UNIVERSITY OF SOUTHAMPTON

GEOMETRICAL NONLINEAR VIBRATION OF BEAMS AND PLATES BY THE HIERARCHICAL FINITE ELEMENT METHOD

VOLUME II – Appendices, Tables and Figures

by

Pedro Manuel Leal Ribeiro

Thesis submitted in fulfilment of the degree of
Doctor of Philosophy

FACULTY OF ENGINEERING AND APPLIED SCIENCE
INSTITUTE OF SOUND AND VIBRATION RESEARCH

June 1998

APPENDIX 1 - SHAPE FUNCTIONS

Out-of-plane shape functions

$f_1= (1/8)-(1/8)\ \xi-(1/8)\ \xi^2+(1/8)\ \xi^3$

$f_2= (1/2)-(3/4)\ \xi+(1/4)\ \xi^3$

$f_3= -(1/8)-(1/8)\ \xi+(1/8)\ \xi^2+(1/8)\ \xi^3$

$f_4= (1/2)+(3/4)\ \xi-(1/4)\ \xi^3$

$f_5= 1/8-(1/4)\ \xi^2+(1/8)\ \xi^4$

$f_6= (1/8)\ \xi-(1/4)\ \xi^3+(1/8)\ \xi^5$

$f_7= -(1/48)+(3/16)\ \xi^2-(5/16)\ \xi^4+(7/48)\ \xi^6$

$f_8= -(1/16)\ \xi+(5/16)\ \xi^3-(7/16)\ \xi^5+(3/16)\ \xi^7$

$f_9= 3/384-(15/96)\ \xi^2+(35/64)\ \xi^4-(63/96)\ \xi^6+(99/384)\ \xi^8$

$f_{10}= (5/128)\ \xi-(35/96)\ \xi^3+(63/64)\ \xi^5-(33/32)\ \xi^7+(143/384)\ \xi^9$

$f_{11}= -1/256+(35/256)\ \xi^2-(105/128)\ \xi^4+(231/128)\ \xi^6-(429/256)\ \xi^8+(143/256)\ \xi^{10}$

$f_{12}= -(7/256)\ \xi+(105/256)\ \xi^3-(231/128)\ \xi^5+(429/128)\ \xi^7-(715/256)\ \xi^9+(221/256)\ \xi^{11}$

$f_{13}= 7/3072-(63/512)\ \xi^2+(1155/1024)\ \xi^4-(1001/256)\ \xi^6+(6435/1024)\ \xi^8-(2431/512)\ \xi^{10}+(4199/3072)\ \xi^{12}$

$f_{14}= (21/1024)\ \xi-(231/512)\ \xi^3+(3003/1024)\ \xi^5-(2145/256)\ \xi^7+(12155/1024)\ \xi^9-(4199/512)\ \xi^{11}+(2261/1024)\ \xi^{13}$

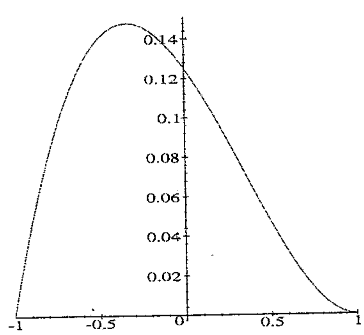

f_1

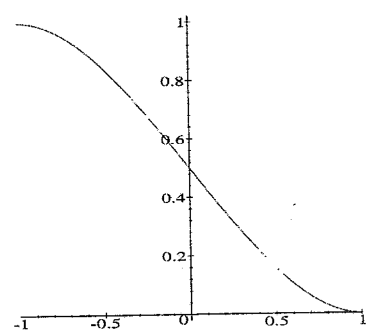

f_2

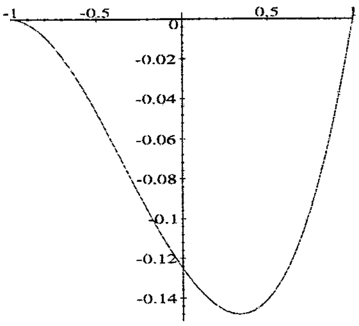

f_3

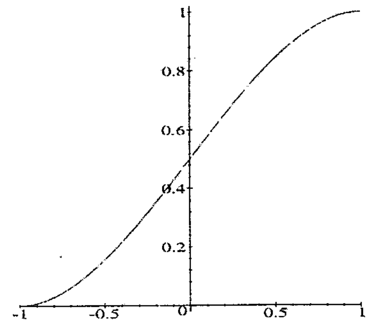

f_4

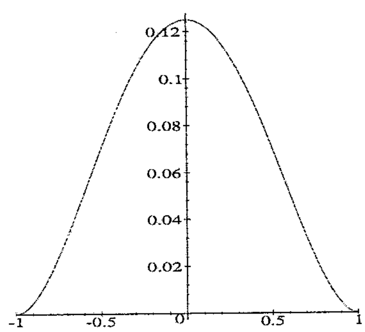

f_5

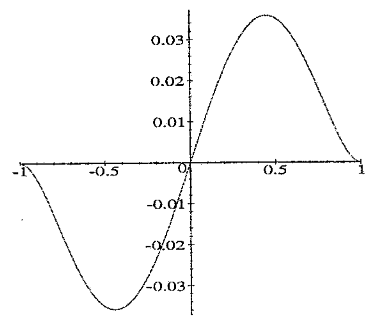

f_6

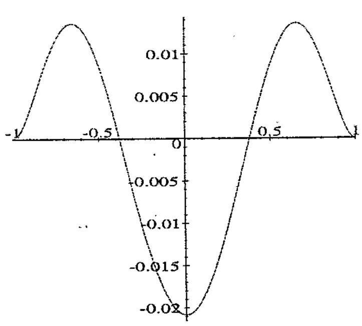

f_7

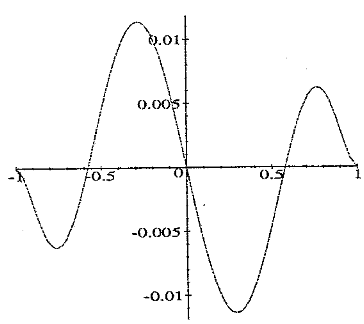

f_8

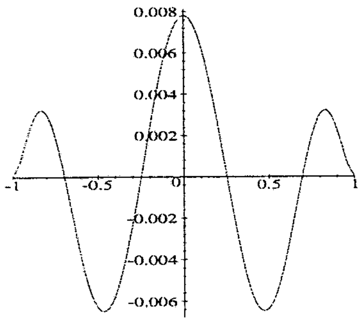

f_9

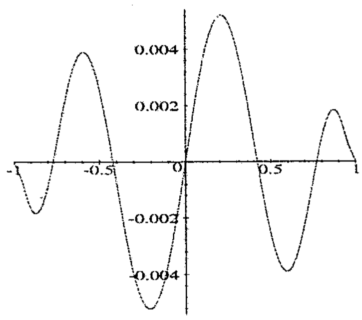

f_{10}

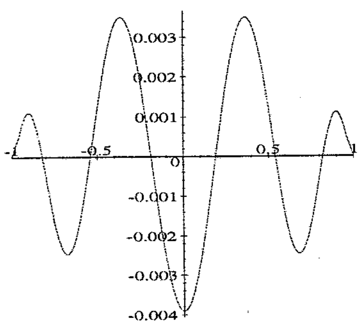

f_{11}

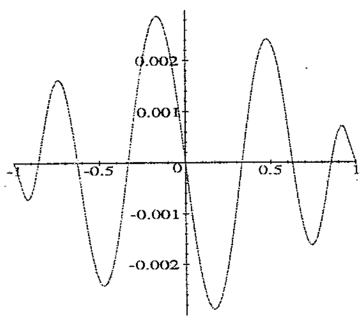

f_{12}

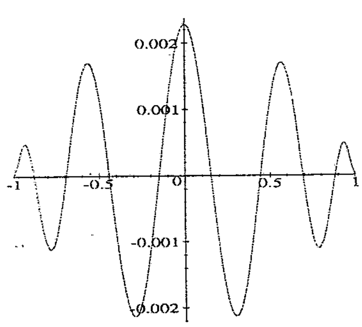

f_{13}

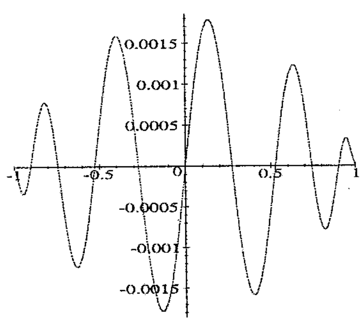

f_{14}

In-plane shape functions

$g_1 = -1/2+(1/2)\,\xi^2$

$g_2 = -(1/2)\,\xi+(1/2)\,\xi^3$

$g_3 = 1/8-(3/4)\,\xi^2+(5/8)\,\xi^4$

$g_4 = (3/8)\,\xi-(5/4)\,\xi^3+(7/8)\,\xi^5$

$g_5 = -1/16+(15/16)\,\xi^2-(35/16)\,\xi^4+(63/48)\,\xi^6$

$g_6 = -(5/16)\,\xi+(35/16)\,\xi^3-(63/16)\,\xi^5+(99/48)\,\xi^7$

$g_7 = 5/128-(105/96)\,\xi^2+(315/64)\,\xi^4-(693/96)\,\xi^6+(1287/384)\,\xi^8$

$g_8 = (35/128)\,\xi-(105/32)\,\xi^3+(693/64)\,\xi^5-(429/32)\,\xi^7+(715/128)\,\xi^9$

$g_9 = -7/256+(315/256)\,\xi^2-(1155/128)\,\xi^4+(3003/128)\,\xi^6-(6435/256)\,\xi^8+(2431/256)\,\xi^{10}$

$g_{10} = -(63/256)\,\xi+(1155/256)\,\xi^3-(3003/128)\,\xi^5+(6435/128)\,\xi^7-(12155/256)$
$\xi^9+(4199/256)\,\xi^{11}$

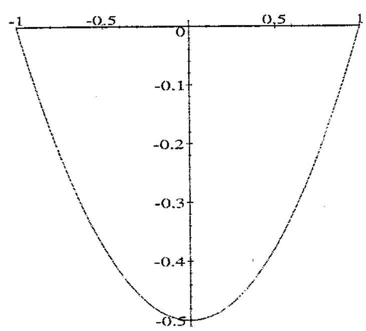

g_1

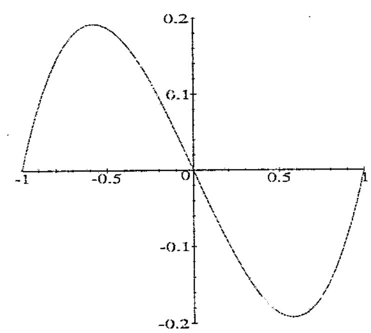

g_2

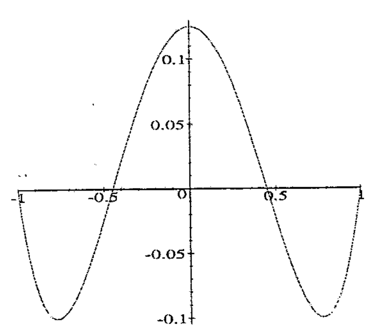

g_3

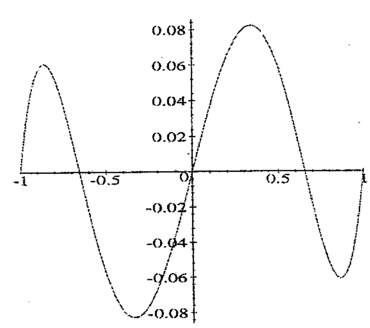

g_4

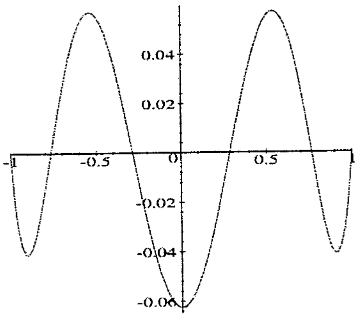

g_5

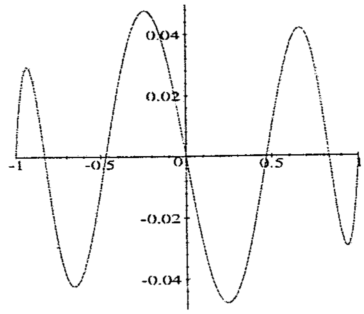

g_6

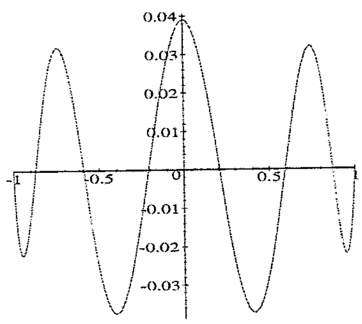

g_7

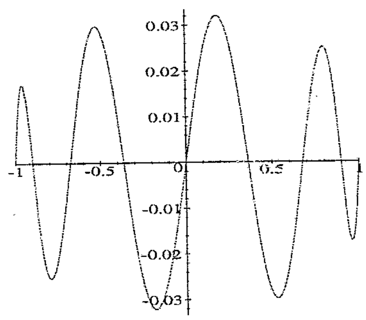

g_8

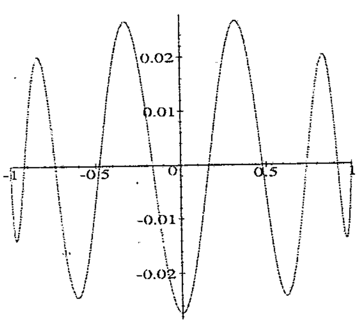

g_9

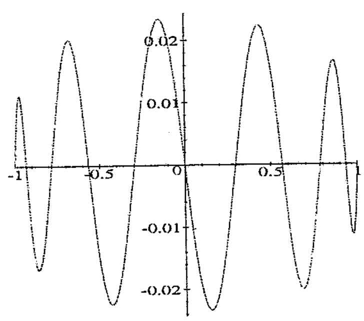

g_{10}

APPENDIX 2 - TRIGONOMETRIC RELATIONS

$$cos^3(\omega t) = \frac{3}{4}cos(\omega t) + \frac{1}{4}cos(3\omega t) \tag{A2.1}$$

$$cos^2(\omega t)cos(3\omega t) = \frac{1}{4}cos(\omega t) + \frac{1}{2}cos(3\omega t) + \frac{1}{4}cos(5\omega t) \tag{A2.2}$$

$$cos(\omega t)cos^2(3\omega t) = \frac{1}{2}cos(\omega t) + \frac{1}{4}cos(5\omega t) + \frac{1}{4}cos(7\omega t) \tag{A2.3}$$

$$cos^3(3\omega t) = \frac{3}{4}cos(3\omega t) + \frac{1}{4}cos(9\omega t) \tag{A2.4}$$

$$cos^2(\omega t)cos(5\omega t) = \frac{1}{4}cos(3\omega t) + \frac{1}{4}cos(7\omega t) + \frac{1}{2}cos(5\omega t) \tag{A2.5}$$

$$cos(\omega t)cos(3\omega t)cos(5\omega t) = \frac{1}{4}cos(\omega t) + \frac{1}{4}cos(3\omega t) + \frac{1}{4}cos(7\omega t) + \frac{1}{4}cos(9\omega t) \tag{A2.6}$$

$$cos(\omega t)cos^2(5\omega t) = \frac{1}{2}cos(\omega t) + \frac{1}{4}cos(9\omega t) + \frac{1}{4}cos(11\omega t) \tag{A2.7}$$

$$cos^2(3\omega t)cos(5\omega t) = \frac{1}{4}cos(\omega t) + \frac{1}{2}cos(5\omega t) + \frac{1}{4}cos(11\omega t) \tag{A2.8}$$

$$cos(3\omega t)cos^2(5\omega t) = \frac{1}{2}cos(3\omega t) + \frac{1}{4}cos(7\omega t) + \frac{1}{4}cos(13\omega t) \tag{A2.9}$$

$$cos^3(5\omega t) = \frac{3}{4}cos(5\omega t) + \frac{1}{4}cos(15\omega t) \tag{A2.10}$$

$$cos^2(\omega t)sin(\omega t) = \frac{1}{4}sin(\omega t) + \frac{1}{4}sin(3\omega t) \tag{A2.11}$$

$$cos(\omega t)sin^2(\omega t) = \frac{1}{4}cos(\omega t) - \frac{1}{4}cos(3\omega t) \tag{A2.12}$$

$$cos^2(\omega t)sin(3\omega t) = \frac{1}{4}sin(\omega t) + \frac{1}{2}sin(3\omega t) + \frac{1}{4}sin(5\omega t) \tag{A2.13}$$

$$cos(\omega t)cos(3\omega t)sin(\omega t) = -\frac{1}{4}sin(\omega t) + \frac{1}{4}sin(5\omega t) \tag{A2.14}$$

$$cos(\omega t)sin(\omega t)sin(3\omega t) = \frac{1}{4}cos(\omega t) - \frac{1}{4}cos(5\omega t) \tag{A2.15}$$

$$cos(\omega t)cos(3\omega t)sin(3\omega t) = \frac{1}{4}sin(5\omega t) + \frac{1}{4}sin(7\omega t) \tag{A2.16}$$

$$cos(\omega t)sin^2(3\omega t) = \frac{1}{2}cos(\omega t) - \frac{1}{4}cos(5\omega t) - \frac{1}{4}cos(7\omega t) \tag{A2.17}$$

$$sin^2(\omega t)cos(3\omega t) = -\frac{1}{4}cos(\omega t) + \frac{1}{2}cos(3\omega t) - \frac{1}{4}cos(5\omega t) \tag{A2.18}$$

$$sin(\omega t)sin(3\omega t)cos(3\omega t) = \frac{1}{4}cos(5\omega t) - \frac{1}{4}cos(7\omega t) \tag{A2.19}$$

$$sin(\omega t)cos^2(3\omega t) = \frac{1}{2}sin(\omega t) - \frac{1}{4}sin(5\omega t) + \frac{1}{4}sin(7\omega t) \tag{A2.20}$$

$$sin(3\omega t)cos^2(3\omega t) = \frac{1}{4}sin(3\omega t) + \frac{1}{4}sin(9\omega t) \tag{A2.21}$$

$$sin(3\omega t)^2\,cos(3\omega t) = \frac{1}{4}cos(3\omega t) - \frac{1}{4}cos(9\omega t) \tag{A2.22}$$

$$sin^3(\omega t) = \frac{3}{4}sin(\omega t) - \frac{1}{4}sin(3\omega t) \tag{A2.23}$$

$$sin^2(\omega t)sin(3\omega t) = -\frac{1}{4}sin(\omega t) + \frac{1}{2}sin(3\omega t) - \frac{1}{4}sin(5\omega t) \tag{A2.24}$$

$$sin(\omega t)sin^2(3\omega t) = \frac{1}{2}sin(\omega t) + \frac{1}{4}sin(5\omega t) - \frac{1}{4}sin(7\omega t) \tag{A2.25}$$

$$sin^3(3\omega t) = \frac{3}{4}sin(3\omega t) - \frac{1}{4}sin(9\omega t) \tag{A2.26}$$

APPENDIX 3 - MATRICES $[M_0]$ AND $[M_1]$

In this appendix the matrices $[M_0]$ and $[M_1]$ present in equations (4.26)-(4.28) are derived for the one and two harmonics' cases.

A3.1 *One harmonic*

When the solution is harmonic,

$$\{q_w\} = \{w_{c1}\}cos(\omega t) + \{w_{s1}\}sin(\omega t), \tag{A3.1}$$

The Fourier expansion of $\partial([Knl]\{q_w\})/\partial\{q_w\}$ is, whithout any approximation:

$$\frac{\partial([Knl]\{q_w\})}{\partial\{q_w\}} = [p_1] + [p_2]cos(2\omega t) + [p_3]sin(2\omega t). \tag{A3.2}$$

$[p_1]$, $[p_2]$ and $[p_3]$, the coefficients of Fourier of $\partial([Knl]\{q_w\})/\partial\{q_w\}$, are defined by (4.7)-(4.9). To study the principal instabilities of the harmonic solution, k=1 is assumed in equation (4.25) arriving at

$$\{\delta\xi\} = e^{\lambda t}(\{b_1\}cos(\omega t) + \{a_1\}sin(\omega t)), \tag{A3.3}$$

and (4.24) becomes

$$\{\delta\ddot{\xi}\} + \left([\omega_j^2] - \frac{1}{4}\left(\frac{\beta}{\omega}\right)^2[I] + [B]^T([p_1] + [p_2]cos(2\omega t) + [p_3]sin(2\omega t))[B]\right)\{\delta\xi\} = \{0\} \tag{A3.4}$$

Inserting (A3.3) into (A3.4) and applying the HBM, results in *terms in cos(ωt)*

$$\left(\left[\omega_{0j}^2\right]+\left(\lambda^2-\omega^2-\frac{1}{4}\left(\frac{\beta}{\omega}\right)^2\right)[I]+[B]^T\left([p_1]+\frac{1}{2}[p_2]\right)[B]\right)\{b_1\}+$$
$$\left(2\lambda\omega+\frac{1}{2}[B]^T[p_3][B]\right)\{a_1\}=\{0\} \tag{A3.5}$$

terms in sin(ωt)

$$\left(\frac{1}{2}[B]^T[p_3][B]-2\lambda\omega\right)\{b_1\}+$$
$$\left(\left[\omega_{0j}^2\right]+\left(\lambda^2-\omega^2-\frac{1}{4}\left(\frac{\beta}{\omega}\right)^2\right)[I]+[B]^T\left([p_1]-\frac{1}{2}[p_2]\right)[B]\right)\{a_1\}=\{0\} \tag{A3.6}$$

Equations (A3.5) and (A3.6) can be written in the following matrix form:

$$\left(\lambda^2[I]+\lambda[M_1]+[M_0]\right)\begin{Bmatrix}b_1\\a_1\end{Bmatrix}=\begin{Bmatrix}0\\0\end{Bmatrix} \tag{A3.7}$$

where [I] is the identity matrix and $[M_1]$ is defined by

$$[M_1]=\begin{bmatrix}0 & 2\omega[I]\\-2\omega[I] & 0\end{bmatrix}. \tag{A3.8}$$

$[M_0]$ is a function of $[p_1]$, $[p_2]$ and $[p_3]$. These are functions of $\{q_w\}$ and can be written in the form

$$[p_1]=\frac{1}{T}\int_0^T\frac{\partial}{\partial\{q_w\}}\left([Knl]\{q_w\}\right)dt=\frac{2}{T}\int_0^T\frac{\partial}{\partial\{q_w\}}\left([Knl]\{q_w\}\right)cos^2(\omega t)\,dt-$$
$$\frac{1}{T}\int_0^T\frac{\partial}{\partial\{q_w\}}\left([Knl]\{q_w\}\right)cos(2\omega t)\,dt=\frac{2}{T}\int_0^T\frac{\partial}{\partial\{q_w\}}\left([Knl]\{q_w\}\right)\frac{\partial\{q_w\}}{\partial\{w_{c1}\}}cos(\omega t)\,dt-\frac{1}{2}[p_2]$$
$$=\frac{\partial\{F_{c1}\}}{\partial\{w_{c1}\}}-\frac{1}{2}[p_2]=[J_{11}]-\frac{1}{2}[p_2] \tag{A3.9}$$

$$[p_2]=\frac{2}{T}\int_0^T\frac{\partial}{\partial\{q_w\}}\left([Knl]\{q_w\}\right)\ cos(2\omega t)dt=\frac{2}{T}\int_0^T\frac{\partial}{\partial\{q_w\}}\left([Knl]\{q_w\}\right)\left(cos^2(\omega t)-sin^2(\omega t)\right)dt$$
$$=2[p_1]-\frac{4}{T}\int_0^T\frac{\partial}{\partial\{q_w\}}\left([Knl]\{q_w\}\right)\frac{\partial\{q_w\}}{\partial\{w_{s1}\}}sin(\omega t)\,dt=2[p_1]-2\frac{\partial\{F_{s1}\}}{\partial\{w_{s1}\}}=2[p_1]-2[J_{22}]$$
(A3.10)

$$[p_3]=\frac{2}{T}\int_0^T\frac{\partial}{\partial\{q_w\}}\left([Knl]\{q_w\}\right)\ sin(2\omega t)dt=$$
$$\frac{4}{T}\int_0^T\frac{\partial}{\partial\{q_w\}}\left([Knl]\{q_w\}\right)\frac{\partial\{q_w\}}{\partial\{w_{c1}\}}sin(\omega t)\,dt=2\frac{\partial\{F_{s1}\}}{\partial\{w_{c1}\}}=2[J_{21}] \qquad \text{(A3.11)}$$

$$[p_3]=\frac{4}{T}\int_0^T\frac{\partial}{\partial\{q_w\}}\left([Knl]\{q_w\}\right)\frac{\partial\{q_w\}}{\partial\{w_{s1}\}}cos(\omega t)\,dt=2\frac{\partial\{F_{c1}\}}{\partial\{w_{s1}\}}=2[J_{12}] \qquad \text{(A3.12)}$$

Above, it was taken into consideration that

$$\frac{\partial\{q_w\}}{\partial\{w_{c1}\}}=[I]cos(\omega t), \quad \text{(A3.13)} \qquad \frac{\partial\{q_w\}}{\partial\{w_{s1}\}}=[I]sin(\omega t). \qquad \text{(A3.14)}$$

$\{F_{c1}\}$ and $\{F_{s1}\}$, defined by (2.133) and (2.134), are the cosine and sine coefficients of $[Knl]\{q_w\}$. Applying the derivation rule for composite functions, the following derivatives of $\{F_{c1}\}$ and $\{F_{s1}\}$ are defined:

$$[J_{11}]=\frac{\partial\{F_{c1}\}}{\partial\{w_{c1}\}}=\frac{2}{T}\int_0^T\frac{\partial}{\partial\{q_w\}}\left([Knl]\{q_w\}\right)\frac{\partial\{q_w\}}{\partial\{w_{c1}\}}cos(\omega t)\,dt, \qquad \text{(A3.15)}$$

$$[J_{12}]=\frac{\partial\{F_{c1}\}}{\partial\{w_{s1}\}}=\frac{2}{T}\int_0^T\frac{\partial}{\partial\{q_w\}}\left([Knl]\{q_w\}\right)\frac{\partial\{q_w\}}{\partial\{w_{s1}\}}cos(\omega t)\,dt, \qquad \text{(A3.16)}$$

$$[J_{21}]=\frac{\partial\{F_{s1}\}}{\partial\{w_{c1}\}}=\frac{2}{T}\int_0^T\frac{\partial}{\partial\{q_w\}}\left([Knl]\{q_w\}\right)\frac{\partial\{q_w\}}{\partial\{w_{c1}\}}sin(\omega t)\,dt, \qquad \text{(A3.17)}$$

$$[J_{22}]=\frac{\partial\{F_{s1}\}}{\partial\{w_{s1}\}}=\frac{2}{T}\int_0^T\frac{\partial}{\partial\{q_w\}}\left([Knl]\{q_w\}\right)\frac{\partial\{q_w\}}{\partial\{w_{s1}\}}sin(\omega t)\,dt. \tag{A3.18}$$

Using (A3.15) to (A3.18), $[M_0]$ can be written as

$$[M_0]=\begin{bmatrix}[B]^T[J_{11}][B]-\left(\omega^2+\left(\frac{1}{2}\frac{\beta}{\omega}\right)^2\right)[I]+[\omega_{0j}^{\;2}] & [B]^T[J_{12}][B]\\ [B]^T[J_{21}][B] & [B]^T[J_{22}][B]-\left(\omega^2+\left(\frac{1}{2}\frac{\beta}{\omega}\right)^2\right)[I]+[\omega_{0j}^{\;2}]\end{bmatrix} \tag{A3.19}$$

A3.2 *Two harmonics*

To study the stability of the two harmonic solutions, k=2 is assumed in equation (4.25) arriving at

$$\{\delta\bar{\xi}\}=e^{\lambda t}\left(\{b_1\}cos(\omega t)+\{a_1\}sin(\omega t)+\{b_3\}cos(3\omega t)+\{a_3\}sin(3\omega t)\right). \tag{A3.20}$$

With this expression, simple instabilities of first and of third order will be detected. Inserting (A3.20) into (4.24) and applying the HBM, neglecting terms of order higher than 3ω, results in an equation of the form (A3.7), with $[M_1]$ defined by

$$[M_1]=\begin{bmatrix}0 & 2\omega[I] & 0 & 0\\ -2\omega[I] & 0 & 0 & 0\\ 0 & 0 & 0 & 6\omega[I]\\ 0 & 0 & -6\omega[I] & 0\end{bmatrix} \tag{A3.21}$$

and the symmetric matrix $[M_0]$ defined by

$$[M_0]=\begin{bmatrix} [B]^T[p_1][B]+\frac{1}{2}[B]^T[p_2][B]+Const1 & \frac{1}{2}[B]^T[p_3][B] & \frac{1}{2}[B]^T[p_2][B]+\frac{1}{2}[B]^T[p_4][B] & \frac{1}{2}[B]^T[p_3][B]+\frac{1}{2}[B]^T[p_5][B] \\ \frac{1}{2}[B]^T[p_3][B] & [B]^T[p_1][B]-\frac{1}{2}[B]^T[p_2][B]+Const1 & -\frac{1}{2}[B]^T[p_3][B]+\frac{1}{2}[B]^T[p_5][B] & \frac{1}{2}[B]^T[p_2][B]-\frac{1}{2}[B]^T[p_4][B] \\ \frac{1}{2}[B]^T[p_2][B]+\frac{1}{2}[B]^T[p_4][B] & -\frac{1}{2}[B]^T[p_3][B]+\frac{1}{2}[B]^T[p_5][B] & [B]^T[p_1][B]+Const2 & 0 \\ \frac{1}{2}[B]^T[p_3][B]+\frac{1}{2}[B]^T[p_5][B] & \frac{1}{2}[B]^T[p_2][B]-\frac{1}{2}[B]^T[p_4][B] & 0 & [B]^T[p_1][B]+Const2 \end{bmatrix} \qquad \text{(A3.22)}$$

The terms *Const*1 and *Const*2 are:

$$Const1=-\left(\omega^2+\left(\frac{1}{2}\frac{\beta}{\omega}\right)^2\right)[I]+\left[\omega_{0j}^{\;2}\right], \qquad \text{(A3.22)}$$

$$Const2=-\left(9\omega^2+\left(\frac{1}{2}\frac{\beta}{\omega}\right)^2\right)[I]+\left[\omega_{0j}^{\;2}\right], \qquad \text{(A3.23)}$$

The matrices $[p_1]$, $[p_2]$, $[p_3]$, $[p_4]$ and $[p_5]$, defined by equations (4.7)-(4.11), were obtained by using the approximation derived in Chapter 3, according to which:

$$\frac{\partial}{\partial q_w}\left([Knl]\{q_w\}\right)\cong 3[Knl]. \qquad \text{(A3.24)}$$

As a result:

$$[p_1]=\frac{3}{2}\left([KNL_1]+[KNL_5]+[KNL_8]+[KNL_{10}]\right), \qquad \text{(A3.25)}$$

$$[p_2]=\frac{3}{2}\left([KNL_1]+[KNL_3]-[KNL_5]+[KNL_7]\right), \qquad \text{(A3.26)}$$

$$[p_3] = \frac{3}{2}\left([KNL_2] + [KNL_4] - [KNL_6]\right), \tag{A3.27}$$

$$[p_4] = \frac{3}{2}\left([KNL_3] - [KNL_7]\right), \tag{A3.28}$$

$$[p_5] = \frac{3}{2}\left([KNL_4] + [KNL_6]\right). \tag{A3.29}$$

The nonlinear stiffness matrices $[KNL_i]$ are defined in Chapter 2.

APPENDIX 4 - THE CHARACTERISTIC EXPONENTS' FORM

The characteristic exponents are defined by the following eigenvalue problem

$$\left(\lambda^2[I]+\lambda[M_1]+[M_0]\right)\{X\}=\begin{Bmatrix}0\\0\end{Bmatrix} \tag{A4.1}$$

Where $[I]$ is the identity matrix, $[M_1]$ and $[M_0]$ are defined in Appendix 3. If the middle plane in-plane displacements are not included in the model, then $\partial([Knl]\{q_w\})/\partial\{q_w\}$ is equal to $3[KNL]$, as was proved in Chapter 3; therefore, $\partial([Knl]\{q_w\})/\partial\{q_w\}$ is a symmetric matrix. When the middle plane in-plane displacements are included in the model, it was verified using *Maple* that $\partial([Knl]\{q_w\})/\partial\{q_w\}$ is still symmetric. Hence, $[M_0]$ is a symmetric matrix.

Eigenvalue problem (A4.1) is typical of a conservative gyroscopic system, because matrices $[I]$ and $[M_0]$ are symmetric and matrix $[M_1]$ is skew-symmetric [4.15]. According to reference [4.12] the resulting eigenvalues are purely real or purely imaginary. If the former was true, stability could only be lost by process (4.32*a*), which would fully justify the simplification of the stability study based on the sign of $|J|$. In fact, for imaginary λ

$$Re\left(\lambda-\frac{1}{2}\frac{\beta}{\omega}\right)=-\frac{1}{2}\frac{\beta}{\omega} \tag{A4.2}$$

and for real λ

$$Re\left(\lambda-\frac{1}{2}\frac{\beta}{\omega}\right)=\lambda-\frac{1}{2}\frac{\beta}{\omega}. \tag{A4.3}$$

Consequently, if λ is imaginary the solution is always stable, if λ is real the stability limit is defined by

$$Re\left(\lambda - \frac{1}{2}\frac{\beta}{\omega}\right) = 0 \Leftrightarrow \lambda = \frac{1}{2}\frac{\beta}{\omega}. \tag{A4.4}$$

and conclusions similar to the ones made in section 4.3 can be taken.

However, no proof was found in the literature that when $[I]$ and $[M_0]$ are symmetric and $[M_1]$ is skew-symmetric, λ is either purely imaginary or purely real.

To verify the form of λ, let us introduce the notation

$$\{X\} = \{Y\} + i\{Z\}, \qquad \{\bar{X}\} = \{Y\} - i\{Z\} \tag{A4.5}$$

where the real vectors $\{Y\}$ and $\{Z\}$ are the real and imaginary parts of $\{X\}$. Introducing equations (A4.5) into (A4.1) one obtains the following quadratic equation

$$\lambda^2\left(\lfloor Y\rfloor[I]\{Y\}+\lfloor Z\rfloor[I]\{Z\}\right)+2\lambda\left(\lfloor Y\rfloor[M_1]\{Z\}\right)i+\left(\lfloor Y\rfloor[M_0]\{Y\}+\lfloor Z\rfloor[M_0]\{Z\}\right)=0 \tag{A4.6}$$

Writing

$$a=\lfloor Y\rfloor[I]\{Y\}+\lfloor Z\rfloor[I]\{Z\},\ b = 2\lfloor Y\rfloor[M_1]\{Z\} \text{ and } c=\lfloor Y\rfloor[M_0]\{Y\}+\lfloor Z\rfloor[M_0]\{Z\}, \tag{A4.7}$$

where a, b and c are real numbers, the following equation is defined

$$\lambda = \frac{-2bi \pm \sqrt{-b^2 - 4ac}}{2a} \tag{A4.8}$$

If matrix $[M_0]$ is positive definite, it is easy to verify that λ is purely imaginary, agreeing with [4.10]. However, if $[M_0]$ is not positive definite, then $-4ac$ can be positive and it can happen that $-b^2 - 4ac > 0$. In this case λ will be complex, with real and imaginary parts both different from zero if $b \neq 0$, and will be purely real if $b=0$.

Concerning the first order type of instability, in the numerical cases tried in this work (with a special attention to the cases in which $-4ac$ was positive) it was verified that $b=0$ and consequently λ was either purely real or purely imaginary. The vectors $\{Y\}$ and $\{Z\}$, and the matrix $[M_1]$, are very sparse, which explains why it is likely to happen that $b=0$, but it does not prove that it always happens. Consequently, a loss of stability, due to an instability of order one, of the types (4.32*b*) or (4.32*c*) is not overridden, but is extremely unlikely to happen.

In what concerns higher order instabilities, it was found that the characteristic exponents can be complex with real and imaginary parts different from zero. Thus, an higher order instability can be of the type (4.32*c*), and will not be detected by an alteration of the Jacobian's sign.

REFERENCES

CHAPTER 1

[1. 1] - Sathyamoorthy, M. Nonlinear vibration analysis of plates: a review and survey of current developments. *Applied Mechanics Review*, 1987, 40(11), 1553-1561.

[1. 2] - Smith, P. W., Malme, C. I. and Gogos, C. M. Nonlinear response of a simple clamped panel. *The Journal of the Acoustical Society of America*, 1961, 33(11), 1476-1482.

[1. 3] - White, R. G. A comparison of some statistical properties of the responses of aluminium alloy and cfrp plates to acoustic excitation. *Composites*, 9, 1978, 251-258.

[1. 4] - Teh, C. E. *Dynamic Behaviour and Acoustic Fatigue of Isotropic and Anisotropic Panels Under Combined Acoustic Excitation and Static In-plane Compression*. Ph.D. Thesis, University of Southampton, 1982.

[1. 5] - Benamar, R. *Nonlinear Dynamic Behaviour of Fully Clamped Beams and Rectangular Isotropic and Laminated Plates*. Ph.D. Thesis, University of Southampton, 1990.

[1. 6] - Benamar, R., Bennouna, M.M.K. and White, R. G. The effects of large vibration amplitudes on the mode shapes and natural frequencies of thin elastic structures. Part III: fully clamped rectangular isotropic plates-measurements of the mode shape amplitude dependence and the spatial distribution of harmonic distortion. *Journal of Sound and Vibration*, 1994, 175(3), 377-395.

[1. 7] - Wolfe, H. *An Experimental Investigation of Nonlinear Behaviour of Beams and Plates Excited to High Levels of Dynamic Response*. Ph.D. Thesis, University of Southampton, 1995.

[1. 8] - Bennouna, M.M.K. *Nonlinear Dynamic Behaviour of a Clamped-clamped Beam with Consideration of Fatigue Life*. Ph.D. Thesis, University of Southampton, 1982.

[1. 9] - Bennouna, M.M., White, R.G. The effects of large vibration amplitudes on the fundamental mode shape of a clamped-clamped uniform beam. *Journal of Sound and Vibration*, 1984, 96(3), 309-331.

[1. 10] - Benamar, R., Bennouna, M.M., White, R.G. The effects of large vibration amplitudes on the mode shapes and natural frequencies of thin elastic structures. Part I: simply supported and clamped-clamped beams. *Journal of Sound and Vibration*, 1991, 149(2), 179-195.

[1. 11] - Benamar, R., Bennouna, M.M.K. and White, R. G. The effects of large vibration amplitudes on the mode shapes and natural frequencies of thin elastic structures. Part II: fully clamped rectangular isotropic plates. *Journal of Sound and Vibration*, 1993, 164(2), 295-316.

[1. 12] - Han, W. *The Analysis of Isotropic and Laminated Rectangular Plates Including Geometrical Non-linearity Using the p-version Finite Element Method.* Ph.D. Thesis, University of Southampton, 1993.

[1. 13] - Han, W. and Petyt, M. Geometrically nonlinear vibration analysis of thin, rectangular plates using the hierarchical finite element method - I: The fundamental mode of isotropic plates. *Computers and Structures*, 1997, 63(2), 295-308.

[1. 14] - Han, W. and Petyt, M. Geometrically nonlinear vibration analysis of thin, rectangular plates using the hierarchical finite element method - II: 1st mode of laminated plates and higher modes of isotropic and laminated plates. *Computers and Structures*, 1997, 63(2), 309-318.

[1. 15] - Nayfeh, A. H. and Mook, D. T. *Nonlinear Oscillations*. New York: John Wiley and Sons, 1995.

[1. 16] - Tseng, W. Y. and Dugundji, J. Nonlinear vibrations of a beam under harmonic excitation. *Transactions of the ASME, Journal of Applied Mechanics*, 1970, 37, 292-297.

[1. 17] - Yamamoto, T., Yasuda, K. and Aoki, K. Subharmonic oscillations of a slender beam. *Bulletin of the JSME*, 1981, 24(192), 1011-1020.

[1. 18] - Yamamoto, T., Yasuda, K. and Aoki, K. Summed and differential harmonic oscillations in a slender beam. *Bulletin of the JSME*, 1982, 24(193), 1214-1222.

[1. 19] - Yamamoto, T., Yasuda, K. and Aoki, K. Super summed and differential harmonic oscillations in a slender beam. *Bulletin of the JSME*, 1982, 25(204), 959-968.

[1. 20] - Maestrello, L., Frendi, A. and Brown, D.E. Nonlinear vibration and radiation from a panel with transition to chaos. *AIAA Journal*, 1992, 30 (11), 2632-2638.

[1. 21] - Moon, F. C. *Chaotic Vibrations. An Introduction for Applied Scientists and Engineers.* New York: John Wiley and Sons, 1987.

[1. 22] - Chia, C.Y. *Nonlinear Analysis of Plates*. New York: McGraw-Hill, 1980.

[1. 23] - Rosenberg, R. M. On non-linear vibrations of systems with many degrees of freedom. *Advances in Applied Mechanics*, 1966, 9,155-242.

[1. 24] - Shaw, S. W. and Pierre, C. Normal modes for non-linear vibratory systems. *Journal of Sound and Vibration*, 1993, 164(1), 85-121.

[1. 25] - Shaw, S. W. and Pierre, C. Normal modes of vibration for non-linear continuous systems. *Journal of Sound and Vibration*, 1994, 169(3), 319-347.

[1. 26] - Burton, T. D. and Hamdan, M.N. On the calculation of non-linear normal modes in continuous systems. *Journal of Sound and Vibration*, 1996, 197(1),117-130.

[1. 27] - Leung, A.Y.T. and Ge, T. Normal multi-modes of non-linear Euler beams. *Journal of Sound and Vibration*, 1997, 202(2), 145-160.

[1. 28] - Woinowski-Krieger, S. The effect of an axial force on the vibration of hinged bars. *Journal of Applied Mechanics*, 1950, 17, 35-36.

[1. 29] - Lewandowski, R. Application of the Ritz method to the analysis of non-linear free vibrations of beams. *Journal of Sound and Vibration*, 1987, 114(1), 91-101.

[1. 30] - Lewandowski, R. Non-linear, steady-state analysis of multispan beams by the finite element method. *Computers and Structures*, 1991, 39(1,2), 83-93.

[1. 31] - Lewandowski, R. Non-linear free vibrations of beams by the finite element and continuation methods. *Journal of Sound and Vibration*, 1994, 170(5), 577-593.

[1. 32] - Lewandowski, R. Solutions with bifurcation points for free vibration of beams: an analytical approach. *Journal of Sound and Vibration*, 1994, 177(2), 239-249.

[1. 33] - Lewandowski, R. On beams membranes and plates vibration backbone curves in cases of internal resonance. *Meccanica*, 1996, 31, 323-346.

[1. 34] - Lewandowski, R. Computational formulation for periodic vibration of geometrically nonlinear structures - Part 1: Theoretical background. *International Journal Solids and Structures*, 1997, 34(15), 1925-1947.

[1. 35] - Lewandowski, R. Computational formulation for periodic vibration of geometrically nonlinear structures - Part 2: Numerical strategy and examples. *International Journal Solids and Structures*, 1997, 34(15), 1949-1964.

[1. 36] - Qaisi, M. I. Application of the harmonic balance principle to the nonlinear free vibration of beams. *Applied Acoustics*, 1993, 40, 141-151.

[1. 37] - Cheung, Y.K., Lau, S.L. Incremental time-space finite strip method for non-linear structural vibrations. *Earthquake Engineering and Structural Dynamics*, 1982, 10, 239-253.

[1. 38] - Szemplinska-Stupnicka, W. *The Behaviour of Non-linear Vibrating Systems*. Dordretch: Kluwer Academic Publishers, 1990.

[1. 39] - Prathap, B. S. and Varadan, T. K. The large amplitude vibrations of hinged beams. *Computers and Structures*, 1978, 9, 219-222.

[1. 40] - Bhashyam, G.R., Prathap, G. Galerkin finite element method for non-linear vibrations. *Journal of Sound and Vibration*, 1980, 72(2), 191-203.

[1. 41] - Sarma, B. S., Varadan, T.K. Lagrange-type formulation for finite element analysis of non-linear beam vibrations. *Journal of Sound and Vibration*, 1983, 86(1), 61-70.

[1. 42] - Sarma, B. S., Varadan, T.K. Ritz finite element approach to non-linear vibrations of beams. *International Journal for Numerical Methods in Engineering*, 1984, 20, 353-367.

[1. 43] - Nayfeh, A. H. and Balachandram, B. *Applied Nonlinear Dynamics: Analytical, Computational, and Experimental Methods*. New York: John Wiley and Sons, 1995.

[1. 44] - Leung, A.Y.T. and Mao, S.G. A symplectic Galerkin method for non-linear vibration of beams and plates. *Journal of sound and Vibration*, 1995, 183(3), 475-491.

[1. 45] - Shi, Y. and Mei, C. A finite element time domain modal formulation for large amplitude free vibration of beams and plates. *Journal of Sound and Vibration*, 1996, 193(2), 453-464.

[1. 46] - Bolotin, V. V. *The Dynamic Stability of Elastic Systems*. San Francisco: Holden Day, 1964.

[1. 47] - Hayashi, C. *Nonlinear Oscillations in Physical Systems*. New York: McGraw-Hill, 1964.

[1. 48] - Bennet, J. A. and Eisley, J. G. A multiple-degree-of freedom approach to nonlinear beam vibrations. *AIAA Journal*, 1970, 8(4), 734-739.

[1. 49] - Atluri, S. Nonlinear vibrations of a hinged beam including nonlinear effects. *Transactions of the ASME, Journal of Applied Mechanics*, 1973, 40, 121-126.

[1. 50] - Takahashi, K. A method of stability analysis for non-linear vibration of beams. *Journal of Sound and Vibration*, 1979, 67(1), 43-54.

[1. 51] - Busby, H.R. and Weingarten, V.I. Nonlinear response of a beam to periodic loading. *International Journal of Non-linear Mechanics*. 1972, 7, 289-303.

[1. 52] - Mei, C. and Decha-Umphai, K. A finite element method for non-linear forced vibrations of beams. *Journal of Sound and Vibration*, 1985, 102(3), 369-380.

[1. 53] - Leung, A.Y.T. and Fung, T.C. Non-linear steady state vibration of frames by finite element method. *International Journal for Numerical Methods in Engineering*, 1989, 28, 1599-1618.

[1. 54] - Ma, A. J., Chen, S. H., Song, D. T. A new method of nonlinear analysis for large deflection forced vibration of beams. *Finite Elements in Analysis and Design*, 1995, 20, 39-46

[1. 55] - Yagasaki, K. Bifurcations and chaos in a quasi-periodically forced beam: theory, simulation and experiment. *Journal Sound Vibration*, 1995, 183(1), 1-31.

[1. 56] - Sathyamoorthy, M. Nonlinear vibration of rectangular plates. *Journal of Sound and Vibration*, 1978, 58(2), 301-304.

[1. 57] - Chu, H.N. and Herrmann, G. Influence of large amplitudes on free flexural vibrations of rectangular elastic plates. *Transactions of the ASME, Journal of Applied Mechanics*, 1956, 23, 532-540.

[1. 58] - Berger, H. M. A new approach to the analysis of large deflections of plates. *Transactions of the ASME, Journal Applied Mechanics*, 1955, 22, 456-472.

[1. 59] - Mei, C. Finite element displacement method for large amplitude free flexural vibration of beams and plates. *Computers and Structures*, 1973, 3, 163-174.

[1. 60] - Rao, G. V., Raju, I. S. and Raju, K. K. A finite element formulation for large amplitude flexural vibrations of thin rectangular plates. *Computers and Structures*, 1976, 6, 163-167.

[1. 61] - Wellford Jr., L. C., Dib, G. M. and Mindle, W. Free and steady state vibration of non-linear structures using a finite element non-linear eigenvalue technique. *Earthquake Engineering and Structural Dynamics*, 1980, 8, 97-115.

[1. 62] - Mei, C. and Decha-Umphai, K. A finite element method for non-linear forced vibrations of rectangular plates. *AIAA Journal*, 1985, 23, 1104-1110.

[1. 63] - Rao, S.R., Sheikh, A. H. and Mukhopadhyay, M. Large-amplitude finite element flexural vibration of plates/stiffened plates. *Journal of the Acoustical Society of America*, 1993, 93(6), 3250-3257.

[1. 64] - Kong, J. and Cheung Y. K. A reduction method for the analysis of non-linear forced vibration of plates. *Journal of Sound and Vibration*, 1995, 184(4), 611-626.

[1. 65] - Lau, S. L., Cheung, Y. K. and Wu, S. Y. Nonlinear vibration of thin elastic plates. Part 1: Generalised incremental Hamilton's principle and element formulation. *Transactions of the ASME, Journal Applied Mechanics*, 1984, 51, 837-844.

[1. 66] - Lau, S. L., Cheung, Y. K. and Wu, S. Y. Nonlinear vibration of thin elastic plates. Part 2: Internal resonance by amplitude-incremental finite element. *Transactions of the ASME, Journal Applied Mechanics*, 1984, 51, 845-851.

[1. 67] - Leung, A.Y.T. and Chui, S.K. On the non-linear vibration of the von Kármán square plate by the IHB method. *Journal of Sound and Vibration*, 1997, 204(2), 239-247.

[1. 68] - Kapania, R. K. and Raciti, S. Recent advances in analysis of laminated beams and plates, Part II: vibrations and wave propagation. *AIAA Journal*, 1989, 27(7), 935-946.

[1. 69] - Schwartz, M. M. *Composite Materials Handbook*. Second Edition. New York: McGraw-Hill, 1992.

[1. 70] - Chia, C.Y. Geometrically nonlinear behavior of composite plates: a review. *Applied Mechanics Review*, 1988, 41(12), 439-451.

[1. 71] - Prabhakara, M. K. and Chia, C. Y. Non-linear flexural vibrations of orthotropic rectangular plates. *Journal of Sound and Vibration*, 1977, 52(4), 511-518.

[1. 72] - Reddy, J. N. and Chao, W. C. Large-deflection and large-amplitude free vibrations of laminated composite-material plates. *Computers and Structures*, 1981, 13, 341-347.

[1. 73] - Eslami, H. and Kandil, O.A. Nonlinear forced vibration of orthotropic rectangular plates using the method of multiple scales. *AIAA Journal*, 1989, 27, 955-960.

[1. 74] - Eslami, H. and Kandil, O.A. Two-mode nonlinear vibration of orthotropic plates using the method of multiple scales. *AIAA Journal*, 1989, 27, 961-967.

[1. 75] - Singh, G., Raju, K. K., Rao, G. V. and Iyengar, N. G. R. Non-linear vibrations of simply supported rectangular cross-ply plates. *Journal of Sound and Vibration*, 1990, 142(2), 213-226.

[1. 76] - Ganapathi, M., Varadan, T. K. and Sarma, B. S. Nonlinear flexural vibrations of laminated orthotropic plates. *Computers and Structures*, 1991, 39(6), 685-688.

[1. 77] - Chiang, C. K., Mei, C. and Gray, C. E. Finite element large-amplitude free and forced vibrations of rectangular thin composite plates. *Transactions of the ASME, Journal of Vibration and Acoustics*, 1991, 113, 309-315.

[1. 78] - Woo, J. and Nair, S. Nonlinear vibrations of rectangular laminated thin plates. *AIAA Journal*, 1992, 30(1), 180-188.

[1. 79] - Sarma, M. S. and Rao, B. N. Applicability of the energy method to non-linear vibrations of thin rectangular plates. *Journal of Sound and Vibration*, 1983, 86(1), 61-70.

[1. 80] - Sarma, M. S., Rao A. V., Pillai, S. R. R. and Rao, B. N. Large amplitude vibrations of laminated hybrid composite plates. *Journal of Sound and Vibration*, 1992, 159(3), 540-545.

[1. 81] - Shi, Y., Lee, R.Y.Y. and Mei, C. Finite element method for nonlinear free vibrations of composite plates. *AIAA Journal*, 1997, 35, 159-166.

[1. 82] - Lee, R.Y.Y., Shi, Y. and Mei, C. Nonlinear response of composite plates to harmonic excitation using the finite element time domain modal method. In N.S. Fergurson, H. F. Wolfe, C. Mei (eds.), *Structural Dynamics Recent Advances, Proceedings of the 6th International Conference*, 1997, Southampton: ISVR, University of Southampton, 1997, 2, 1423-1436.

[1. 83] - Abe, B., Kobayashi, Y. and Yamada, G. Two-mode response of simply supported, rectangular laminated plates. *International Journal of Non-Linear Mechanics*, 1998, 33, 675-690.

[1. 84] - Peano, A. Hierarchies of conforming finite elements for plane elasticity and plate bending. *Computers and Mathematics with Applications*, 1976, 2, 211-224.

[1. 85] - Meirovitch, L., Baruh, H. On the inclusion principle for the hierarchical finite element method. *International Journal for Numerical Methods in Engineering*, 1983, 19, 281-291.

[1. 86] - Zienkiewicz, O.C. and Taylor, R.L. *The Finite Element Method*. 4th Edition. London: McGraw-Hill, 1988.

[1. 87] - Meirovitch, L., Silverberg, L.M. Two bracketing theorems characterizing the eigensolution for the *h*-version of the finite element method. *International Journal for Numerical Methods in Engineering*, 1983, 19, 1691-1704.

[1. 88] - Meirovitch, L. *Elements of Vibration Analysis*. Singapore: McGraw-Hill, 1986.

[1. 89] - Szabó, B.A. and Babuska, I. *Finite Element Analysis*. New York: John Wiley and Sons, 1991.

[1. 90] - Szabó, B. A. and Sahrmann, G.J. Hierarchic plate and shell models based on p-extension. *International Journal for Numerical Methods in Engineering*, 1988, 26, 1855-1881.

[1. 91] - Han, W., Petyt, M. and Hsiao, K.M. An investigation into geometrically nonlinear analysis of rectangular laminated plates using the hierarchical finite element method. *Finite Elements in Analysis and Design*, 1994, 18, 273-288.

[1. 92] - Zhu, D.C. Development of hierarchical finite element methods at BIAA. In *Proceedings of International Conference on Computational Mechanics*, May 1986, Tokyo. Tokyo: Springer-Verlag, 1986.

[1. 93] - Houmat, A. Hierarchical finite element analysis of the vibration of membranes. *Journal of Sound and Vibration*, 1997, 201(4), 465-472.

[1. 94] - Houmat, A. An alternative hierarchical finite element formulation applied to plate vibrations. *Journal of Sound and Vibration*, 1997, 206(2), 201-215.

[1. 95] - Bardell, N. S. Free vibration analysis of a flat plate using the hierarchical finite element method. *Journal of Sound and Vibration*, 1991, 151(2), 263-289.

[1. 96] - Han, W. and Petyt, M. Linear vibration analysis of laminated rectangular plates using the hierarchical finite element method - I: Free vibration analysis. *Computers and Structures*, 1996, 61(4), 705-712.

[1. 97] - Han, W. and Petyt, M. Linear vibration analysis of laminated rectangular plates using the hierarchical finite element method - II: Forced vibration analysis. *Computers and Structures*, 1996, 61(4), 713-724.

[1. 98] - Redfern, D. *The Maple Handbook*. New York: Springer-Verlag, 1994.

CHAPTER 2

[2. 1] - Chia, C.Y. *Nonlinear Analysis of Plates*. New York: McGraw-Hill, 1980.

[2. 2] - Zienkiewicz, O.C. and Taylor, R.L. *The Finite Element Method*. 4th Edition. London: McGraw-Hill, 1988.

[2. 3] - Federkov, G. V. On the damping of the free vibrations of systems with many degrees of freedom. *Tr. Mosk. Inst. Inzh. Transp.*, 1952, 76, 135-140.

[2. 4] - Bolotin, V. V. *The Dynamic Stability of Elastic Systems*. San Francisco: Holden Day, 1964.

[2. 5] - Rayleigh, J.W.S. *The Theory of Sound*, vol. 1. New York: Dover, pag. 130, 1877.

[2. 6] - Caughey, T. K. Classical normal modes in damped linear dynamic systems. *Transactions of the ASME, Journal of Applied Mechanics*, 1960, 27, 269-271.

[2. 7] - Lazan, B. J. *Damping of Materials and Members in Structural Mechanics*. Oxford: Pergamon Press, 1968.

[2. 8] - Meirovitch, L. *Elements of Vibration Analysis*. Singapore: McGraw-Hill, 1986.

[2. 9] - Petyt, M. *Introduction to Finite Element Vibration Analysis*. Cambridge: Cambridge University Press, 1990.

[2. 10] - Mentel, T. J. Vibrational energy dissipation at structural support junctions. In J. E. Ruzicka (ed.), *Colloquium on Structural Damping*, New York: The American Society of Mechanical Engineers, 1959, 89-116.

[2. 11] - Cheung, Y.K., Lau, S.L. Incremental time-space finite strip method for non-linear structural vibrations. *Earthquake Engineering and Structural Dynamics*, 1982, 10, 239-253.

[2. 12] - Han, W. *The Analysis of Isotropic and Laminated Rectangular Plates Including Geometrical Non-linearity Using the p-version Finite Element Method*. Ph.D. Thesis. University of Southampton, UK, 1993.

[2. 13] - Mei, C. and Prasad, C. B. Effects of large deflection and transverse shear on responses of symmetrical composite laminates subjected to acoustic excitation. *Journal of Composite Materials*, 1989, 23(6), 606-639.

[2. 14] - Kapania, R. K. and Raciti, S. Recent advances in analysis of laminated beams and plates, Part II: vibrations and wave propagation. *AIAA Journal*, 1989, 27(7), 935 - 946.

[2. 15] - Redfern, D. *The Maple Handbook*. New York: Springer-Verlag, 1994.

[2. 16] - Bardell, N. S. *Wave Propagation in Periodically Stiffned Plates and Shells*. Ph.D. Thesis. University of Southampton. UK, 1990.

[2. 17] - Bardell, N. S. Free vibration analysis of a flat plate using the hierarchical finite element method. *Journal of Sound and Vibration*, 1991, 151(2), 263-289.

[2. 18] - Han, W. and Petyt, M. Linear vibration analysis of laminated rectangular plates using the hierarchical finite element method - I: Free vibration analysis. *Computers and Structures*, 1992, 61 (4), 705-712.

[2. 19] - Han, W. and Petyt, M. Linear vibration analysis of laminated rectangular plates using the hierarchical finite element method - II: Forced vibration analysis. *Computers and Structures*, 1996, 61 (4), 713-724.

[2. 20] - Han, W. and Petyt, M. Geometrically nonlinear vibration analysis of thin, rectangular plates using the hierarchical finite element method - I: The fundamental mode of isotropic plates. *Computers and Structures,* 1997, 63 (2), 295-308.

[2. 21] - Han, W. and Petyt, M. Geometrically nonlinear vibration analysis of thin, rectangular plates using the hierarchical finite element method - II: 1st mode of laminated plates and higher modes of isotropic and laminated plates. *Computers and Structures*, 1997, 63 (2), 309-318.

[2. 22] - Houmat, A. An alternative Hierarchical finite element formulation applied to plate vibrations. *Journal of Sound and Vibration*, 1997, 206(2), 201-215.

[2. 23] - Bhat, R. B. Natural frequencies of rectangular plates using characteristic orthogonal polynomials in Rayleigh-Ritz method. *Journal of Sound and Vibration*, 1985, 102(4), 493-499.

[2. 24] - Leung, A. Y. T. and Chan, J. K. W. Fourier p-element for the analysis of beams and plates. *Journal of Sound and Vibration*, 1998, 212(1), 179-185.

[2. 25] - Conte, S. and de Boor, C. *Elementary Numerical Analysis. An Algorithmic Approach*. Third edition. Auckland: McGraw-Hill, 1987.

[2. 26] - Moon, F. C. *Chaotic Vibrations. An Introduction for Applied Scientists and Engineers*. New York: John Wiley and Sons, 1987.

[2. 27] - *MATLAB Reference Guide*. Natick, Mass.: The Math Works, 1992.

[2. 28] - Bennouna, M.M., White, R.G., The effects of large vibration amplitudes on the fundamental mode shape of a clamped-clamped uniform beam. *Journal of Sound and Vibration* , 1984, 96 (3), 309-331.

[2. 29] - Benamar, R., Bennouna, M.M.K. and White, R. G. The effects of large vibration amplitudes on the mode shapes and natural frequencies of thin elastic structures. Part III: fully clamped rectangular isotropic plates-measurements of the mode shape amplitude dependence and the spatial distribution of harmonic distortion. *Journal of Sound and Vibration*, 1994, 175(3), 377-395.

[2. 30] - Wolfe, H. *An Experimental Investigation of Nonlinear Behaviour of Beams and Plates Excited to High Levels of Dynamic Response*. Ph.D. Thesis, University of Southampton, UK, 1995.

[2. 31] - Farkas, M. *Periodic Motions*. New York: Springer-Verlag, 1994, p. 110 and 179.

[2. 32] - Nayfeh, A. H. *Introduction to Perturbation Techniques*. New York: John Willey, 1983.

[2. 33] - Nayfeh, A. H. and Mook. *Nonlinear Oscillations*. New York: John Wiley and Sons, 1995.

[2. 34] - Mickens, R.E. Comments on the method of harmonic balance. *Journal of Sound and Vibration*, 1984, 94(3), 456-460.

[2. 35] - Szemplinska-Stupnicka, W. *The Behaviour of Non-linear Vibrating Systems*. Dordretch: Kluwer Academic Publishers, 1990.

[2. 36] - Hamdan, M.N. and Burton, T.D. On the steady state response and stability of non-linear oscillators using harmonic balance. *Journal of Sound and Vibration*, 166(2), 255-266, 1993.

[2. 37] - Rosenberg, R. M. On non-linear vibrations of systems with many degrees of freedom. *Advances in Applied Mechanics*, 1966, 9, 155-242.

[2. 38] - Benamar, R., Bennouna, M.M., White, R.G. The effects of large vibration amplitudes on the mode shapes and natural frequencies of thin elastic structures. Part I: simply supported and clamped-clamped beams. *Journal of Sound and Vibration*, 1991, 149(2), 179-195.

[2. 39] - Benamar, R., Bennouna, M.M.K. and White, R. G. The effects of large vibration amplitudes on the mode shapes and natural frequencies of thin elastic structures. Part II: fully clamped rectangular isotropic plates. *Journal of Sound and Vibration*, 1993, 164(2), 295-316.

[2. 40] - Bennouna, M.M.K. *Nonlinear Dynamic Behaviour of a Clamped-clamped Beam with Consideration of Fatigue Life*. PhD Thesis, University of Southampton, UK, 1982.

[2. 41] - Wang, S. S., Huseyn, K. 1993. Bifurcations and stability properties of nonlinear systems with symbolic software. *Mathematical Comput. Modelling*, 1993, 18 (8), 21-38.

CHAPTER 3

[3. 1] - Mei, C. and Decha-Umphai, K. A finite element method for non-linear forced vibrations of beams. *Journal of Sound and Vibration*, 1985, 102(3), 369-380.

[3. 2] - Mei, C. and Decha-Umphai, K. A finite element method for non-linear forced vibrations of rectangular plates. *AIAA Journal*, 1985, 23(7), 1104-1110.

[3. 3] - Mei, C. and Prasad, C.B. Effects of large deflection and transverse shear on responses of symmetrical composite laminates subjected to acoustic excitation. *Journal of Composite Materials*, 1989, 23(6), 606-639.

[3. 4] - Chiang, C. K., Mei, C. and Gray, C. E. Finite element large-amplitude free and forced vibrations of rectangular thin composite plates. *Transactions of the ASME, Journal of Vibration and Acoustics*, 1991, 113, 309-315.

[3. 5] - Han, W. *The Analysis of Isotropic and Laminated Rectangular Plates Including Geometrical Non-linearity Using the p-version Finite Element Method*. Ph.D. Thesis, University of Southampton, 1993.

[3. 6] - Han, W. and Petyt, M. Geometrically nonlinear vibration analysis of thin, rectangular plates using the hierarchical finite element method - I: The fundamental mode of isotropic plates. *Computers and Structures*, 1997, 63 (2), 295-308.

[3. 7] - Han, W. and Petyt, M. Geometrically nonlinear vibration analysis of thin, rectangular plates using the hierarchical finite element method - II: 1st mode of laminated plates and higher modes of isotropic and laminated plates, *Computers and Structures*, 1997, 63 (2), 309-318.

[3. 8] - Rao, S.R., Sheikh, A. H. and Mukhopadhyay, M. Large-amplitude finite element flexural vibration of plates/stiffened plates, *Journal of the Acoustical Society of America*, 1993, 93(6), 3250-3257.

[3. 9] - Ren, B.S., Chen, D.Y. Non-linear vibration of a composite annular plate. In *Proceedings of the International Conference on Vibration Engineering*, Beijing, 1994. Beijing: International Academic Publishers, 1994, 353-358.

[3. 10] - Chia, C.Y. *Nonlinear Analysis of Plates*. New York: McGraw-Hill, 1980.

[3. 11] - Zienkiewicz, O.C. and Taylor, R.L. *The Finite Element Method*. 4th Edition. London: McGraw-Hill, 1988.

[3. 12] - Conte, S. and de Boor, C. *Elementary Numerical Analysis. An Algorithmic Approach*. Third edition. Auckland: McGraw-Hill, 1987.

[3. 13] - Riks, E. An incremental approach to the solution of snapping and buckling problems, *International Journal of Solids and Structures*, 1979, 15, 529-551.

[3. 14] - Crisfield, M. A. A fast incremental/iterative solution procedure that handles "snap-through", *Computers and Structures*, 1981, 13, 55-62.

[3. 15] - Lewandowski, R. Non-linear, steady-state analysis of multispan beams by the finite element method. *Computers and Structures*, 1991, 39(1,2), 83-93.

[3. 16] - Lewandowski, R. Non-linear steady-state vibration of structures by harmonic balance/finite element method. *Computers and Structures*, 1992, 44(1/2), 287-296.

[3. 17] - Lewandowski, R. Non-linear free vibrations of beams by the finite element and continuation methods. *Journal of Sound and Vibration*, 1994, 170(5), 577-593.

[3. 18] - Lewandowski, R. Computational formulation for periodic vibration of geometrically nonlinear structures - Part 1: Theoretical background. *International Journal of Solids and Structures*, 1997, 34(15), 1925-1947.

[3. 19] - Lewandowski, R. Computational formulation for periodic vibration of geometrically nonlinear structures - Part 2: Numerical strategy and examples. *Int. Journal of Solids and Structures*, 1997, 34(15), 1949-1964.

[3. 20] - Sundarajan, P. and Noah, S. T. Dynamics of forced nonlinear systems using shooting/arc-length continuation method-application to rotor systems. *Transactions of the ASME, Journal of Vibration and Acoustics*, 1997, 119, 9-20.

[3. 21] - Seydel, R. *From Equilibrium to Chaos. Pratical Bifurcation and Stability Analysis*. New York: Elsevier Science, 1988.

[3. 22] - Wagner, W., Wriggers, P. A simple method for the calculation of poscritical branches. *Engineering Computation*, 1988, 5, 103-109.

[3. 23] - Redfern, D. *The Maple Handbook*. New York: Springer-Verlag, 1994.

[3. 24] - Waszczyszyn, Z., Cichon, C. and Radwanska, M. *Stability of Structures by Finite Element Methods*. Amsterdam: Elsevier Science B.V, 1994.

CHAPTER 4

[4. 1] - Szemplinska-Stupnicka, W. *The Behaviour of Non-linear Vibrating Systems*. Dordretch: Kluwer Academic Publishers, 1990.

[4. 2] - Nayfeh, A. H. and Mook, D.T. *Nonlinear Oscillations*. New York: John Wiley and Sons, 1995.

[4. 3] - Hsu, C. S. On the parametric excitation of a dynamic system having multiple degrees of freedom. *Transactions of the ASME, Journal of Applied Mechanics*, 1963, 30, 367-372.

[4. 4] - Szemplinska-Stupnicka, W. The generalised harmonic balance method for determining the combination resonance in the parametric dynamic systems. *Journal of Sound and Vibration*, 1978, 58(3), 347-361.

[4. 5] - Wolfe, H. *An Experimental Investigation of Nonlinear Behaviour of Beams and Plates Excited to High Levels of Dynamic Response*. Ph.D. Thesis, University of Southampton, 1995.

[4. 6] - Bolotin, V. V. *The Dynamic Stability of Elastic Systems*. San Francisco: Holden Day, 1964.

[4. 7] - Takahashi, K. Instability of parametric systems with non-uniform damping. *Journal of Sound and Vibration*, 1982, 85(2), 257-262.

[4. 8] - Hayashi, C. *Nonlinear Oscillations in Physical Systems*. New York: McGraw-Hill, 1964.

[4. 9] - Takahashi, K. A method of stability analysis for non-linear vibration of beams. *Journal of Sound and Vibration*, 1979, 67(1), 43-54.

[4. 10] - Meirovitch, L. A new method of solution of the eigenvalue problem for gyroscopic systems. *AIAA Journal*, 1974, 12, 1337-1342.

[4. 11] - Seydel, R. *From Equilibrium to Chaos. Pratical Bifurcation and Stability Analysis*. New York: Elsevier Science, 1988.

[4. 12] - Lewandowski, R. Non-linear, steady-state analysis of multispan beams by the finite element method. *Computers and Structures*, 1991, 39, 83-93.

[4. 13] - Lewandowski, R. Computational formulation for periodic vibration of geometrically nonlinear structures - Part 1: Theoretical background. *International Journal of Solids and Structures*, 1997, 34, 1925-1947.

[4. 14] - Lewandowski, R. Computational formulation for periodic vibration of geometrically nonlinear structures - Part 2: Numerical strategy and examples. *International Journal of Solids and Structures*, 1997, 34, 1949-1964.

[4. 15] - Meirovitch, L. *Computational Methods in Structural Dynamics*. Rockville: Sijthoff and Noordhof, 1980.

CHAPTER 5

[5. 1] - Bennouna, M.M.K. *Nonlinear Dynamic Behaviour of a Clamped-clamped Beam with Consideration of Fatigue Life*. PhD Thesis, University of Southampton, 1982.

[5. 2] - Bennouna, M.M., White, R.G. The effects of large vibration amplitudes on the fundamental mode shape of a uniform clamped-clamped beam. *Journal of Sound and Vibration*, 1984, 96(3), 309-331.

[5. 3] - Harris, C. M. *Shock and Vibration Handbook*, Third edition. New York: Mc Graw-Hill, 1988.

[5. 4] - Benamar, R., Bennouna, M.M., White, R.G. The effects of large vibration amplitudes on the mode shapes and natural frequencies of thin elastic structures. Part I: simply supported and clamped-clamped beams. *Journal of Sound and Vibration*, 1991, 149(2), 179-195.

[5. 5] - Wolfe, H. *An Experimental Investigation of Nonlinear Behaviour of Beams and Plates Excited to High Levels of Dynamic Response*, Ph.D. Thesis, University of Southampton, 1995.

[5. 6] - Atluri, S. Nonlinear vibrations of a hinged beam including nonlinear effects. *Transactions of the ASME, Journal of Applied Mechanics*, 1973, 40, 121-126.

[5. 7] - Mei, C. and Decha-Umphai, K. A finite element method for non-linear forced vibrations of beams. *Journal of Sound and Vibration*, 1985, 102, 369-380.

CHAPTER 6

[6. 1] - Szemplinska-Stupnicka, W. *The Behaviour of Non-linear Vibrating Systems*. Dordretch: Kluwer Academic Publishers, 1990.

[6. 2] - Nayfeh, A. H. and Mook, D. T. *Nonlinear Oscillations*. New York: John Wiley and Sons, 1995.

[6. 3] - Nayfeh, A. H. and Balachandran, B. Modal interactions in dynamical and structural systems. *Applied Mechanics Review*, 1989, 42(11 - Part 2): S175 - S201.

[6. 4] - Bennouna, M.M. and White, R.G. The effects of large vibration amplitudes on the fundamental mode shape of a clamped-clamped uniform beam. *Journal of Sound and Vibration*, 1984, 96(3), 309-331.

[6. 5] - Benamar, R., Bennouna, M.M.K. and White, R. G. The effects of large vibration amplitudes on the mode shapes and natural frequencies of thin elastic structures. Part III: fully clamped rectangular isotropic plates-measurements of the mode shape amplitude dependence and the spatial distribution of harmonic distortion. *Journal of Sound and Vibration*, 1994, 175(3), 377-395.

[6. 6] - Leung, A.Y.T. and Fung, T.C. Non-linear steady state vibration of frames by finite element method. *International Journal for Numerical Methods in Engineering*, 1989, 28, 1599-1618.

[6. 7] - Lewandowski, R. Non-linear free vibrations of beams by the finite element and continuation methods. *Journal of Sound and Vibration*, 1994, 170(5), 577-593.

[6. 8] - Lewandowski, R. Computational formulation for periodic vibration of geometrically nonlinear structures - Part 1: Theoretical background. *International Journal Solids Structures*, 1997, 34(15), 1925-1947.

[6. 9] - Lewandowski, R. Computational formulation for periodic vibration of geometrically nonlinear structures - Part 2: Numerical strategy and examples. *International Journal Solids Structures*, 1997, 34(15), 1949-1964.

[6. 10] - Lewandowski, R. Solutions with bifurcation points for free vibration of beams: an analytical approach. *Journal of Sound and Vibration*, 1994, 177(2), 239-249.

[6. 11] - Lewandowski, R. On beams membranes and plates vibration backbone curves in cases of internal resonance. *Meccanica*, 1996, 31, 323-346.

[6. 12] - Lau, S. L., Cheung, Y. K. and Wu, S. Y. Nonlinear vibration of thin elastic plates. Part 2: Internal resonance by amplitude-incremental finite element. *Transactions of the ASME, Journal Applied Mechanics*, 1984, 51, 845-851.

[6. 13] - Abe, B., Kobayashi, Y. and Yamada, G. Two-mode response of simply supported, rectangular laminated plates. *International Journal of Non-Linear Mechanics*, 1998, 33, 675-690.

[6. 14] - Harris, C. M. *Shock and Vibration Handbook*, Third edition. New York: McGraw-Hill, 1988.

[6. 15] - Sarma, B. S. and Varadan, T.K. Ritz finite element approach to non-linear vibrations of beams. *International Journal for Numerical Methods in Engineering*, 1984, 20, 353-367.

[6. 16] - Cheung, Y.K. and Lau, S.L. Incremental time-space finite strip method for non-linear structural vibrations. *Earthquake Engineering and Structural Dynamics*, 1982, 10, 239-253.

[6. 17] - Woinowski-Krieger, S. The effect of an axial force on the vibration of hinged bars. *Journal of Applied Mechanics*, 1950, 17, 35-36.

[6. 18] - Benamar, R. *Nonlinear Dynamic Behaviour of Fully Clamped Beams and Rectangular Isotropic and Laminated Plates*. Ph.D. Thesis. University of Southampton. UK, 1990.

[6. 19] - Benamar, R., Bennouna, M.M., White, R.G. The effects of large vibration amplitudes on the mode shapes and natural frequencies of thin elastic structures. Part I: simply supported and clamped-clamped beams. *Journal of Sound and Vibration*, 1991, 149(2), 179-195.

[6. 20] - Qaisi, M. I. Application of the harmonic balance principle to the nonlinear free vibration of beams. *Applied Acoustics*, 1993, 40, 141-151.

CHAPTER 7

[7. 1] - Benamar, R., Bennouna, M.M.K. and White, R. G. The effects of large vibration amplitudes on the mode shapes and natural frequencies of thin elastic structures. Part III: fully clamped rectangular isotropic plates-measurements of the mode shape amplitude dependence and the spatial distribution of harmonic distortion. *Journal of Sound and Vibration*, 1994, 175(3), 377-395.

[7. 2] - Benamar, R. *Nonlinear Dynamic Behaviour of Fully Clamped Beams and Rectangular Isotropic and Laminated Plates.* Ph.D. Thesis. University of Southampton. UK, 1990.

[7. 3] - Han, W. and Petyt, M. Geometrically nonlinear vibration analysis of thin, rectangular plates using the hierarchical finite element method - I: The fundamental mode of isotropic plates. *Computers and Structures*, 1997, 63 (2), 295-308.

[7. 4] - Rao, S., Sheikh, A. and Mukhopadhyay, M. Large-amplitude finite element flexural vibration of plates/stiffened plates. *Journal of the Acoustical Society of America*, 1993, 93(6), 3250-3257.

[7. 5] - Mei, C. and Decha-Umphai, K. A finite element method for non-linear forced vibrations of rectangular plates. *AIAA Journal*, 1985, 23(7), 1104-1110.

[7. 6] - Mei, C. and Prasad, C.B. Effects of large deflection and transverse shear on responses of symmetrical composite laminates subjected to acoustic excitation. *Journal of Composite Materials*, 1989, 23(6), 606-639.

[7. 7] - Lau, S. L., Cheung, Y. K. and Wu, S. Y., Nonlinear vibration of thin elastic plates. Part 1: Generalised incremental Hamilton's principle and element formulation. *Transactions of the ASME, Journal of Applied Mechanics*, 1984, 51, 837-844.

[7. 8] - Han, W. and Petyt, M. Geometrically nonlinear vibration analysis of thin, rectangular plates using the hierarchical finite element method - II: 1st mode of laminated plates and higher modes of isotropic and laminated plates. *Computers and Structures*, 1997, 63 (2), 309-318.

[7. 9] - Chiang, C. K., Mei, C. and Gray, C. E. Finite element large-amplitude free and forced vibrations of rectangular thin composite plates. *Transactions of the ASME, Journal of Vibration and Acoustics*, 1991, 113, 309-315.

[7. 10] - Han, W. *The Analysis of Isotropic and Laminated Rectangular Plates Including Geometrical Non-linearity Using the p-version Finite Element Method.* Ph.D. Thesis. University of Southampton. UK.1993.

[7. 11] - Chia, C.Y. Geometrically nonlinear behavior of composite plates: a review. *Applied Mechanics Review*, 1988, 41(12), 439-451.

CHAPTER 8

[8. 1] - Benamar, R. *Nonlinear Dynamic Behaviour of Fully Clamped Beams and Rectangular Isotropic and Laminated Plates*. Ph.D. Thesis. University of Southampton. UK, 1990.

[8. 2] - ESDU Data Items, *Natural Frequencies of Rectangular, Specially Orthotropic Laminated Plates*, item No 83036 with Amendments A and B, December 1992, ESDU International plc.

[8. 3] - Chia, C.Y. *Nonlinear Analysis of Plates*. New York: McGraw-Hill, 1980.

[8. 4] - Chow, S.T., Liew, k.M. and Lam, K.Y., Transverse Vibration of Symmetrically Laminated Rectangular Composite Plates, *Composite Structures*, 1992, 20, 213-226.

CHAPTER 10

[10. 1] - Popovic, P., Nayfeh, A. H., Oh, K. and Nayfeh, S. A. An experimental investigation of energy transfer from a high-frequency mode to a low-frequency mode in a flexible structure. *Journal of Vibration and Control*, 1995, 1, 115-128.

[10. 2] - Tabaddor, M. and Nayfeh, A. H. An experimental investigation of multimode responses in a cantilever beam. *Journal of Vibration and Acoustics, Transactions of the ASME*, 1997, 119, 532-538.

[10. 3] - Oh, K. and Nayfeh, A.H. High- to low-frequency modal interactions in a cantilever composite plate. *Journal of Vibration and Acoustics, Transactions of the ASME*, 1998, 120, 579-587.

[10. 4] - Bennouna, M.M. and White, R.G. The effects of large vibration amplitudes on the fundamental mode shape of a clamped-clamped uniform beam. *Journal of Sound and Vibration*, 1984, 96(3), 309-331.

[10. 5] - Benamar, R., Bennouna, M.M.K. and White, R. G. The effects of large vibration amplitudes on the mode shapes and natural frequencies of thin elastic structures. Part III: fully clamped rectangular isotropic plates-measurements of the mode shape amplitude dependence and the spatial distribution of harmonic distortion. *Journal of Sound and Vibration*, 1994, 175(3), 377-395.

[10. 6] - Hassan, A. & Burton, T. D. Extraneous solutions predicted by the harmonic balance method. *Journal of Sound and Vibration*, 1995, 182(4), 523-539.

[10. 7] - Wolfe, H. *An Experimental Investigation of Nonlinear Behaviour of Beams and Plates Excited to High Levels of Dynamic Response*. Ph.D. Thesis, University of Southampton, 1995.

[10. 8] - Sundarajan, P. and Noah, S. T. Dynamics of forced nonlinear systems using shooting/arc-length continuation method-application to rotor systems. *Transactions of the ASME, Journal of Vibration and Acoustics*, 1997, 119, 9-20.

[10. 9] - Padmanabhan, C. and Singh, R. Analysis of periodically excited non-linear systems by a parametric continuation technique. *Journal of Sound and Vibration*, 1995, 184(1), 35-58.

[10. 10] - Seydel, R. *From Equilibrium to Chaos. Pratical Bifurcation and Stability Analysis.* New York: Elsevier Science, 1988.

[10. 11] - Locke, J.E. Finite element non-linear random response of beams. *Journal of Sound and Vibration*, 1994, 178(2), 201-210

[10. 12] - Caughey, T. K. Equivalent linearization techniques. *Journal of Acoustical Society of America*, 1963, 35, 1706-1711.

[10. 13] - Mei, C. and Prasad, C.B. Effects of large deflection and transverse shear on responses of symmetrical composite laminates subjected to acoustic excitation. *Journal of Composite Materials*, 1989, 23(6), 606-639.

[10. 14] - Hwang, C. and Pi, W. S. Nonlinear acoustic response analysis of plates using the finite element method. *AIAA Journal*, 1972, 10, 276-281.

Table 5.1 - Geometric properties of beams analysed.

Beam	h (mm)	b (mm)	L (mm)	Ω (m^2)	$I = (1/12)bh^3$ (m^4)	$r = \sqrt{I/\Omega}$
1	2	20	580	4×10^{-5}	$1.333(3)\ \times10^{-11}$	5.7735×10^{-4}
2	2	20	406	4×10^{-5}	$1.333(3)\ \times10^{-11}$	5.7735×10^{-4}

Table 5.2 - Material properties of beams analysed.

Beam	Material	E (N/m^2)	ρ (Kg/m^3)	ν
1	Aluminium DTDSO 70	7×10^{10}	2778	0.34
2	Aluminium 7075-T6	7.172×10^{10}	2800	0.33

Table 5.3 - Linear natural frequencies of Beam 1 *cc* (rad/s).

Mode	1	2	3	4
Exact [5.3] *	192.8	531.3	1041.6	1722
HFEM	192.8	531.3	1041.6	1722

* the data in ref. [5.3] is provided with four significant digits

Table 5.4 - Convergence of non-dimensional ($\omega/\omega_{\ell 1}$) first natural frequency values with number of shape functions.

w_m/h	1.75	2
$p_o = p_i = 5$	1.61170	1.75300
$p_o = p_i = 7$	1.61169	1.75301

Table 5.5 - Nondimensional first nonlinear frequencies of Beam 1 *cc* ($\omega/\omega_{\ell 1}$).

w_m/h	0.5	1.0	1.5	2.0	2.25
LUM 1	1.06505	1.23773	1.47701	1.75299	1.89925
LUM 2	1.06506	1.23773	1.47701	1.75299	1.89923
LUM 3	1.06506	1.23773	1.47714	1.75308	1.89908
LUM 4	1.06505	1.23772	1.47711	1.75299	1.89943
w_m/h	2.50	2.75	3.00	3.25	3.5
LUM 1	(2.06063)*	-	-	-	-
LUM 2	2.04930	2.20211	2.35716	2.51395	*
LUM 3	(2.04329)*	-	-	-	-
LUM 4	2.04809	2.20211	2.35696	2.51369	*

* - convergence not achieved in less then 300 iterations.

( ) - indicates the value correspondent to the 300th iteration

LUM 1 - method without linear combination, starting from linear solution.

LUM 2- method with linear combination, starting from linear solution.

LUM 3- method without linear combination, starting from nonlinear solution.

LUM 4 - method with linear combination and starting from nonlinear solution.

Table 5.6 - HFEM (LUM) and experimental nonlinear frequencies (rad/s).

Max. Deflection at midpoint/beam thickness	≈0 (linear)	0.33	0.61	1.16	1.53	1.66	1.83
ω_e [5.1]	177.8	187.9	201.1	271.4	302.5	321.4	345.6
ω_{HFEM}	192.8	198.3	211.2	252.3	287.7	301.1	319.2
$(\omega_{HFEM} - \omega_e)/\omega_e \times 100$	+8.44	+5.53	+5.02	-7.04	-4.89	-6.32	-7.64

Table 5.7 - Nonlinear resonance frequencies of Beam 1 *cc*.

w_m/h	≈ 0	0.5	1.0	1.25	1.5	1.75
$\omega_1/\omega_{\ell 1}$	1	1.06505	1.23772	1.35133	1.47711	1.61169
$\omega_2/\omega_{\ell 2}$	2.75654	3.29558	4.36057	4.97419	5.60927	6.26078
$\omega_3/\omega_{\ell 3}$	5.40392	6.35857	8.44891	9.68956	11.0010	-
w_m/h	2.0	2.50	3.00	3.25	3.3125	3.625
$\omega_1/\omega_{\ell 1}$	1.752993	2.048089	2.356959	2.513686	2.548723	-
$\omega_2/\omega_{\ell 2}$	6.92491	8.27701	9.64886	10.3399	10.5130	11.3816

Table 5.8 - Convergence of fundamental linear frequency of Beam 2 *cc* (rad/s) with p_o. Only symmetric shape functions used.

Exact [5.3]	$p_o=2$	$p_o=3$	$p_o=4$	$p_o=5$	$p_o=9$
396.6	396.613 239	396. 605 011	396. 605 008	396. 605 008	396. 605 008

Table 5.9 - Natural linear frequencies of Beam 2 *cc* (rad/s): p_o=10 (both symmetric and anti-symmetric) and p_o=9 *(only symmetric).

Mode	1	2	3	4
ω	396. 6050	1093. 257	2143. 221	3542. 857
Mode	5	6	7	9
ω	5295. 504 *5292. 411	7405. 836	10382. 49 *9841. 260	*15790. 94

Table 6.1 - Nonlinear resonance frequencies calculated using the LUM; Beam 1 *cc*.

w_m/h	≈ 0	0.5	1.0	1.25	1.5	1.75
$(\omega_1/\omega_{\ell 1})$ - 1 harmonic	1	1.06505	1.23772	1.35133	1.47711	1.61169
$(\omega_1/\omega_{\ell 1})$ - 2 harmonics	1	1.06483	1.23602	1.34885	1.47473	1.61153
relative error*		+2.06E-4	+1.36E-3	+1.84E-3	+1.61E-3	+9.56E-5
$(\omega_2/\omega_{\ell 2})$ - 1 harmonic	2.75654	3.29558	4.36057	4.97419	5.60927	6.26078
$(\omega_2/\omega_{\ell 2})$ - 2 harmonics	2.75654	3.31671	4.36196	4.95557	5.57698	6.21992
relative error		-6.37E-3	-3.20E-4	+3.76E-3	+5.79E-3	+6.57E-3
$(\omega_3/\omega_{\ell 3})$ - 1 harmonic	5.40392	6.35857	8.44891	9.68956	11.0010	-
$(\omega_3/\omega_{\ell 3})$ - 2 harmonics	5.40392	6.33843	8.32205	-	-	-
relative error*		+3.17E-3	+1.52E-2	-	-	-

* the values obtained with two harmonics were taken as reference.

Table 6.2 - Nonlinear fundamental frequencies of Beam 1 *cc*.

w_m/h	$.18\times10^{-5}$	.500	.998	1.491	1.978	2.498	3.014
$\omega/\omega_{\ell 1}$	1.00000	1.06485	1.23509	1.46991	1.74530	2.09573	2.59260
w_m/h	3.508	4.008	4.508	5.007	5.507	6.007	-
$\omega/\omega_{\ell 1}$	3.21820	3.8709	4.50414	5.11761	5.71659	6.30542	-

Table 6.3 - Natural frequencies ($\omega/\omega_{\ell 1}$) obtained with one harmonic (iterative procedure) and with two and three harmonics (continuation method). Beam 1 *cc*.

w_m/h *	0.5	1.0	1.5	2.0	2.25
One harmonic	1.0651	1.2377	1.4771	1.7530	1.8994
Two harmonics	1.0649	1.2351	1.4699	1.7453	1.9280
Three harmonics	1.0648	1.2370	1.4754	1.7631	1.9227
w_m/h *	2.50	2.75	3.00	3.25	-
One harmonic	2.0481	2.2021	2.3570	2.5137	-
Two harmonics	2.0957	2.2919	2.5926	2.8946	
Three harmonics	2.1052	2.3204	2.6122	2.9791	

* For two and three harmonics the value of w_m/h is approximated (error<0.6% and <0.16%, respectively)

Table 6.4 - Fundamental linear frequency parameter $\lambda = \omega_\ell^2 mL^4/EI$. Beam 1 *ss*.

Exact [6.14]	FEM [6.15] (eight elements - 32 DOF)	FEM [6.7] (six elements - 12 DOF)	HFEM (1 element - 4 DOF*)
97.409	97.409	97.419	97.409

* 6 DOF, if symmetries are not used to reduce the number of DOF.

m - mass per unit length

Table 6.5 - Natural linear frequencies (rad/s) of Beam 1 *ss*. 12 DOF.

Mode	1	2	3	4	5	6
Exact [6.4]	85.03	340.1	765.2	1360	2126	3061
HFEM	85.03	340.1	765.3	1360	2126	3062

Table 6.6 - Comparison of $\omega/\omega_{\ell 1}$ of Beam 1 *ss*. Two harmonics.

w_m/r	$\omega/\omega_{\ell 1}$ Exact [6.17]	$\omega/\omega_{\ell 1}$ [6.16] 48 DOF	w_m/r	$\omega/\omega_{\ell 1}$ [6.7] 24 DOF	w_m/r	$\omega/\omega_{\ell 1}$ HFEM 14 DOF (10 DOF*)	w_m/r	$\omega/\omega_{\ell 1}$ HFEM 16 DOF (10 DOF*)
1.0	1.0892	1.0892	1.0087	1.0906	0.9995	1.0891	1.0014	1.0894
2.0	1.3177	1.3178	1.9738	1.3106	2.0021	1.3185	2.0001	1.3180
3.0	1.6256	1.6255	2.9808	1.6198	3.0012	1.6268	3.0033	1.6275

* If symmetries are used to reduce the number of degrees of freedom of HFEM model

Table 7.1 - Geometric properties of isotropic plates.

Plate	a (mm)	b (mm)	h (mm)
1	486	322.9	1.2
2	500	500	2.0833
3	300	320	1

Table 7.2 - Material properties of isotropic plates.

Plate	Material	E (N/m^2)	ρ (Kg/m^3)	ν
1 and 2	Steel	21.0×10^{10}	7800	0.3
3	Aluminium DTDSO 70	7×10^{10}	2778	0.34

Table 7.3 - Convergence of linear natural frequencies of Plate 1 with p_o. Doubly-symmetric modes.

p_o	2	3	4	5
$\omega_{\ell 1}$ (rad/s)	487.343	487.283	487.276	487.276
$\omega_{\ell 2}$ (rad/s)	1233.04	1197.30	1195.92	1195.91
$\omega_{\ell 3}$ (rad/s)	2378.31	2267.64	2263.73	2263.69

Table 7.4 - Convergence of frequency ratios $\omega/\omega_{\ell 1}$ of the fundamental mode with p_o. Plate 1. p_i=6.

p_o=2		p_o=3		p_o=4		p_o=5	
$\frac{w_m}{h}$	$\omega/\omega_{\ell 1}$	$\frac{w_m}{h}$	$\omega/\omega_{\ell 1}$	$\frac{w_m}{h}$	$\omega/\omega_{\ell 1}$	$\frac{w_m}{h}$	$\omega/\omega_{\ell 1}$
0.20112	1.0075	0.19308	1.0069	0.25820	1.0123	0.19935	1.0073
0.39781	1.0290	0.40502	1.0299	0.41981	1.0321	0.39991	1.0291
0.59444	1.0637	0.59830	1.0644	0.60211	1.0653	0.59950	1.0644
0.79931	1.1129	0.79760	1.1124	0.79957	1.1131	0.79906	1.1121
1.0004	1.1730	1.0003	1.1729	1.0265	1.1817	1.0000	1.1711

Table 7.5 - Convergence of the frequency ratios $\omega/\omega_{\ell 1}$ of the second mode with p_o. Plate 1. p_i=6.

p_o=2		p_o=3		p_o=4		p_o=5	
$\frac{w_m}{h}$	$\omega/\omega_{\ell 1}$	$\frac{w_m}{h}$	$\omega/\omega_{\ell 1}$	$\frac{w_m}{h}$	$\omega/\omega_{\ell 1}$	$\frac{w_m}{h}$	$\omega/\omega_{\ell 1}$
0.22911	2.6121	0.22982	2.5369	0.22991	2.5324	0.23046	2.5325

Table 7.6 - Convergence of the frequency ratios $\omega/\omega_{\ell l}$ of the third mode with p_o. Plate 1. p_i=6.

$p_o=2$		$p_o=3$		$p_o=4$		$p_o=5$	
$\frac{w_m}{h}$	$\omega/\omega_{\ell l}$	$\frac{w_m}{h}$	$\omega/\omega_{\ell l}$	$\frac{w_m}{h}$	$\omega/\omega_{\ell l}$	$\frac{w_m}{h}$	$\omega/\omega_{\ell l}$
0.25094	5.1332	0.25010	4.8929	0.24903	4.8770	0.24971	4.8761

Table 7.7 - Convergence of frequency ratios $\omega/\omega_{\ell l}$ of the fundamental mode with p_i. Plate 1. p_o=3.

$p_i=0$		$p_i=2$		$p_i=3$		$p_i=4$	
$\frac{w_m}{h}$	$\omega/\omega_{\ell l}$	$\frac{w_m}{h}$	$\omega/\omega_{\ell l}$	$\frac{w_m}{h}$	$\omega/\omega_{\ell l}$	$\frac{w_m}{h}$	$\omega/\omega_{\ell l}$
0.19725	1.0105	0.20767	1.0116	0.20553	1.0107	0.20124	1.0080
0.41032	1.0443	0.39996	1.0421	0.39880	1.0398	0.39927	1.0309
0.59209	1.0899	0.60250	1.0928	0.59809	1.0872	0.59901	1.0682
0.79722	1.1566	0.79983	1.1574	0.80076	1.1509	0.80063	1.1188
1.0025	1.2363	0.99991	1.2353	1.0002	1.2261	0.99971	1.1799

$p_i=5$		$p_i=6$	
$\frac{w_m}{h}$	$\omega/\omega_{\ell l}$	$\frac{w_m}{h}$	$\omega/\omega_{\ell l}$
0.20369	1.0081	0.19308	1.0069
0.40135	1.0309	0.40502	1.0299
0.59977	1.0679	0.59830	1.0644
0.79990	1.1179	0.79760	1.1124
1.0003	1.1792	1.0003	1.1729

Table 7.8 - Convergence of frequency ratios ω/ω_l of the second mode with p_i. Plate 1. p_o=3.

HFEM $p_i=0$		HFEM $p_i=2$		HFEM $p_i=3$		HFEM $p_i=4$		HFEM $p_i=5$	
$\frac{w_m}{h}$	$\omega/\omega_{\ell l}$	$\frac{w_m}{h}$	$\omega/\omega_{\ell l}$	$\frac{w_m}{h}$	$\omega/\omega_{\ell l}$	$\frac{w_m}{h}$	$\omega/\omega_{\ell l}$	$\frac{w_m}{h}$	$\omega/\omega_{\ell l}$
0.25000	2.5553	0.24996	2.5523	0.25004	2.5523	0.24993	2.5517	0.24990	2.5515

Table 7.9 - Convergence of the frequency ratios $\omega/\omega_{\ell l}$ of the third mode with p_i. Plate 1. p_o=3.

p_i=0		p_i=2		p_i=3		p_i=4	
$\frac{w_m}{h}$	$\omega/\omega_{\ell l}$	$\frac{w_m}{h}$	$\omega/\omega_{\ell l}$	$\frac{w_m}{h}$	$\omega/\omega_{\ell l}$	$\frac{w_m}{h}$	$\omega/\omega_{\ell l}$
0.25011	4.9037	0.25001	4.8941	0.24993	4.8934	0.25007	4.8936

p_i=5		p_i=6	
$\frac{w_m}{h}$	$\omega/\omega_{\ell l}$	$\frac{w_m}{h}$	$\omega/\omega_{\ell l}$
0.24994	4.8932	0.25010	4.8929

Table 7.10 - Comparison of frequency ratios $\omega/\omega_{\ell l}$ of immovable fully clamped square isotropic plates.

$\frac{w_m}{h}$	Ref [7.4] 133 DOF	Ref. [7.3] 49 DOF	HFEM 9 DOF (p_o=3, p_i=6)		HFEM 16 DOF (p_o=4, p_i=7)	
			$\frac{w_m}{h}$	$\omega/\omega_{\ell l}$	$\frac{w_m}{h}$	$\omega/\omega_{\ell l}$
0.2	1.0095	1.0068	0.2099	1.0079	0.21377	1.0082
0.6	1.0825	1.0600	0.6007	1.0632	0.60780	1.0647
1	1.2149	1.1599	1.0011	1.1670	1.0012	1.1668

Table 7.11 - Frequency ratio ω/ω_l of immovable fully clamped isotropic square plates under uniform harmonic distributed force $P_0=0.2^*$ (P_d=873.82 N/m^2).

$\frac{w_m}{h}$	Elliptic function solution*	Perturbation solution*	Finite element* 54 DOF	HFEM 9 DOF (p_o=3 p_i=6)		HFEM 16 DOF (p_o=4 p_i=7)	
				$\frac{w_m}{h}$	$\omega/\omega_{\ell l}$	$\frac{w_m}{h}$	$\omega/\omega_{\ell l}$
±0.2	0.1944	0.1987	0.1643	+.2001	0.2442	+0.2000	0.2432
	1.4281	1.4281	1.4238	-.2005	1.4399	-0.2072	1.4275
±0.6	0.8951	0.8956	0.8905	+.5992	0.8962	+0.6008	0.8971
	1.2117	1.2119	1.2083	-.5997	1.2114	-0.59011	1.2120
±1	1.0822	1.0845	1.0700	+1.000	1.0800	1.0013	1.0803
	1.2540	1.255	1.2429	-1.001	1.2491	-0.9952	1.2475

* From reference [7.5]: $P_0 = cF_0/\rho h^2\omega_1^2$ $c=\iint\phi dxdy/\iint\phi^2 dxdy$, ϕ - normalised mode shape. F_0 - amplitude of external applied force (N/m^2).

Table 7.12 - Geometric properties of laminated plates.

Plate	Number of layers	Orientation of principal axes	a (mm)	b (mm)	h (mm)
4	3	(45, -45, 45)	500	500	5
5	8	$(90, -45, 45\ 0)_{sym.}$	480	320	1
6	16	$(45, -45, 0, -45, 45, -45, 0, 45)_{sym}$	300	150	2.72
7	5	(θ, -θ, θ, -θ, θ)	300	300	1

Table 7.13 - Material properties of laminated plates (graphite/epoxy).

Plate	E_L (GNm^{-2})	E_G (GNm^{-2})	G_{LT} (GNm^{-2})	ν_{LT}	ρ (Kgm^{-3})
4	206.84	5.171	2.5855	0.25	2564.856
5	120.5	9.63	3.58	0.32	1540
6	173.0	7.2	3.76	0.29	1540
7	173.0	E_L / 15.4	0.79 E_G	0.3	1540

Table 7.14 - Convergence of linear natural frequencies of Plate 4 with number of out-of-plane shape functions.

p_o	3 9 DOF	4 16 DOF	5 25 DOF	6 36 DOF	ref [7.9] 36 elem. 24 DOF* each
ω_1 (rad/s)	1587.01	1580.36	1576.72	1574.96	1592.30
ω_2 (rad/s)	2688.01	2580.91	2578.71	2577.55	—
ω_3 (rad/s)	4041.70	3759.85	3690.61	3671.02	—

*Only 16 are necessary in linear analysis (conforming element)

Table 7.15 - Free vibration. Plate 4. $\xi=\eta=0$.

HFEM and LUM method [7.8]		HFEM and Continuation Met.	
	$p_o=p_i=5$		$p_o=p_i=5$
$\frac{w_m}{h}$	$\omega/\omega_{\ell l}$	$\frac{w_m}{h}$	$\omega/\omega_{\ell l}$
1	1.2268	0.99897	1.2259

Table 7.16 - Forced vibration. Plate 4. P_0=0.1* (P_d = 3454.6650 N/m^2). $\xi=\eta=0$. Number of DOF of HFEM = p_o^2.

p_o=4 p_i=6		p_o=4 p_i=7		p_o=5 p_i=5		p_o=6 p_i=5		[7.9] 67 DOF	
$\frac{w_m}{h}$	$\omega/\omega_{\ell 1}$	$\frac{w_m}{h}$	$\omega/\omega_{\ell 1}$	$\frac{w_m}{h}$	$\omega/\omega_{\ell 1}$	$\frac{w_m}{h}$	$\omega/\omega_{\ell 1}$	$\frac{w_m}{h}$	$\omega/\omega_{\ell 1}$
0.20163	0.73401	0.20184	0.73401	0.20117	0.73570	0.19861	0.73162	±0.2	0.7219
-0.19709	1.24655	-0.20000	1.24321	-0.19981	1.24520	-0.20026	1.24448		1.2333
0.39441	0.91119	0.39631	0.91119	0.40336	0.91963	0.40141	0.91887	±0.4	0.9129
-0.39993	1.15836	-0.40036	1.15726	-0.39407	1.16099	-0.39538	1.16083		1.1548
0.59965	1.00845	0.60001	1.00687	0.60199	1.01498	0.59513	1.01253	±0.6	1.0085
- 0.60001	1.16395	-0.59972	1.16225	-0.60311	1.16824	-0.59528	1.16749		1.1621
0.800173	1.091817	0.799681	1.08950	0.79874	1.09893	0.80049	1.10059	±0.8	1.0929
-0.79988	1.201822	-0.80035	1.19995	-0.80208	1.20842	-0.80315	1.20950		1.2018
1.00053	1.17560	0.99984	1.17312	1.00172	1.18607	0.99623	1.18492	±1	1.1787
-0.99987	1.25782	-0.99993	1.25580	-0.99818	1.26571	-1.00263	1.26840		1.2607

* From reference [7.9]. $P_0 = cF_0/\rho h^2\omega_1^2$ $c=\iint\phi dxdy/\iint\phi^2 dxdy$, ϕ - normalised mode shape. F_0 - amplitude of external applied force (N/m^2).

Table 7.17 - Convergence of the HFEM linear natural frequencies. Plate 5.

p_o	3	4	5	6	7
$\omega_{\ell 1}$ (rad/s)	511.577	511.440	511.405	511.390	511.387
$\omega_{\ell 2}$ (rad/s)	646.264	645.576	645.365	645.296	645.281
$\omega_{\ell 3}$ (rad/s)	907.776	903.155	886.902	886.855	886.217

Table 7.18 - Convergence of frequency ratios $\omega/\omega_{\ell 1}$ of the fundamental mode with p_o. Plate 5. $\xi=\eta=0$.

p_o=3 p_i=5		p_o=4 p_i=5		p_o=5 p_i=5		p_o=6 p_i=6	
$\frac{w_m}{h}$	$\omega/\omega_{\ell 1}$	$\frac{w_m}{h}$	$\omega/\omega_{\ell 1}$	$\frac{w_m}{h}$	$\omega/\omega_{\ell 1}$	$\frac{w_m}{h}$	$\omega/\omega_{\ell 1}$
0.20064	1.0060	0.20930	1.0064	0.19964	1.0059	0.21421	1.0063
0.39990	1.0234	0.39586	1.0229	0.39951	1.0232	0.39765	1.0217
0.59977	1.0519	0.60113	1.0521	0.60012	1.0518	0.60266	1.0495
0.80010	1.0907	0.80035	1.0908	0.79988	1.0904	0.80520	1.0872
1.0000	1.1389	0.99978	1.1389	0.99988	1.1382	0.99661	1.1315
1.2495	1.2106	1.2494	1.2108	1.2499	1.2092	1.2501	1.2018
1.4993	1.2935	1.4992	1.2938	1.5001	1.2904	1.5040	1.2835

Table 7.19 - Convergence of frequency ratios $\omega/\omega_{\ell l}$ of the second mode with p_o. Plate 5. ξ= 0.4, η=0.

p_o=3 p_i=5		p_o=4 p_i=5		p_o=5 p_i=5		p_o=6 p_i=6	
$\frac{w_m}{h}$	$\omega/\omega_{\ell l}$	$\frac{w_m}{h}$	$\omega/\omega_{\ell l}$	$\frac{w_m}{h}$	$\omega/\omega_{\ell l}$	$\frac{w_m}{h}$	$\omega/\omega_{\ell l}$
0.19938	1.2827	0.20010	1.2824	0.20021	1.2820	0.20189	1.2786
0.40007	1.3397	0.40001	1.3399	0.40309	1.3406	0.40413	1.3271
0.59996	1.4297	0.59993	1.4299	0.60258	1.4308	0.59489	1.3978
0.80000	1.5465	0.80021	1.5466	0.79913	1.5457	0.79984	1.4964
1.0001	1.6850	0.99569	1.6814	0.99883	1.6840	0.99869	1.6104
1.2496	1.8812	1.2476	1.8793	1.2500	1.8825	1.2498	1.7752
1.4999	2.0977	1.4999	2.0988	1.4999	2.1006	1.4985	1.9564

Table 7.20 - Convergence of frequency ratios $\omega/\omega_{\ell l}$ of the third mode with p_o. Plate 5. ξ = 0, η = 0.

p_o=3 p_i=5		p_o=4 p_i=5		p_o=5 p_i=5		p_o=6 p_i=6	
$\frac{w_m}{h}$	$\omega/\omega_{\ell l}$	$\frac{w_m}{h}$	$\omega/\omega_{\ell l}$	$\frac{w_m}{h}$	$\omega/\omega_{\ell l}$	$\frac{w_m}{h}$	$\omega/\omega_{\ell l}$
0.19989	1.8391	0.20072	1.8313	0.19989	1.7971	0.20158	1.7978
0.39903	2.0180	0.39917	2.0046	0.40062	1.9686	0.39868	1.9665
0.60074	2.2674	0.59974	2.2557	0.59964	2.2190	0.59897	2.2192
0.79806	2.5607	0.80000	2.5592	0.80027	2.5332	0.80069	2.5378
1.0000	2.9056	1.0002	2.9024	1.0001	2.8957	0.99887	2.9010
—	—	—	—	1.2500	3.4033	1.2487	3.4133
—	—	—	—	1.4999	3.9556	1.4999	3.9727

Table 7.21 - Convergence of frequency ratios $\omega/\omega_{\ell l}$ of the fundamental mode. with p_i. Plate 5. p_o=5. $\xi = 0$, $\eta = 0$.

p_i=0		p_i=3		p_i=4	
$\frac{w_m}{h}$	$\omega/\omega_{\ell l}$	$\frac{w_m}{h}$	$\omega/\omega_{\ell l}$	$\frac{w_m}{h}$	$\omega/\omega_{\ell l}$
0.19985	1.0081	0.19975	1.0076	0.19959	1.0059
0.39984	1.0319	0.39948	1.0301	0.39990	1.0236
0.59991	1.0704	0.60000	1.0667	0.59978	1.0522
0.80003	1.1218	0.80002	1.1156	0.79990	1.0912
1.0000	1.1840	0.99999	1.1753	0.99987	1.1392
1.2526	1.2746	1.2500	1.2618	1.2499	1.21031
1.5012	1.3734	1.4999	1.3583	1.5000	1.2914

p_i=5		p_i=6		p_i=7	
$\frac{w_m}{h}$	$\omega/\omega_{\ell l}$	$\frac{w_m}{h}$	$\omega/\omega_{\ell l}$	$\frac{w_m}{h}$	$\omega/\omega_{\ell l}$
0.19964	1.0059	0.2006	1.0057	0.19992	1.0055
0.39951	1.0232	0.4013	1.0222	0.40364	1.0224
0.60012	1.0518	0.6003	1.0491	0.61101	1.0508
0.79988	1.0904	0.8013	1.0864	0.80613	1.0874
0.99988	1.1382	0.9999	1.1324	0.99977	1.1324
1.2499	1.2092	1.2532	1.2028	1.2531	1.2029
1.5001	1.2904	1.4977	1.2814	1.4976	1.2816

Table 7.22 - Convergence of frequency ratios $\omega/\omega_{\ell 1}$ of the second mode with p_i. Plate 5. p_o=5. $\xi = 0.4$, $\eta = 0$.

p_i=0		p_i=3		p_i=4	
$\frac{w_m}{h}$	$\omega/\omega_{\ell 1}$	$\frac{w_m}{h}$	$\omega/\omega_{\ell 1}$	$\frac{w_m}{h}$	$\omega/\omega_{\ell 1}$
0.19986	1.2848	0.19941	1.2844	0.19979	1.2831
0.39933	1.3503	0.39990	1.3484	0.39942	1.3440
0.59848	1.4516	0.60002	1.4483	0.59895	1.4391
0.79757	1.5816	0.80001	1.5775	0.79865	1.5624
0.99666	1.7346	0.99986	1.7299	1.0015	1.7109
1.2455	1.9501	1.2501	1.9459	1.2496	1.9175
1.5044	2.1953	1.5000	2.1822	1.4994	2.1465
p_i=5		p_i=6		p_i=7	
$\frac{w_m}{h}$	$\omega/\omega_{\ell 1}$	$\frac{w_m}{h}$	$\omega/\omega_{\ell 1}$	$\frac{w_m}{h}$	$\omega/\omega_{\ell 1}$
0.20021	1.2820	0.19988	1.2784	0.20030	1.2781
0.40309	1.3406	0.40009	1.32593	0.39250	1.3224
0.60258	1.4308	0.59970	1.40017	0.60010	1.3981
0.79913	1.5457	0.80099	1.4978	0.79787	1.4930
0.99883	1.6840	0.99935	1.6127	0.99745	1.6076
1.2500	1.8825	1.2500	1.7801	1.2478	1.7732
1.4999	2.1006	1.4999	1.9657	1.5021	1.9611

Table 7.23 - Convergence of frequency ratios $\omega/\omega_{\ell 1}$ of the third mode with p_i. Plate 5. p_o=5. $\xi = 0$, $\eta = 0$.

p_i=0		p_i=3		p_i=4	
$\frac{w_m}{h}$	$\omega/\omega_{\ell 1}$	$\frac{w_m}{h}$	$\omega/\omega_{\ell 1}$	$\frac{w_m}{h}$	$\omega/\omega_{\ell 1}$
0.20004	1.7999	0.19995	1.7974	0.20014	1.7972
0.39979	1.9766	0.39989	1.9705	0.39988	1.9696
0.59902	2.2337	0.60005	2.2261	0.60016	2.2230
0.79799	2.5528	0.79998	2.5439	0.80006	2.5378
1.00192	2.9317	1.0000	2.9111	1.0001	2.9026
p_i=5		p_i=6		p_i=7	
$\frac{w_m}{h}$	$\omega/\omega_{\ell 1}$	$\frac{w_m}{h}$	$\omega/\omega_{\ell 1}$	$\frac{w_m}{h}$	$\omega/\omega_{\ell 1}$
0.19989	1.7971	0.20078	1.7973	0.20094	1.7962
0.40062	1.9686	0.40040	1.9684	0.39886	1.9630
0.59964	2.2190	0.60002	2.2213	0.59930	2.2131
0.80027	2.5332	0.79985	2.5366	0.80077	2.5290
1.0001	2.8957	0.95691	2.8189	1.0004	2.8936
1.2500	3.4033	1.2495	3.4145	1.2494	3.4053
1.4999	3.9556	1.4997	3.9716	1.4983	3.9641

Table 7.24 - Comparison of frequency ratios $\omega/\omega_{\ell l}$ of the fundamental mode. Plate 5. p_o=5 p_i=5. ξ=η=0.

HFEM and LUM [7.8], [7.10]		HFEM and Continuation Method	
$\frac{w_m}{h}$	$\omega/\omega_{\ell l}$	$\frac{w_m}{h}$	$\omega/\omega_{\ell l}$
0.2	1.0058	0.19964	1.0059
0.4	1.0232	0.39951	1.0232
0.6	1.0516	0.60012	1.0518
0.8	1.0903	0.79988	1.0904
1.0	1.1382	0.99988	1.1382
1.2	1.1941	1.1999	1.1941

Table 8.1 - Convergence of linear natural frequencies (rad/s) of Plate 1 with number of out-of-plane shape functions.

p_o	5 25 DOF	6 36 DOF	7 49 DOF	8 64 DOF	10 100 DOF
ω_1 (1,1)	487.28261	487.28261	487.27635	487.27635	487.27568
ω_2 (2,1)	750.90400	750.74748	750.74620	750.73935	750.73829
ω_3 (1,2)	1194.6916	1194.3609	1194.3426	1194.3416	1194.3389
ω_4 (3,1)	1197.3040	1197.3040	1195.9236	1195.9236	1195.9100
ω_5 (2,2)	1440.2864	1439.6702	1439.6702	1439.6446	1439.6402
ω_6 (4,1)	1960.2411	1819.7703	1819.7614	1811.3413	1811.1831
ω_7 (3,2)	1859.3470	1859.0321	1857.8927	1857.8902	1857.8711
ω_8 (1,3)	2267.6416	2267.6416	2263.7338	2263.7338	2263.6930
ω_9 (4,2)	2548.5234	2455.4194	2455.4194	2449.1365	2449.0494
ω_{10} (2,3)	2507.3497	2506.4230	2503.0925	2503.0163	2502.9808

Table 8.2 - Convergence of linear natural frequencies (rad/s) of aluminium plate - Plate 3 - with number of out-of-plane shape functions.

p_o	5 25 DOF	7 49 DOF	10 100 DOF
ω_1 (1,1)	579.44641	579.44156	579.44116
ω_2 (1,2)	1135.0211	1134.7515	1134.7469
ω_3 (2,1)	1227.6215	1227.3118	1227.3079
ω_4 (2,2)	1742.2799	1741.6415	1741.6187
ω_5 (1,3)	2014.3183	2011.3691	2011.3424
ω_6 (3,1)	2235.7076	2232.2331	2232.2004
ω_7 (2,3)	2590.7982	2587.9560	2587.9135
ω_8 (3,2)	2725.4862	2722.0562	2721.9965
ω_9 (1,4)	3499.4726	3210.4784	3192.9034
ω_{10} (3,3)	3545.1451	3540.5456	3540.5106

Table 8.3 - Convergence of linear natural frequencies (rad/s) of Plate 6 with the number of out-of-plane shape functions.

p_o	5 25 DOF	6 36 DOF	7 49 DOF	10 100 DOF
ω_1 (1,1)	4941.817	4941.817	4941.533	4941.484
ω_2 (2,1)	7302.876	7300.268	7300.230	7299.848
ω_3 (3,1)	10904.63	10904.63	10894.69	10894.44
ω_4 (1,2)	12223.93	12220.70	12219.51	12219.32
ω_5 (2,2)	14994.59	14979.04	14979.04	14977.37
ω_6 (4,1)	16601.79	15728.35	15727.96	15671.68
ω_7 (3,2)	19117.22	19112.66	19095.75	19094.79
ω_8 (5,1)	24368.49	24368.49	21860.24	21637.69
ω_9 (1,3)	23079.46	23079.46	23039.20	23038.16
ω_{10} (4,2)	24847.44	24411.66	24411.66	24362.53
ω_{11} (2,3)	26090.00	26057.08	26025.04	26018.49
ω_{12}(6,1)	-	34972.02	34969.89	28814.58

Table 8.4 - Convergence of linear natural frequencies (rad/s) of Plate 7, θ=45°, with the number of out-of-plane shape functions.

p_o	5 25 DOF	6 36 DOF	7 49 DOF	8 64 DOF
ω_1	763.1592	763.1008	763.0973	763.0961
ω_2	1420.456	1419.971	1419.934	1419.927
ω_3	1648.234	1647.451	1647.383	1647.361
ω_4	2220.854	2220.103	2219.165	2219.133
ω_5	2657.120	2654.918	2650.820	2650.651
ω_6	2872.601	2869.397	2865.341	2865.101
ω_7	3210.336	3198.623	3194.657	3193.688
ω_8	3793.948	3730.628	3721.229	3715.734
ω_9	4444.815	4265.583	4258.766	4234.946
ω_{10}	4632.294	4368.324	4353.888	4346.652
ω_{11}	4798.930	4455.886	4452.876	4431.806
ω_{12}	5434.871	5064.244	5016.991	4989.541

Table 8.5 - Linear natural frequency parameter of Plate 7, θ=45°. $\lambda = \left(\rho h \omega^2 a^4 / D_0\right), D_0 = \left(E_L h^3\right) / \left(12\left(1 - \nu_{LT} \nu_{TL}\right)\right)$.

Mode	1	2	3	4	5	6	7	8
HFEM p_o=8 64 DOF	22.38	41.65	48.32	65.09	77.74	84.03	93.67	109.0
HFEM p_o=6 36 DOF	22.38	41.65	48.32	65.11	77.87	84.16	93.81	109.4
Rayleigh-Ritz[8.4] 50 terms	22.40	41.64	48.32	65.09	77.76	84.06	93.58	109.0

Table 8.6 - Convergence of linear natural frequencies (rad/s) of Plate 7, θ=15°, with the number of out-of-plane shape functions.

p_o	n	ω_1	ω_2	ω_3	ω_4	ω_5	ω_6	ω_7	ω_8
6	36	799.652	1073.32	1562.72	2058.84	2263.52	2318.30	2775.89	3318.54
8	64	799.650	1073.30	1561.23	2058.71	2253.53	2317.71	2773.88	3142.39

Table 8.7 - Linear natural frequency parameter of Plate 7, θ=15°. $\lambda = \left(\rho h \omega^2 a^4 / D_0\right), D_0 = \left(E_L h^3\right) / \left(12\left(1 - \nu_{LT} \nu_{TL}\right)\right)$.

Mode	1	2	3	4	5	6	7	8
HFEM p_o=6 36 DOF	23.45	31.48	45.83	60.38	66.39	67.99	81.41	97.32
Rayleigh-Ritz [8.4] 50 terms	23.46	31.48	45.86	60.38	66.47	67.96	81.36	92.42

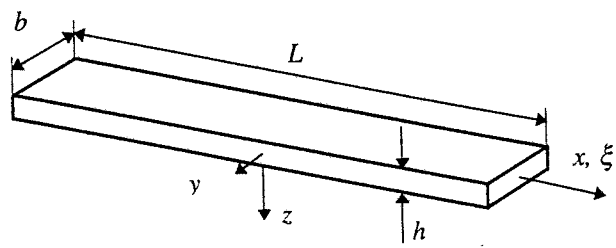

Figure 2.1 - Beam, local and global co-ordinate systems.

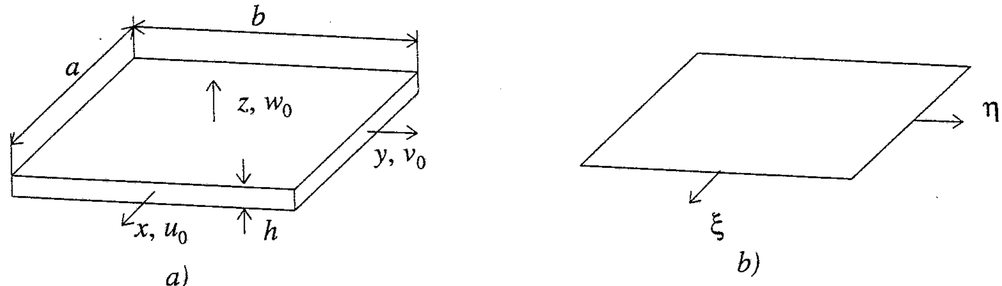

Figure 2.2 - *a)* Rectangular plate: x, y and z - global coordinate system; u_0, v_0 and w_0 - middle-plane displacements; a, b and h - plate dimensions. *b)* ξ, η - local coordinate system.

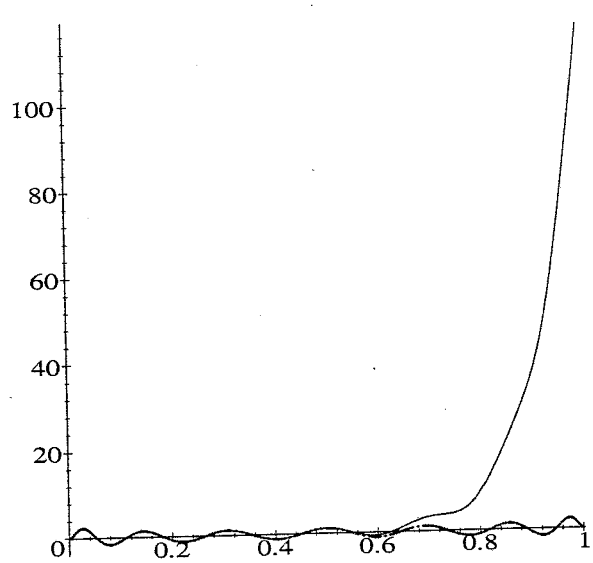

Figure 2.3 - Bhat's polynomial of order 16: - plotted using 10 digits, + plotted using 14 digits.

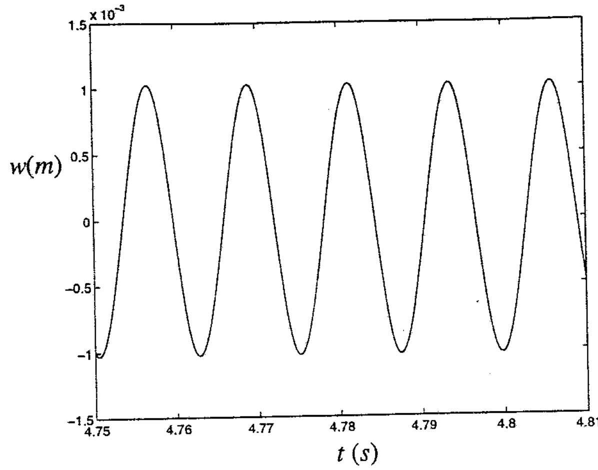

Figure 2.4 - Time domain response of Plate 5 to harmonic excitation by a plane wave.

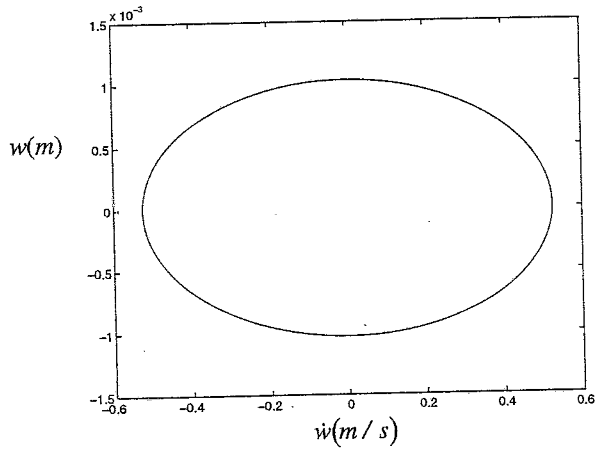

Figure 2.5 - Phase plane of the steady-state vibration of Plate 5 due to harmonic excitation by a plane wave.

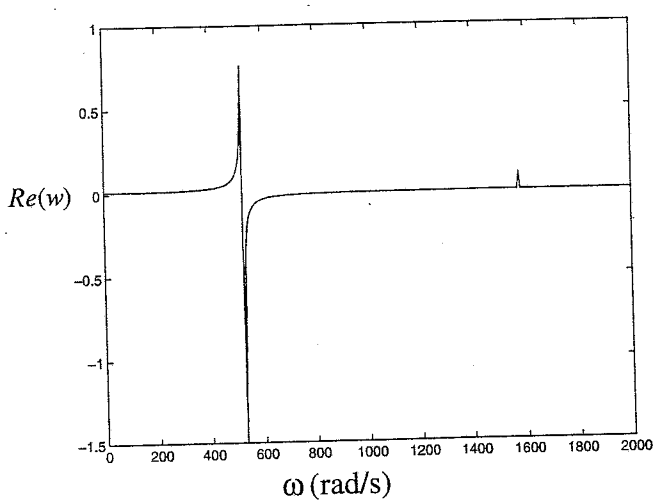

Figure 2.6 - Fourier transform of the steady-state vibration of Plate 5 due to harmonic excitation by a plane wave.

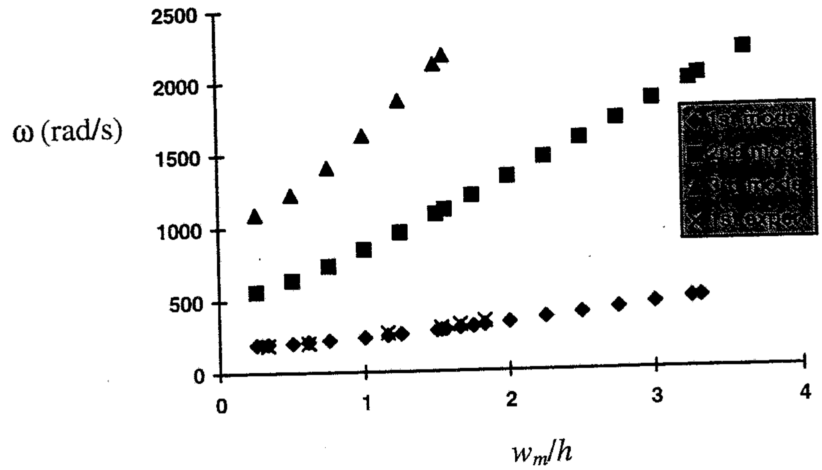

Figure 5.1 - First three nonlinear frequencies calculated by the HFEM and first nonlinear frequency obtained experimentally by Bennouna [5.1].

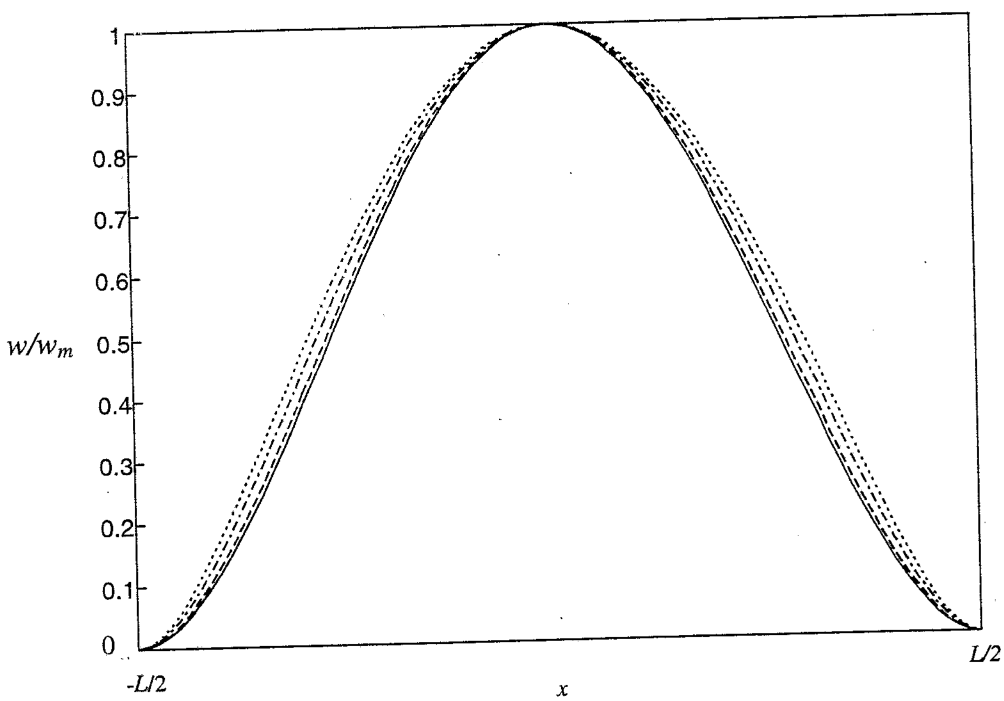

Figure 5.2 - First mode shape calculated with one harmonic

linear mode — ; nonlinear mode: - - w_m/h=1; — - w_m/h =2; ····· w_m/h =3

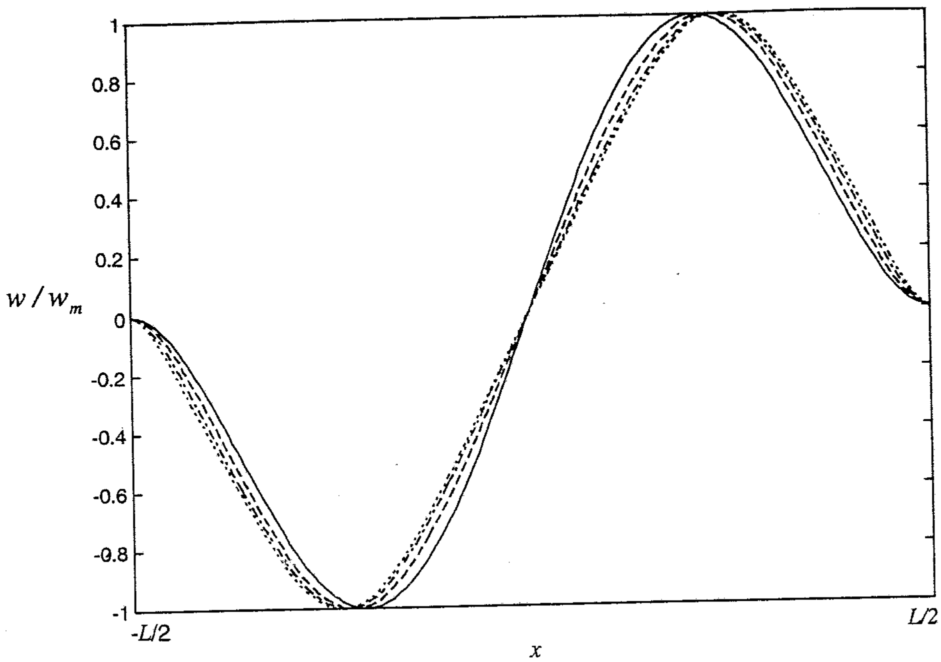

Figure 5.3 - Second mode shape

—— linear mode; nonlinear mode - - w_m/h =1; — - w_m/h =2; ····· w_m/h =3

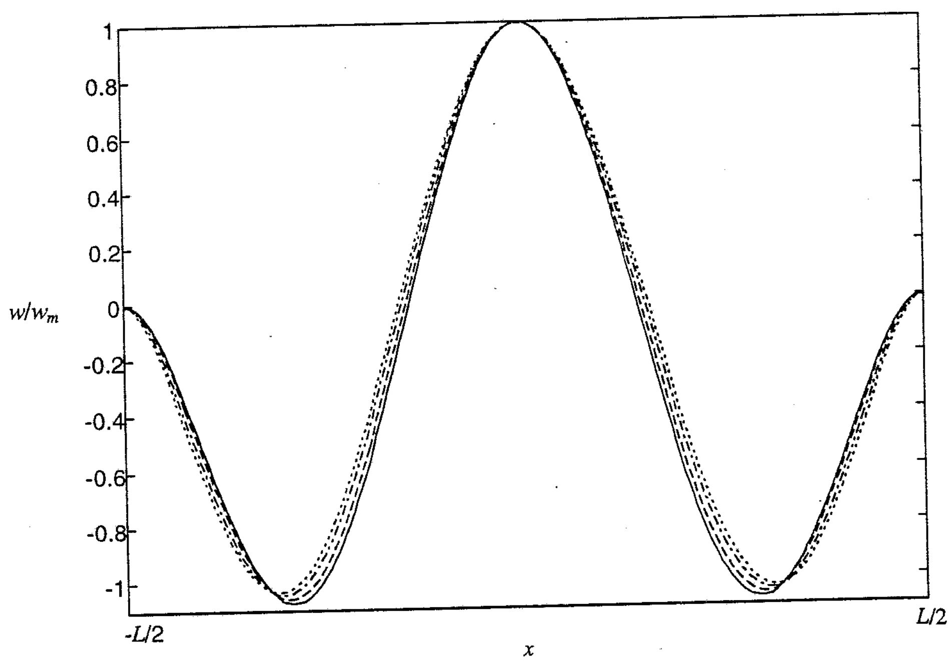

Figure 5.4 - Third mode shape.

—— linear mode; nonlinear mode - - w_m/h =0.5; — - w_m/h =1; ····· w_m/h =1.5.

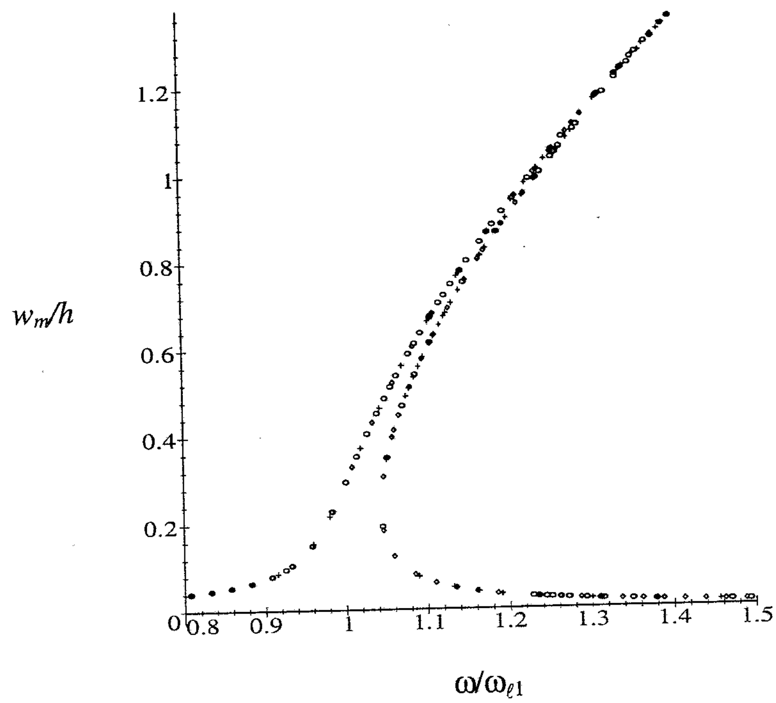

Figure 5.5 - FRF in the vicinity of the first mode calculated with: ◊ $p_o = 4$, + $p_o = 5$, o $p_o = 6$, at point x=0. In all cases p_i=9.

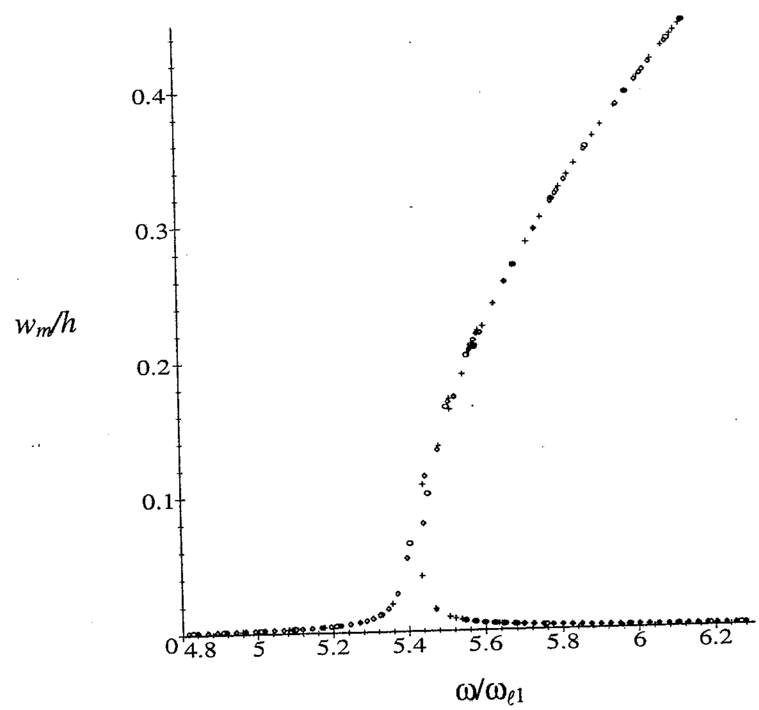

Figure 5.6 - FRF in the vicinity of the third mode calculated with: ◊ $p_o = 4$, + $p_o = 5$, o $p_o = 6$, at point x=0. In all cases p_i=9.

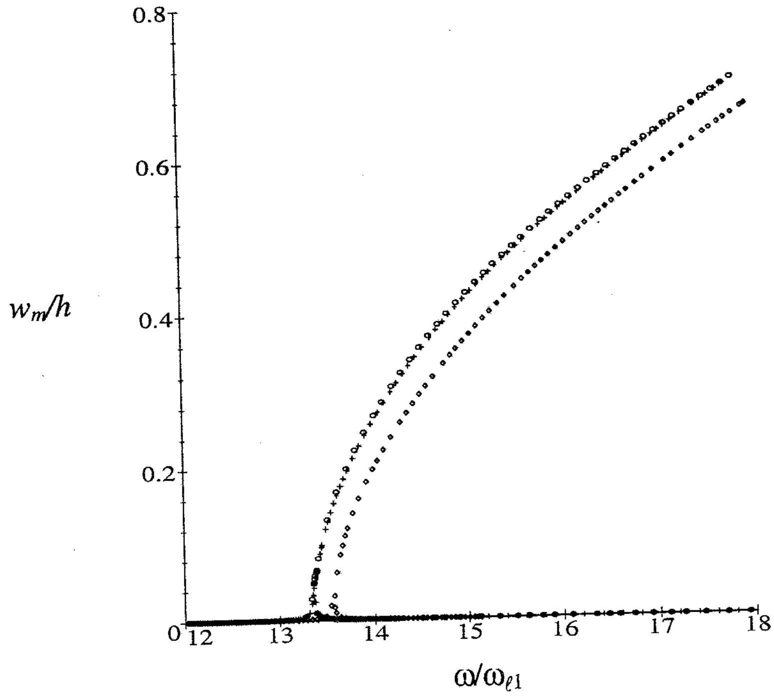

Figure 5.7 - FRF in the vicinity of the fifth mode calculated with: ◊ $p_o = 4$, + $p_o = 5$, o $p_o = 6$, at point x=0. In all cases p_i=9.

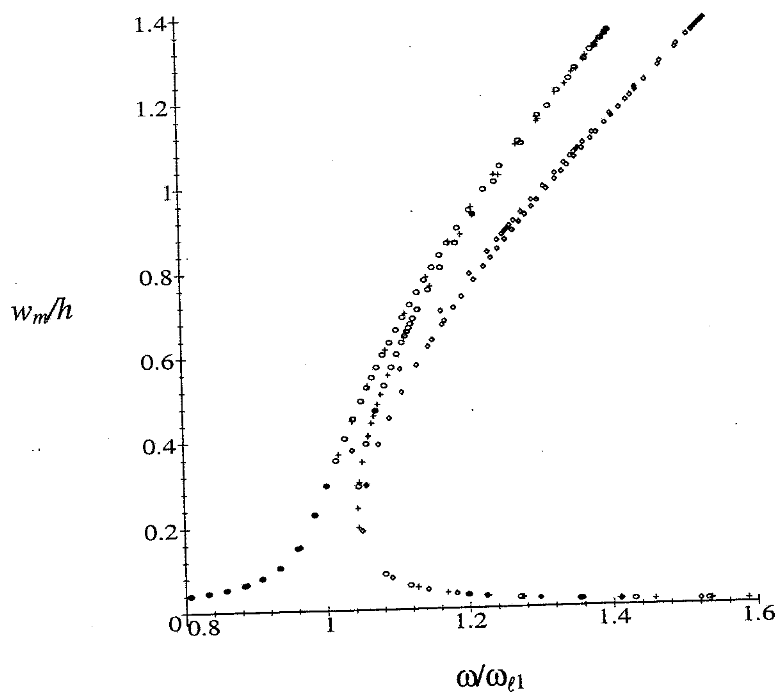

Figure 5.8 - FRF in the vicinity of the first mode calculated with: ◊ $p_i = 0$, + $p_i = 4$, o $p_i = 8$, at point x=0. In all cases p_o=6.

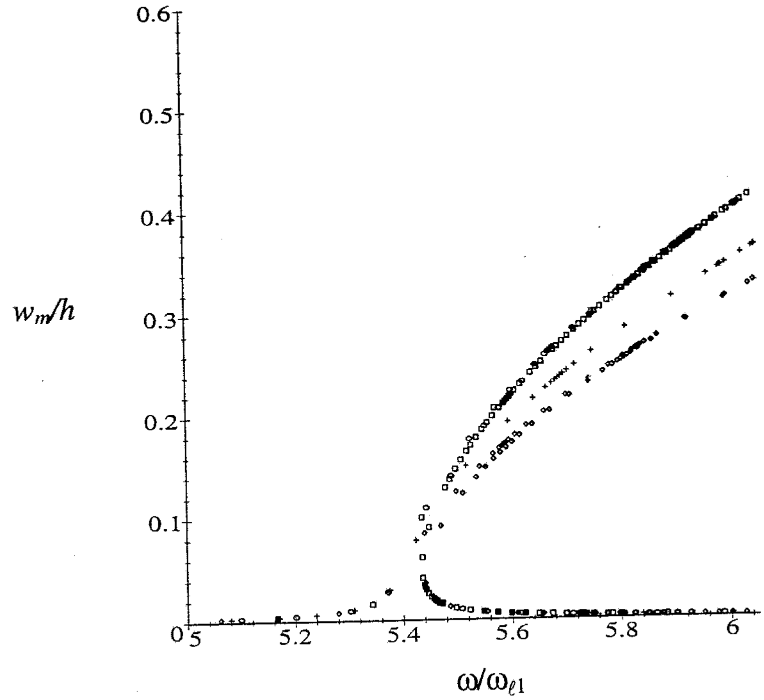

Figure 5.9 - FRF in the vicinity of the third mode calculated with: $\Diamond$ $p_i = 0$, $+$ $p_i = 4$, o $p_i = 8$, $\square$ $p_i = 10$; at point x=0. In all cases p_o=6.

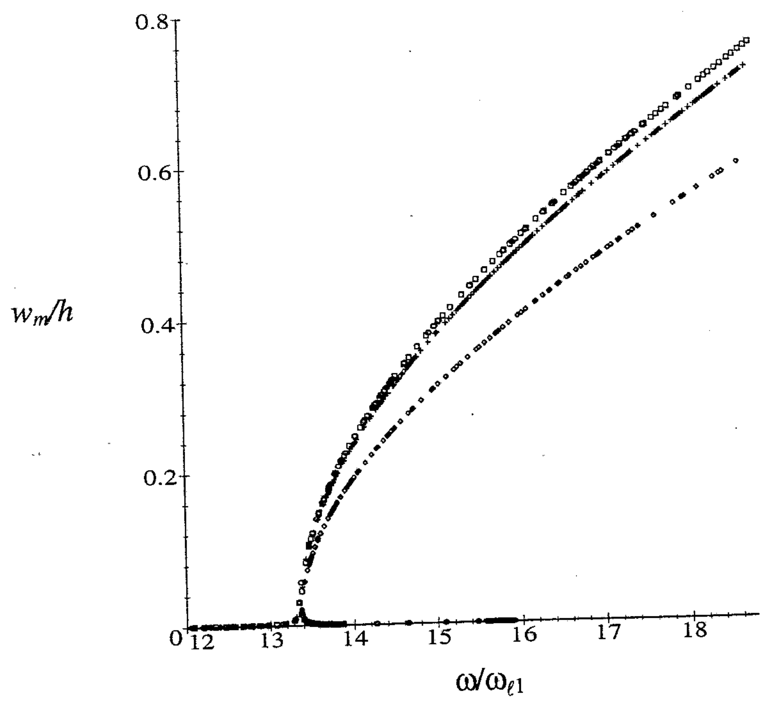

Figure 5.10 - FRF in the vicinity of the fifth mode calculated with: $\Diamond$ $p_i = 0$, $+$ $p_i = 8$, o $p_i = 10$, $\square$ $p_i = 12$; at point x=0. In all cases p_o=6.

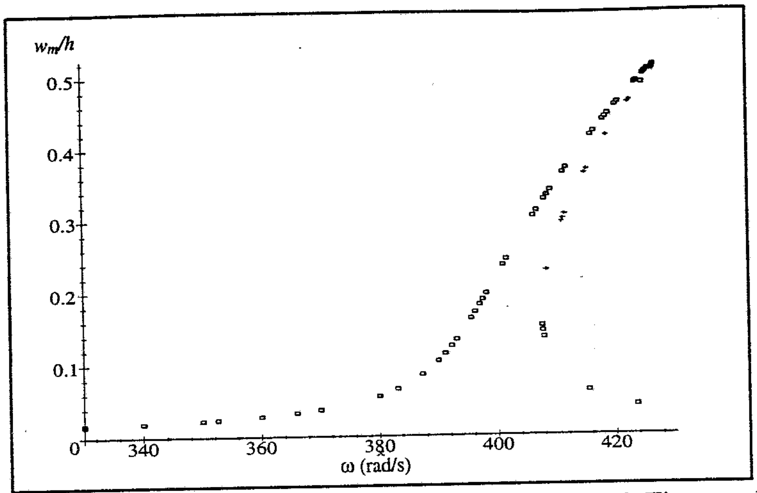

Figure 5.11 – Stability study using the perturbation method. First mode. x=0. ❑ stable solution; + unstable solution; p_o=p_i=6.

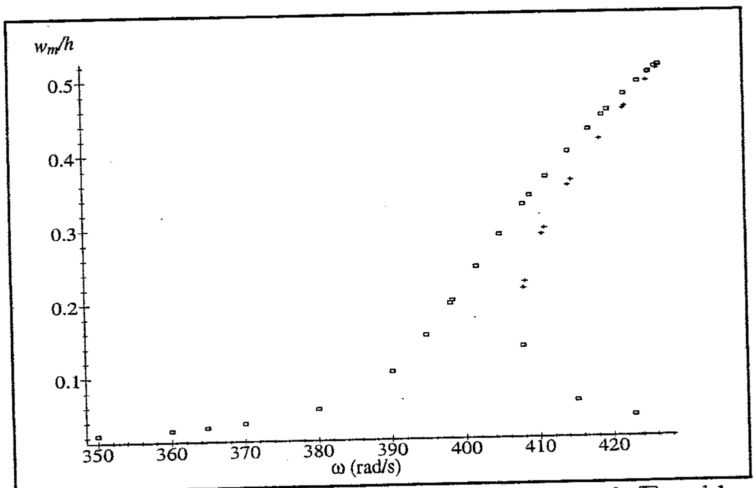

Figure 5.12 – Stability study by the HBM. First mode. x=0. ❑ stable solution; + unstable solution; p_o=p_i=6.

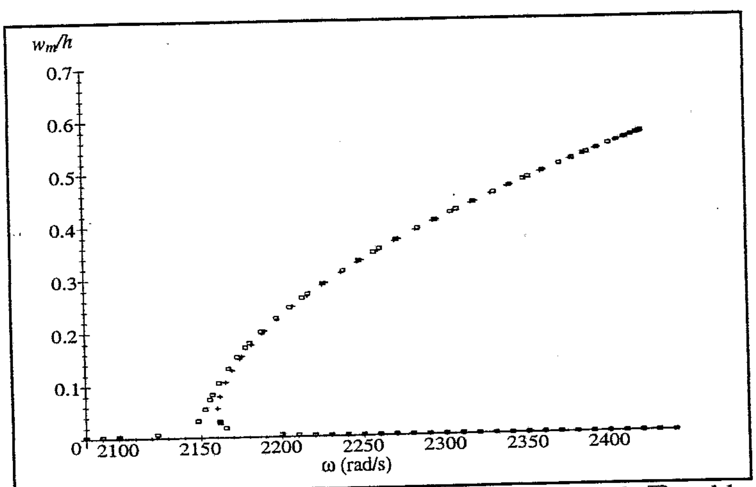

Figure 5.13 – Stability study by the HBM. Third mode. x=0. ❑ stable solution; + unstable solution; p_o=p_i=6.

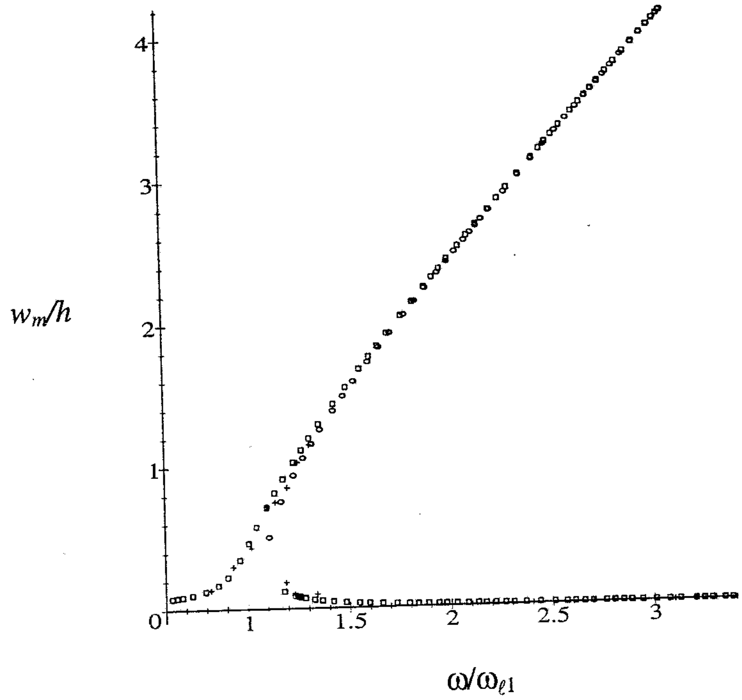

Figure 5.14 - FRF due to a point excitation of 0.134 N: experimental +, HFEM (p_o=6, p_i = 8, α=0.01) □ stable, o unstable. Values at point x=0.

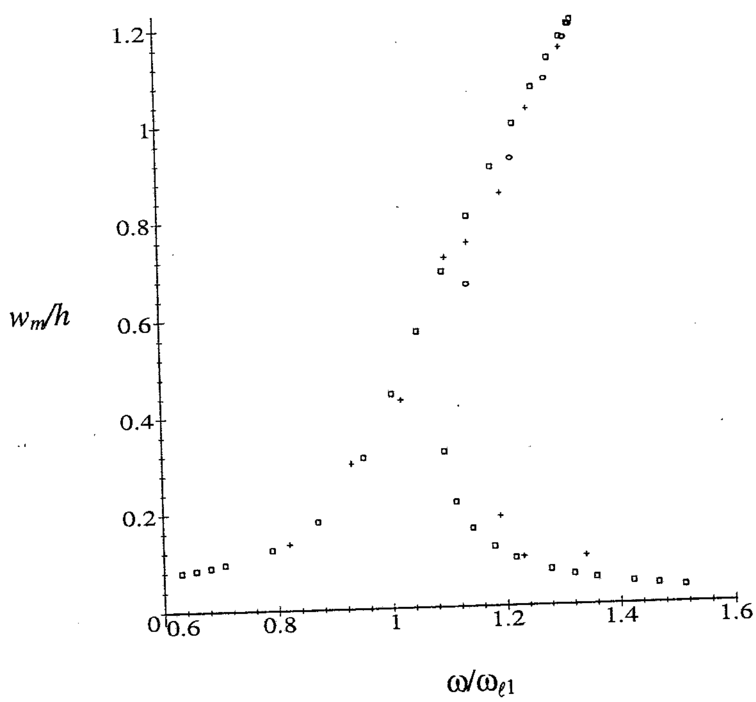

Figure 5.15 - FRF due to a point excitation of 0.134 N: experimental +, HFEM (p_o=6, p_i = 8, α=0.038) □ stable, o unstable. Values at point x=0.

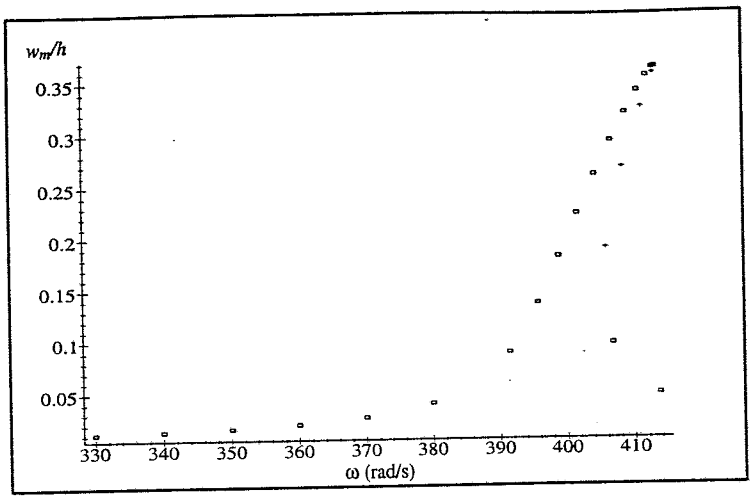

Figure 5.16 – FRF due to an harmonic plane wave at perpendicular incidence, first mode. ❑ stable,+ unstable. x=0.

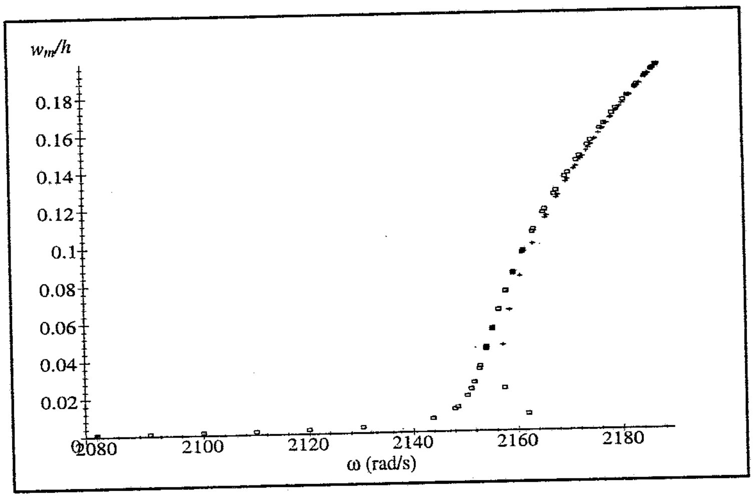

Figure 5.17 – FRF due to an harmonic plane wave at perpendicular incidence, third mode. ❑ stable,+ unstable. x=0.

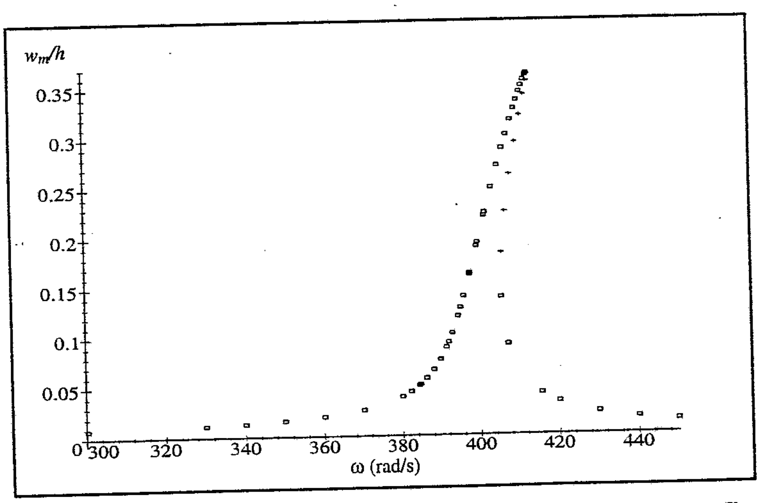

Figure 5.18 – FRF due to an harmonic wave at grazing incidence, first mode. ❑ stable,+ unstable. x=0.

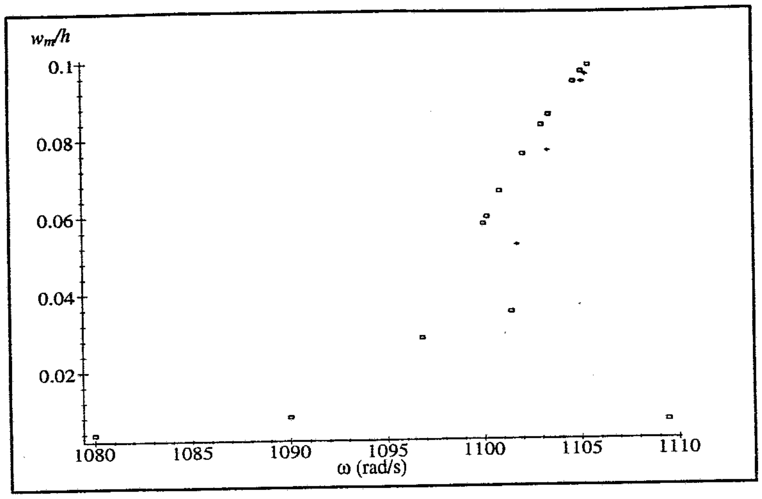

Figure 5.19 – FRF due to an harmonic wave at grazing incidence, second mode.
❑ stable, + unstable. x=0.25×L.

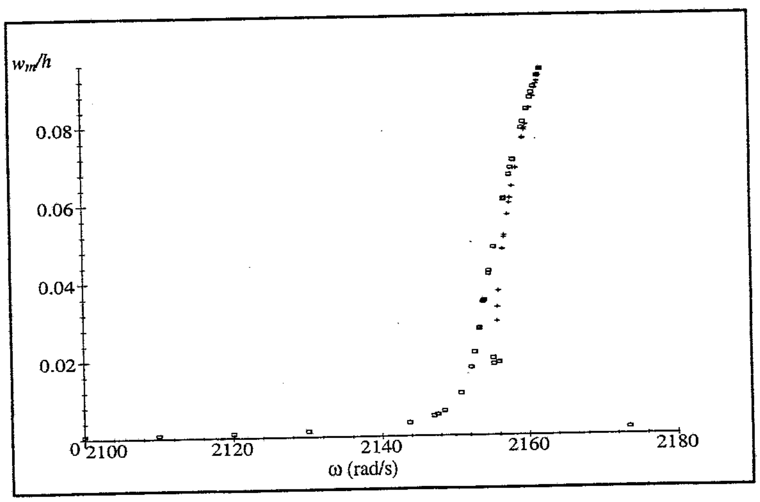

Figure 5.20 – FRF due to an harmonic wave at grazing incidence, third mode.
❑ stable, + unstable. x=0.

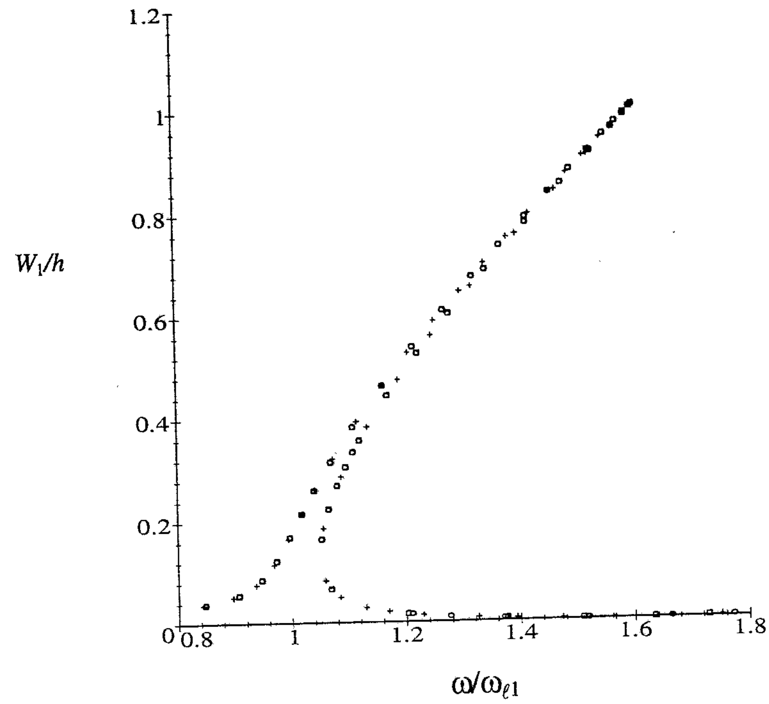

Figure 6.1 - First harmonic amplitude near first resonance frequency of *cc* beam calculated with: o $p_o = 5$, + $p_o = 7$,□ $p_o = 9$, at point x=0.25×L. In all cases p_i=10.

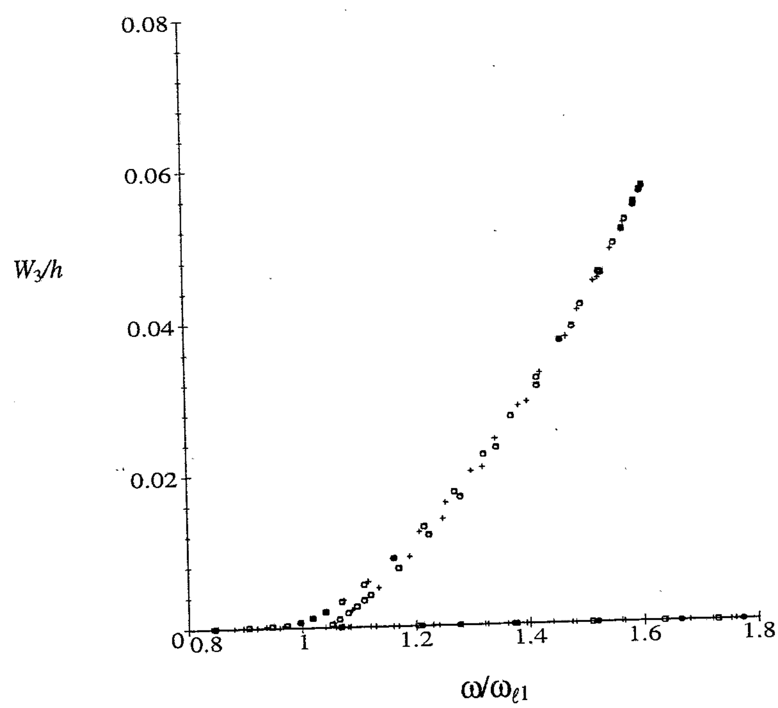

Figure 6.2 - Third harmonic amplitude near first resonance frequency of *cc* beam calculated with: o $p_o = 5$, + $p_o = 7$,□ $p_o = 9$, at point x=0.25×L. In all cases p_i=10.

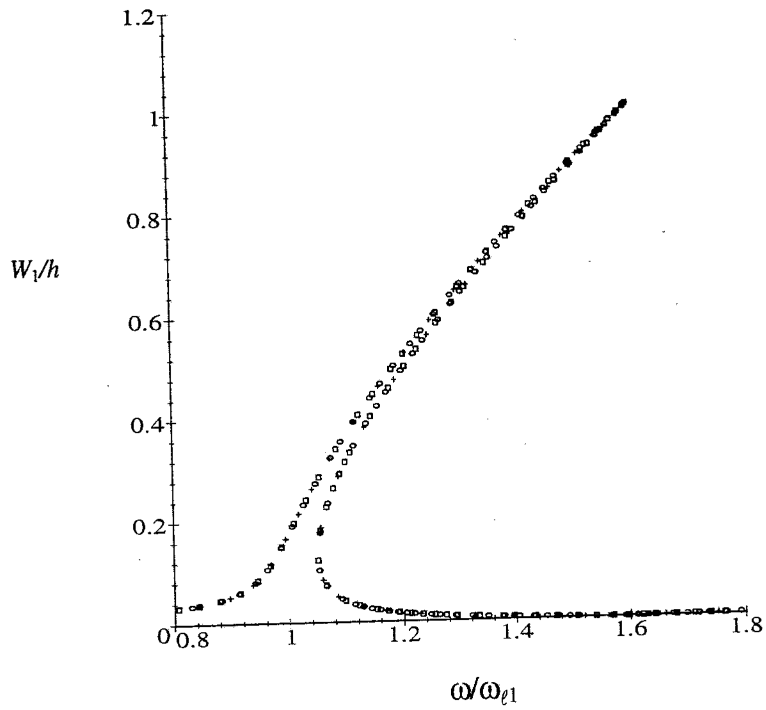

Figure 6.3 - First harmonic amplitude near first resonance frequency of *cc* beam calculated with: o $p_i = 8$, + $p_i = 10$,□ $p_i = 12$, at point x=0.25×L. In all cases p_o=7.

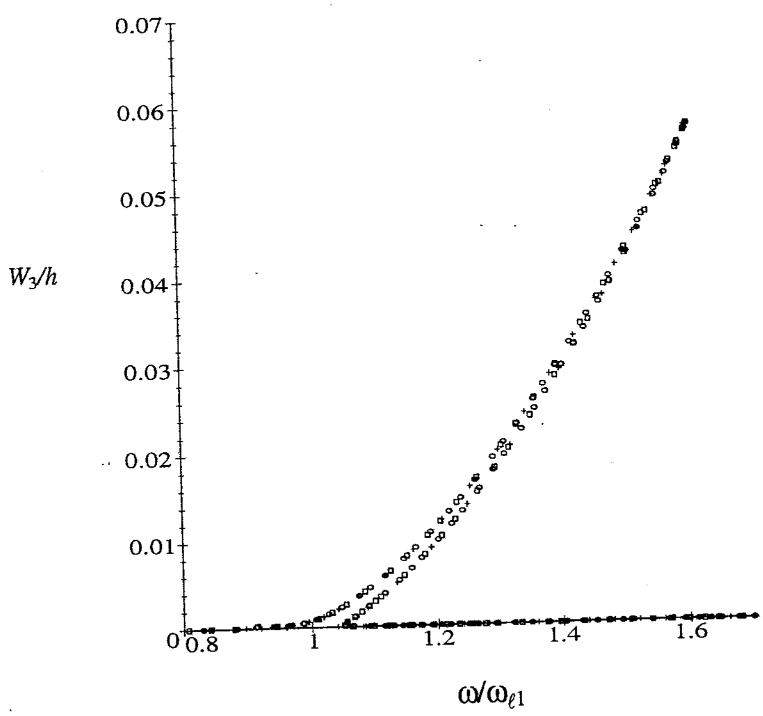

Figure 6.4 - Third harmonic amplitude near first resonance frequency of *cc* beam calculated with: o $p_i = 8$, + $p_i = 10$,□ $p_i = 12$, at point x=0.25×L. In all cases p_o=7.

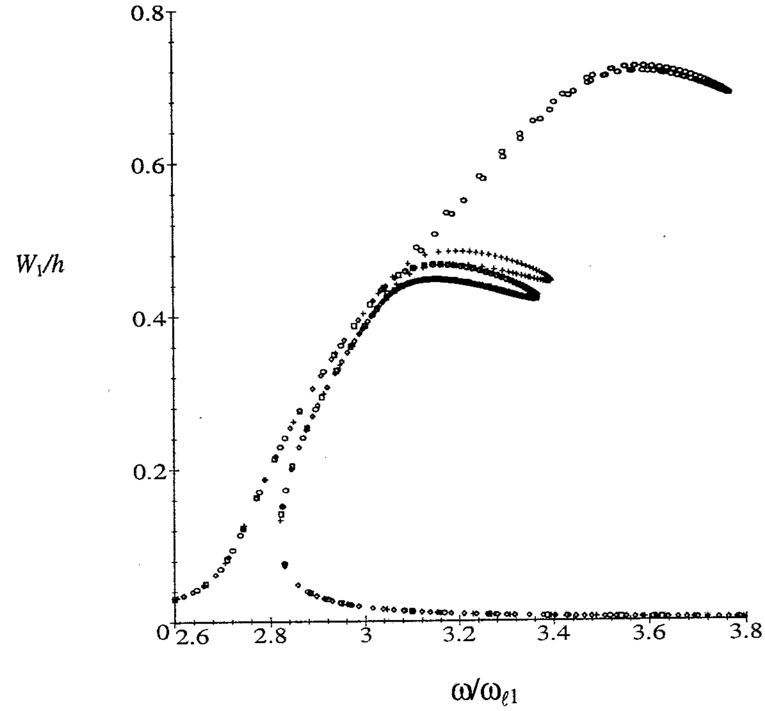

Figure 6.5 - First harmonic amplitude near second resonance frequency of *cc* beam calculated with p_i=10 and: o p_o = 5, + p_o =7,□ p_o = 9, ◊ p_o = 11 (x=0.25×L).

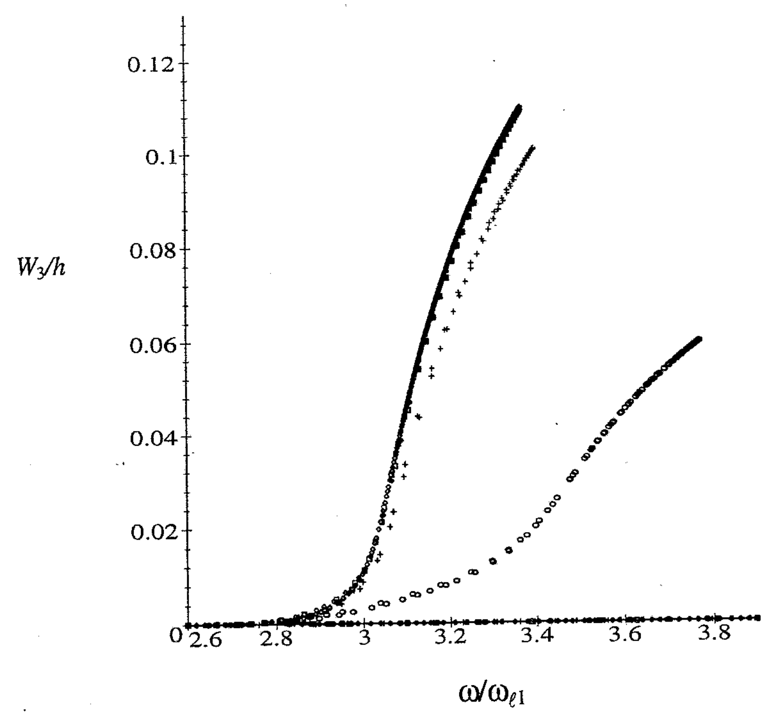

Figure 6.6 - Third harmonic amplitude near second resonance frequency of *cc* beam calculated with p_i=10 and: o p_o =5, + p_o =7,□ p_o =9, ◊ p_o =11 (x=0.25×L).

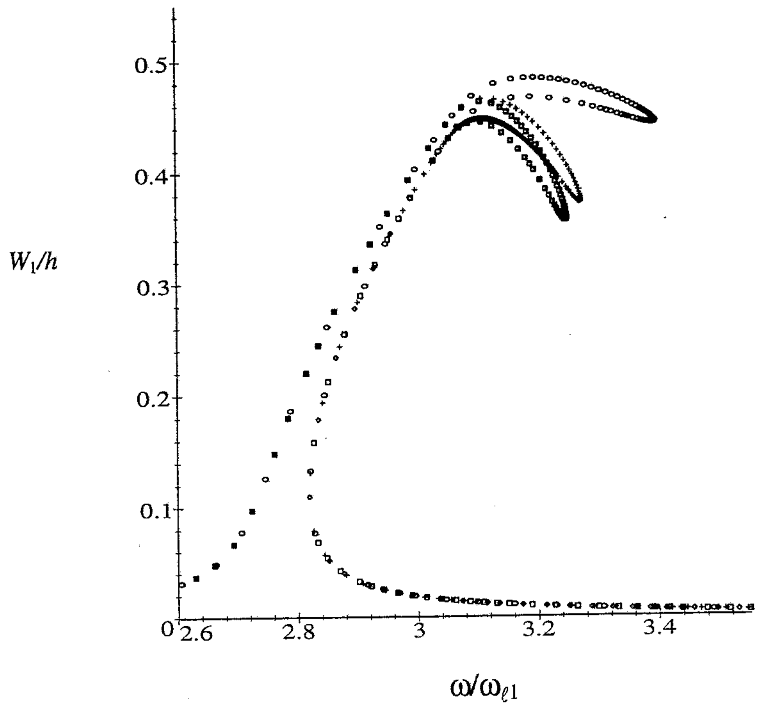

Figure 6.7 - First harmonic amplitude near second resonance frequency of *cc* beam calculated with p_o=7 and: o p_i = 10, + p_i = 12,□ p_i = 14, ◊ p_i = 16 (0.25×L).

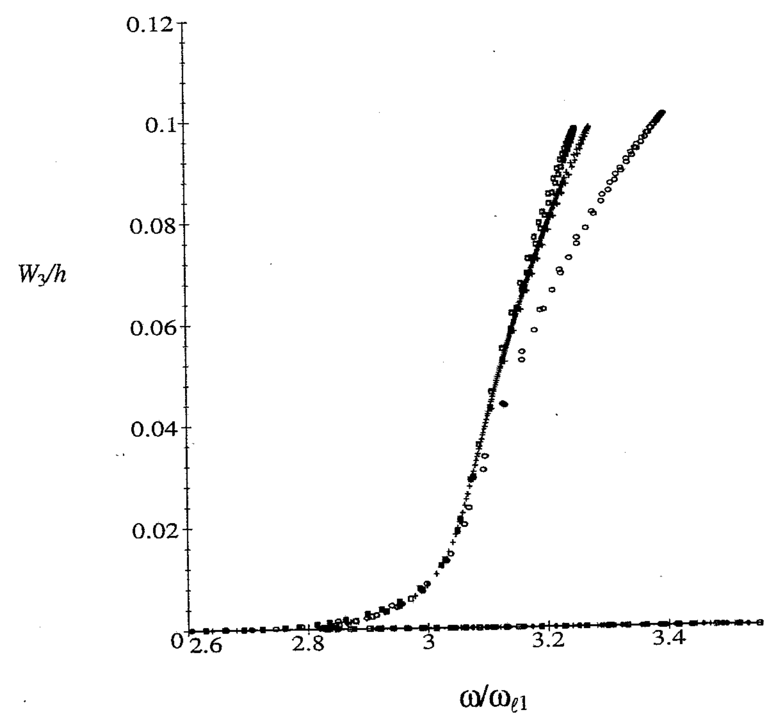

Figure 6.8 - Third harmonic amplitude near second resonance frequency of *cc* beam calculated with p_o=7 and: o p_i =10, + p_i =12,□ p_i =14, ◊ p_i =16 (x=0.25×L).

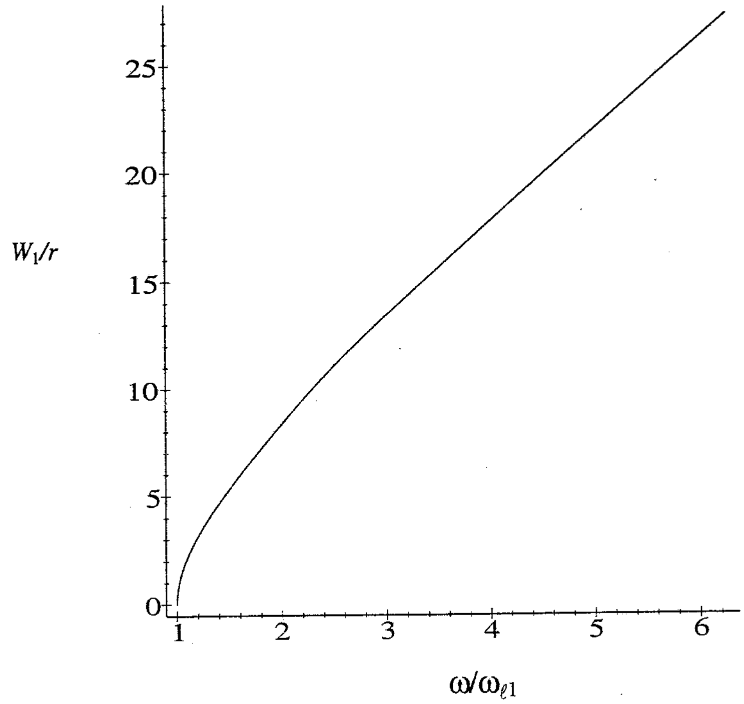

Figure 6.9 - Backbone curve of *cc* beam defined by W_1/r (x=0) and $\omega/\omega_{\ell 1}$.

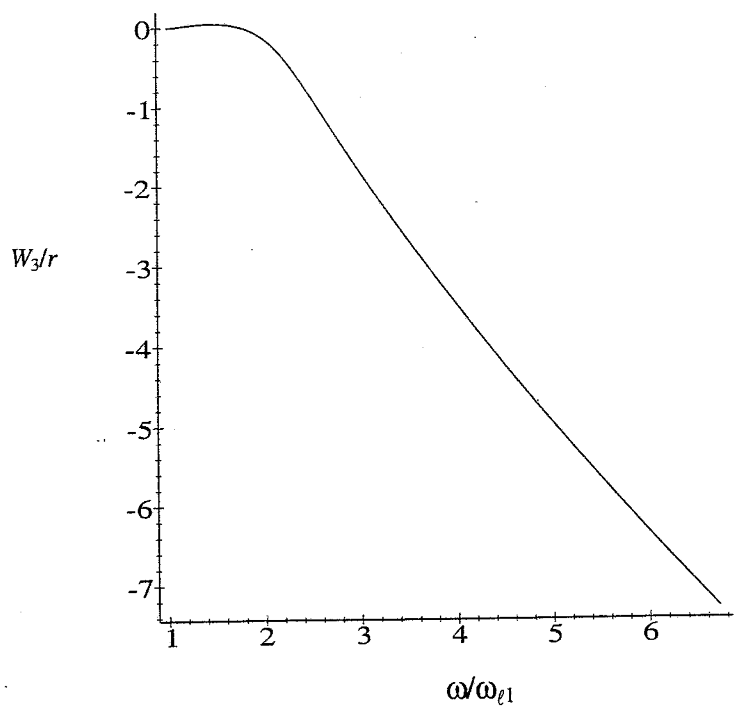

Figure 6.10 - Backbone curve of *cc* beam defined by W_3/r (x=0) and $\omega/\omega_{\ell 1}$.

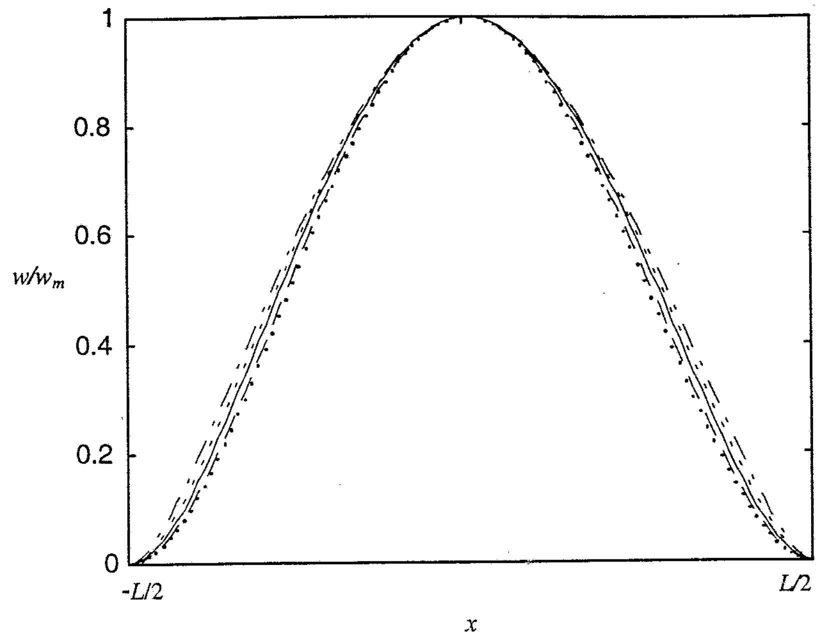

Figure 6.11 - Mode shape of the first harmonic of the clamped-clamped beam
.... linear mode; -- $\omega/\omega_{\ell 1}$=1.2351; — $\omega/\omega_{\ell 1}$=1.7453; ⁻⁻ $\omega/\omega_{\ell 1}$=2.5926;
—- $\omega/\omega_{\ell 1}$=3.8709.

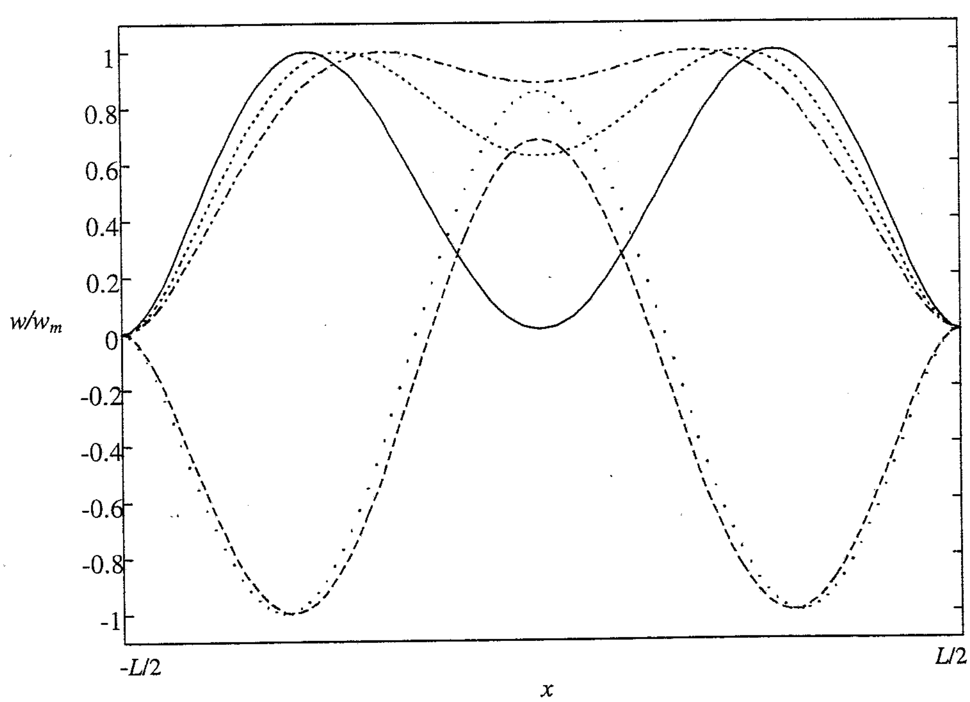

Figure 6.12 - Mode shape of the third harmonic of the clamped-clamped beam
—- $W_1/h \langle\langle 1$, $\omega/\omega_{\ell 1}\cong 1$; -- $\omega/\omega_{\ell 1}$=1.2351; — $\omega/\omega_{\ell 1}$=1.7453; ⁻⁻ $\omega/\omega_{\ell 1}$=2.5926;
.... $\omega/\omega_{\ell 1}$=3.8709.

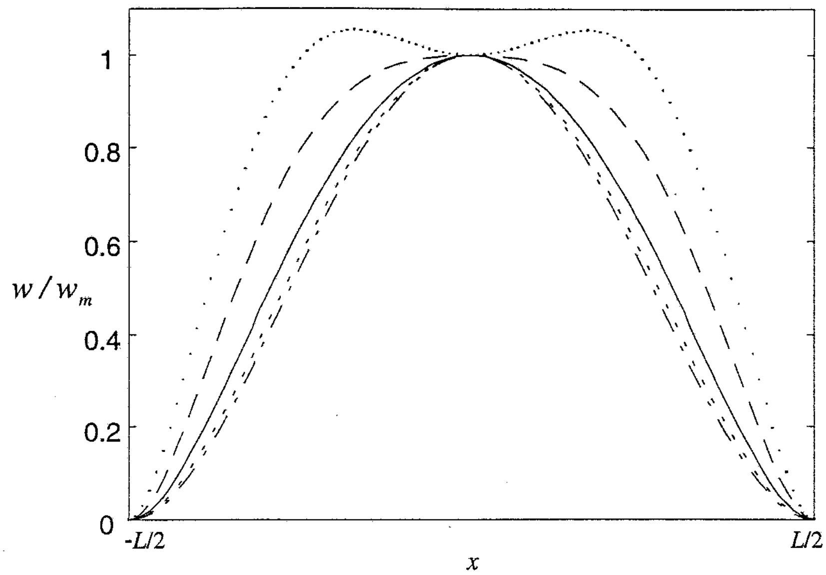

Figure 6.13 - Shape of *cc* beam at t=2πmT: — - $\omega/\omega_{\ell 1}$= 1.0001, ··· $\omega/\omega_{\ell 1}$=1.2351, — $\omega/\omega_{\ell 1}$=1.7453, ------ $\omega/\omega_{\ell 1}$=2.5926, ···· $\omega/\omega_{\ell 1}$=3.8709.

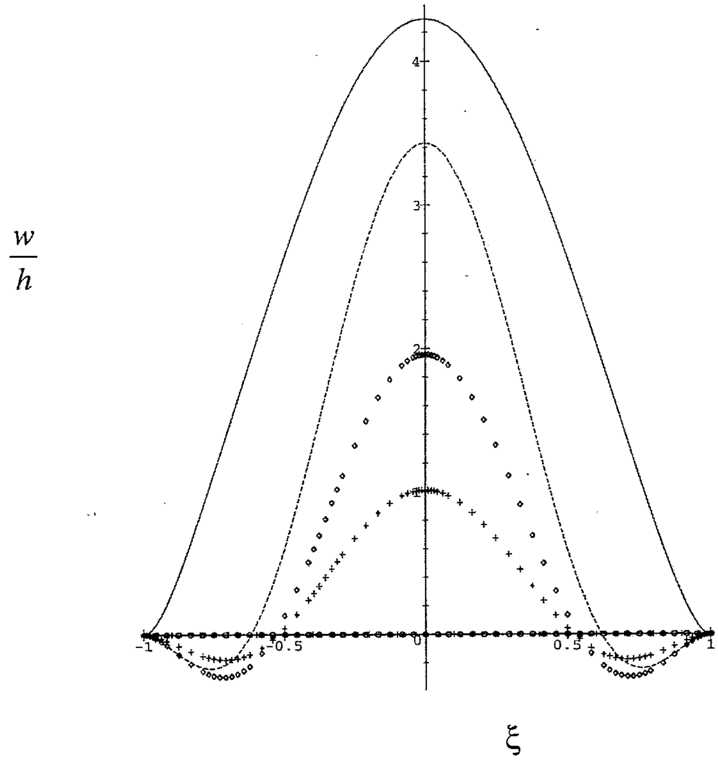

Figure 6.14 - Vibration of *cc* beam at $\omega/\omega_{\ell 1}$= 3.84. Plots at
o t=T/4, + (1/48)T+T/4, ◊ (1/24)T+T/4, -- (1/12)T+T/4, - (1/6)T+T/4

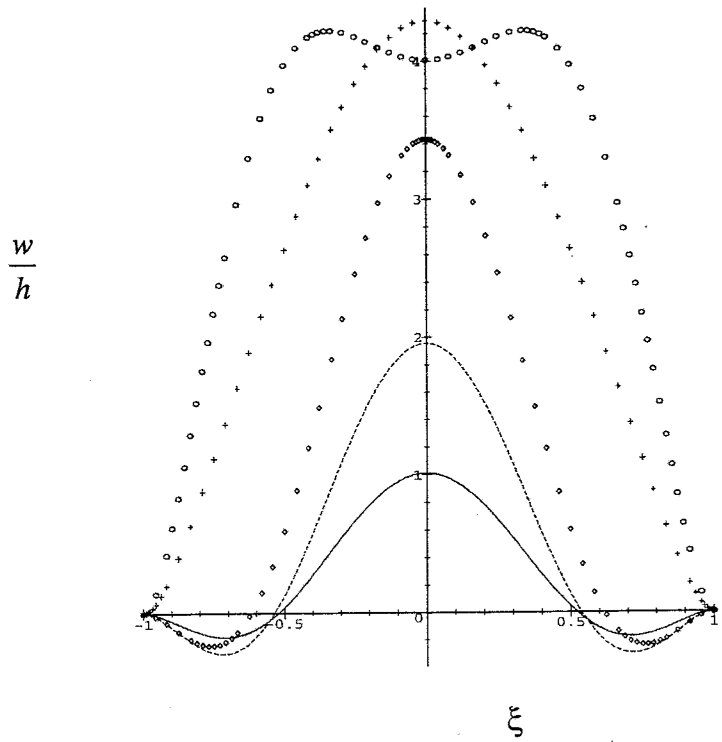

Figure 6.15 - Vibration of *cc* beam at $\omega/\omega_{\ell 1}$= 3.84
o (1/4)T+T/4, + (4/12)T+T/4, ◊ (5/12)T+T/4, -- (11/24)T+T/4, —(23/48)T+T/4

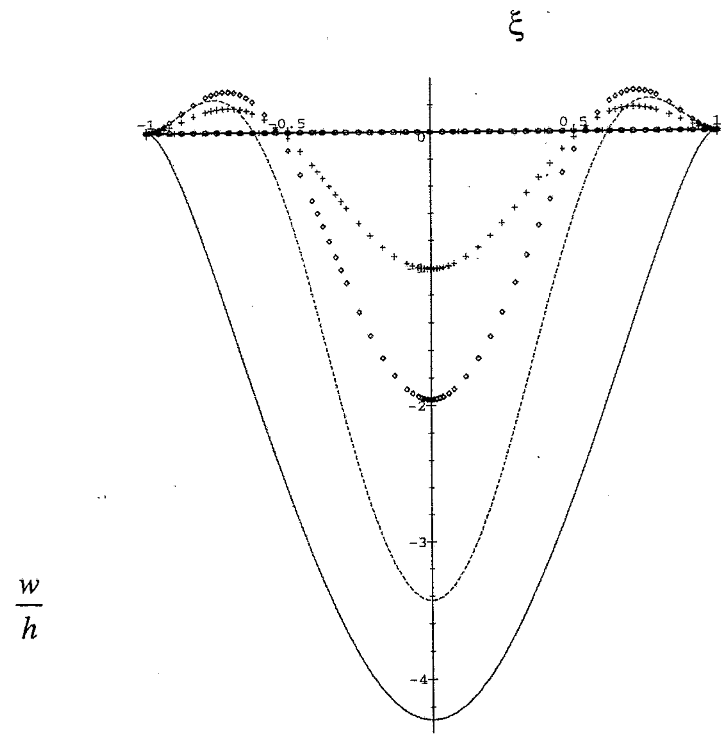

Figure 6.16 - Vibration of *cc* beam at $\omega/\omega_{\ell 1}$= 3.84
o T/2+T/4, + T/4+(25/48)T , ◊ T/4+(13/24)T, -- (7/12)T+T/4, —(8/12)T+T/4

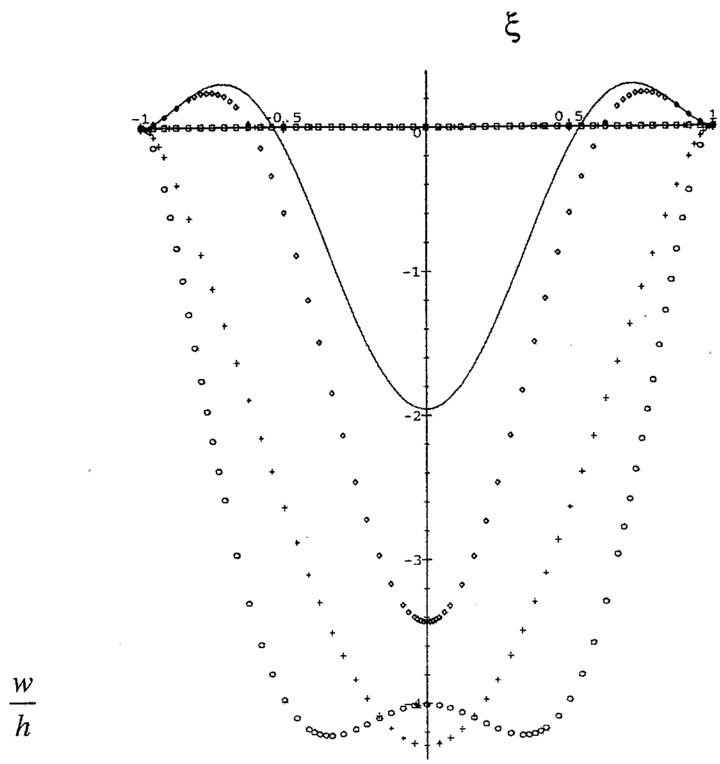

Figure 6.17 - Vibration of *cc* beam at $\omega/\omega_{\ell 1}$= 3.84
o (3/4)T+T/4, + (10/12)T+T/4, ◊ (11/12)T+T/4, — (23/24)T+T/4, □T+T/4

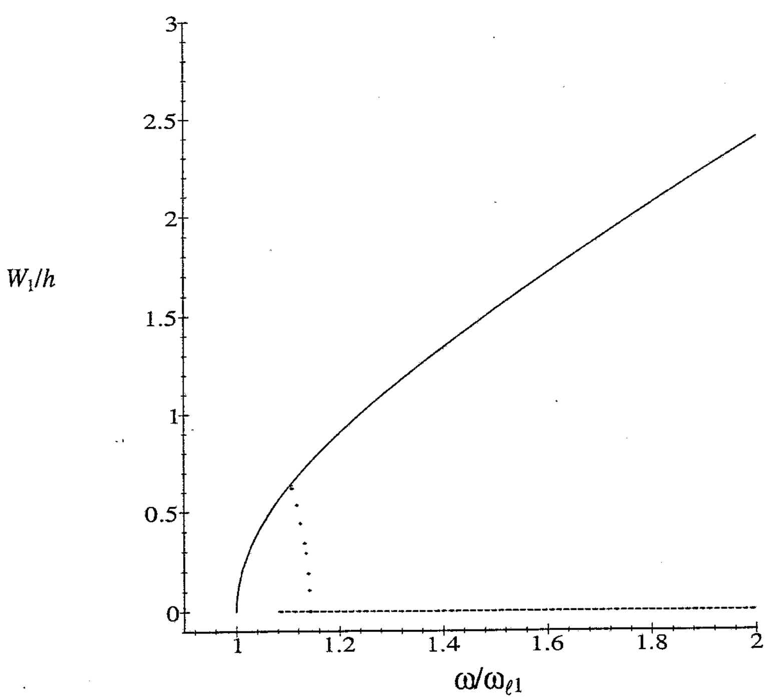

Figure 6.18 - Backbone curve of *cc* beam defined by W_1/h (x=0) and $\omega/\omega_{\ell 1}$.
— first main branch, + + + secondary branch, ········ second main branch.

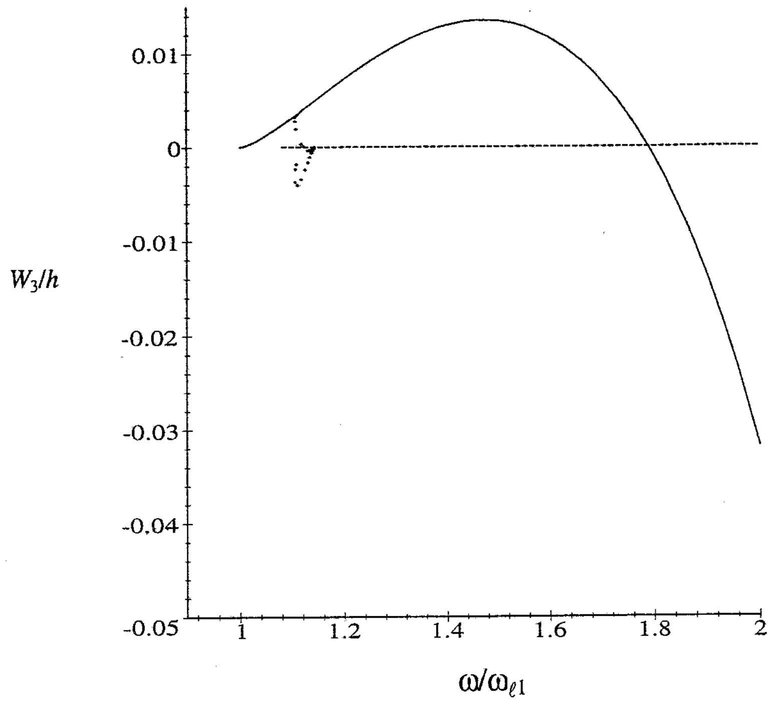

Figure 6.19 - Backbone curve of *cc* beam defined by W_3/h (x=0) and $\omega/\omega_{\ell 1}$.
—first main branch, + + + secondary branch, ········ second main branch.

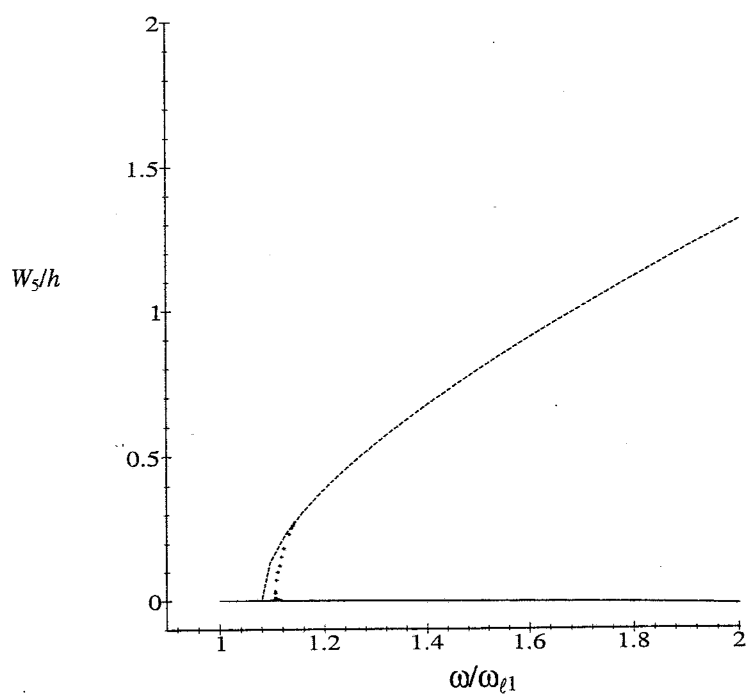

Figure 6.20 - Backbone curve of beam defined by W_5/h (x=0) and $\omega/\omega_{\ell 1}$.
—first main branch, + + + secondary branch, ········ second main branch.

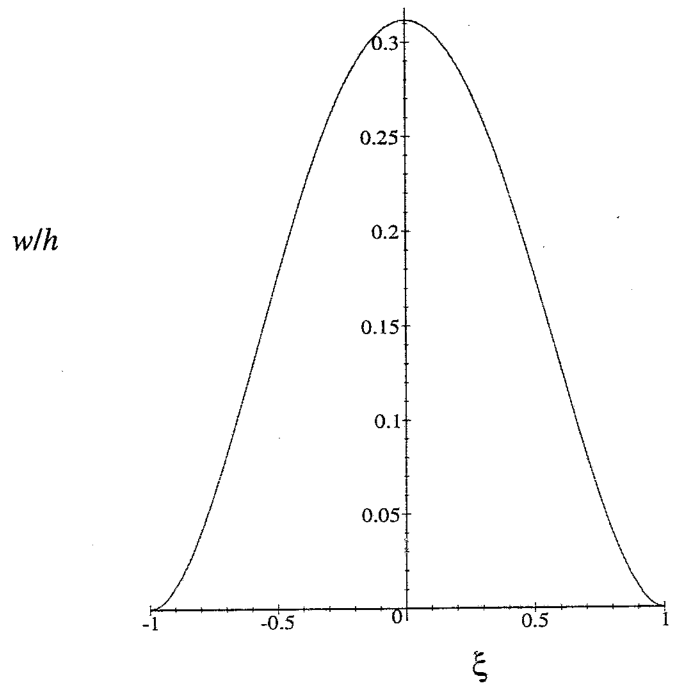

Figure 6.21 - Mode shape of the first harmonic of clamped-clamped beam at point $\omega/\omega_{\ell 1}$= 1.1339 of secondary branch.

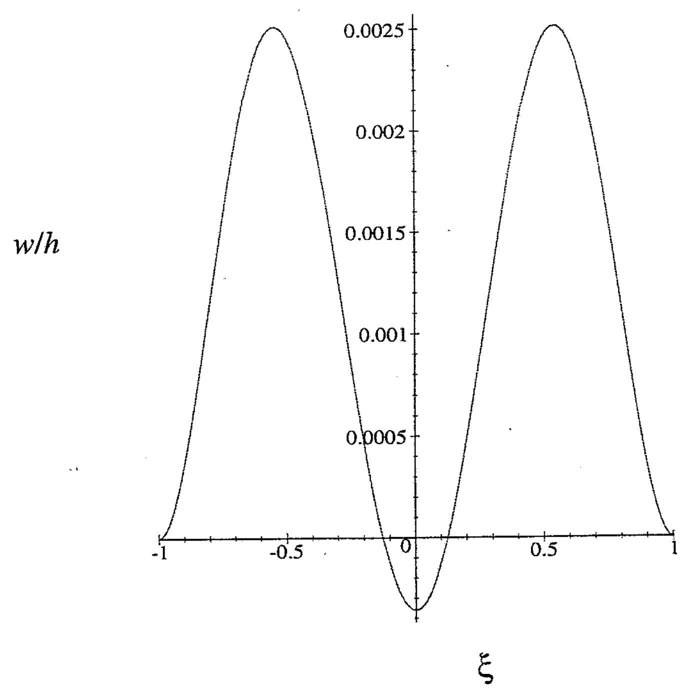

Figure 6.22 - Mode shape of the second harmonic of clamped-clamped beam at point $\omega/\omega_{\ell 1}$=1.1339 of secondary branch.

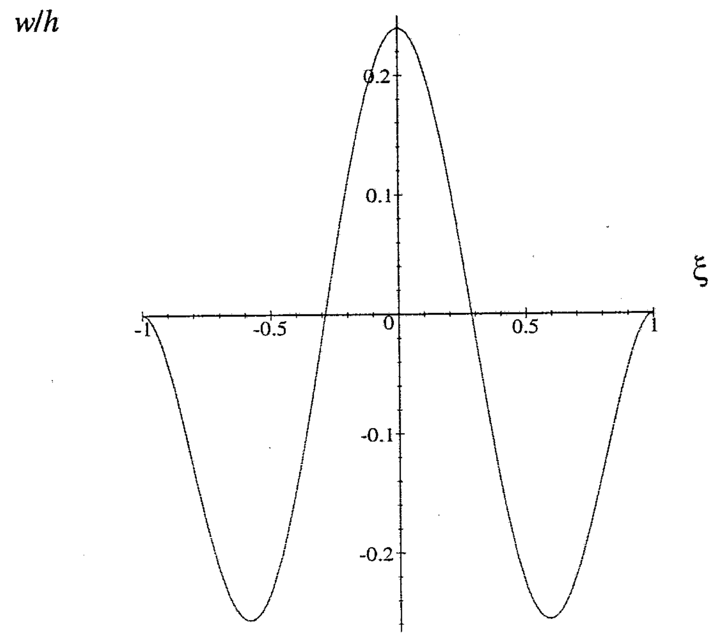

Figure 6.23 - Mode shape of the third harmonic of clamped-clamped beam at point $\omega/\omega_{\ell 1}$= 1.1339 of secondary branch.

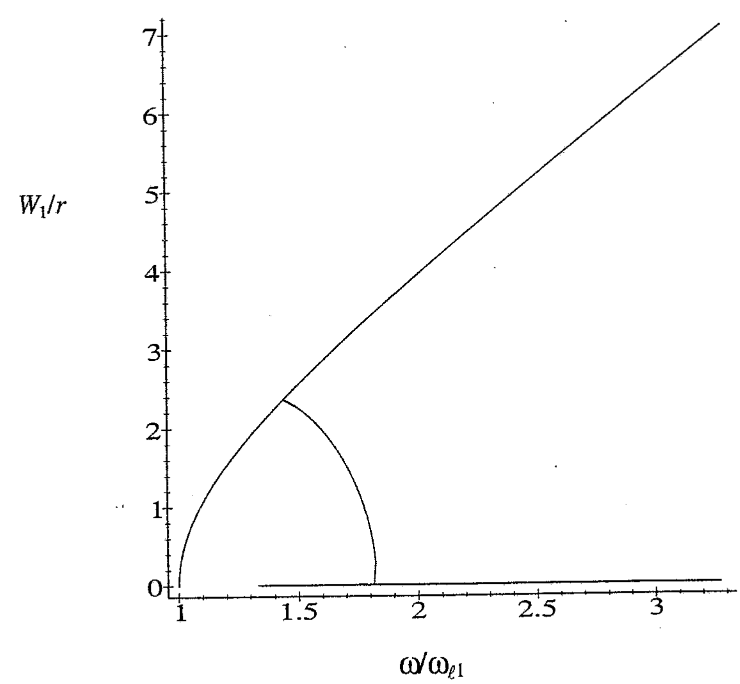

Figure 6.24 - Backbone curve of *ss* beam defined by W_1/r (at x= 0) and $\omega/\omega_{\ell 1}$.
From above: first main branch, secondary branch, second main branch.

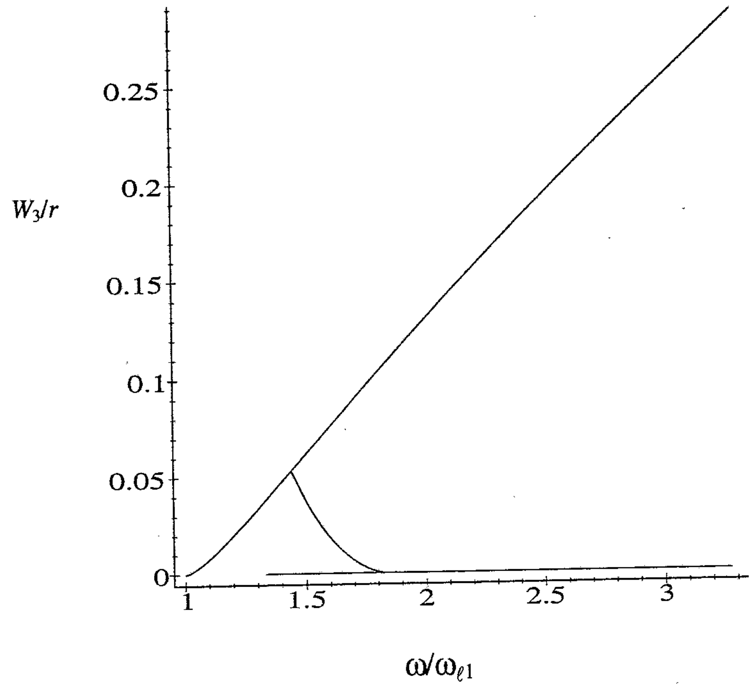

Figure 6.25 - Backbone curve of *ss* beam defined by W_3/r (x=0) and $\omega/\omega_{\ell 1}$.
From above: first main branch, secondary branch, second main branch.

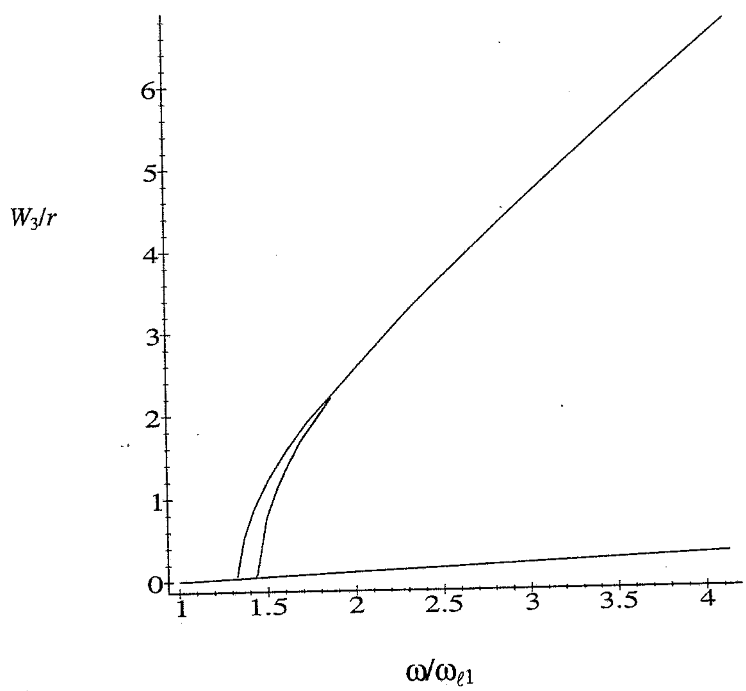

Figure 6.26 - Backbone curve of *ss* beam defined by W_3/r (x=0.25×L) and $\omega/\omega_{\ell 1}$.
From above: second main branch, secondary branch, first main branch.

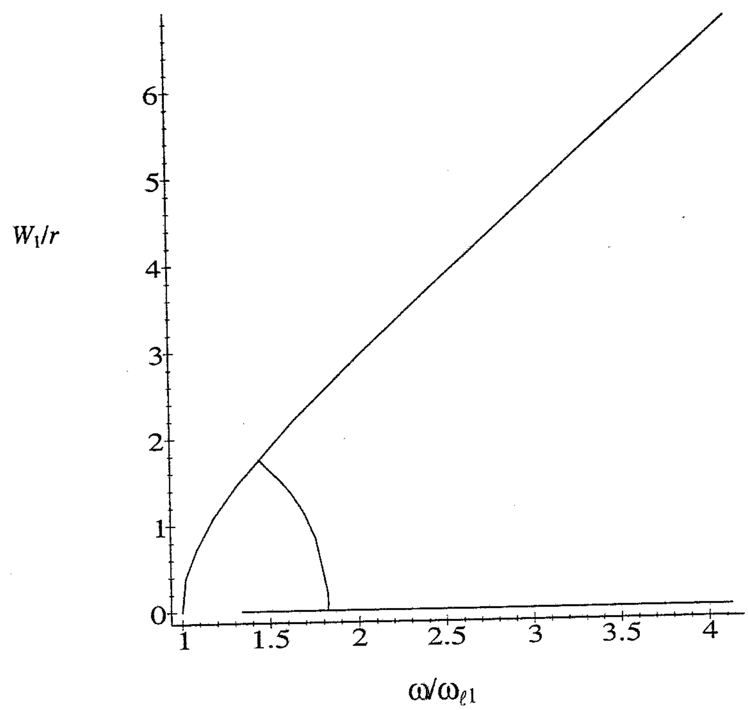

Figure 6.27 - Backbone curve of *ss* beam defined by W_1/r (x=0.25×L), $\omega/\omega_{\ell 1}$. From above: first main branch, secondary branch, second main branch.

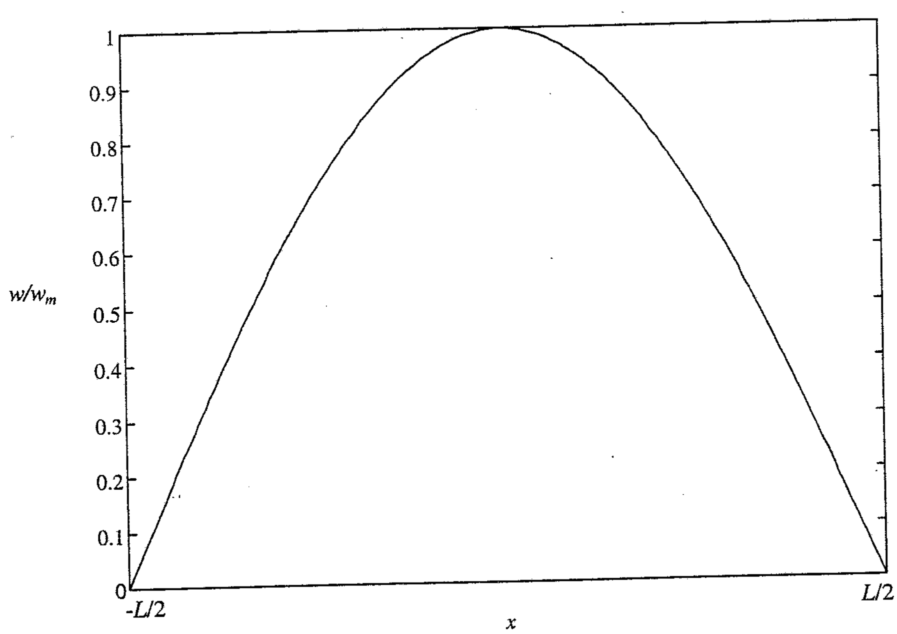

Figure 6.28 - Normalised linear mode shape (-); first (-·) and third harmonics (..) at $W_1/r \cong 6.09$. Difference not visible

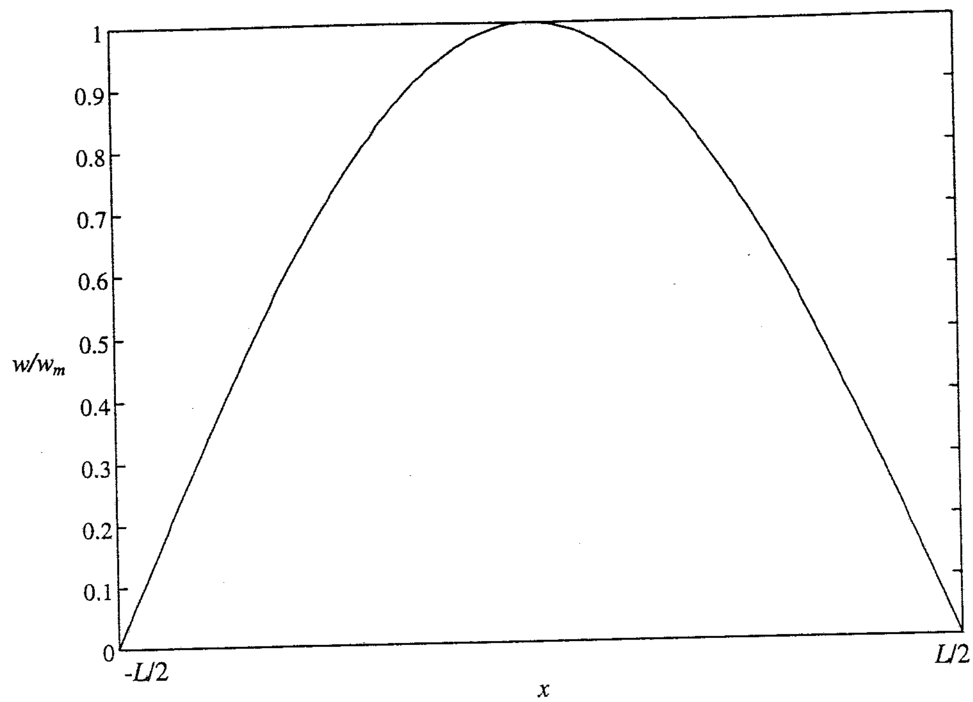

Figure 6.29 - Mode shape of the first harmonic for all points of the secondary branch

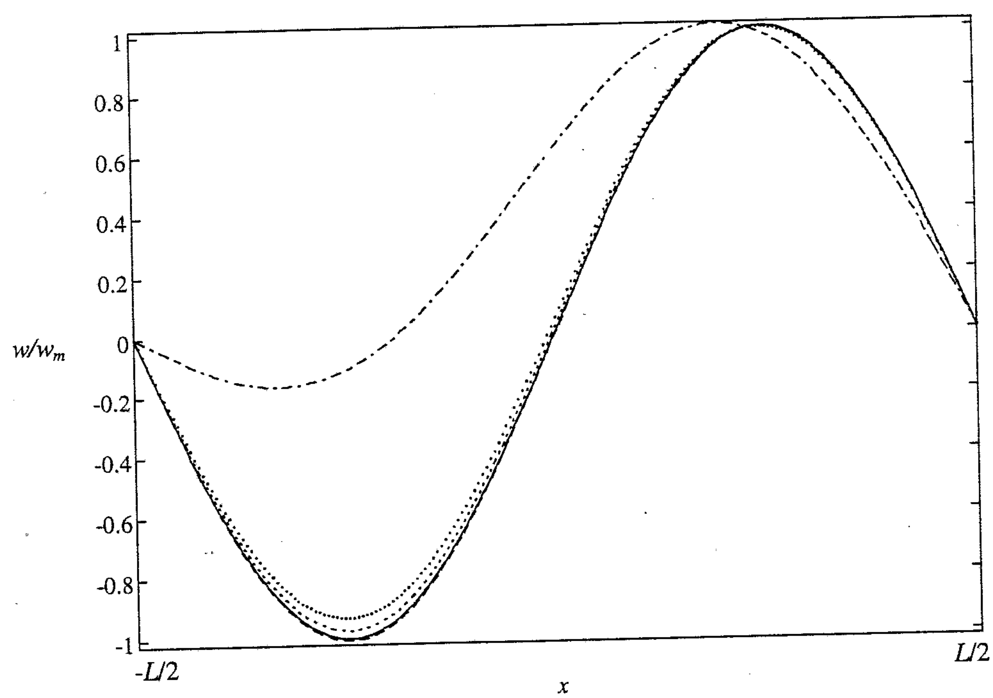

Figure 6.30 - Mode shape of the third harmonic for points of the secondary branch
—·· $\omega/\omega_{\ell 1}$=1.3025, ... $\omega/\omega_{\ell 1}$=1.3520, --- $\omega/\omega_{\ell 1}$=1.4105, — $\omega/\omega_{\ell 1}$=1.5304,
- - $\omega/\omega_{\ell 1}$=1.6469

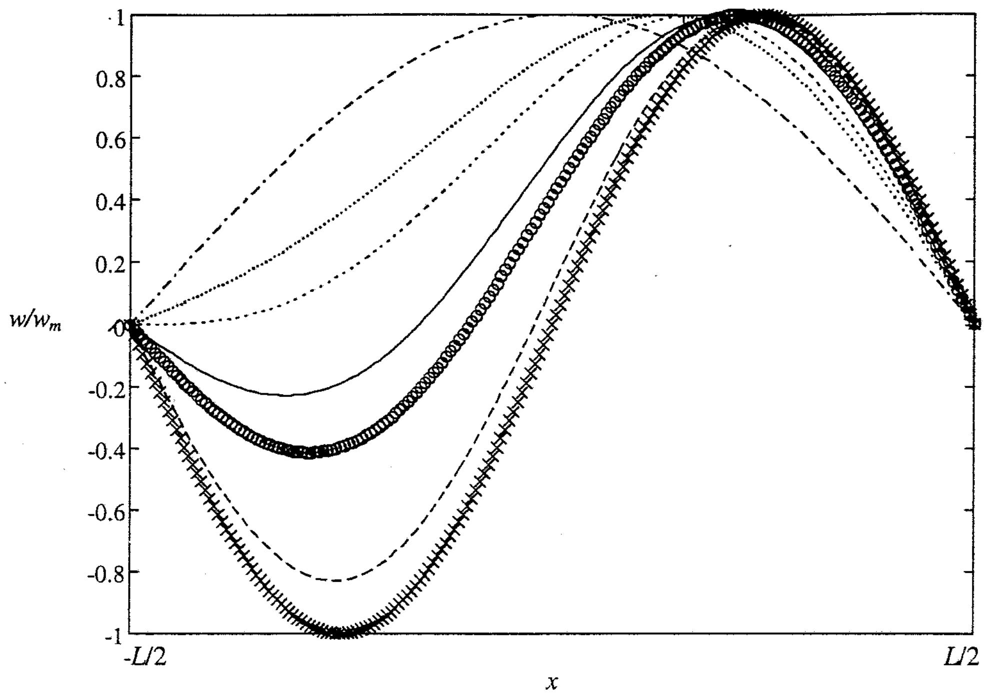

Figure 6.31 - Sum of first and third harmonic for points of the secondary branch at $t=2\pi mT$.— - $\omega/\omega_{\ell 1}=1.3025$, ... $\omega/\omega_{\ell 1}=1.3520$, --- $\omega/\omega_{\ell 1}=1.4105$,— $\omega/\omega_{\ell 1}=1.5304$, o $\omega/\omega_{\ell 1}=1.5892$, - - $\omega/\omega_{\ell 1}=1.6469$, + $\omega/\omega_{\ell 1}=1.6501$.

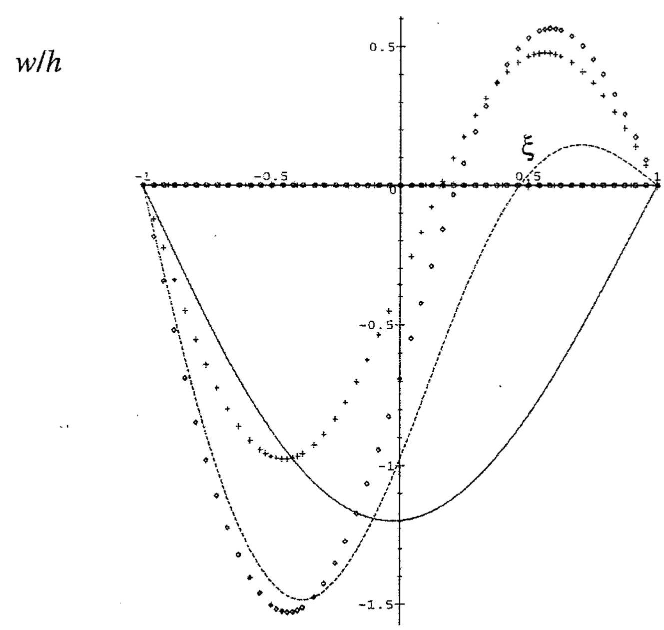

Figure 6.32 - Vibration of *ss* beam at $\omega/\omega_{\ell 1} = 1.693$. Plots at o $t=T/4$, + $(1/24)T+T/4$, ◊ $(2/24)T+T/4$, -- $(3/24)T+T/4$, —$(4/24)T+T/4$

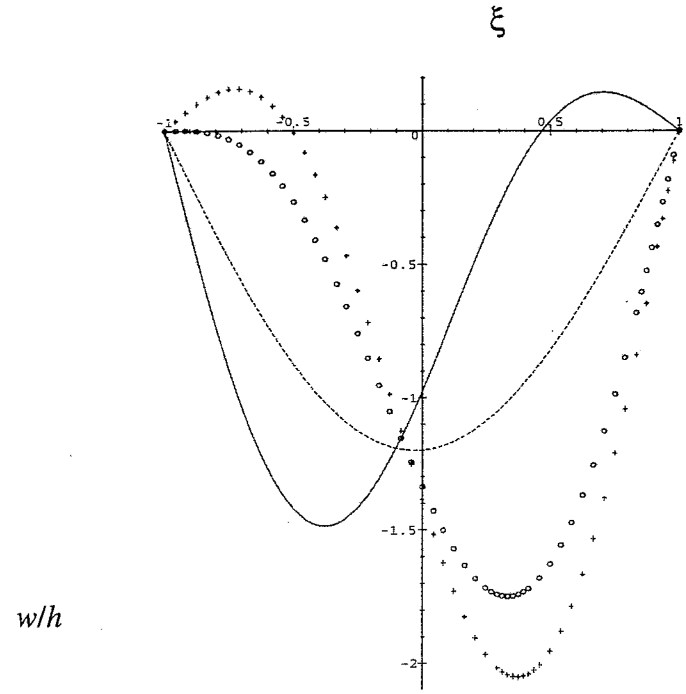

Figure 6.33 - Vibration of *ss* beam at $\omega/\omega_{\ell 1}$=1.693. Plots at
o t= (5/24)T+T/4, + (6/24)T+T/4, o (7/24)T+T/4, -- (8/24)T+T/4,
— (9/24)T+T/4

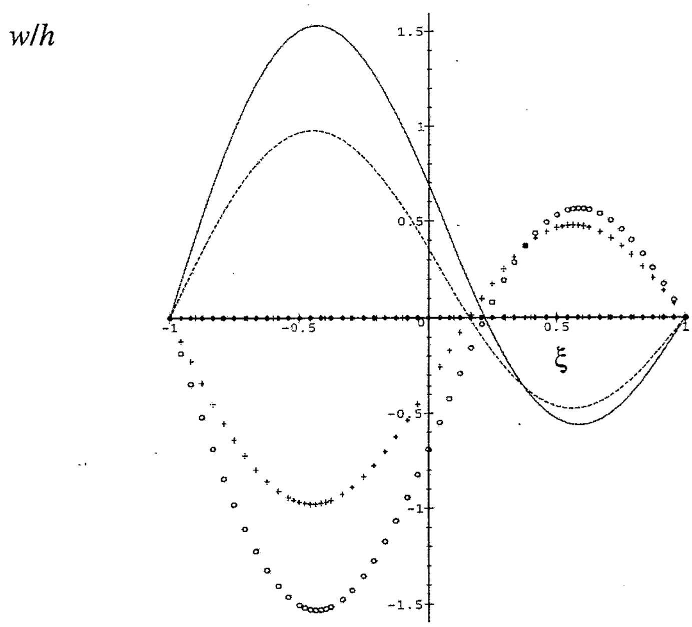

Figure 6.34 - Vibration of *ss* beam at $\omega/\omega_{\ell 1}$= 1.693. Plots at
o t= (10/24)T+T/4, + (11/24)T+T/4, ◊ (12/24)T+T/4, -- (13/24)T+T/4,
— (14/24)T+T/4

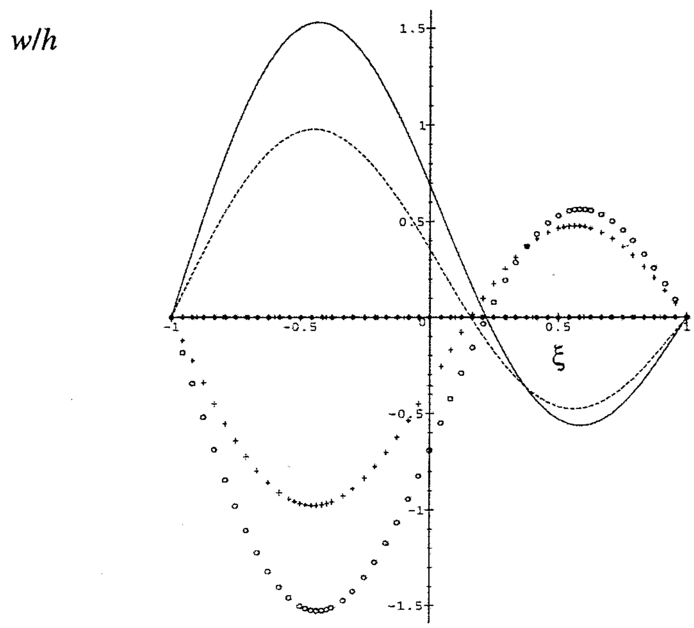

Figure 6.35 - Vibration of *ss* beam at $\omega/\omega_{\ell 1}$=1.693. Plots at
o t= (15/24)T+T/4, + (16/24)T+T/4, ◊ (17/24)T+T/4, -- (18/24)T+T/4,
— (19/24)T+T/4

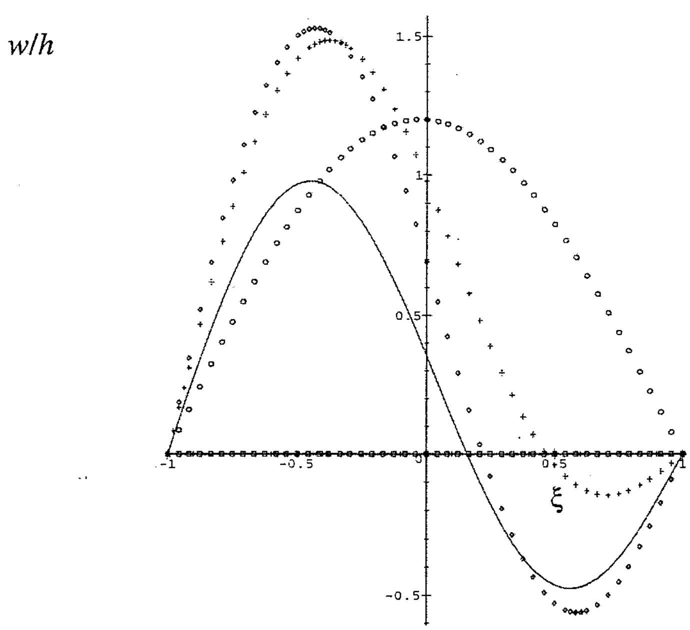

Figure 6.36 - Vibration of *ss* beam at $\omega/\omega_{\ell 1}$=1.693. Plots at
o t= (20/24)T+T/4, + (21/24)T+T/4, ◊ (22/24)T+T/4,
— (23/24)T+T/4, □ T+T/4

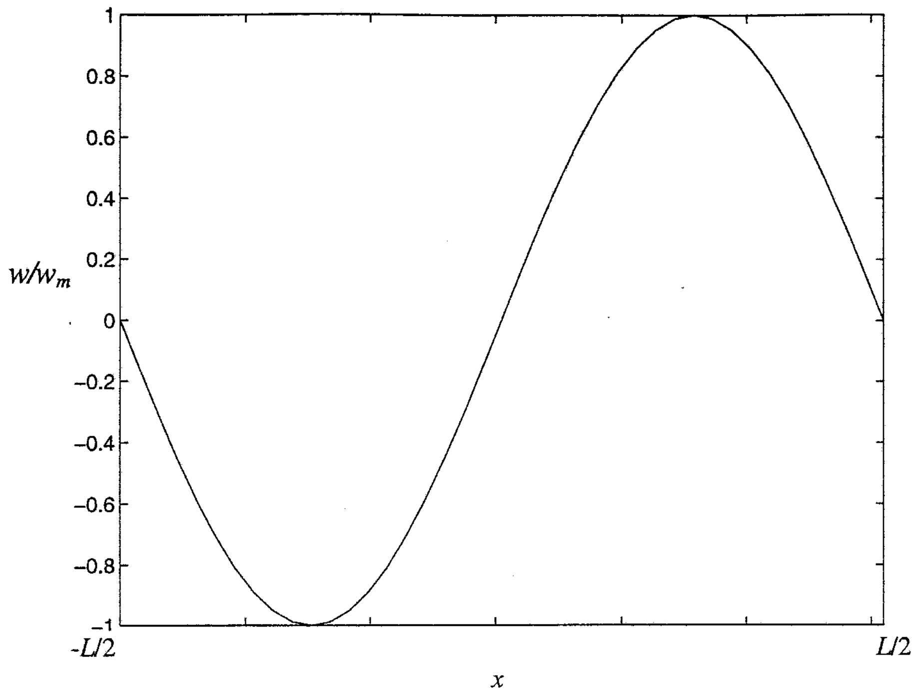

Figure 6.37 - Nonlinear mode shapes of the third or second main branch.

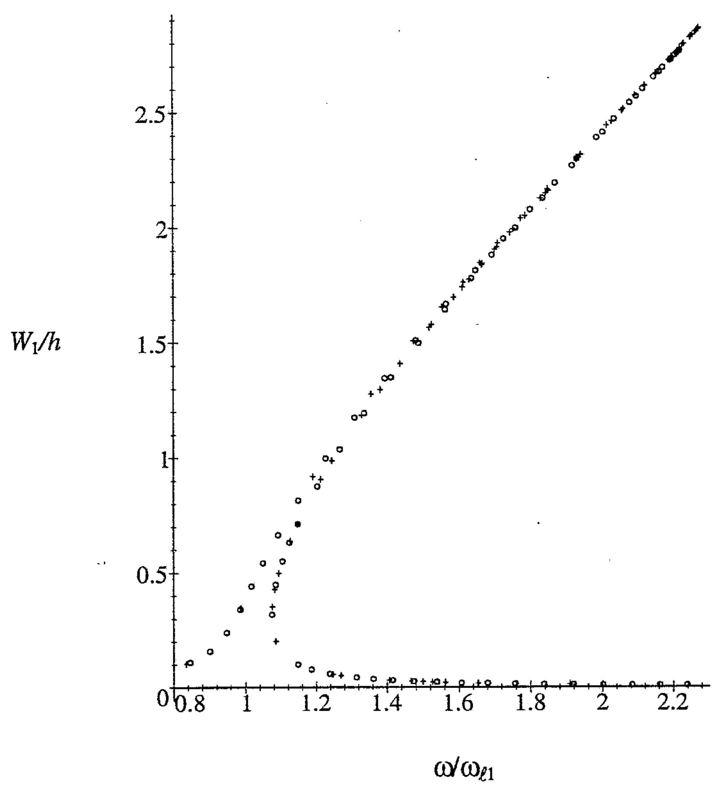

Figure 6.38 - Amplitude of first harmonic (at x=0) due to point harmonic excitation of 0.03 N amplitude, applied in the middle of *cc* beam: + harmonic solution, o two-harmonics solution. α=0.01, p_o=7, p_i=10.

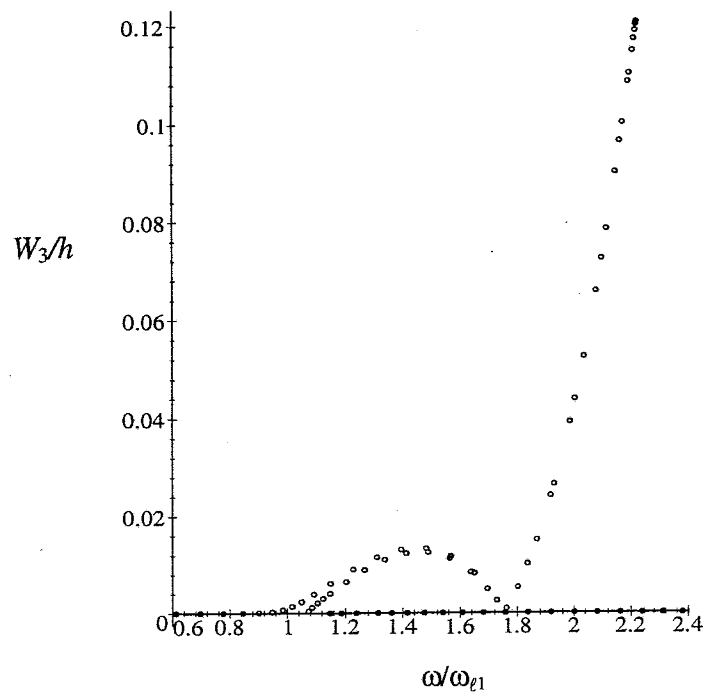

Figure 6.39 - Amplitude (at x=0) of third harmonic due to point harmonic excitation of 0.03 N amplitude, applied in the middle of cc beam, two-harmonics solution. α=0.01, p_o=7, p_i=10.

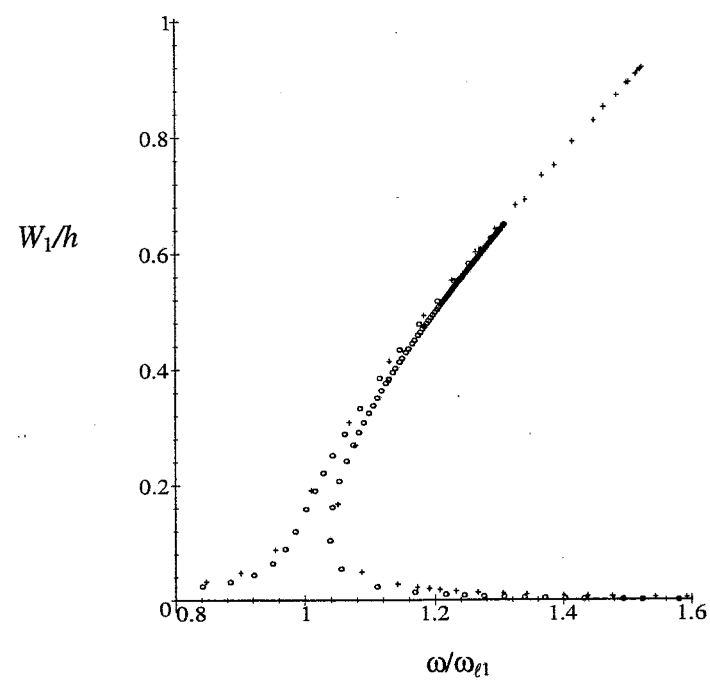

Figure 6.40 - Amplitude of first harmonic (at x=L/4) due to point harmonic excitation of 0.02 N amplitude, applied at x=L/4 (cc beam): + harmonic solution, o two-harmonics solution. α=0.01, p_o=7, p_i=10. First mode.

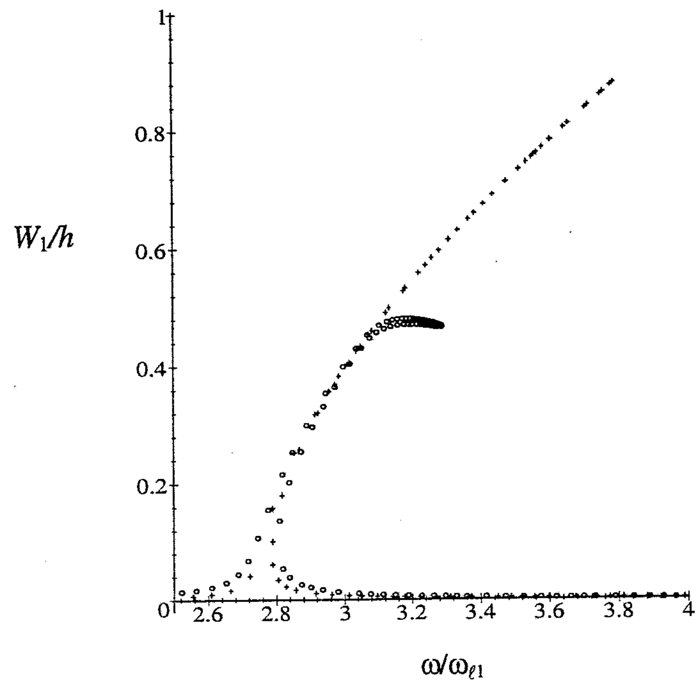

Figure 6.41 - Amplitude of first harmonic (at x=L/4) due to point harmonic excitation of 0.02 N amplitude, applied at x=L/4 (cc beam): + harmonic solution, o two-harmonics solution. α=0.01, p_o=7, p_i=10. Second mode.

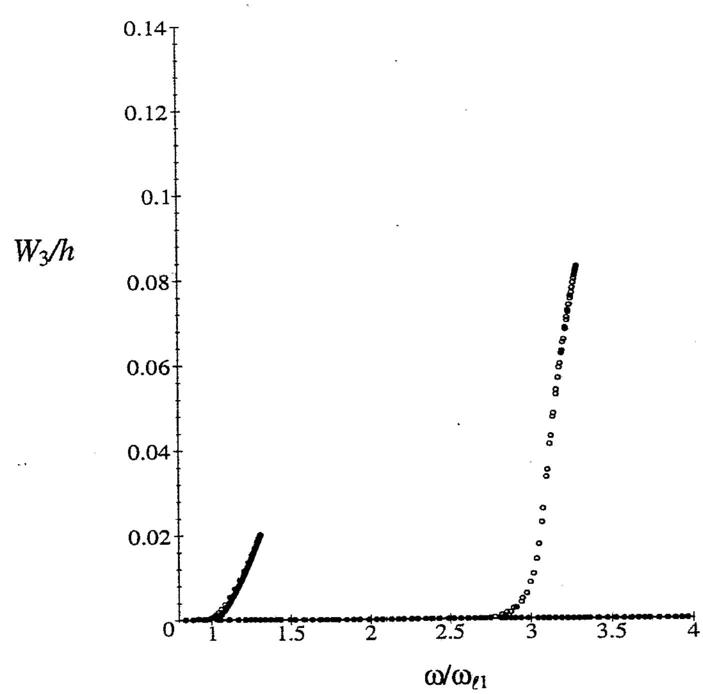

Figure 6.42 - Amplitude (at x=L/4) of third harmonic due to point harmonic excitation of 0.02 N amplitude, applied at x=L/4 (cc beam), two-harmonics solution. α=0.01, p_o=7, p_i=10.

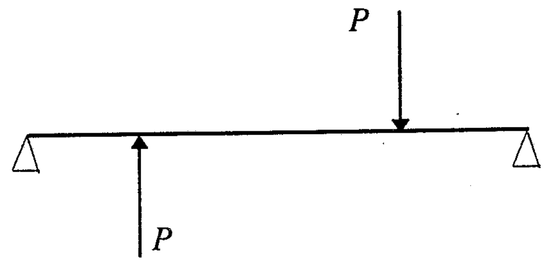

Figure 6.43 - Antissymetric excitation

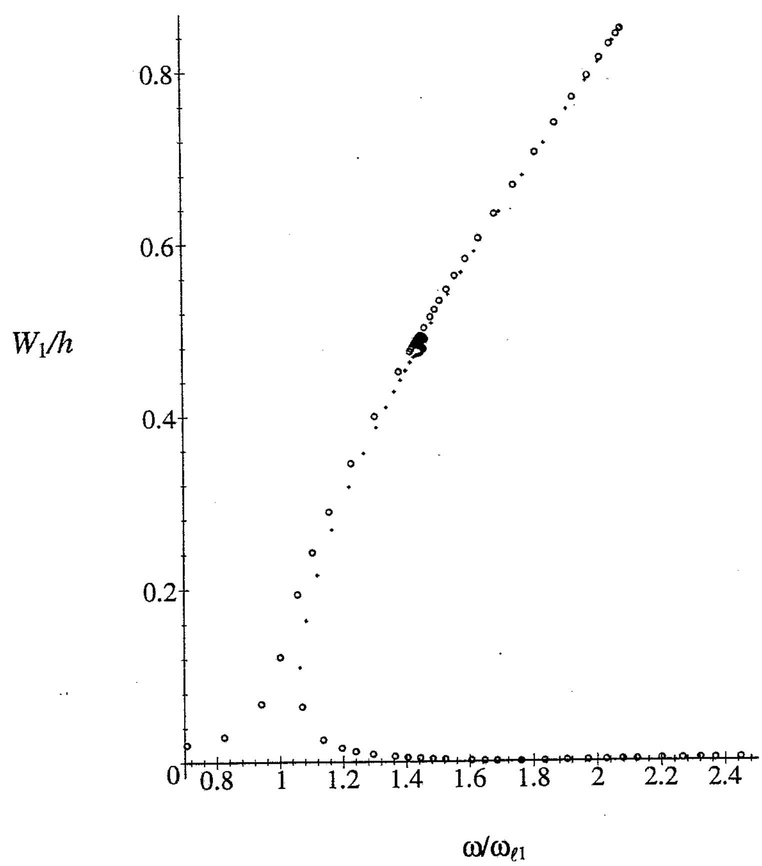

Figure 6.44 - Amplitude of first harmonic (at $x=L/4$) due to antissymmetric excitation: + unstable solution, o stable solution. $\alpha=0.01$, $p_o=10$, $p_i=10$.

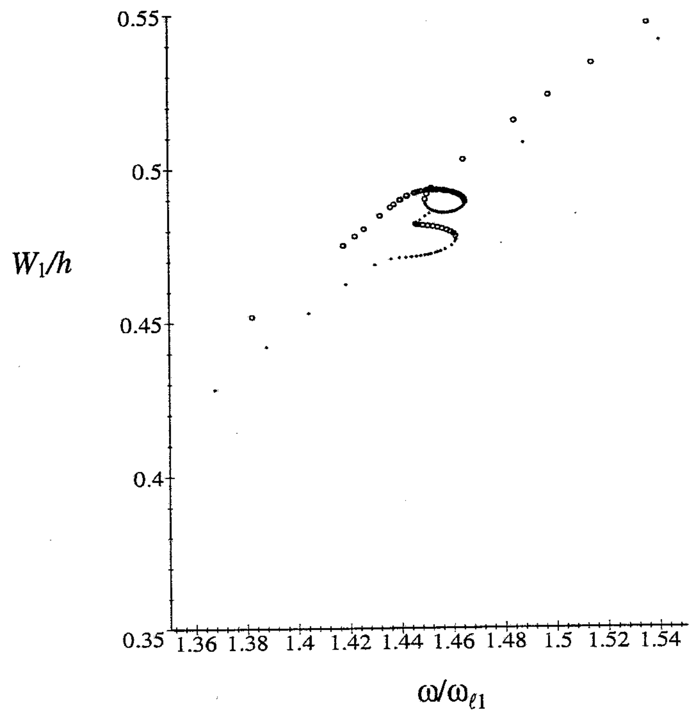

Figure 6.45 - Detail of internal resonance from Figure 6.44.

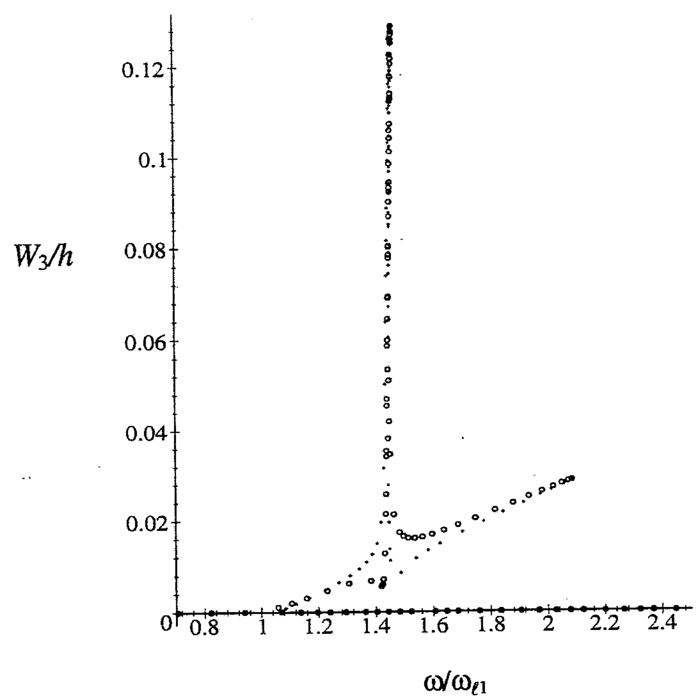

Figure 6.46 - Amplitude of third harmonic (at $x=L/4$) due to antissymmetric excitation: + unstable solution, o stable solution. $\alpha=0.01$, $p_o=10$, $p_i=10$.

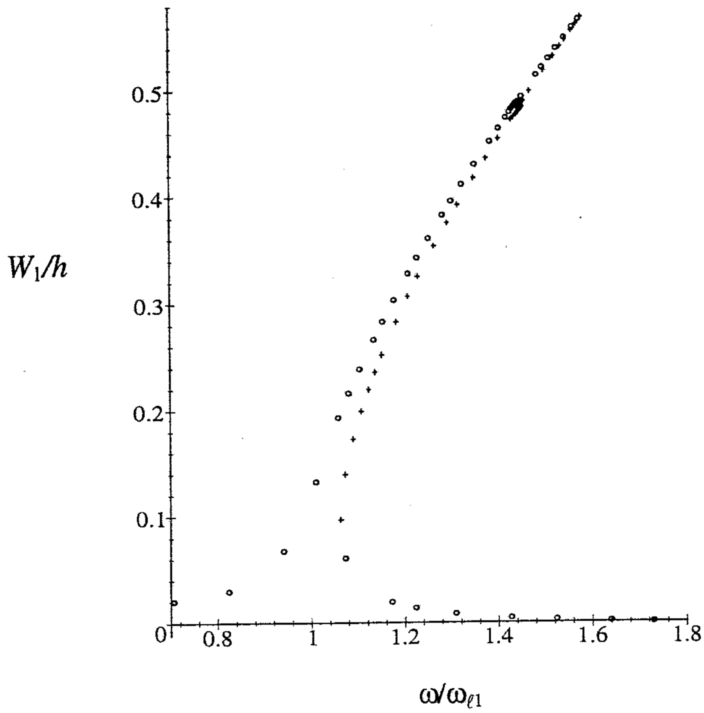

Figure 6.47 - Amplitude of first harmonic (at $x=L/4$) due to antissymmetric excitation: + unstable solution, o stable solution. $\alpha=0.015$, $p_o=10$, $p_i=10$.

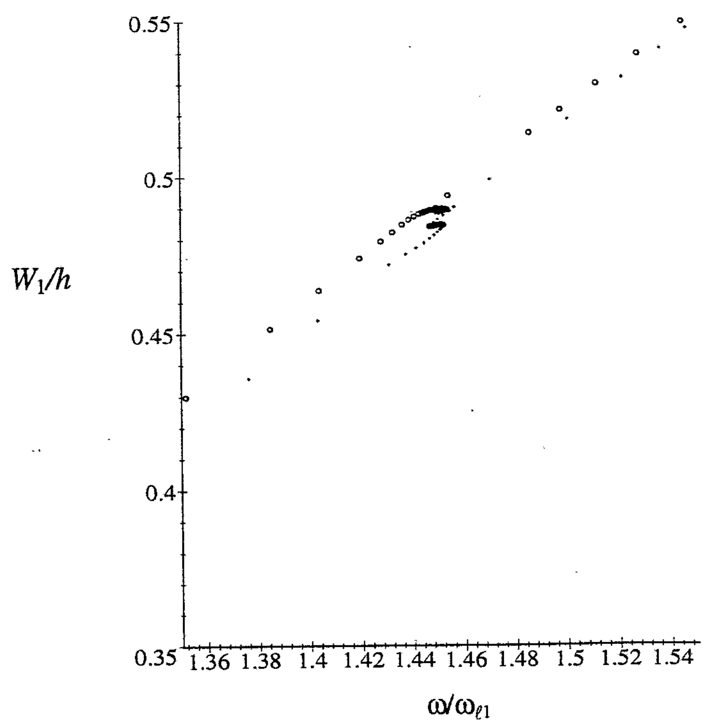

Figure 6.48 - Detail of internal resonance from figure 6.47.

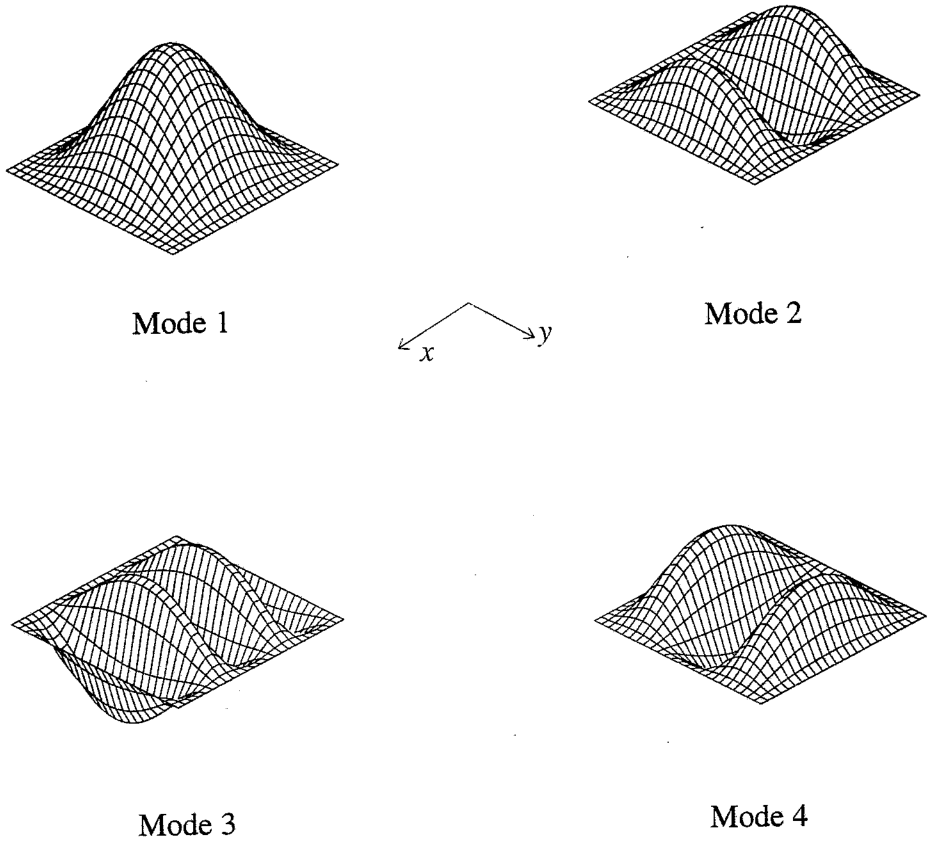

Figure 7.1 - First four bi-symmetric linear modes of vibration of Plate 1. p_o=5.

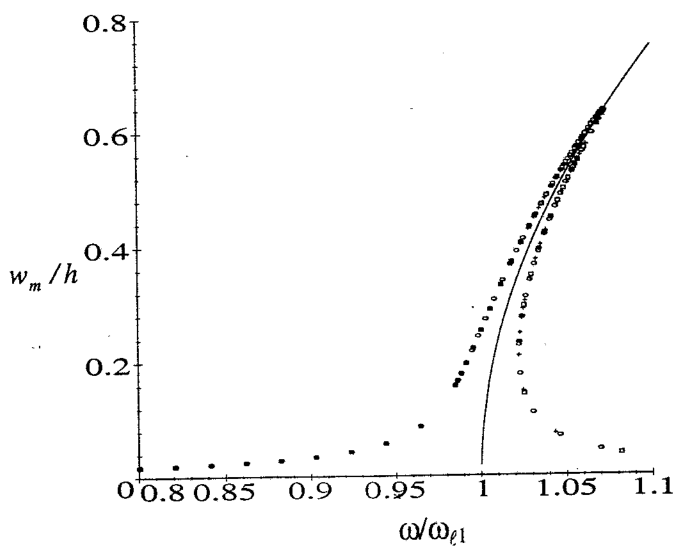

Figure 7.2 - Convergence with p_o in the vicinity of the first mode. FRFs:□ p_o=2, o p_o= 3, + p_o=4; Backbone curves: —.

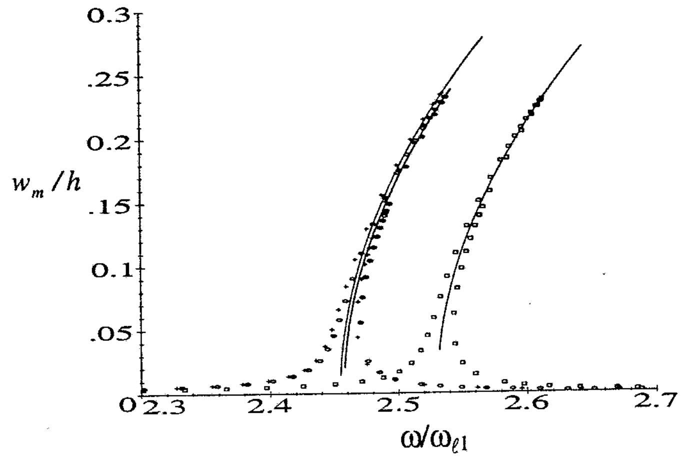

Figure 7.3 - Convergence with p_o in the vicinity of the second mode. Legend as in Fig. 7.2.

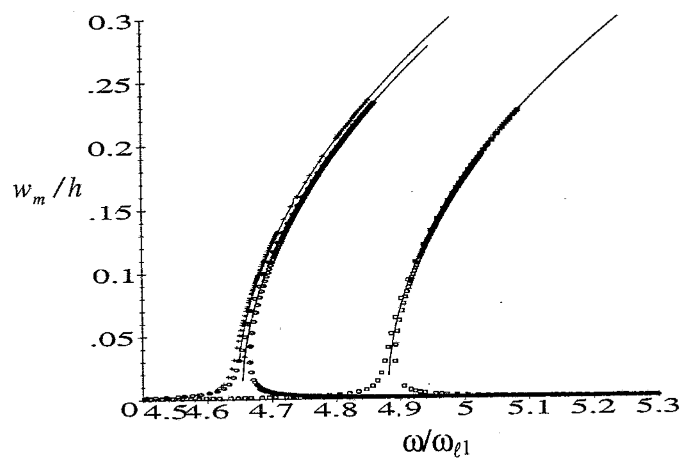

Figure 7.4 - Convergence with p_o in the vicinity of the third mode. Legend as in Figure 7.2.

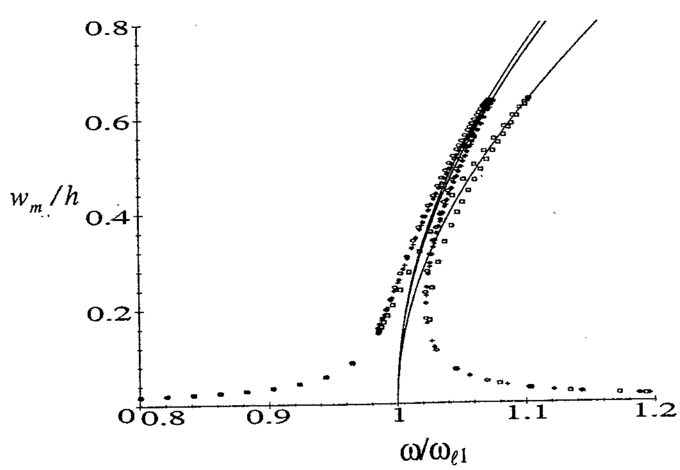

Figure 7.5 - Convergence with p_i in the vicinity of the first mode. FRFs:□ $p_i = 0$, + $p_i = 4$, ◊ $p_i = 5$, o p_i=6; Backbone curves: —.

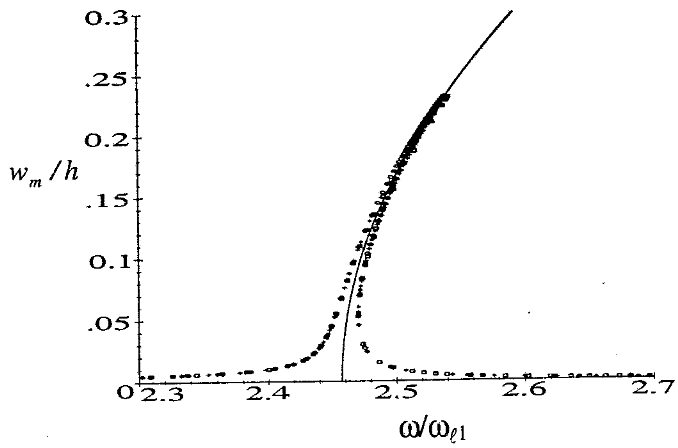

Figure 7.6 - Convergence with p_i in the vicinity of the second mode. FRFs:□ p_i = 0, + p_i = 3, ◊ p_i = 4, o p_i=5; Backbone curves: —.

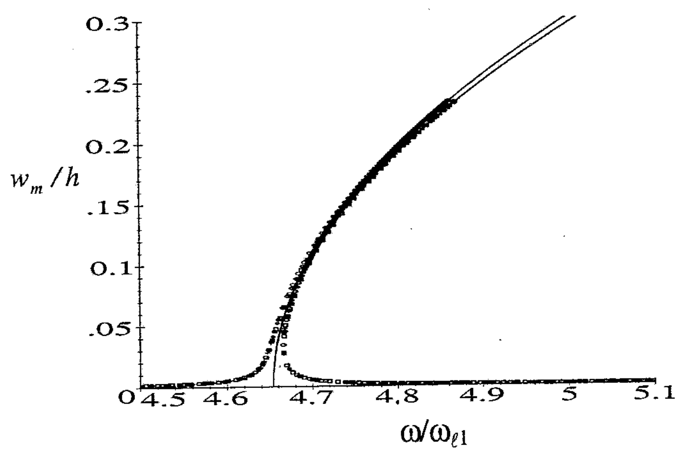

Figure 7.7 - Convergence with p_i in the vicinity of the third mode. Legend as in Fig. 7.6.

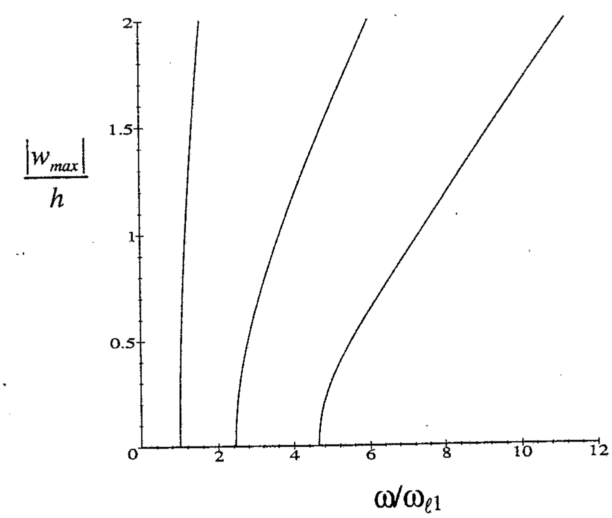

Figure 7.8 - Backbone curves of first three double-symmetric modes of vibration of Plate 1. p_o=5, p_i=6. $(x, y) = (0,0)$.

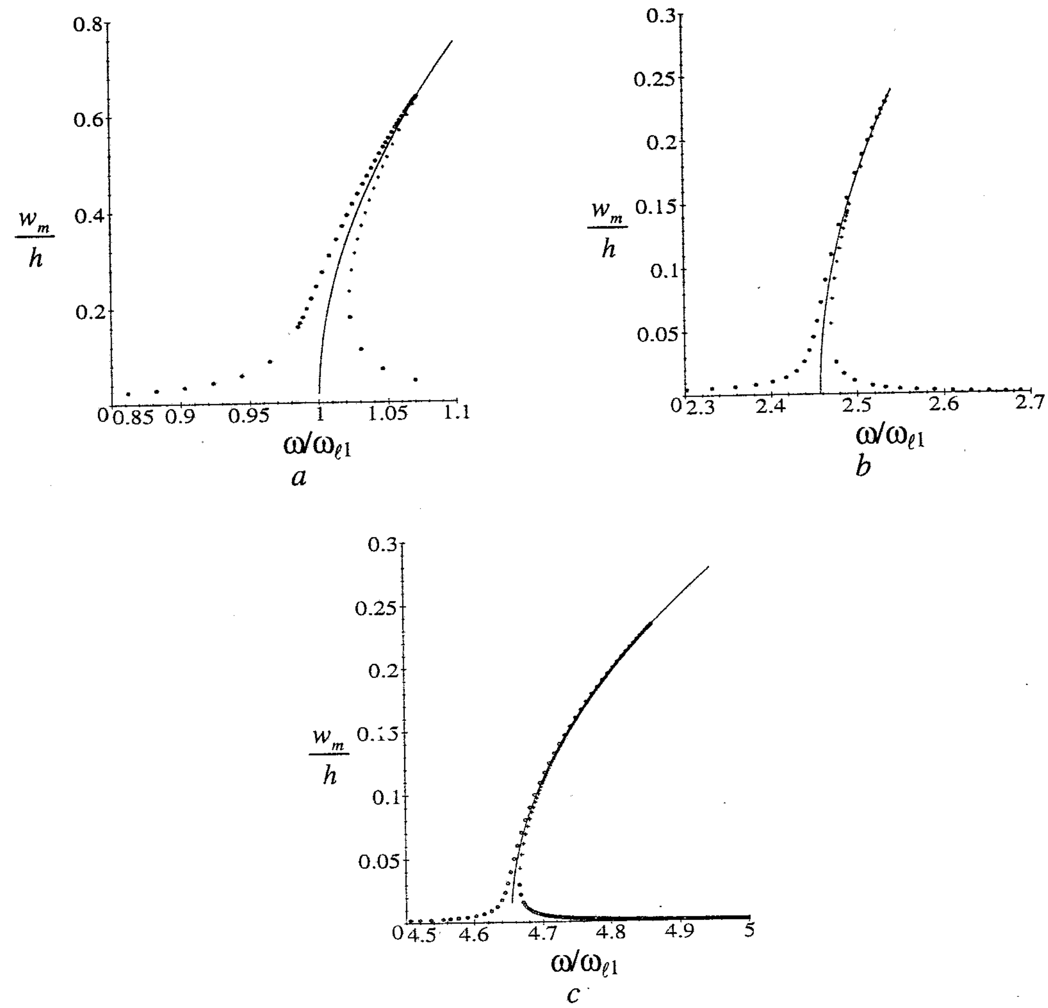

Figure 7.9 - FRF in the vicinity of the first (a), second (b) and third (c) double-symmetric modes. o stable solutions, + unstable solutions. Plate 1. $(x, y) = (0,0)$.

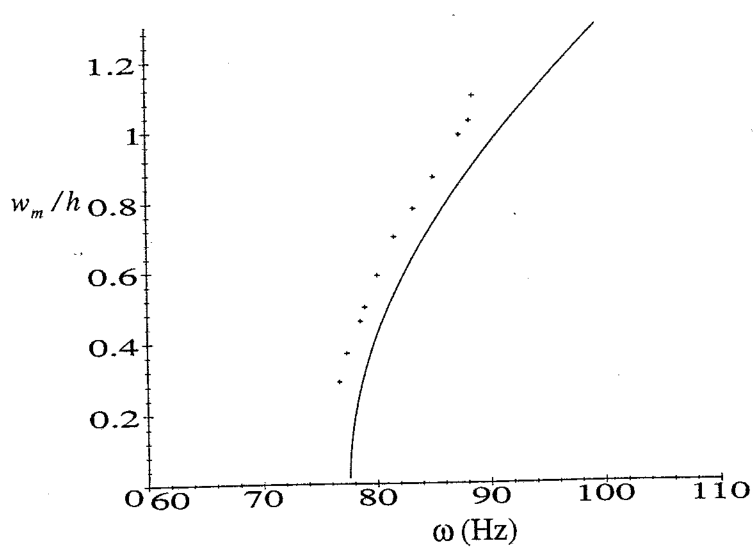

Figure 7.10 - Comparison between the first resonance frequency predicted by the HFEM, —, and the measured one, + [7.2].

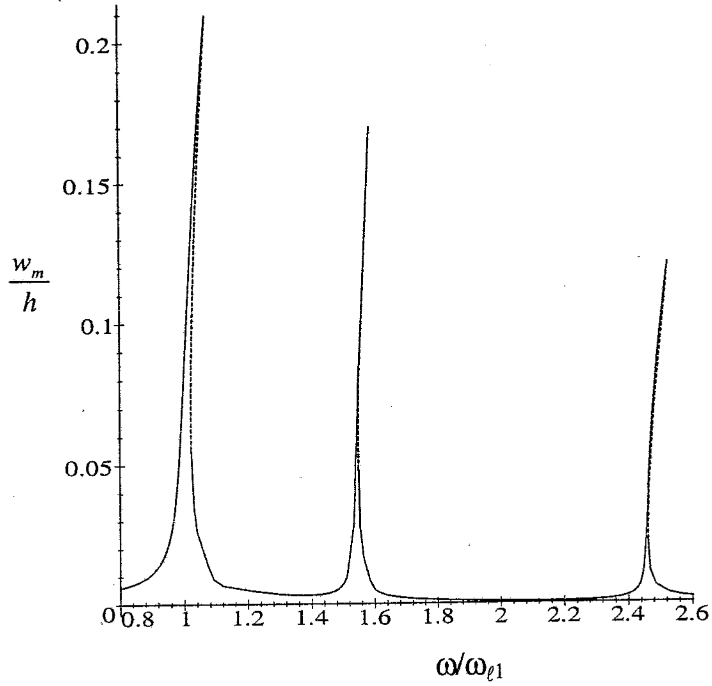

Figure 7.11 - FRF due to excitation by harmonic plane wave at grazing incidence with P_g=10 N/m^2.— stable solutions,---------- unstable solutions. $(x, y)=(a/4, b/4)$, p_o=5, p_i=6.

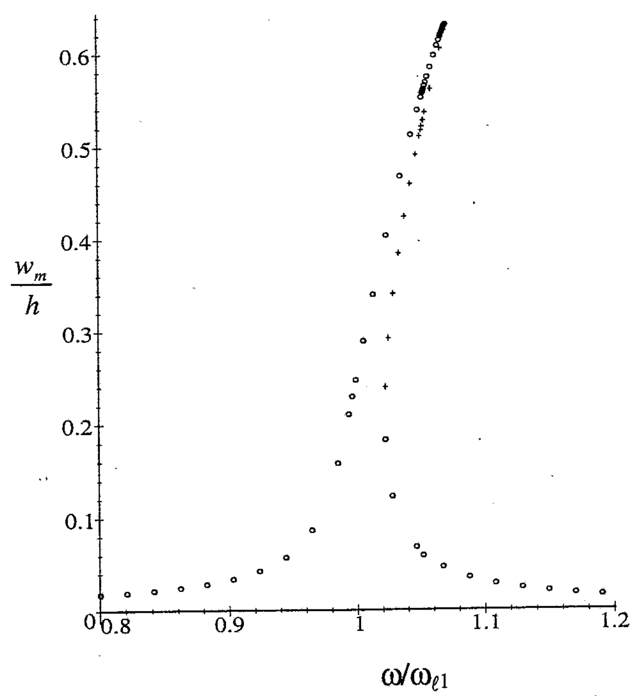

Figure 7.12 - FRF in the vicinity of the first mode due to excitation by harmonic plane wave at grazing incidence with P_g=10 N/m^2. o stable solutions, + unstable solutions. Plate 1. $(x, y) = (0,0)$, p_o=5, p_i=6.

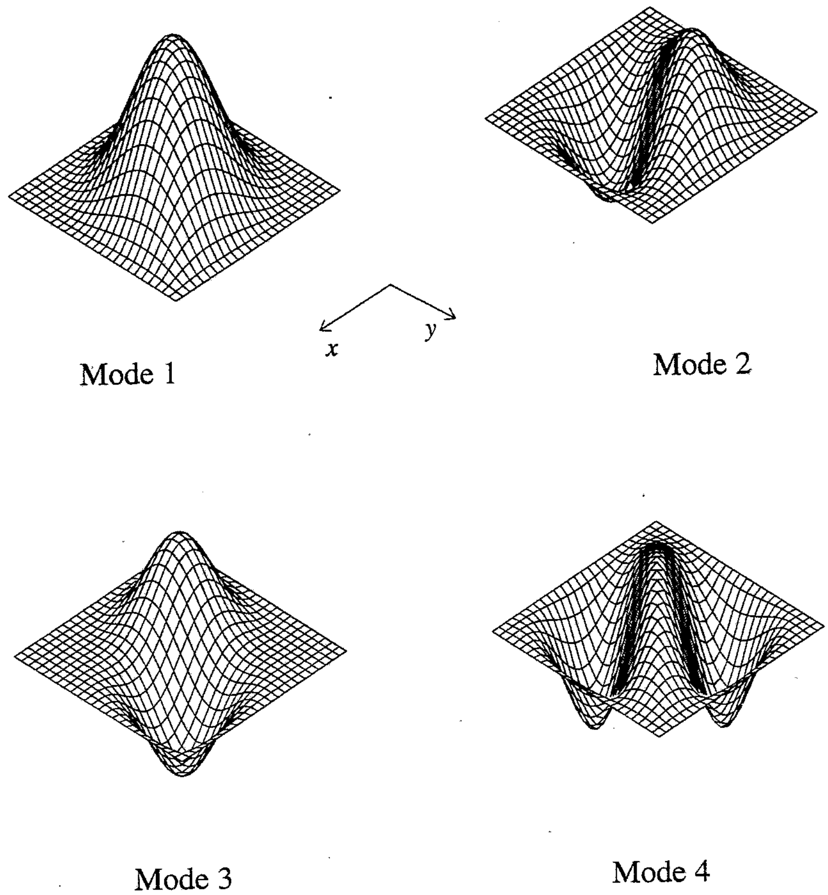

Figure 7.13 - First four linear modes of vibration of Plate 4. p_o=5.

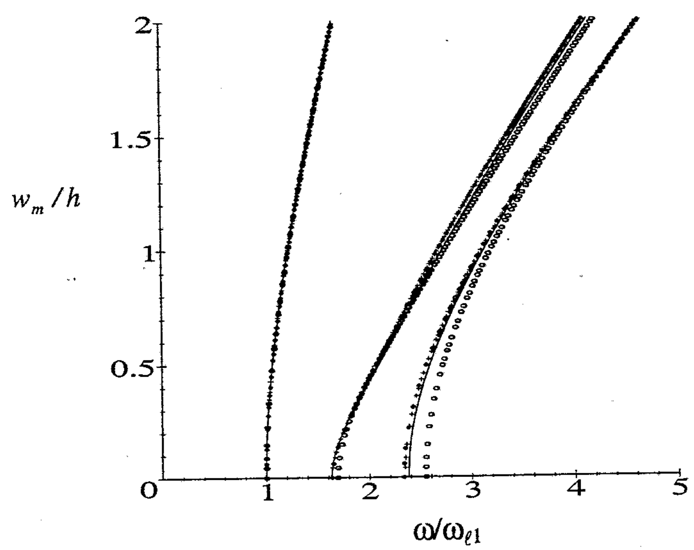

Figure 7.14 - Convergence in free vibration with p_o for the first three modes of Plate 4. $p_i = 5$ and: o $p_o = 3$, — $p_o = 4$, + $p_o = 5$, ◊ $p_o = 6$. First mode calculated at ξ=η=0, second at ξ=0.4, η=-0.4 and third at ξ=0.4,η= 0.4.

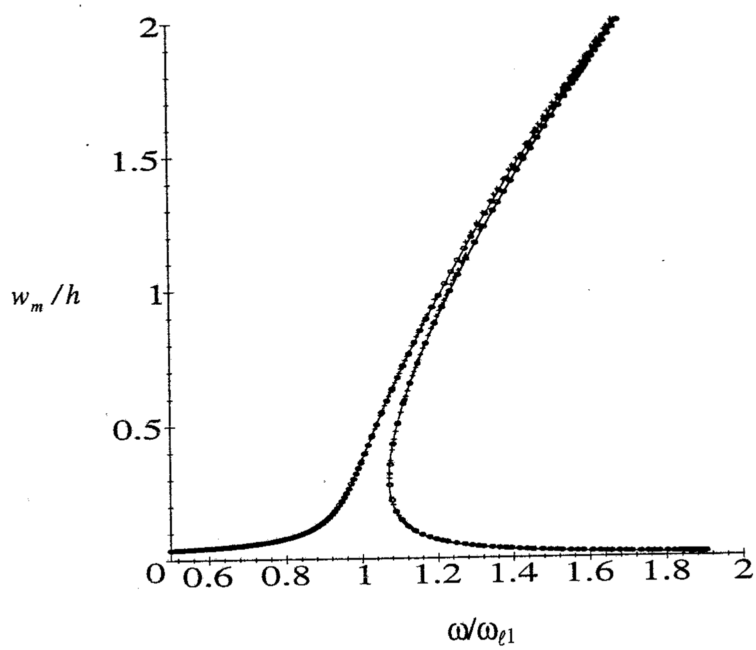

Figure 7.15 - Convergence in forced vibration with p_o. First mode.
Plate 4. P_d=1000 N/m^2. $p_i = 5$ and: + $p_o = 3$,— $p_o = 4$ and ∘ $p_o = 5$. $\xi=\eta=0$.

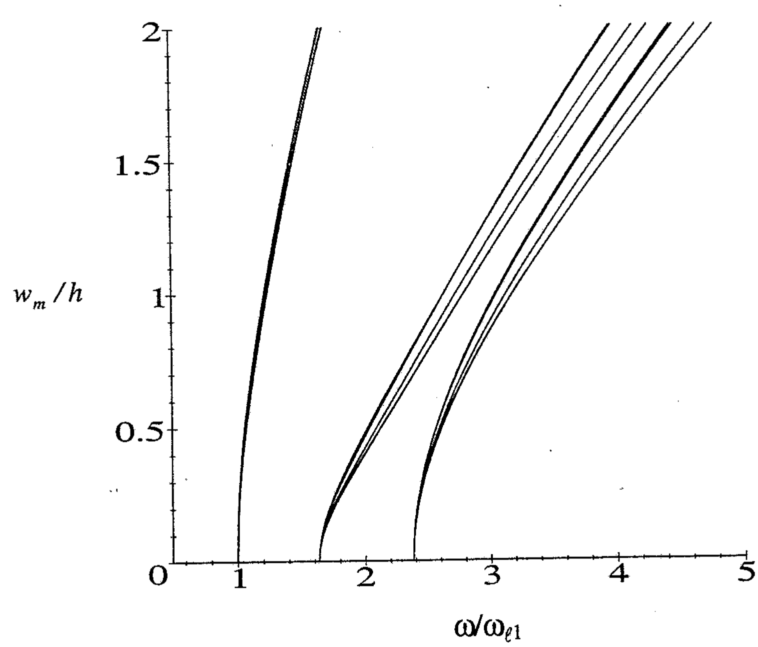

Figure 7.16 - Convergence in free vibration with p_i for Plate 4. $p_o = 4$; in each mode from right to left: $p_i = 4$, $p_i = 5$, $p_i = 6$, $p_i = 7$. First mode calculated at $\xi=\eta=0$, second at $\xi=0.4$, $\eta=-0.4$ and third at $\xi=0.4$, $\eta= 0.4$.

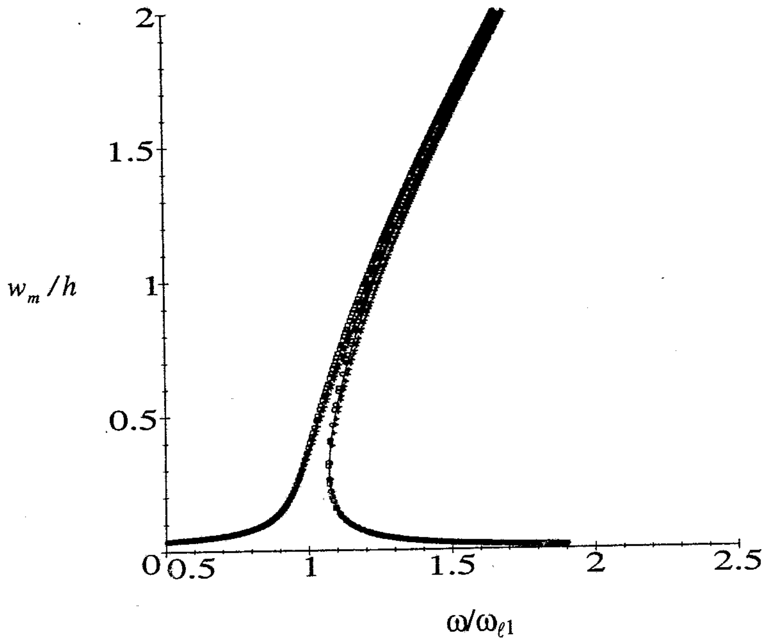

Figure 7.17 - Convergence with p_i in forced vibration. First mode. Plate 4. P_d=1000 N/m^2. $p_o = 4$ and: + $p_i = 4$, — $p_i = 5$, ∘ $p_i = 6$, □ $p_i = 7$. $\xi=\eta=0$.

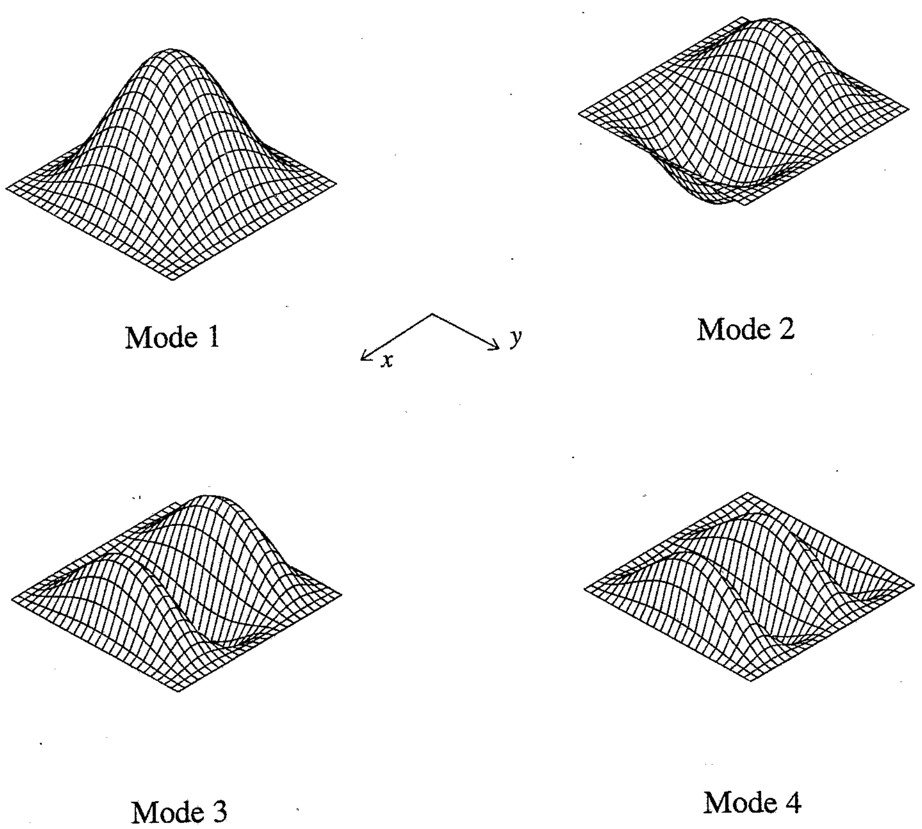

Figure 7.18 - First four linear modes of vibration of Plate 5. p_o=6.

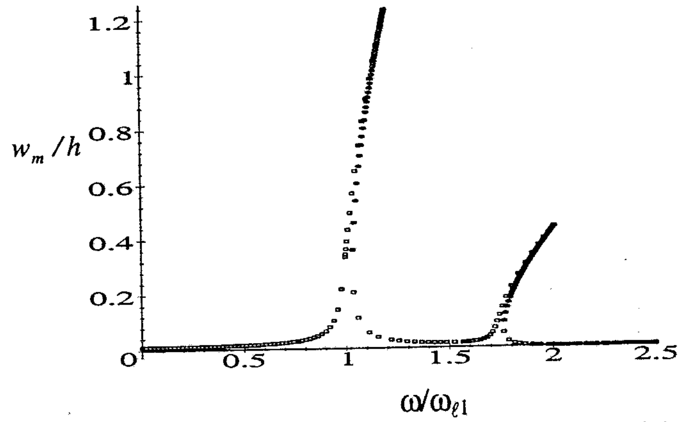

Figure 7.19 - Response to an harmonic plane wave at normal incidence, p_o=5, p_i=6 and P_d=3 N/m^2.□ stable solutions, o unstable solutions. ξ=η=0. Plate 5.

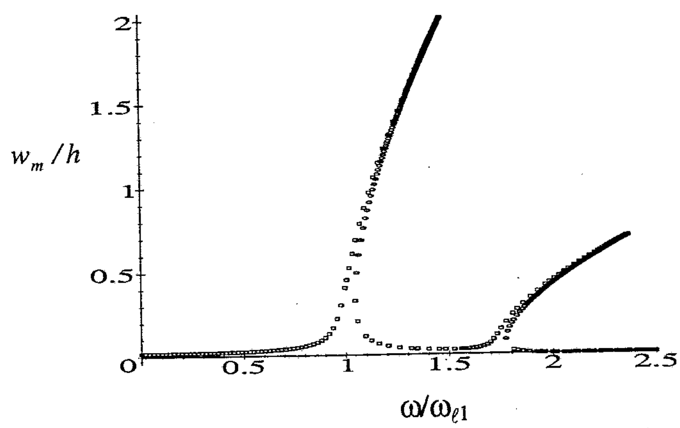

Figure 7.20 - Response to an harmonic plane wave at normal incidence, p_o=5, p_i=6 and P_d=5 N/m^2.□ stable solutions, o unstable solutions. ξ=η=0. Plate 5.

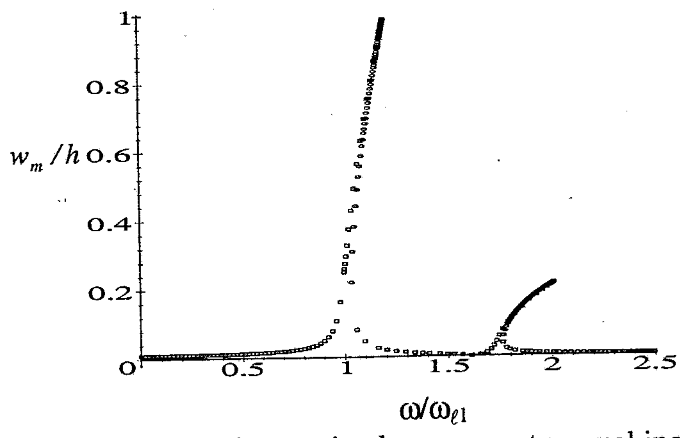

Figure 7.21 - Response to an harmonic plane wave at normal incidence, p_o=5, p_i=6 and P_d=3 N/m^2. □ stable solutions, o unstable solutions. ξ=0.4, η=0. Plate 5.

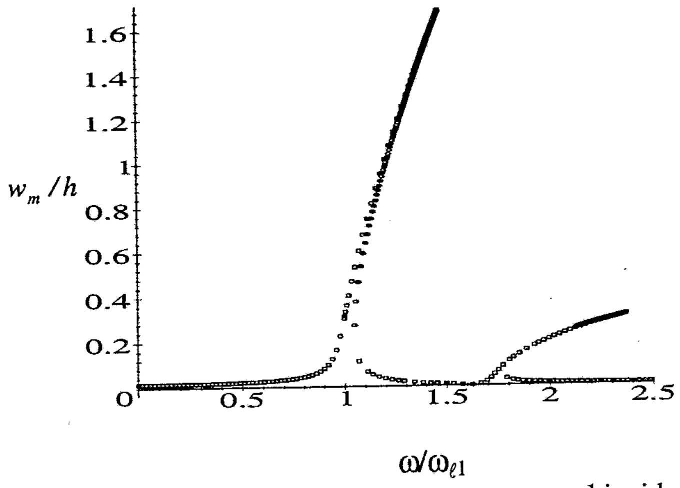

Figure 7.22 - Response to an harmonic plane wave at normal incidence, p_o=5, p_i=6 and P_d=5 N/m^2. □ stable solutions, o unstable solutions. ξ=0.4, η=0. Plate 5.

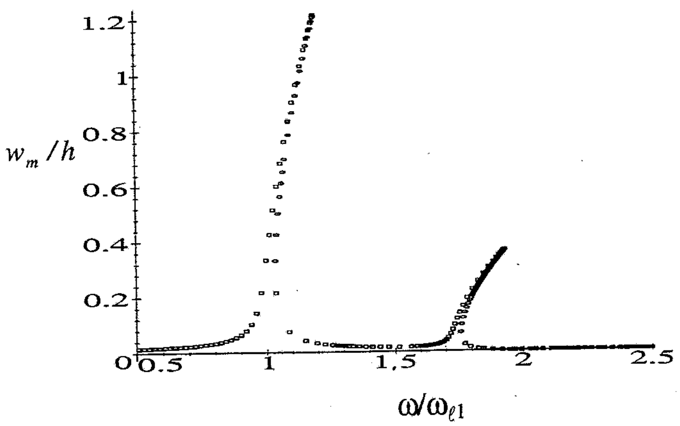

Figure 7.23 - Response to an harmonic plane wave at grazing incidence, α=0°, p_o=5, pi=6 and P_g=3 N/m^2. □ stable solutions, o unstable solutions. ξ=0, η=0. Plate 5.

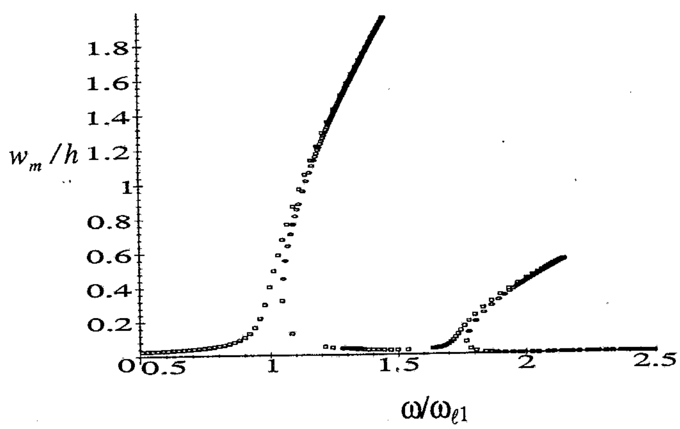

Figure 7.24 - Response to an harmonic plane wave at grazing incidence, α=0°, p_o=5, p_i=6 and P_g =5 N/m^2. □ stable solutions, o unstable solutions. ξ=0, η=0. Plate 5.

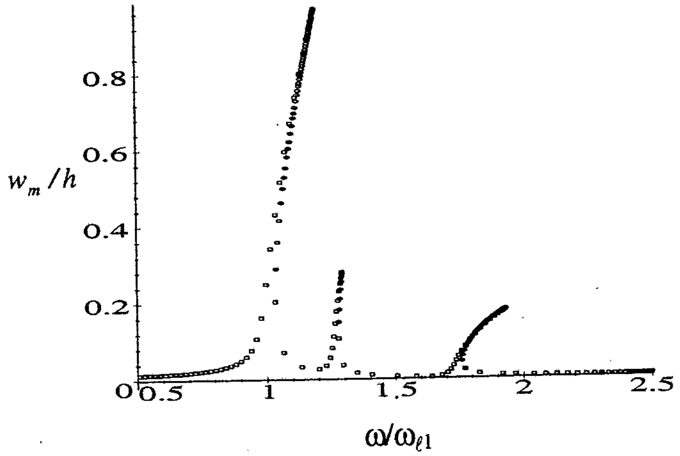

Figure 7.25 - Response to an harmonic plane wave at grazing incidence, $\alpha=0^{\circ}$, $p_o=5$, $p_i=6$ and $P_g=3$ N/m^2. □ stable solutions, o unstable solutions. $\xi=0.4$, $\eta=0$.

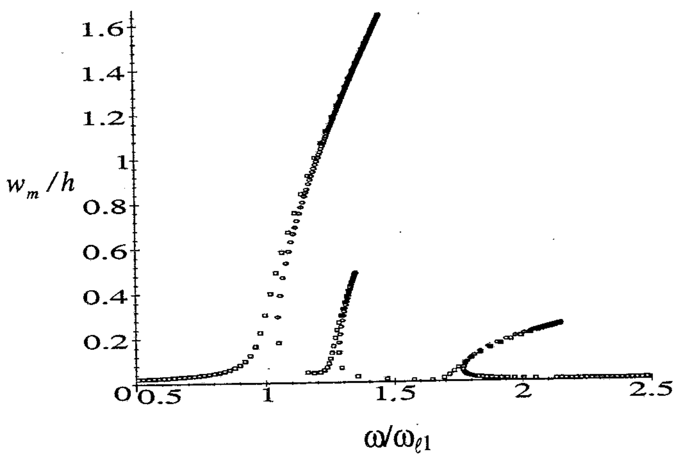

Figure 7.26 - Response to an harmonic plane wave at grazing incidence, $\alpha=0^{\circ}$, $p_o=5$, $p_i=6$ and $P_g=5$ N/m^2. □ stable solutions, o unstable solutions. $\xi=0.4$, $\eta=0$.

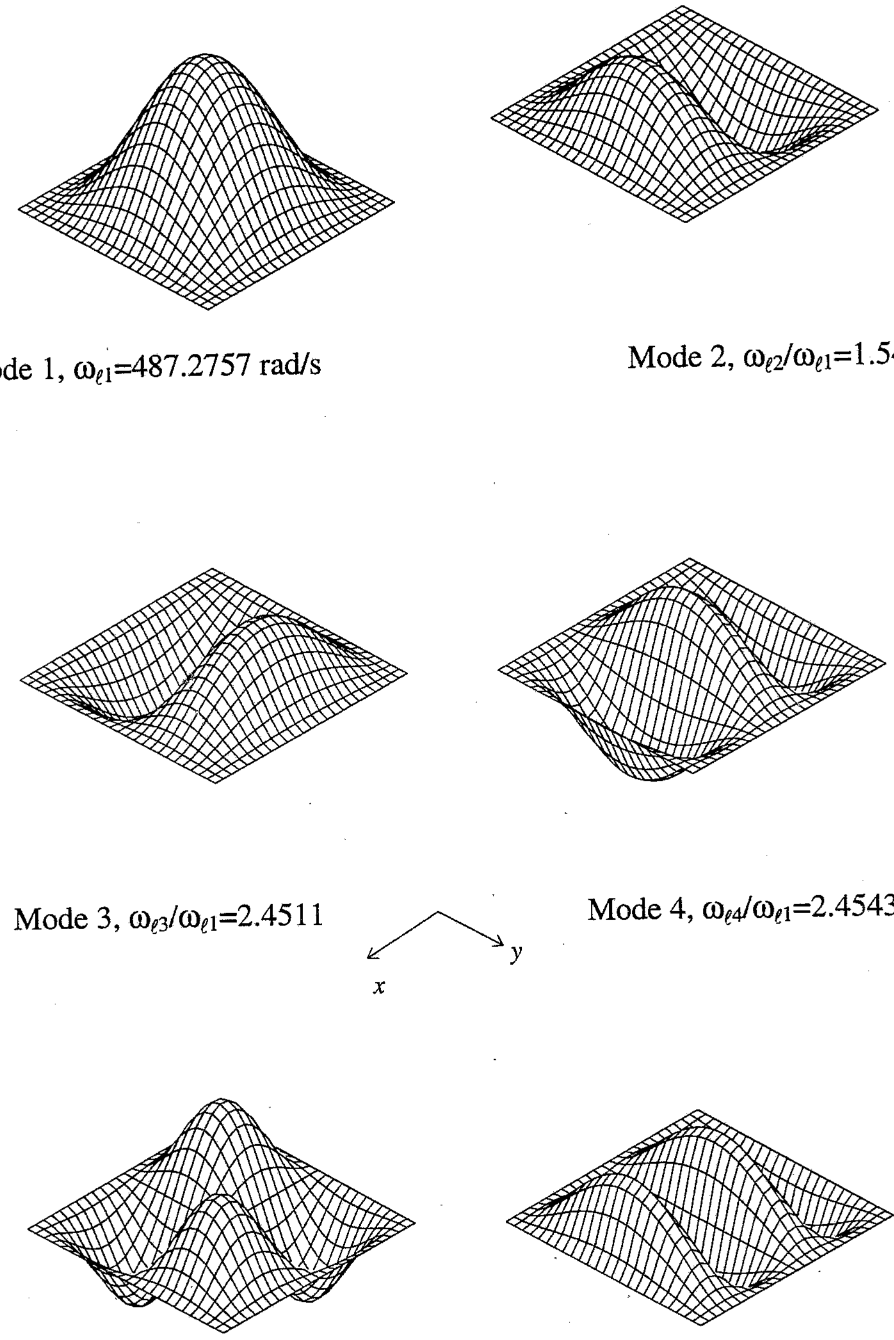

Mode 1, $\omega_{\ell 1}$=487.2757 rad/s

Mode 2, $\omega_{\ell 2}/\omega_{\ell 1}$=1.5407

Mode 3, $\omega_{\ell 3}/\omega_{\ell 1}$=2.4511

Mode 4, $\omega_{\ell 4}/\omega_{\ell 1}$=2.4543

Mode 5, $\omega_{\ell 5}/\omega_{\ell 1}$=2.9545

Mode 6, $\omega_{\ell 6}/\omega_{\ell 1}$=3.7170

Figure 8.1a - First to sixth linear mode shapes and natural frequencies of Plate 1. p_o=10.

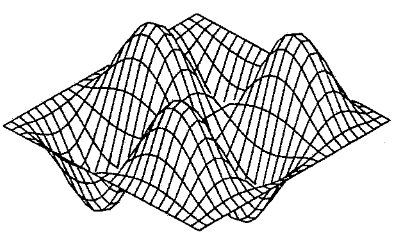

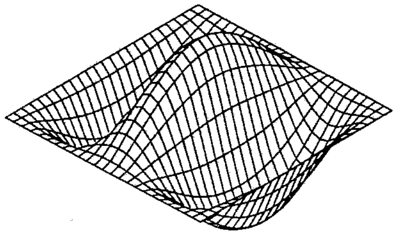

Mode 7, $\omega_{\ell 7}/\omega_{\ell 1}$=3.8128

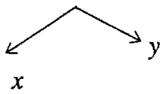

Mode 8, $\omega_{\ell 8}/\omega_{\ell 1}$=4.6456

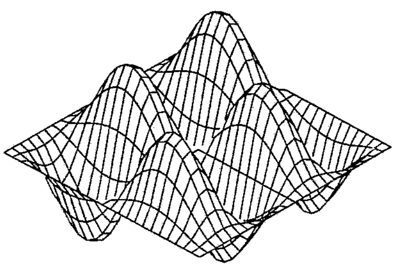

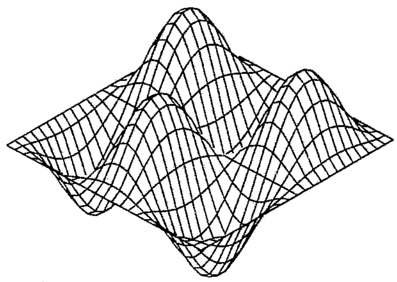

Mode 9, $\omega_{\ell 9}/\omega_{\ell 1}$=5.0260

Mode 10, $\omega_{\ell 10}/\omega_{\ell 1}$=5.1367

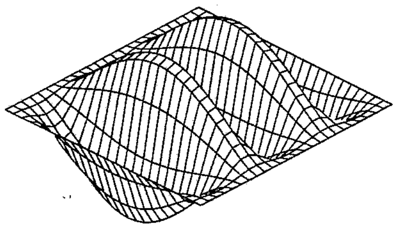

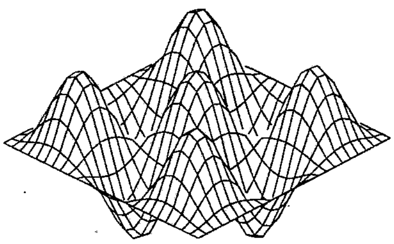

Mode 11, $\omega_{\ell 11}/\omega_{\ell 1}$=5.3175

Mode 12, $\omega_{\ell 12}/\omega_{\ell 1}$=5.9682

Figure 8.1*b* - Seventh to twelveth linear mode shapes and natural frequencies of Plate 1. p_o=10.

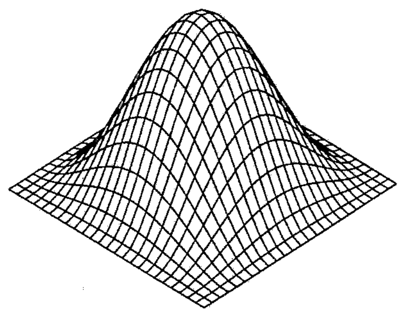

Mode 1, $\omega_{\ell 1}$=579.4412 rad/s

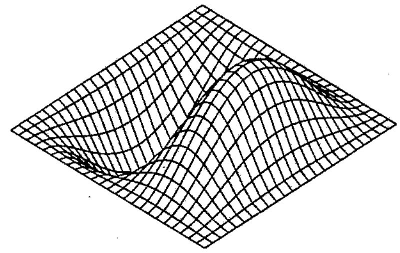

Mode 2, $\omega_{\ell 2}/\omega_{\ell 1}$=1.9583

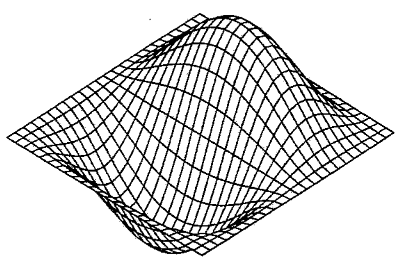

Mode 3, $\omega_{\ell 3}/\omega_{\ell 1}$=2.1181

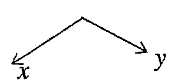

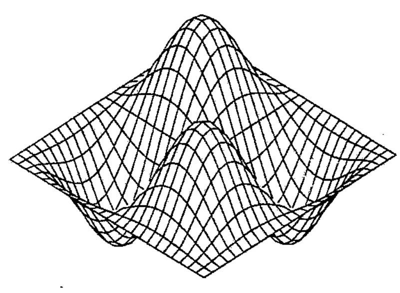

Mode 4, $\omega_{\ell 4}/\omega_{\ell 1}$=3.0057

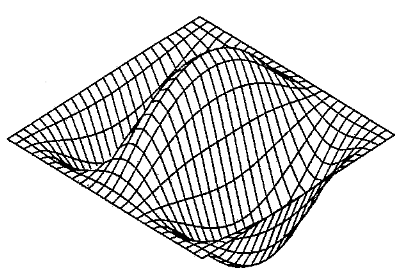

Mode 5, $\omega_{\ell 5}/\omega_{\ell 1}$=3.4712

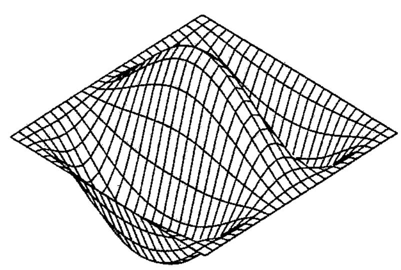

Mode 6, $\omega_{\ell 6}/\omega_{\ell 1}$=3.8523

Figure 8.2*a* - First to sixth linear mode shapes and natural frequencies of Plate 3. p_o=10.

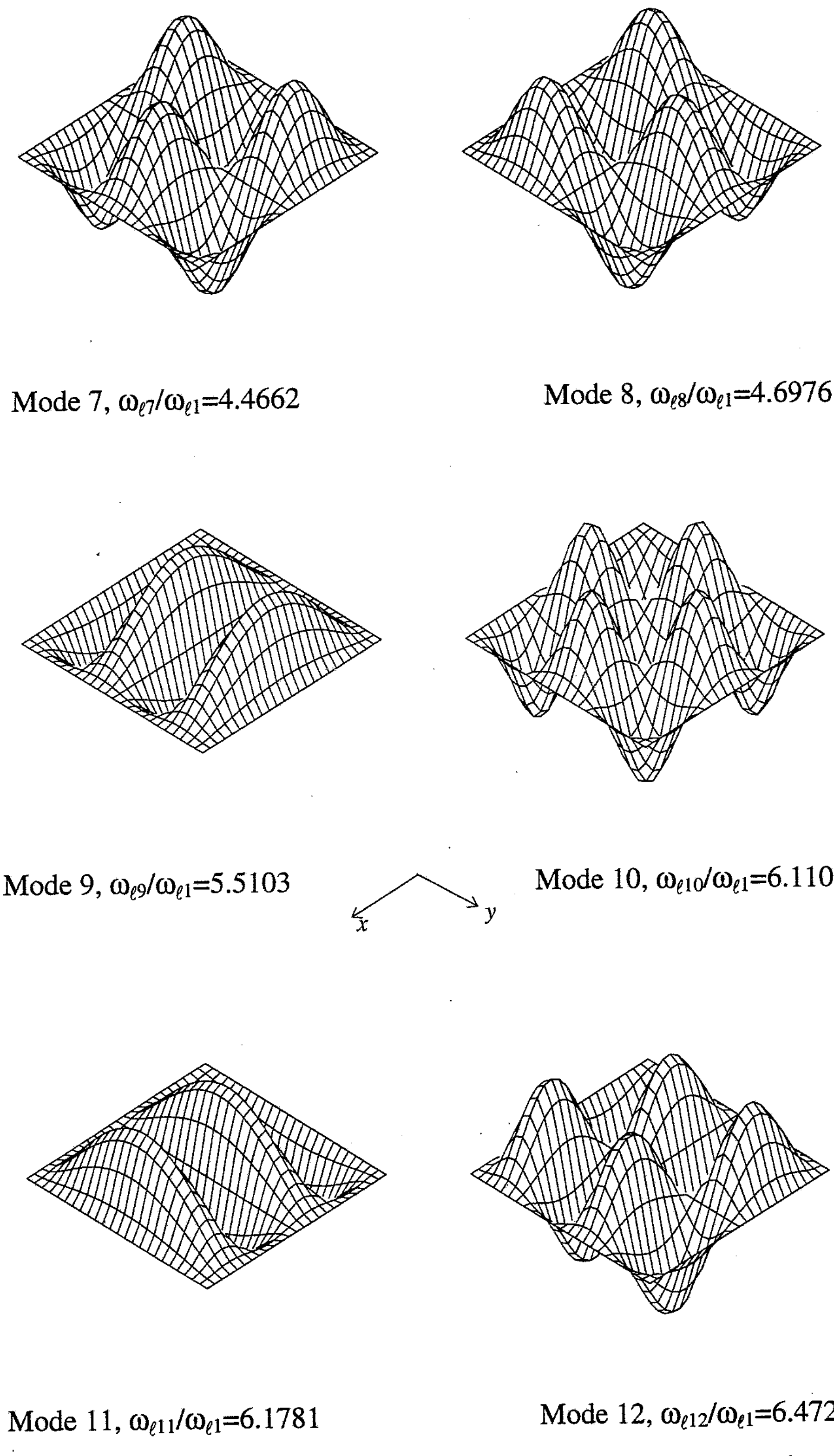

Figure 8.2*b* - Seventh to twelveth linear mode shapes and natural frequencies of Plate 3. p_o=10.

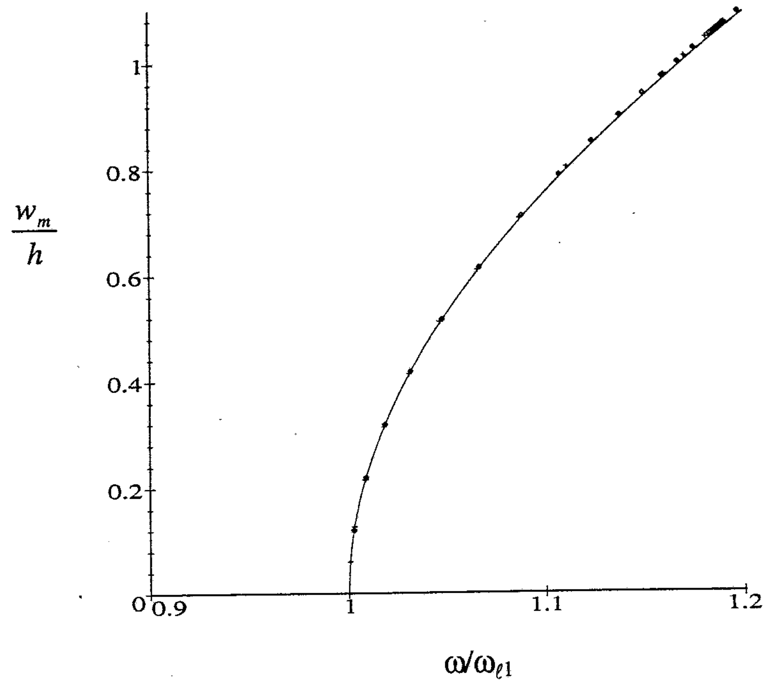

Figure 8.3 - Convergence with the number of harmonics. Plate 1, p_i=6, p_o=6. Total displacement calculated at (ξ, η)=(0, 0): - 1 harmonic, ◊ 2 harmonics, + three harmonics.

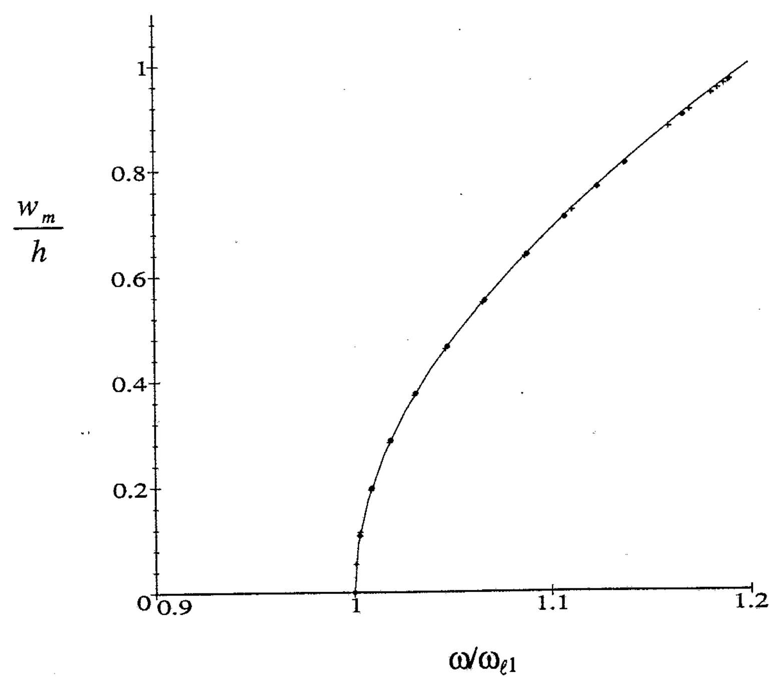

Figure 8.4 - Convergence with the number of harmonics. Plate 1, p_i=6, p_o=6. Total displacement calculated at (ξ, η)=(0.23, 0): - 1 harmonic, ◊ 2 harmonics, + three harmonics.

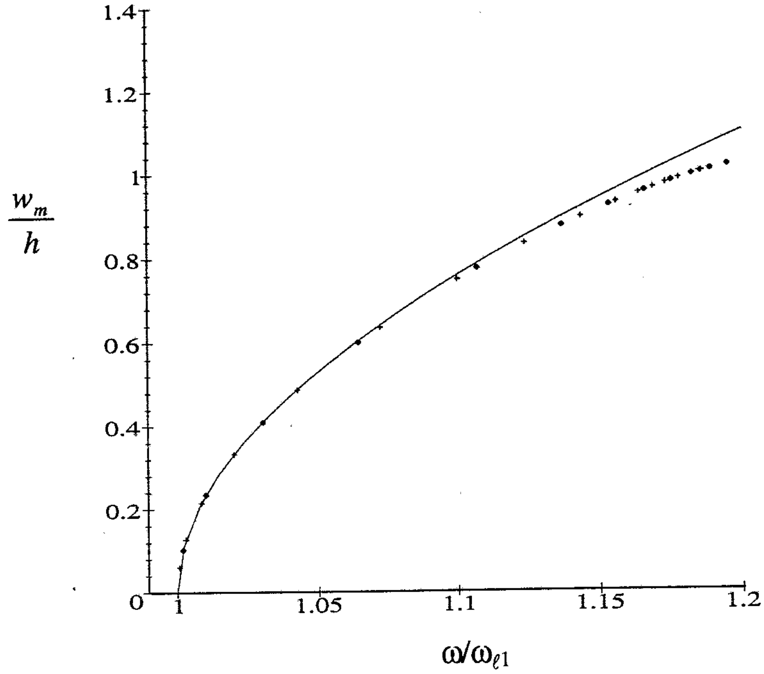

Figure 8.5 - Plate 3. Convergence with the number of harmonics (p_o=5, p_i=8). - 1 harmonic, ◊ 2 harmonics, + three harmonics; (ξ, η)=(0, 0).

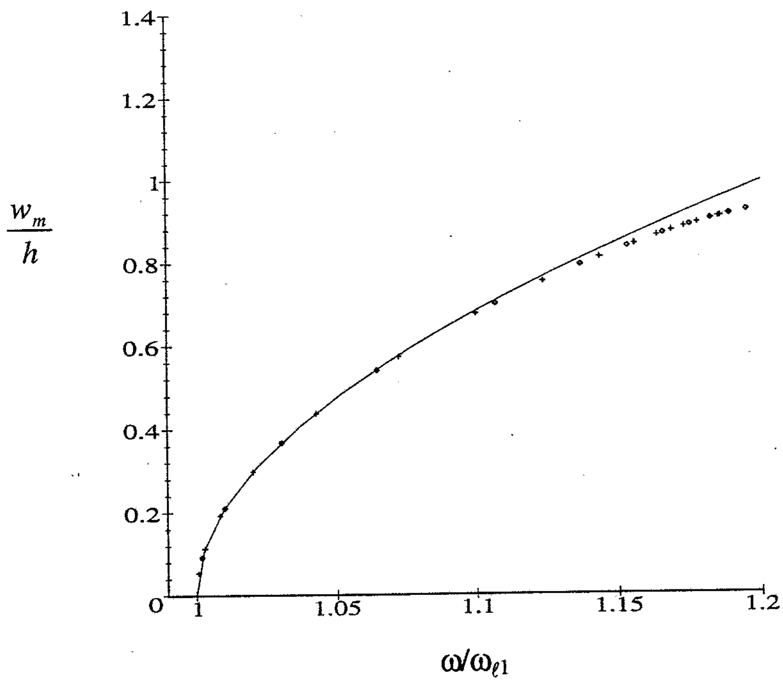

Figure 8.6 - Plate 3. Convergence with the number of harmonics (p_o=5, p_i=8). - 1 harmonic, ◊ 2 harmonics, + three harmonics; (ξ, η)=(0.23, 0).

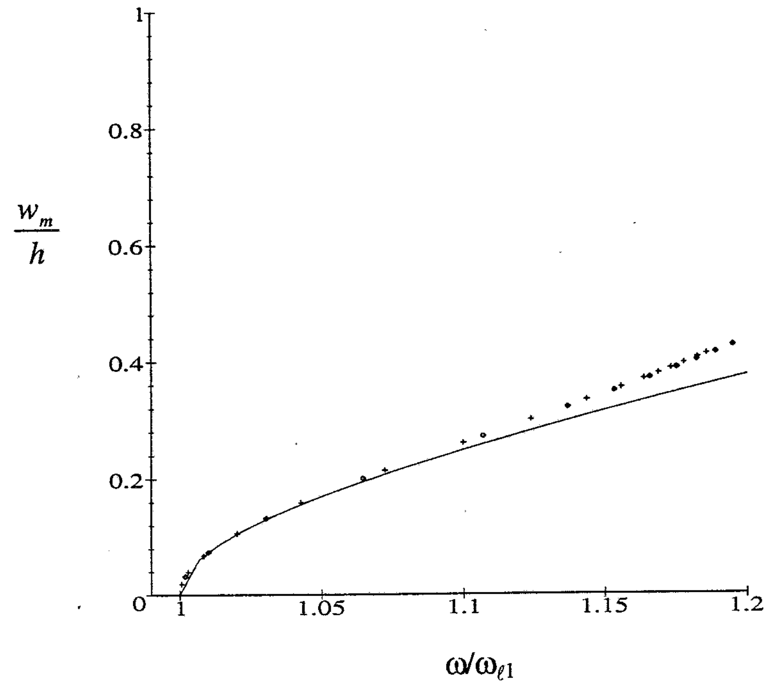

Figure 8.7 - Plate 3. Convergence with the number of harmonics (p_o=5, p_i=8). - 1 harmonic, ◊ 2 harmonics, + three harmonics; (ξ, η)=(0.5, 0.5).

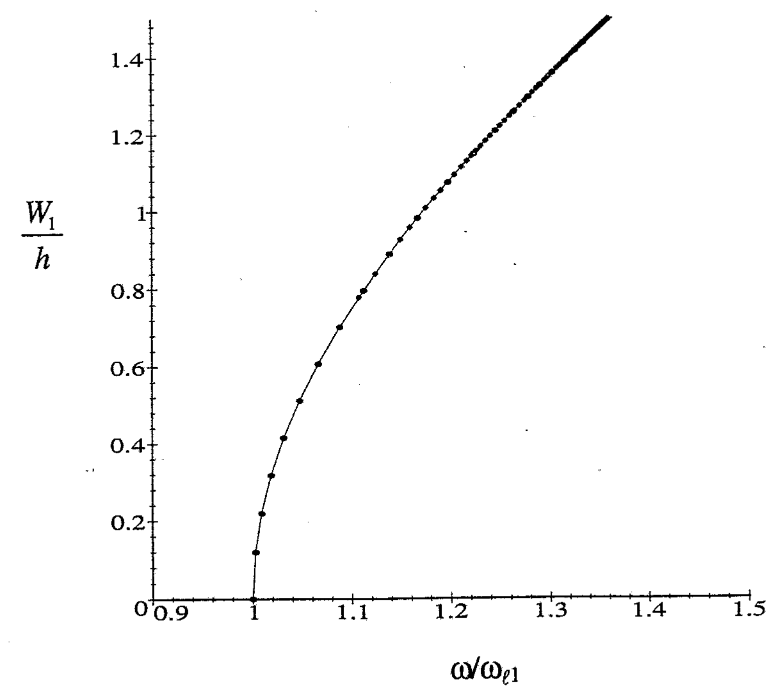

Figure 8.8 - Plate 1. Convergence with the number of out-of-plane shape functions. p_i=6 and: - p_o=5, ◊ p_o = 6, + p_o=7, o p_o=8; (ξ, η)=(0, 0). First harmonic.

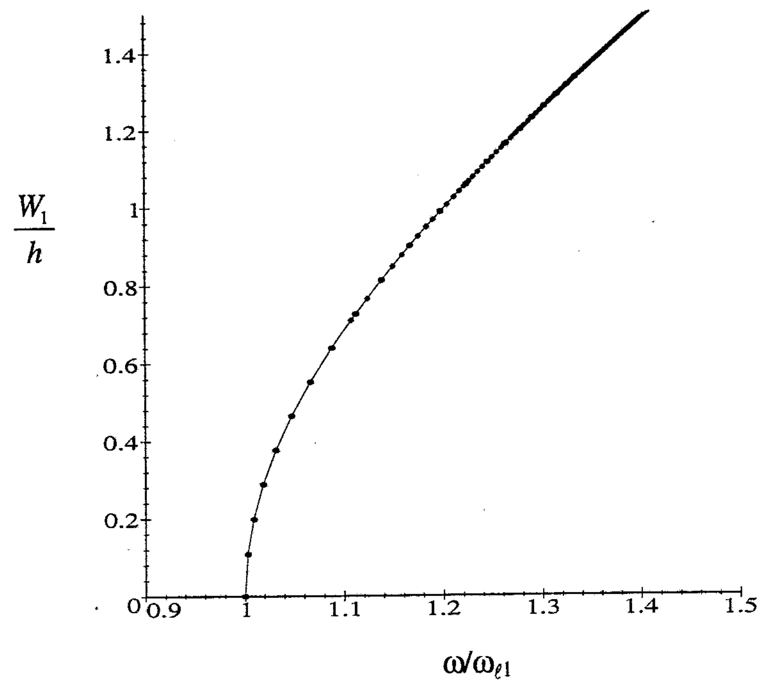

Figure 8.9 - Plate 1. Convergence with the number of out-of-plane shape functions. p_i=6 and: - p_o=5, ◊ p_o = 6, + p_o=7, o p_o=8; (ξ, η)=(0.23, 0). First harmonic.

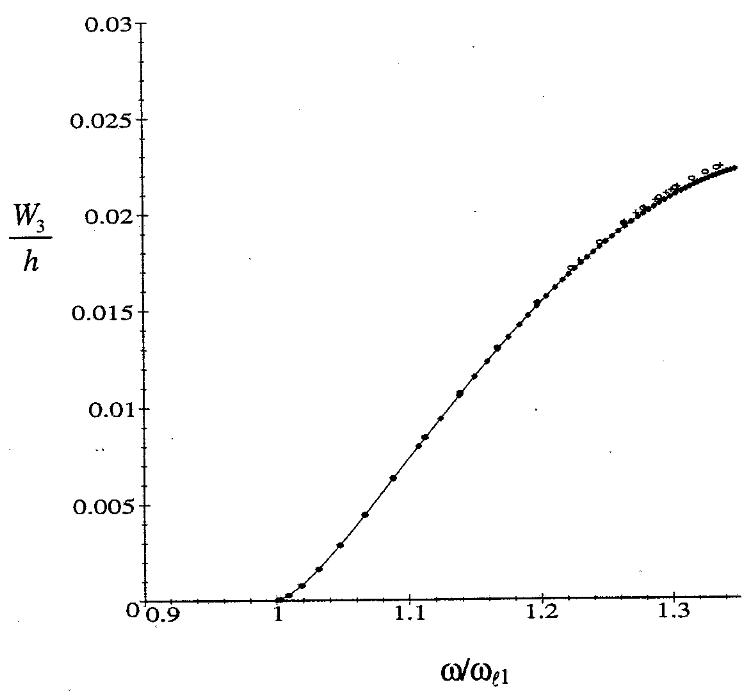

Figure 8.10 - Plate 1. Convergence with the number of out-of-plane shape functions. p_i=6 and: - p_o=5, ◊ p_o = 6, + p_o=7, o p_o=8; (ξ,η)=(0,0). Third harmonic.

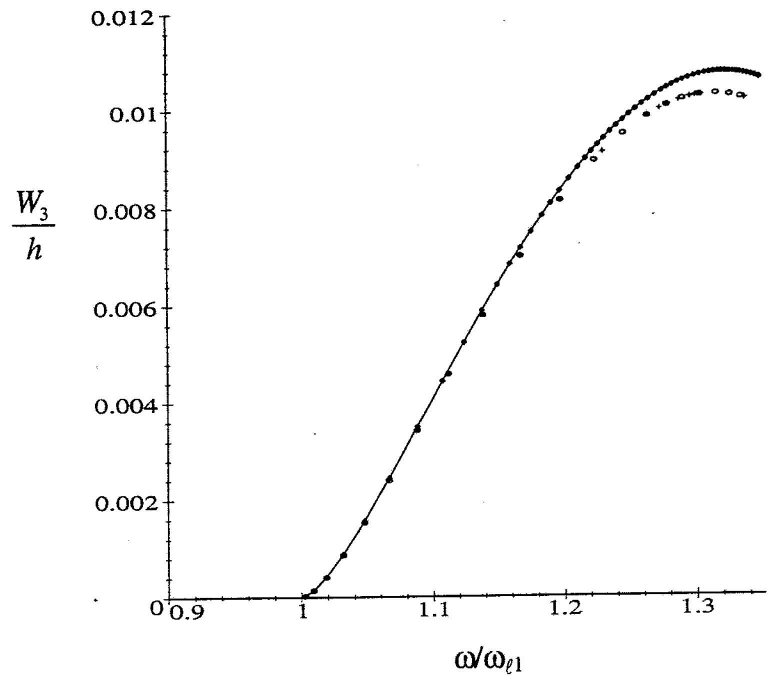

Figure 8.11 - Plate 1. Convergence with the number of out-of-plane shape functions. p_i=6 and: - p_o=5, ◊ $p_o = 6$, + p_o=7, o p_o=8; (ξ,η)=(0.23,0). Third harmonic.

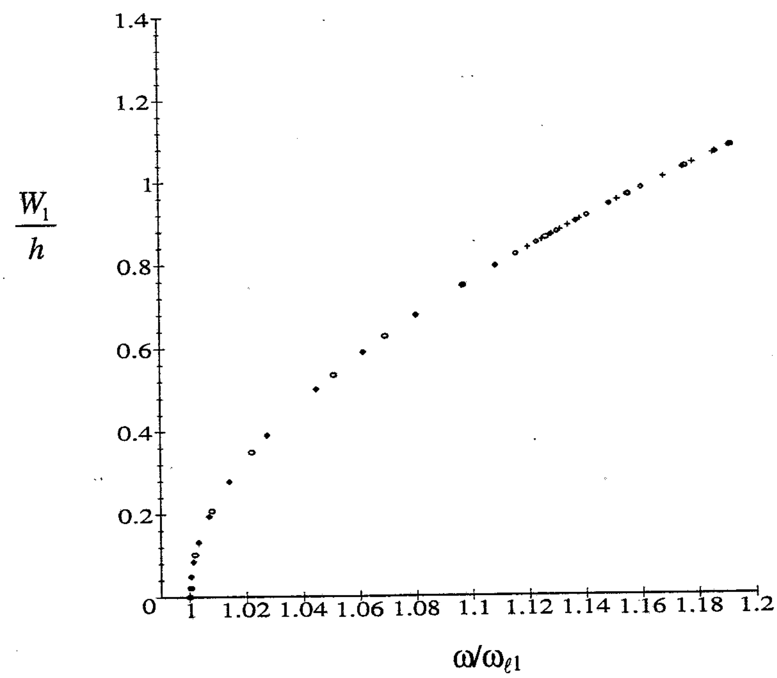

Figure 8.12 - Plate 3. Convergence with the number of out-of-plane shape functions. p_i=10 and: o p_o=5, ◊ $p_o = 6$, + p_o=7; (ξ, η)=(0, 0). First harmonic.

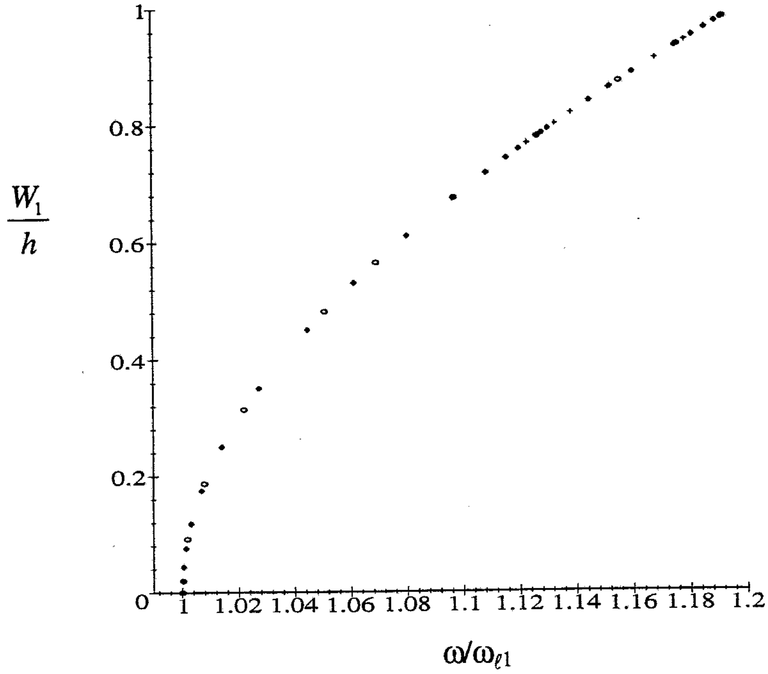

Figure 8.13 - Plate 3. Convergence with the number of out-of-plane shape functions. p_i=10 and: o p_o=5, ◊ p_o = 6, + p_o=7; (ξ, η)=(0.23, 0). First harmonic.

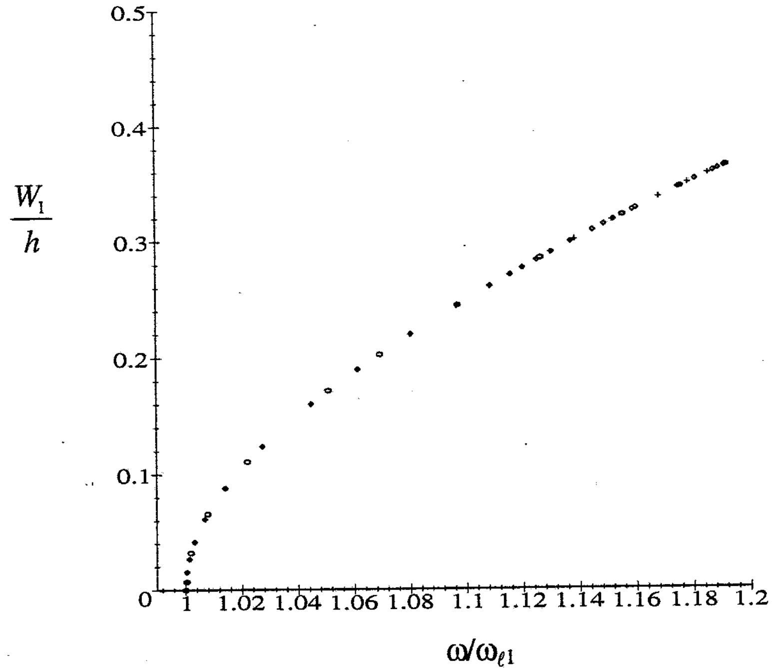

Figure 8.14 - Plate 3. Convergence with the number of out-of-plane shape functions. p_i=10 and: o p_o=5, ◊ p_o = 6, + p_o=7; (ξ, η)=(0.5, 0.5). First harmonic.

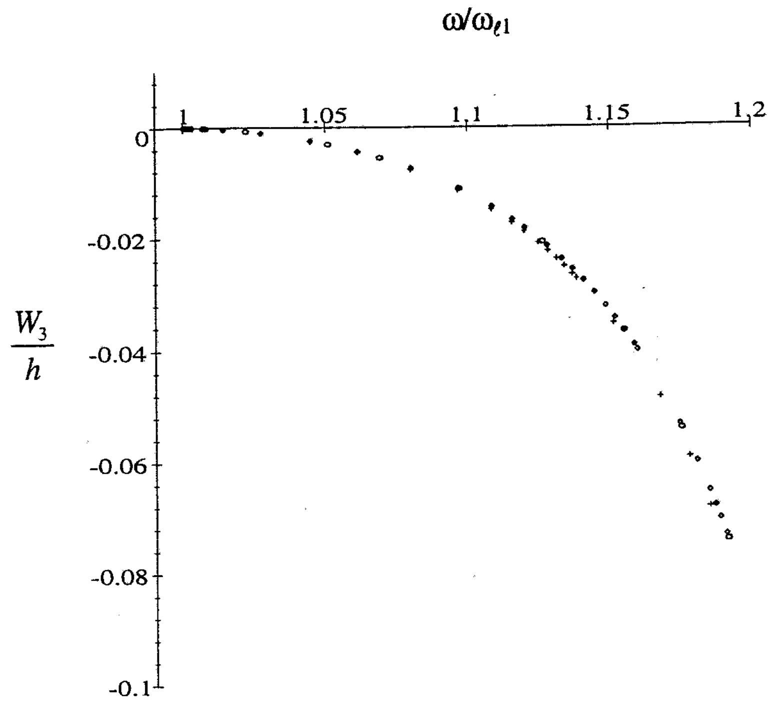

Figure 8.15 - Plate 3. Convergence with the number of out-of-plane shape functions. p_i=6 and: o p_o=5, ◊ p_o = 6, + p_o=7; (ξ, η)=(0, 0). Third harmonic.

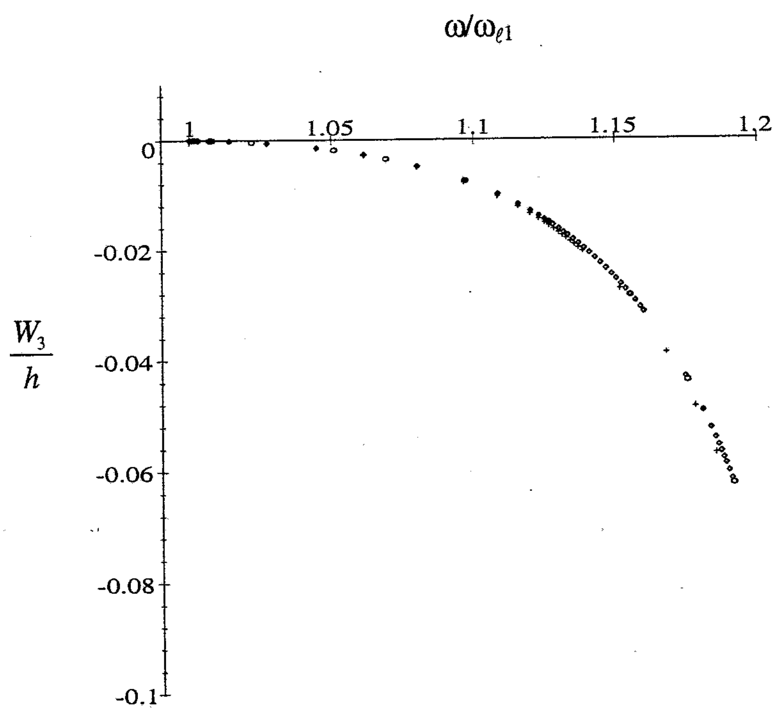

Figure 8.16 - Plate 3. Convergence with the number of out-of-plane shape functions. p_i=6 and: o p_o=5, ◊ p_o = 6, + p_o=7; (ξ, η)=(0.23, 0). Third harmonic.

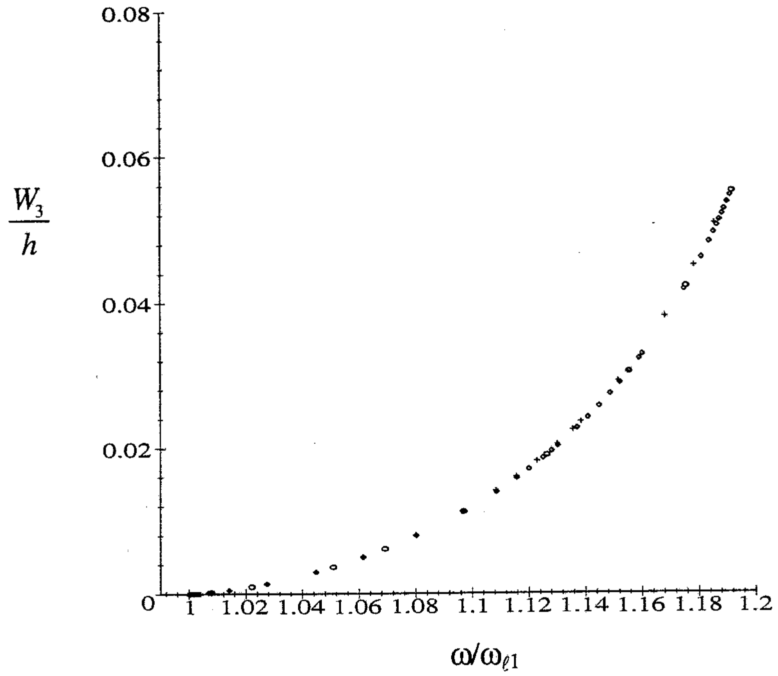

Figure 8.17 - Plate 3. Convergence with the number of out-of-plane shape functions. p_i=6 and: o p_o=5, ◊ $p_o = 6$, + p_o=7; (ξ, η)=(0.5, 0.5). Third harmonic.

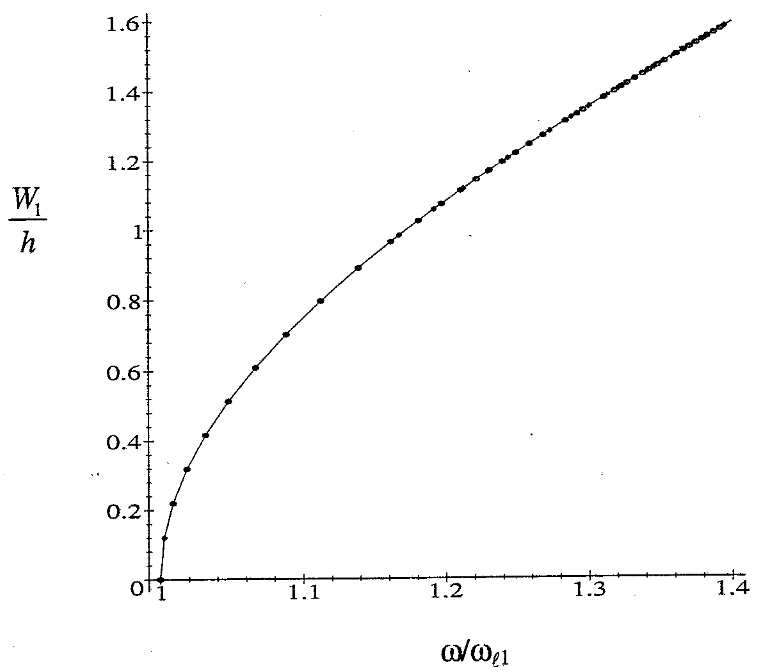

Figure 8.18 - Plate 1. Convergence with the number of in-plane shape functions. p_o=6 and: — $p_i = 6$, ◊ p_i=7, + p_i=8; (ξ, η)=(0, 0). First harmonic.

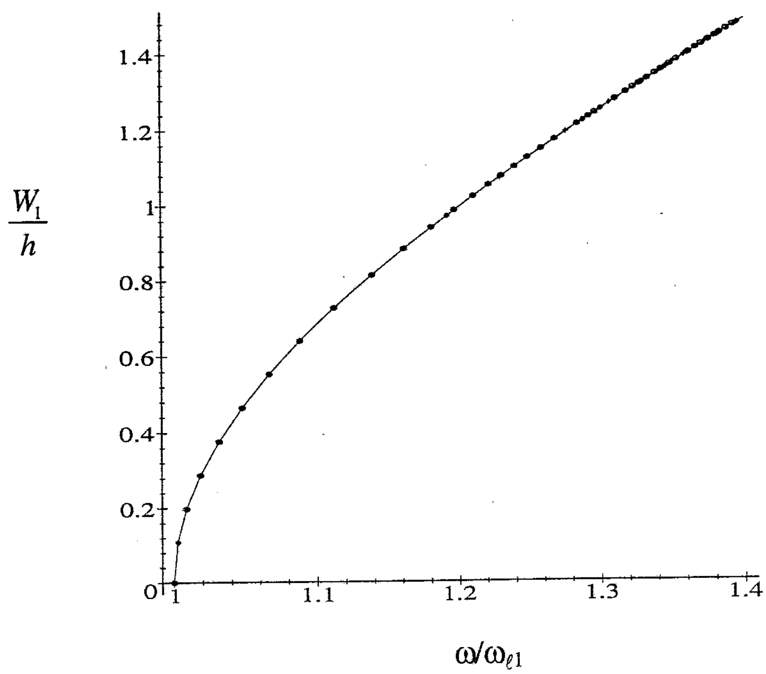

Figure 8.19 - Plate 1. Convergence with the number of in-plane shape functions. p_o=6 and: — $p_i = 6$, ◊ p_i=7, + p_i=8; (ξ, η)=(0.23, 0). First harmonic.

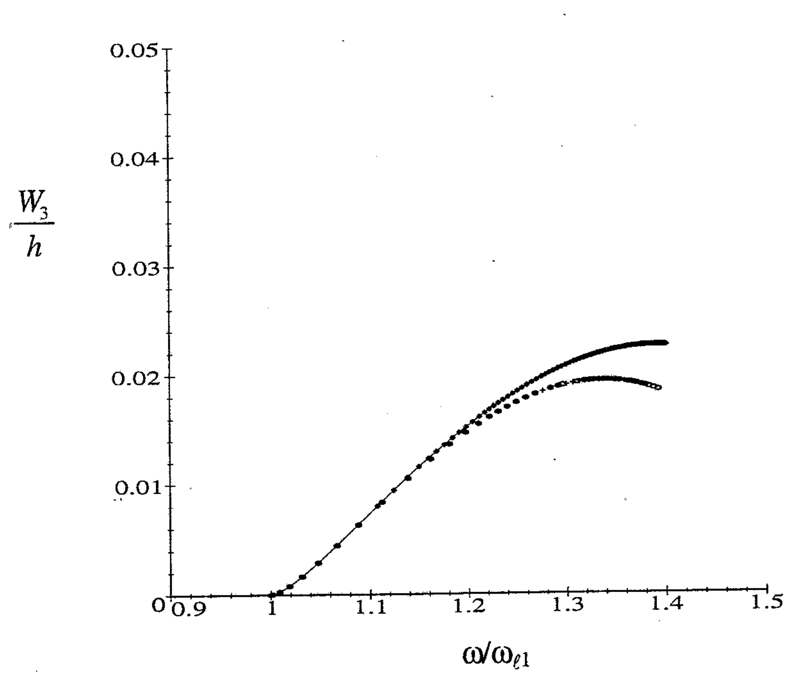

Figure 8.20 - Plate 1. Convergence with the number of in-plane shape functions. p_o=6 and: — $p_i = 6$, ◊ p_i=7, + p_i=8, o p_i=10; (ξ, η)=(0, 0). Third harmonic.

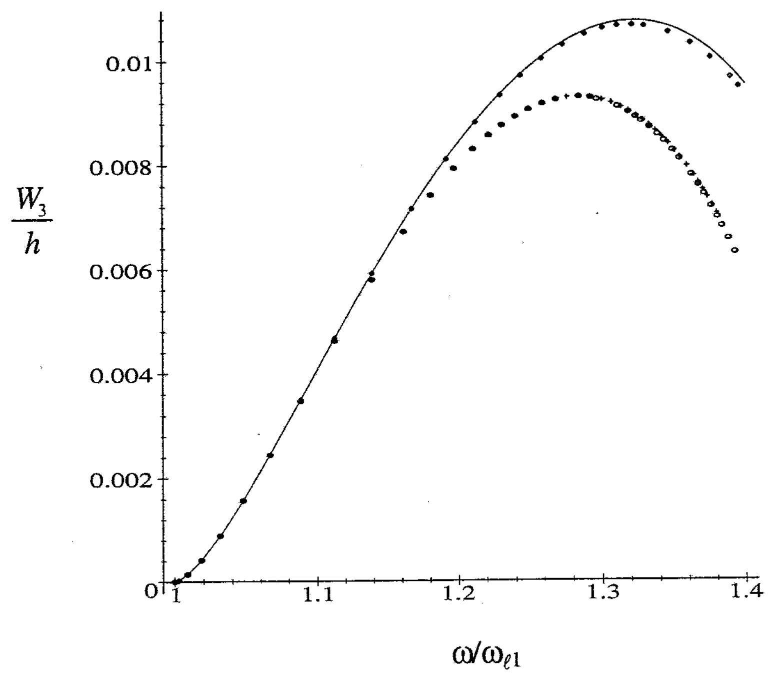

Figure 8.21 - Plate 1. Convergence with the number of in-plane shape functions. p_o=6 and: — $p_i = 6$, ◊ p_i=7, + p_i=8, o p_i=10; (ξ, η)=(0.23, 0). Third harmonic.

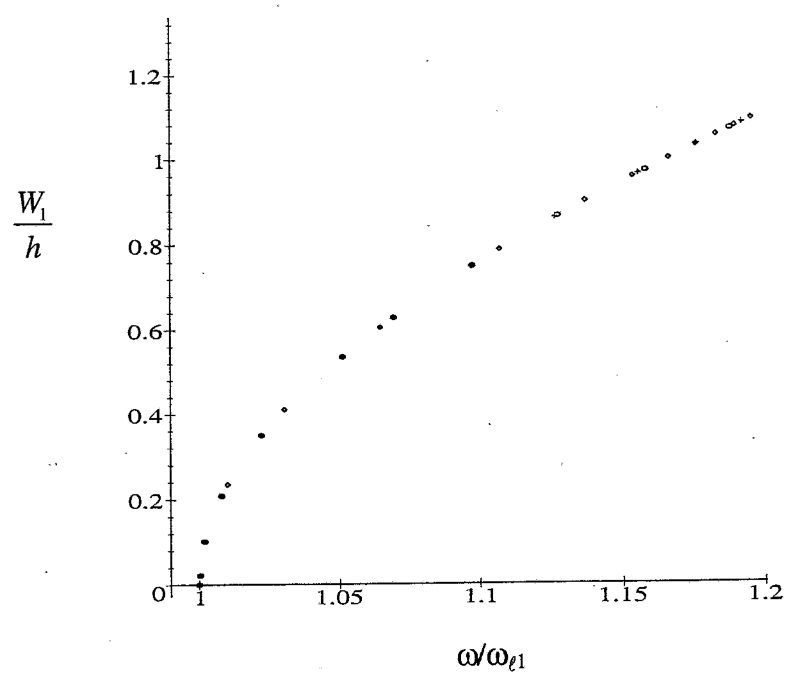

Figure 8.22 - Plate 3. Convergence with the number of in-plane shape functions. p_o=5 and: o $p_i = 7$, ◊ p_i=8, + p_i=10; (ξ, η)=(0, 0). First harmonic.

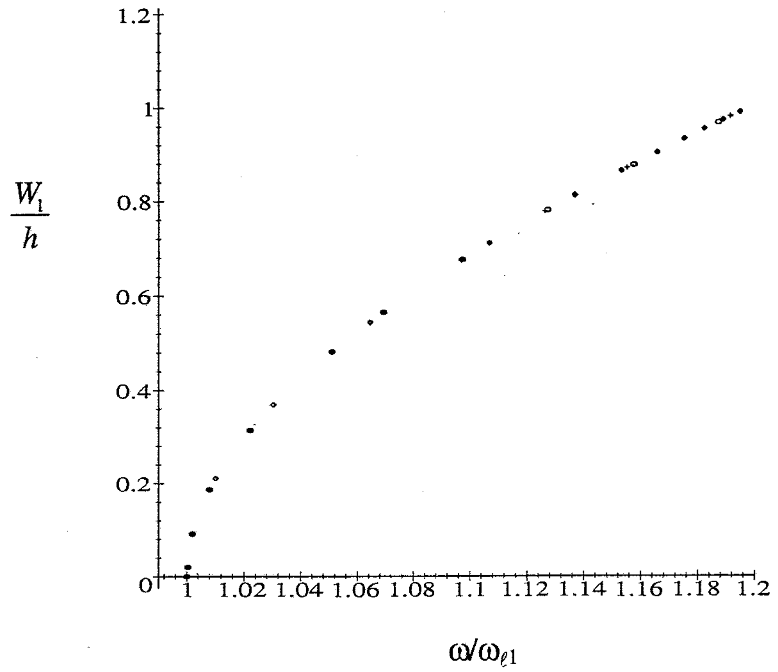

Figure 8.23 - Plate 3. Convergence with the number of in-plane shape functions. p_o=5 and: o $p_i = 7$, ◊ p_i=8, + p_i=10; (ξ, η)=(0.23, 0). First harmonic.

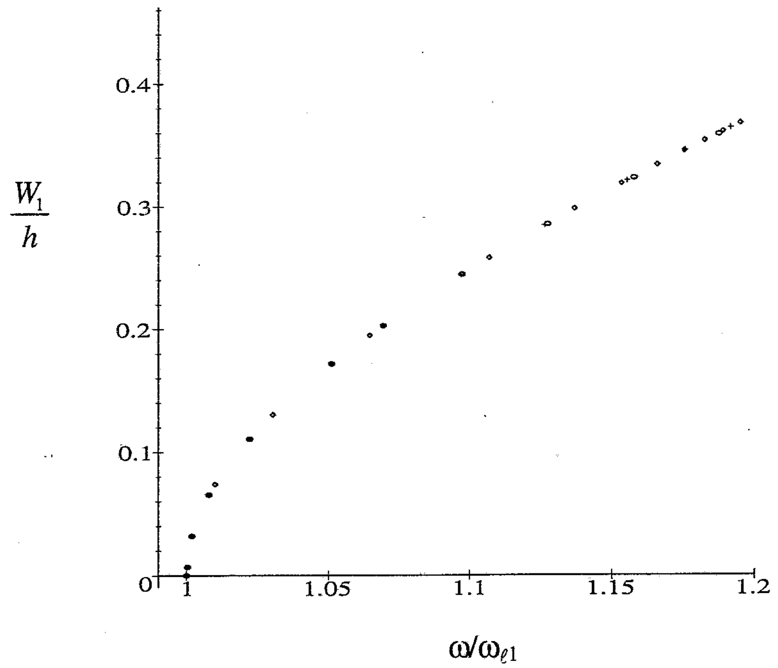

Figure 8.24 - Plate 3. Convergence with the number of in-plane shape functions. p_o=5 and: o $p_i = 7$, ◊ p_i=8, + p_i=10; (ξ, η)=(0.5, 0.5). First harmonic.

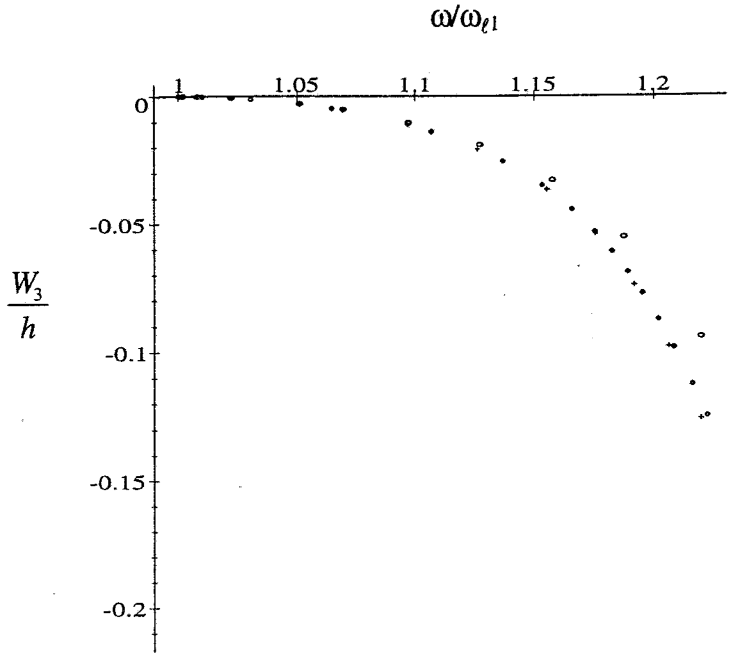

Figure 8.25 - Plate 3. Convergence with the number of in-plane shape functions. p_o=5 and: o $p_i = 7$, ◊ p_i=8, + p_i=10; (ξ, η)=(0, 0). Third harmonic.

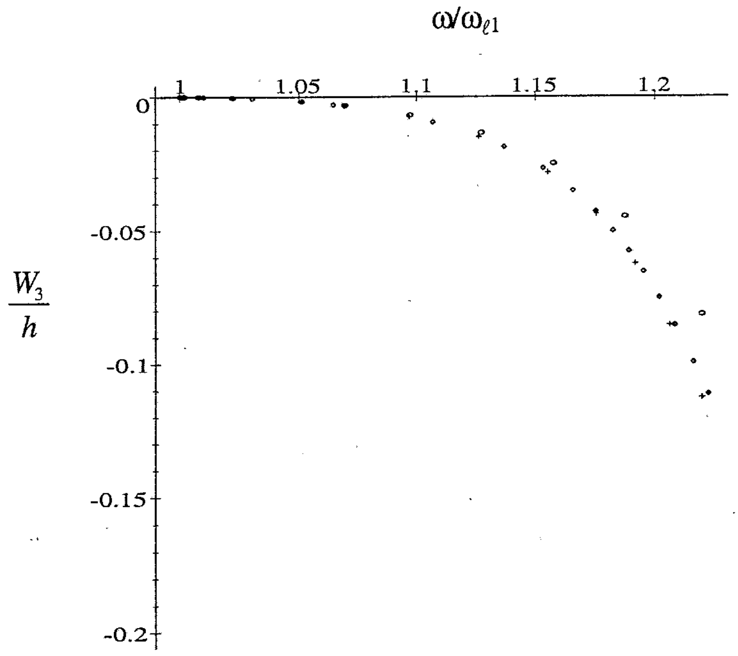

Figure 8.26 - Plate 3. Convergence with the number of in-plane shape functions. p_o=5 and: o $p_i = 7$, ◊ p_i=8, + p_i=10; (ξ, η)=(0.23, 0). Third harmonic.

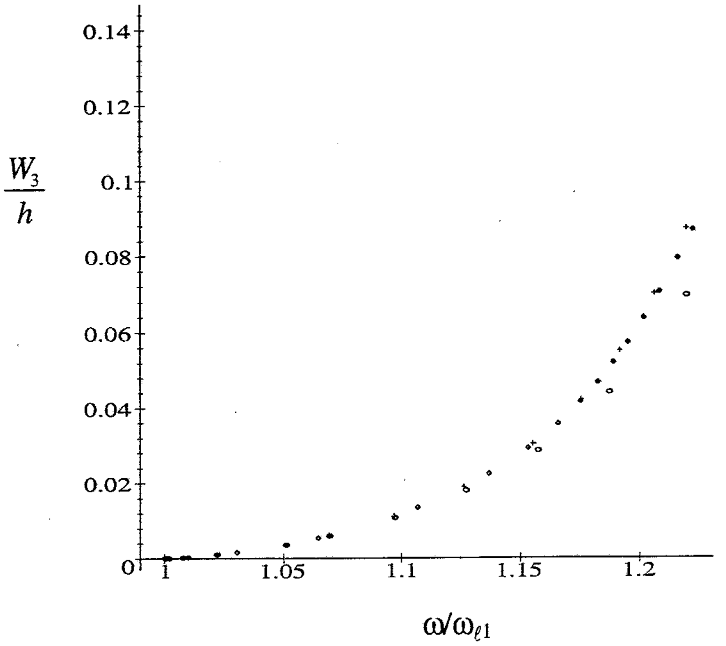

Figure 8.27 - Plate 3. Convergence with the number of in-plane shape functions. p_o=5 and: o p_i = 7, ◊ p_i=8, + p_i=10; (ξ, η)=(0.5, 0.5). Third harmonic.

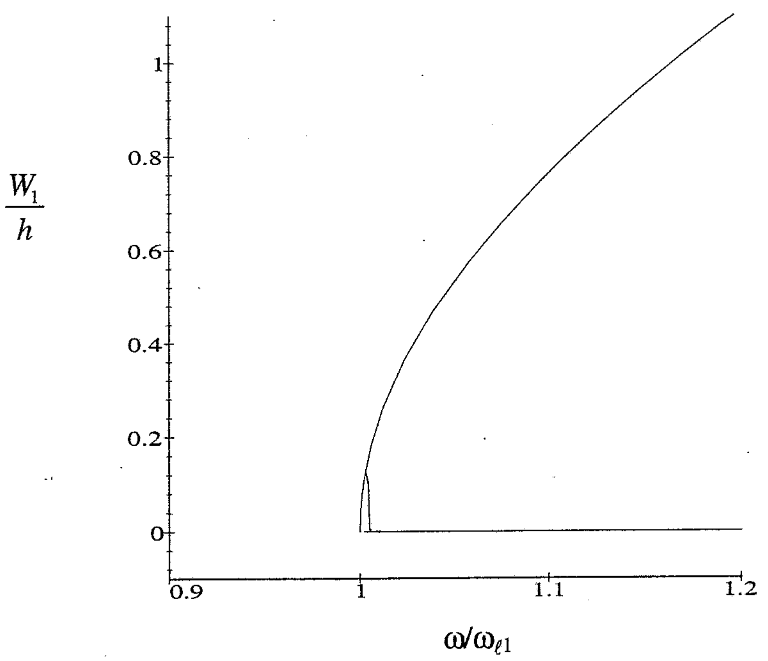

Figure 8.28 - Branch diagram of Plate 3. p_o=5, p_i=10; (ξ, η)=(0, 0), first harmonic. From the top: First main branch, secondary branch and second main branch.

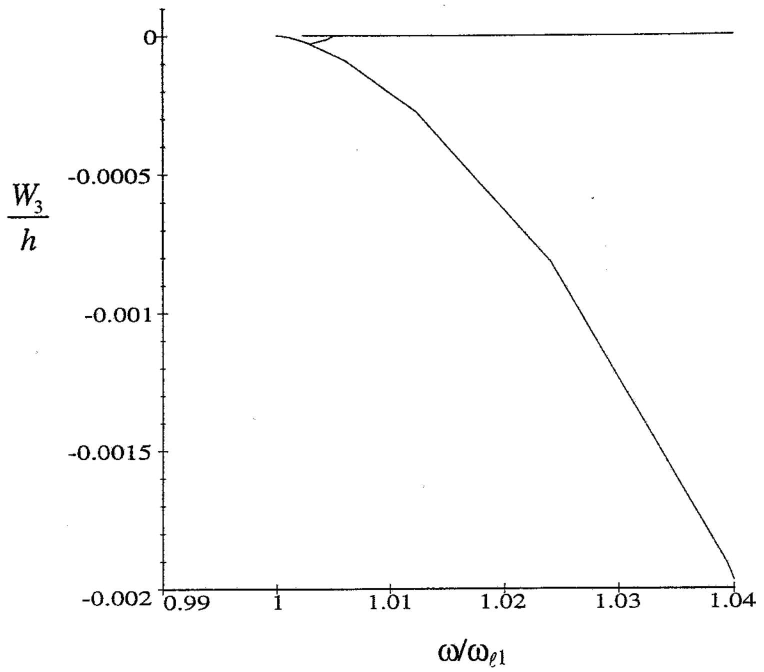

Figure 8.29 - Branch diagram of Plate 3. p_o=5, p_i=10; (ξ, η)=(0, 0), third harmonic. From the top: First main branch, secondary branch and second main branch.

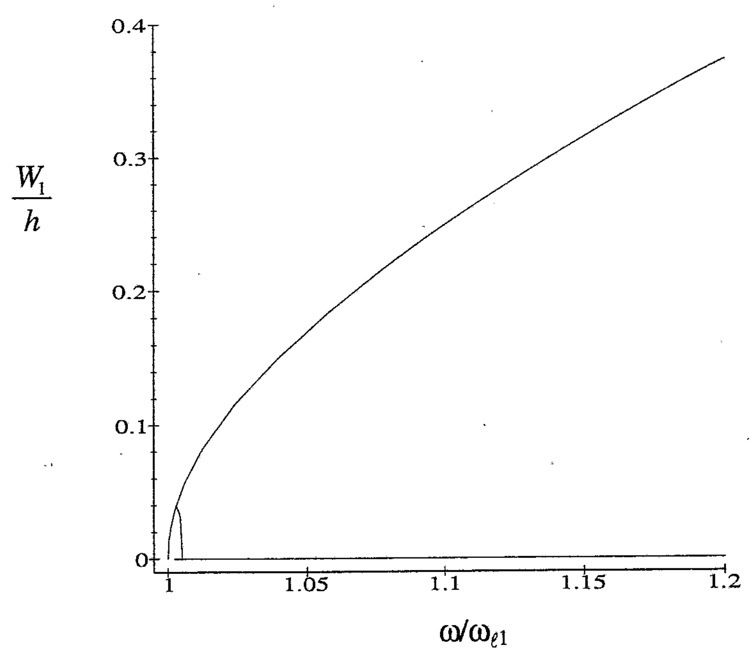

Figure 8.30 - Branch diagram of Plate 3. p_o=5, p_i=10; (ξ, η)=(0.5, 0.5), first harmonic. From the top: First main branch, secondary branch and second main branch.

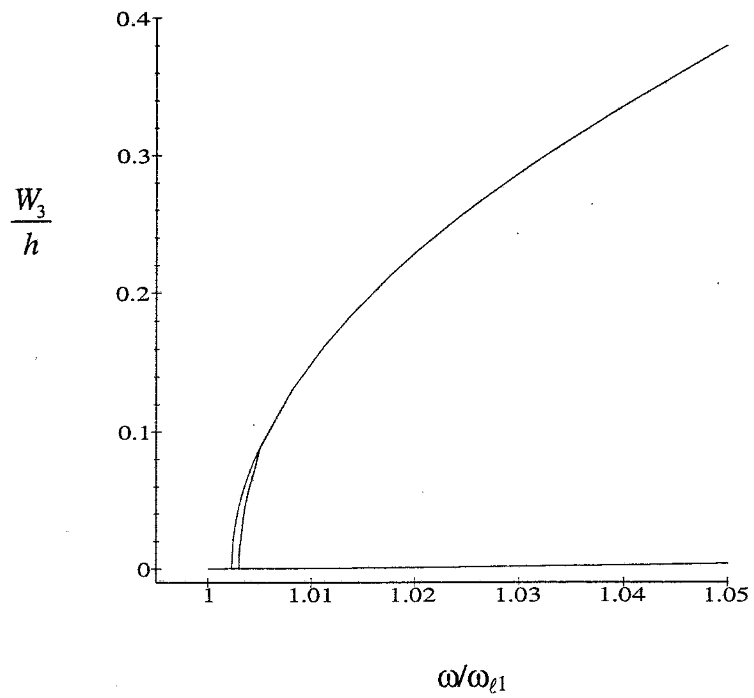

Figure 8.31 - Branch diagram of Plate 3. p_o=5, p_i=10; (ξ, η)=(0.5, 0.5), third harmonic. From the top: First main branch, secondary branch and second main branch.

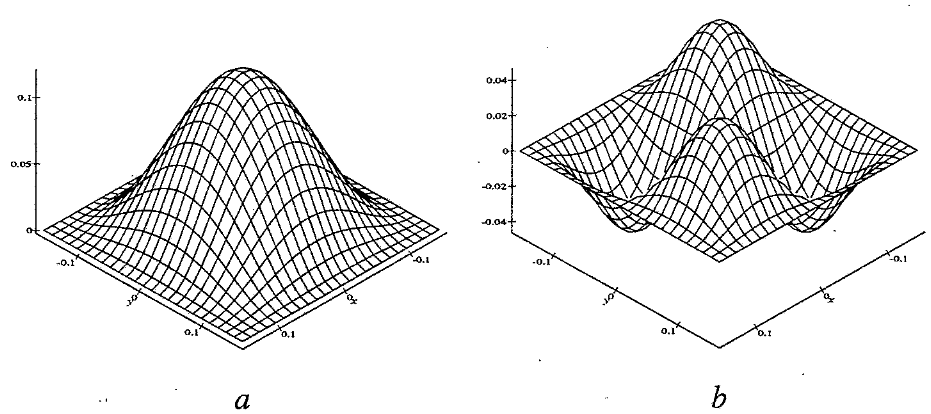

Figure 8.32 - Mode shapes associated with first and third harmonics, at point $\omega/\omega_{\ell 1}$ = 1.0035 of secondary branch.

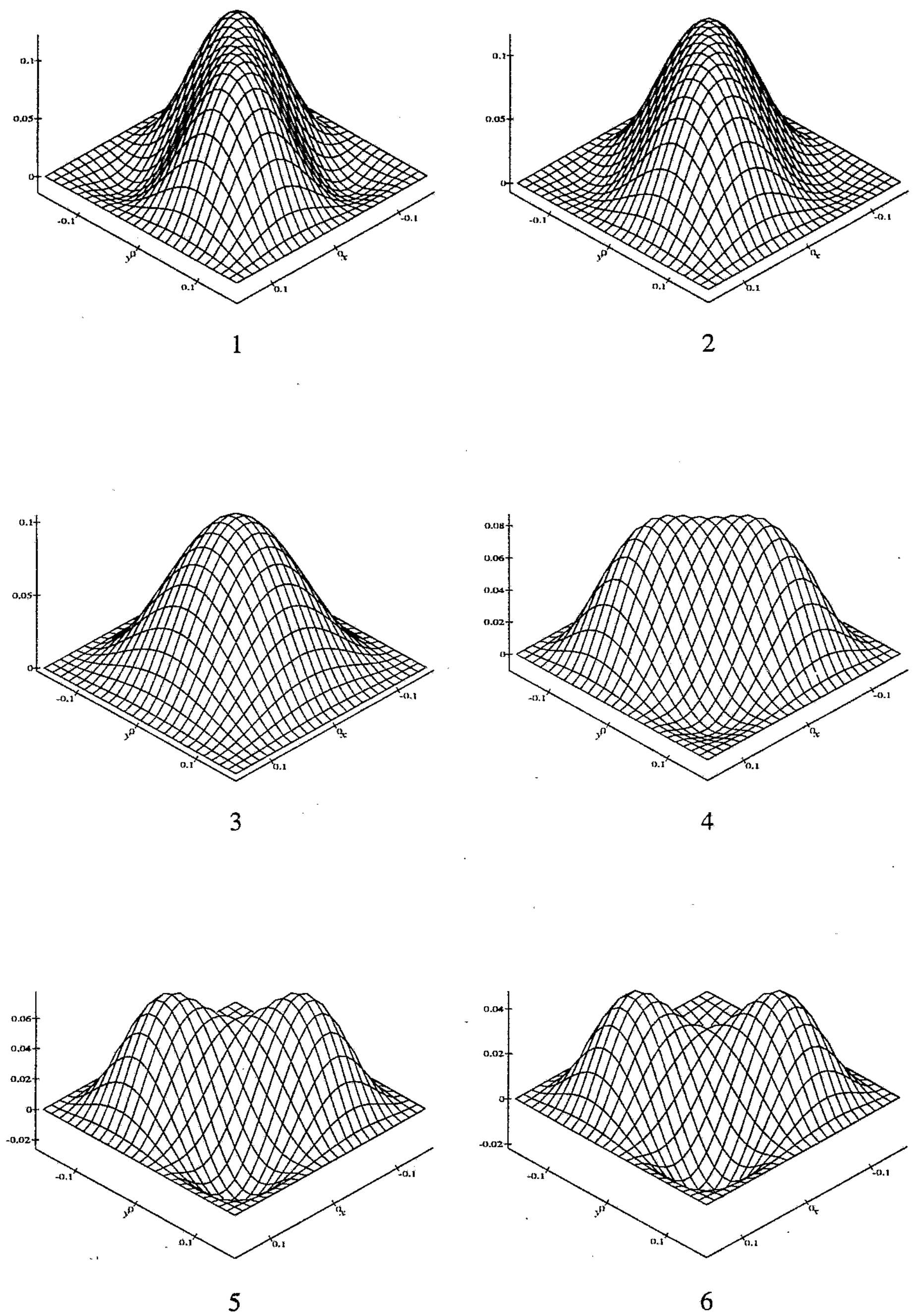

Figure 8.33 (continued) - Vibration of Plate 3 during half a cycle, at point $\omega/\omega_{\ell 1}$ = 1.0035 of secondary branch.

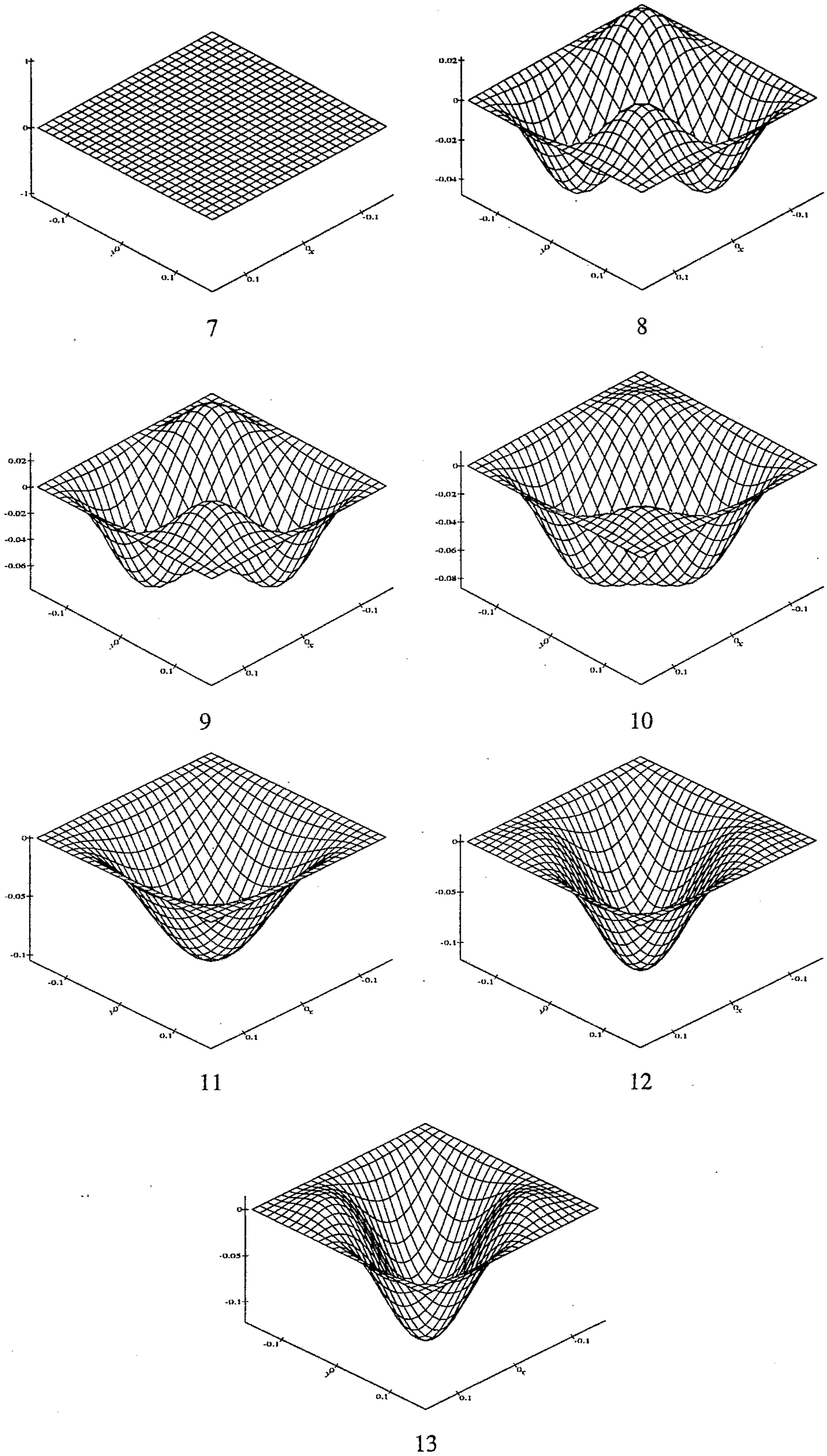

Figure 8.33 - Vibration of Plate 3 during half a cycle, at point $\omega/\omega_{\ell 1} = 1.0035$ of secondary branch.

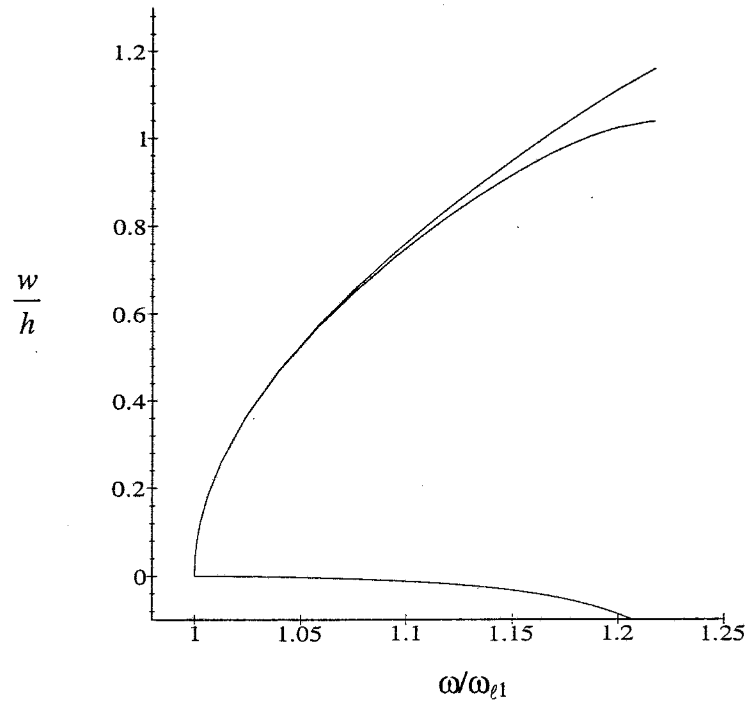

Figure 8.34 - Main branch Plate 3. p_o=5, p_i=10; (ξ, η)=(0, 0), From the top: first harmonic displacement, total displacement, third harmonic displacement.

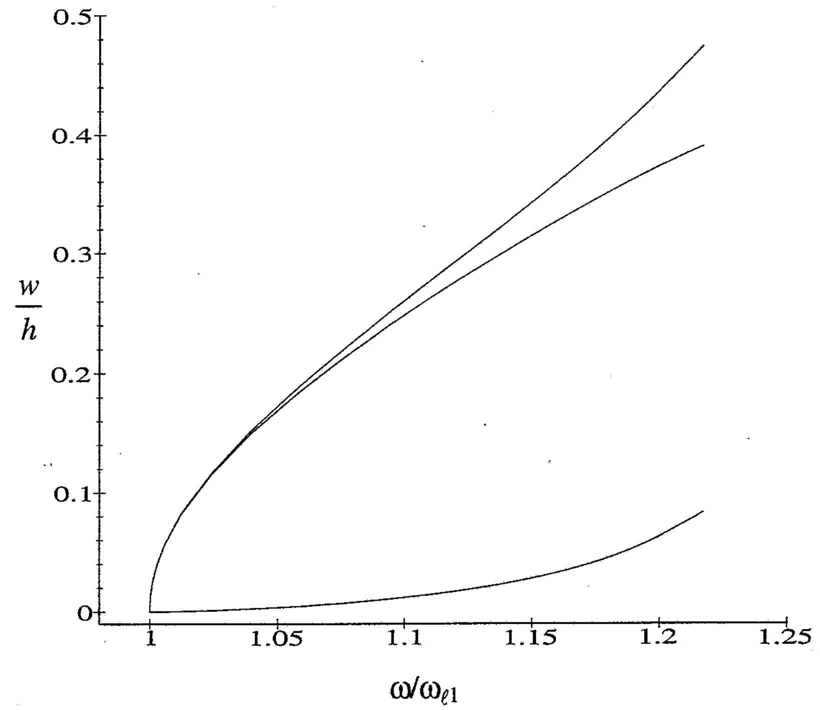

Figure 8.35 - Main branch Plate 3. p_o=5, p_i=10; (ξ, η)=(0.5, 0.5), From the top: total displacement, first harmonic displacement, third harmonic displacement.

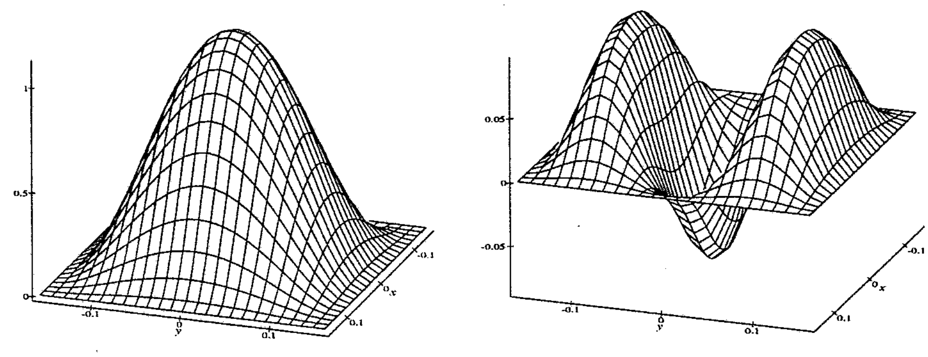

a *b*

Figure 8.36 - Mode shapes associated with first (a) and third (b) harmonics, at point $\omega/\omega_{\ell 1} = 1.1993$ of first main branch.

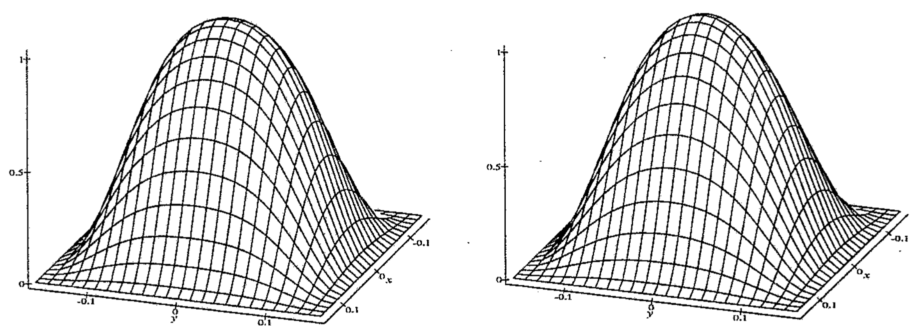

1 2

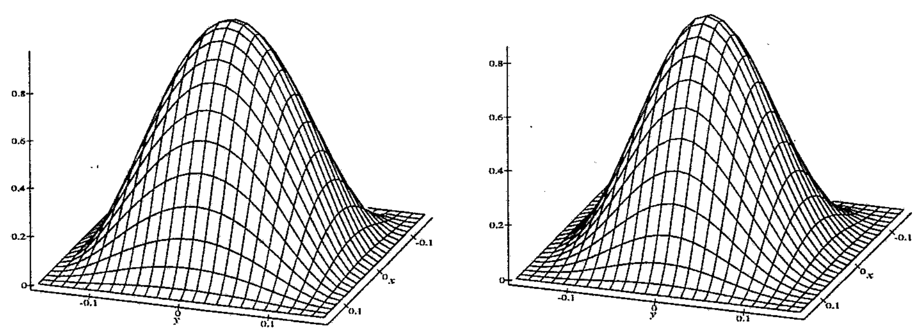

3 4

Figure 8.37 (continued) - Vibration of Plate 3 during half a cycle, at point $\omega/\omega_{\ell 1} = 1.1993$ of first main branch.

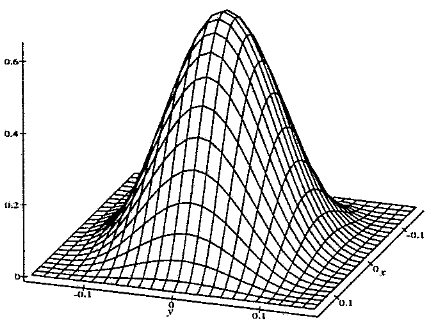

5

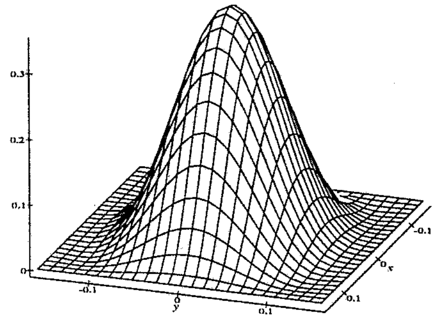

6

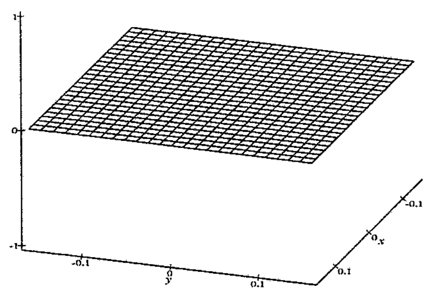

7

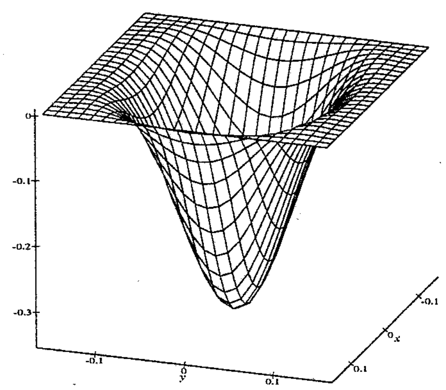

8

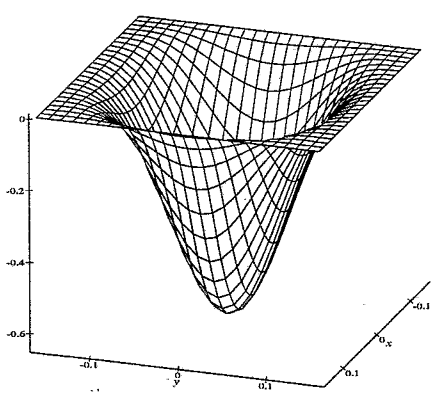

9

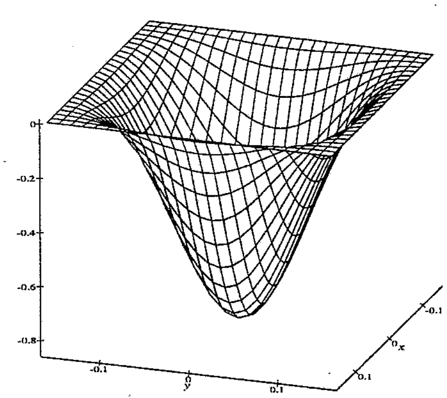

10

Figure 8.37 (continued) - Vibration of Plate 3 during half a cycle, at point $\omega/\omega_{\ell 1}$ = 1.1993 of first main branch.

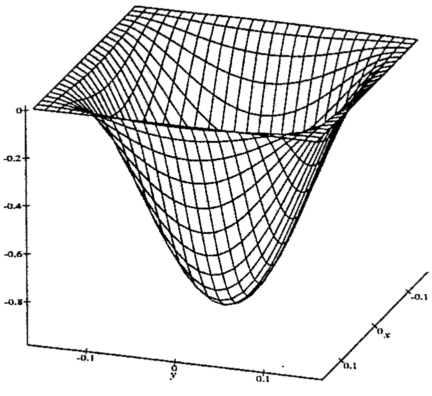

11

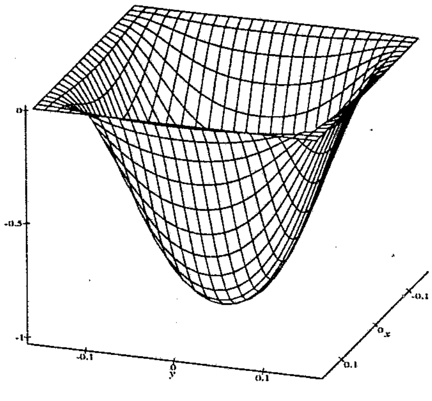

12

Figure 8.37 - Vibration of Plate 3 during half a cycle, at point $\omega/\omega_{\ell 1} = 1.1993$ of first main branch.

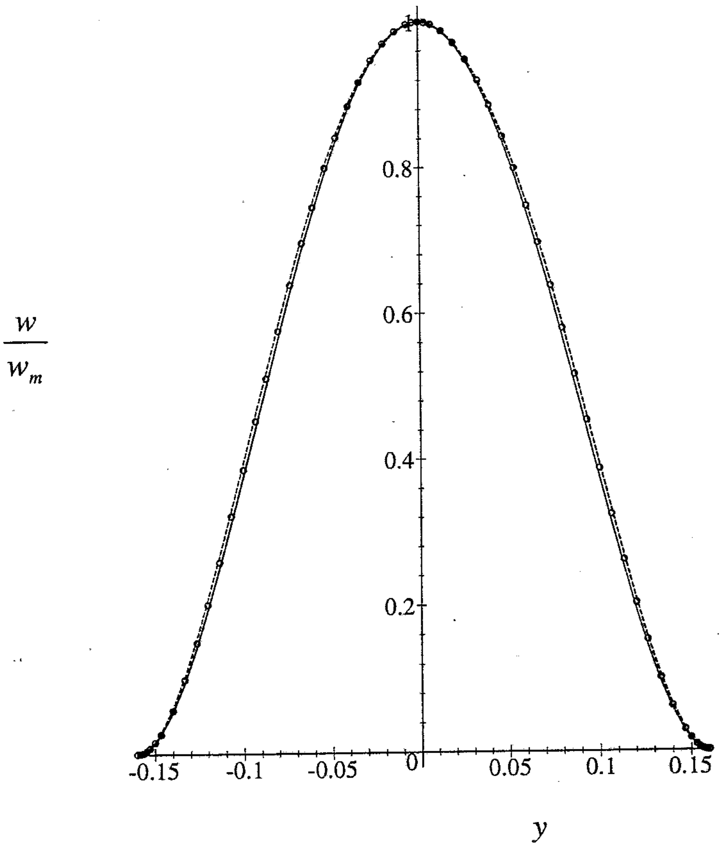

Figure 8.38 - Sections of modes of first harmonic of Plate 3 at x=0, first main branch at points - $\omega/\omega_{\ell 1} = 1.0025$, o $\omega/\omega_{\ell 1} = 1.0944$, -- $\omega/\omega_{\ell 1} = 1.1993$.

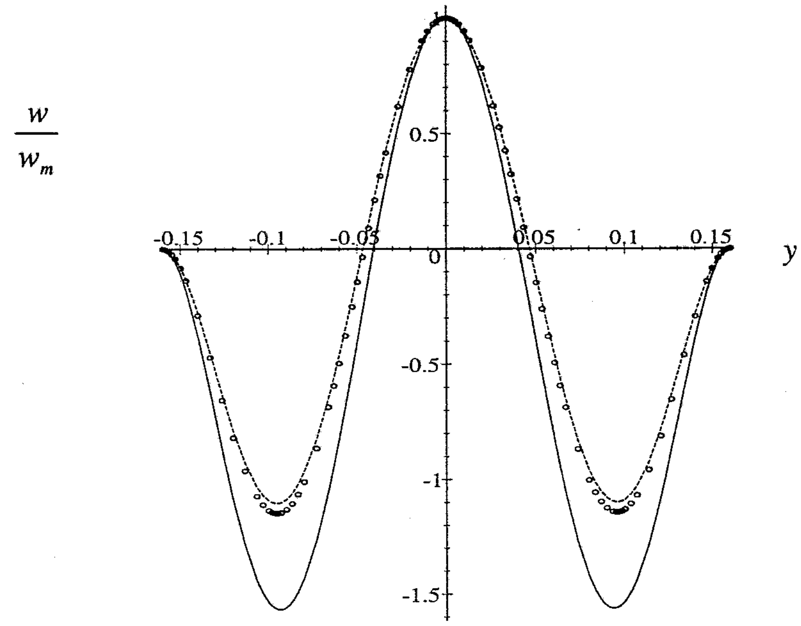

Figure 8.39 - Sections of modes of second harmonic of Plate 3 at x=0, first main branch at points - $\omega/\omega_{\ell 1}$ = 1.0025, o $\omega/\omega_{\ell 1}$ = 1.0944, -- $\omega/\omega_{\ell 1}$ = 1.1993.

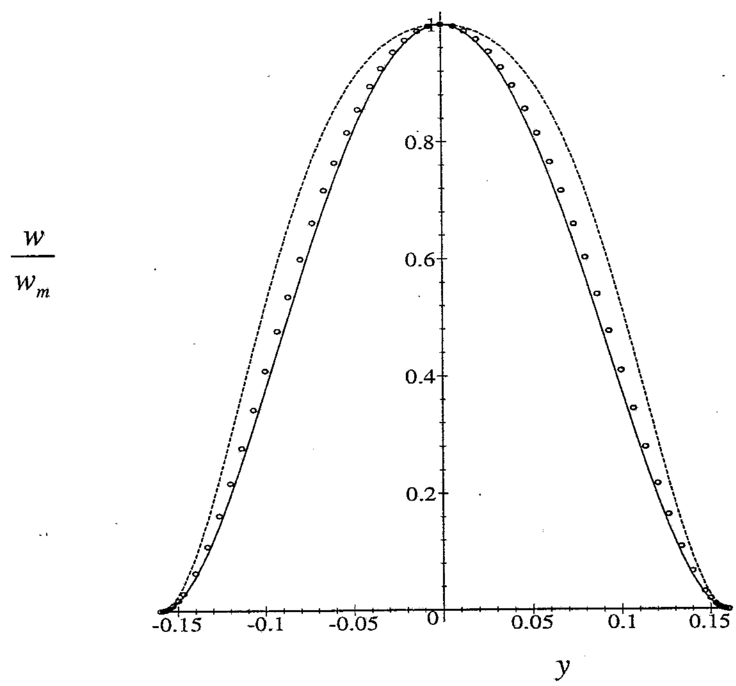

Figure 8.40 - Sections of shape of vibration (both harmonics) of Plate 3 at x=0, first main branch, points - $\omega/\omega_{\ell 1}$ = 1.0025, o $\omega/\omega_{\ell 1}$ = 1.0944, -- $\omega/\omega_{\ell 1}$ = 1.1993.

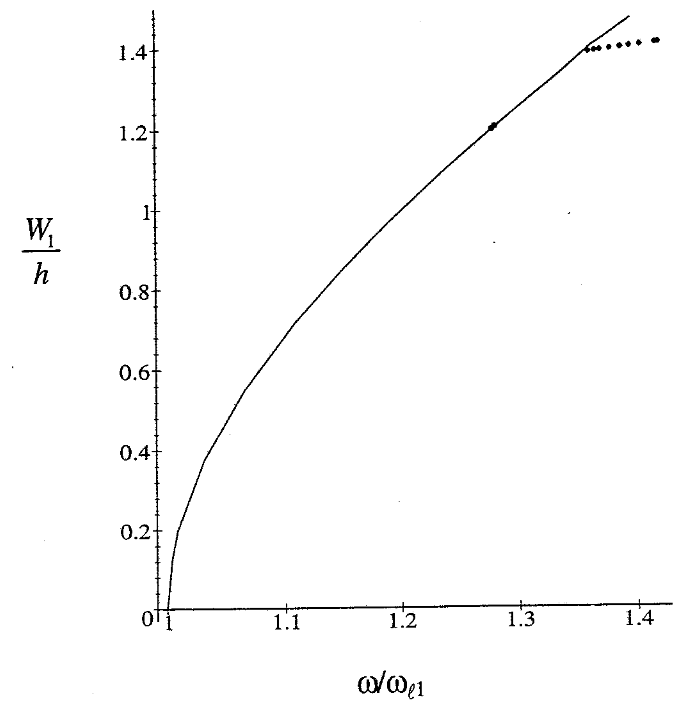

Figure 8.41 - Branch diagram of Plate 1. First harmonic calculated at $(\xi,\eta)=(0.23,0)$. - main branch, o bifurcation points, ◊ secondary branch. $p_o=7$, $p_i=10$.

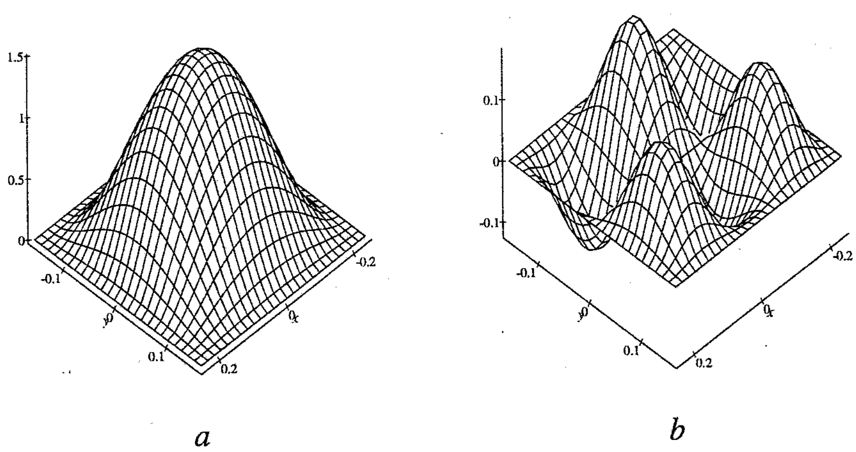

Figure 8.42 - Mode shapes associated with first and third harmonics, at point $\omega/\omega_{\ell 1} = 1.36528$ of second branch of Plate 1.

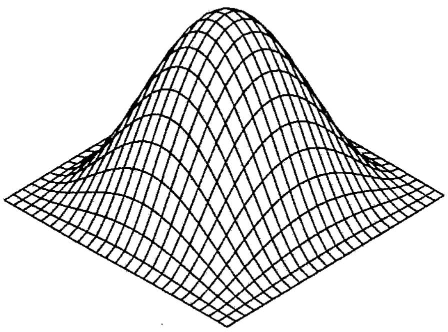

Mode 1, $\omega_{\ell 1}$=4941.4835 rad/s

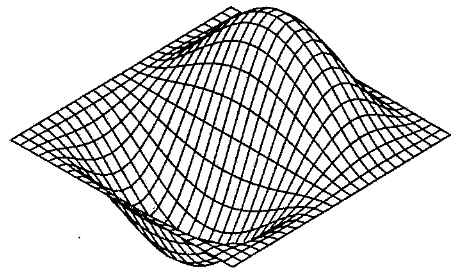

Mode 2, $\omega_{\ell 2}/\omega_{\ell 1}$=1.4773

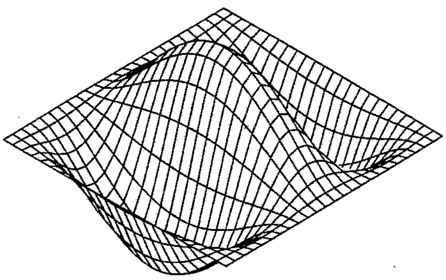

Mode 3, $\omega_{\ell 3}/\omega_{\ell 1}$= 2.2047

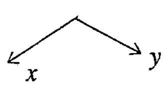

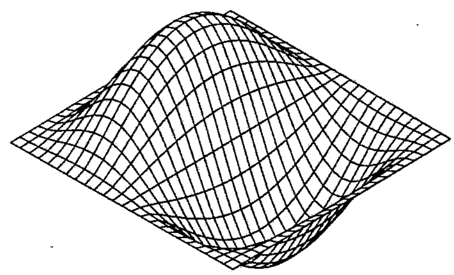

Mode 4, $\omega_{\ell 4}/\omega_{\ell 1}$= 2.4728

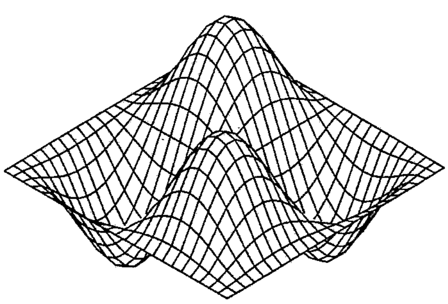

Mode 5, $\omega_{\ell 5}/\omega_{\ell 1}$= 3.0309

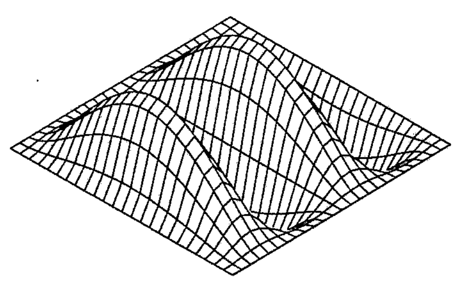

Mode 6, $\omega_{\ell 6}/\omega_{\ell 1}$= 3.1715

Figure 8.43*a* - Linear mode shapes and natural frequencies of Plate 6. p_o=10.

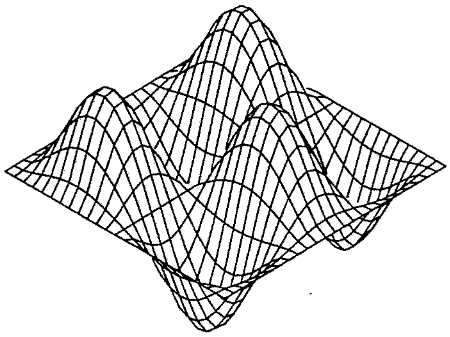

Mode 7, $\omega_{\ell 7}/\omega_{\ell 1}$=3.8642

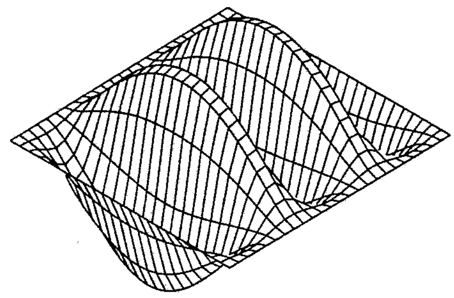

Mode 8, $\omega_{\ell 8}/\omega_{\ell 1}$=4.3788

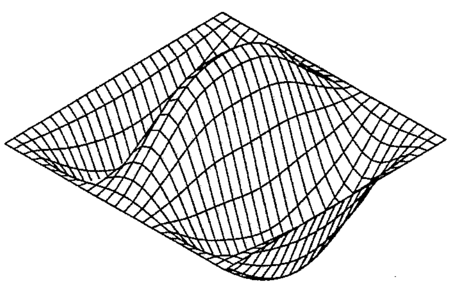

Mode 9, $\omega_{\ell 9}/\omega_{\ell 1}$=4.6622

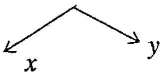

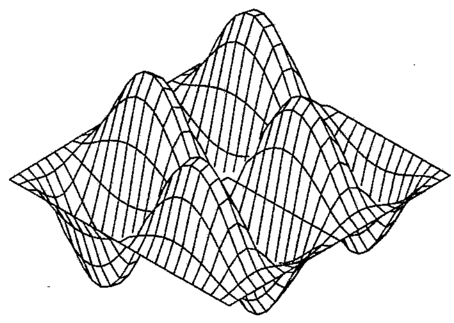

Mode 10, $\omega_{\ell 10}/\omega_{\ell 1}$=4.9302

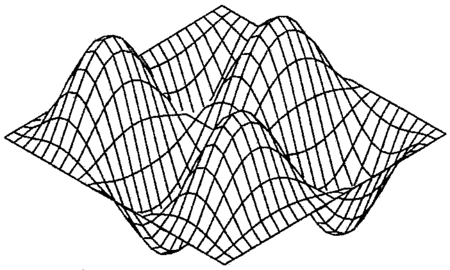

Mode 11, $\omega_{\ell 11}/\omega_{\ell 1}$=5.2653

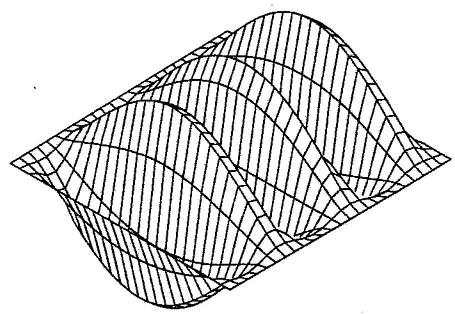

Mode 12, $\omega_{\ell 12}/\omega_{\ell 1}$=5.8312

Figure 8.43b - Linear mode shapes and natural frequencies of Plate 6. p_o=10.

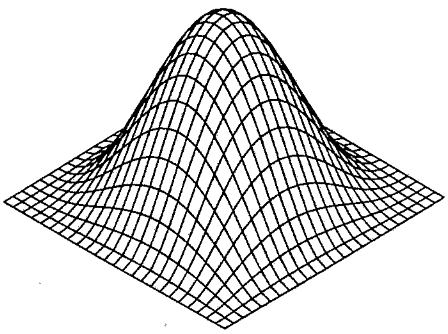

Mode 1, $\omega_{\ell 1}$=763.0961 rad/s

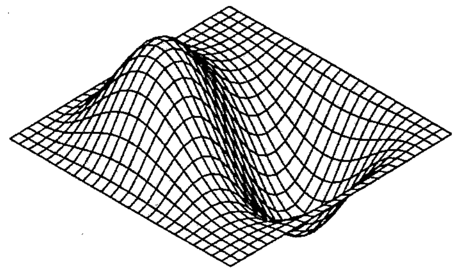

Mode 2, $\omega_{\ell 2}/\omega_{\ell 1}$=1.8607

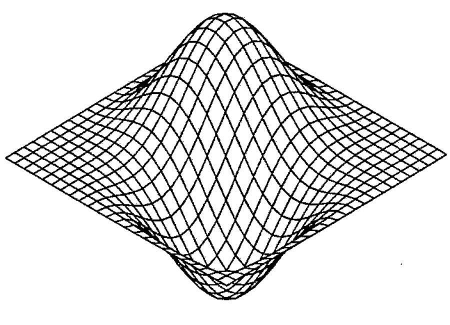

Mode 3, $\omega_{\ell 3}/\omega_{\ell 1}$=2.1588

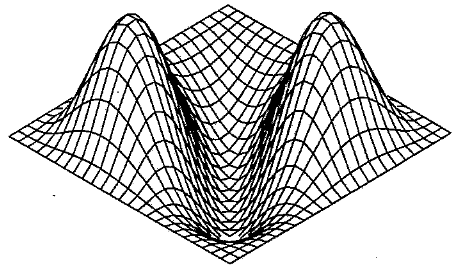

Mode 4, $\omega_{\ell 4}/\omega_{\ell 1}$=2.9081

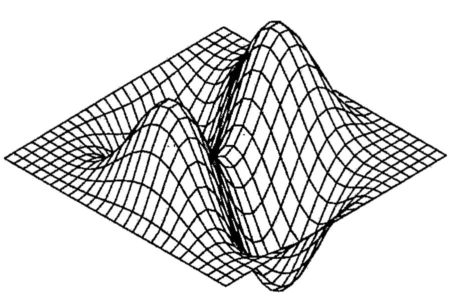

Mode 5, $\omega_{\ell 5}/\omega_{\ell 1}$=3.4735

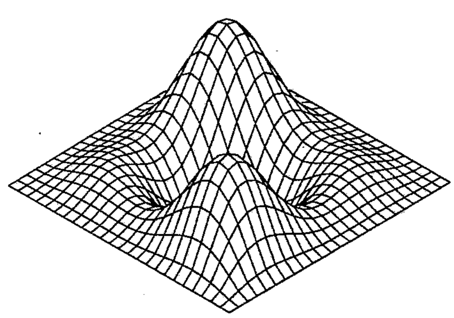

Mode 6, $\omega_{\ell 6}/\omega_{\ell 1}$=3.7546

Figure 8.44*a* - Linear mode shapes and natural frequencies of Plate 7. p_o=8.

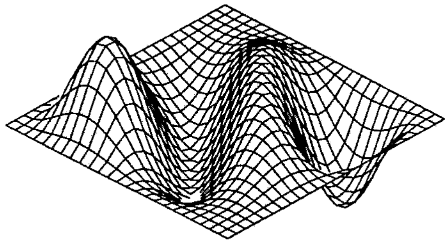

Mode 7, $\omega_{\ell 7}/\omega_{\ell 1}$=4.1852

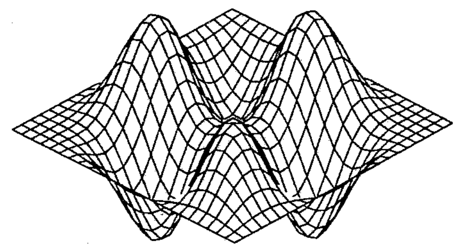

Mode 8, $\omega_{\ell 8}/\omega_{\ell 1}$=4.8693

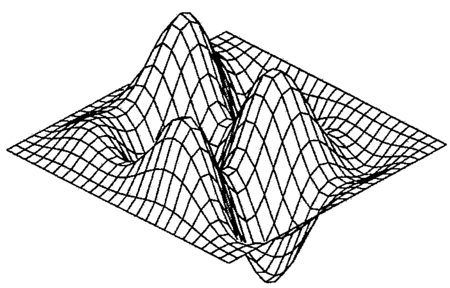

Mode 9, $\omega_{\ell 9}/\omega_{\ell 1}$=5.5497

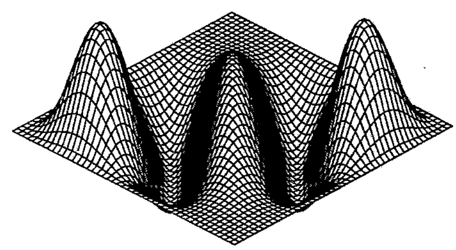

Mode 10, $\omega_{\ell 10}/\omega_{\ell 1}$=5.6961

Figure 8.44*b* - Linear mode shapes and natural frequencies of Plate 7. p_o=8.

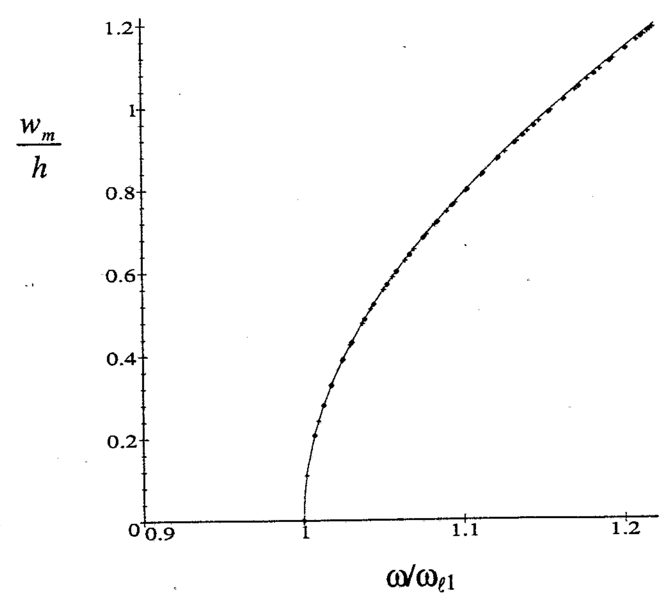

Figure 8.45 - Plate 6. Total displacement calculated at (ξ,η)=(0,0) (p_o=6, p_i=6):
- 1 harmonic, ◊ 2 harmonics, + three harmonics.

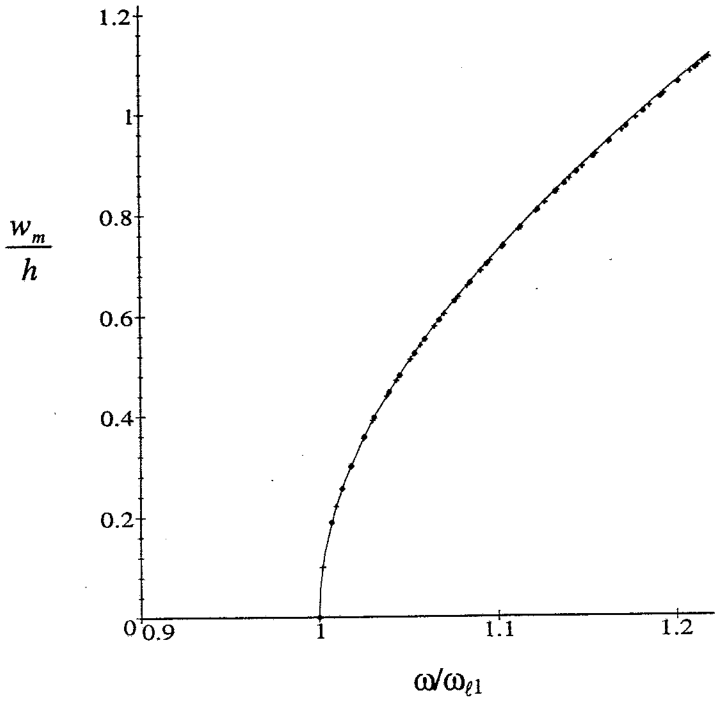

Figure 8.46 - Plate 6. Total displacement calculated at $(\xi,\eta)=(0.23,0)$ (p_o=6, p_i=6):
- 1 harmonic, ◊ 2 harmonics, + three harmonics.

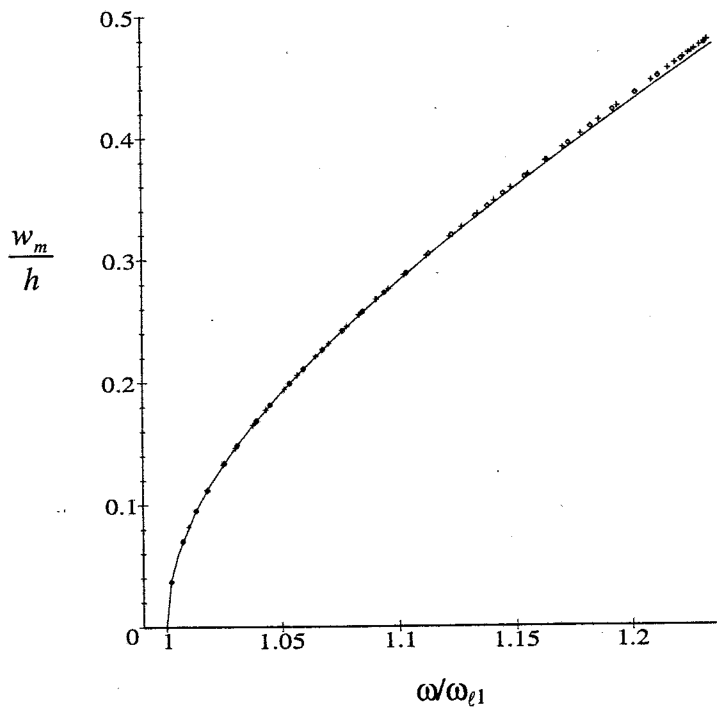

Figure 8.47 - Plate 6. Total displacement calculated at $(\xi,\eta)=(0.5,0.5)$ (p_o=6, p_i=6):
- 1 harmonic, ◊ 2 harmonics, + three harmonics.

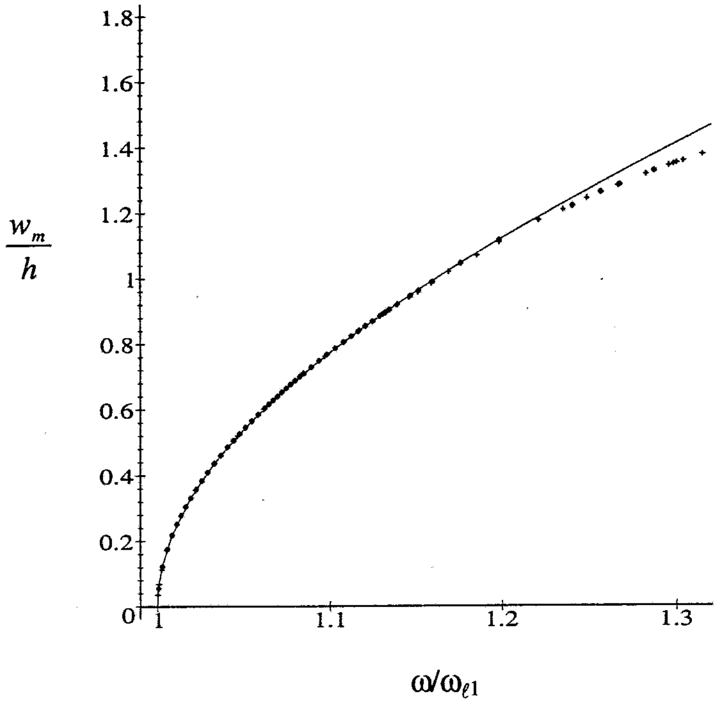

Figure 8.48 - Plate 7. Total displacement calculated at $(\xi,\eta)=(0,0)$ ($p_o=5$, $p_i=10$): - 1 harmonic, ◊ 2 harmonics, + three harmonics.

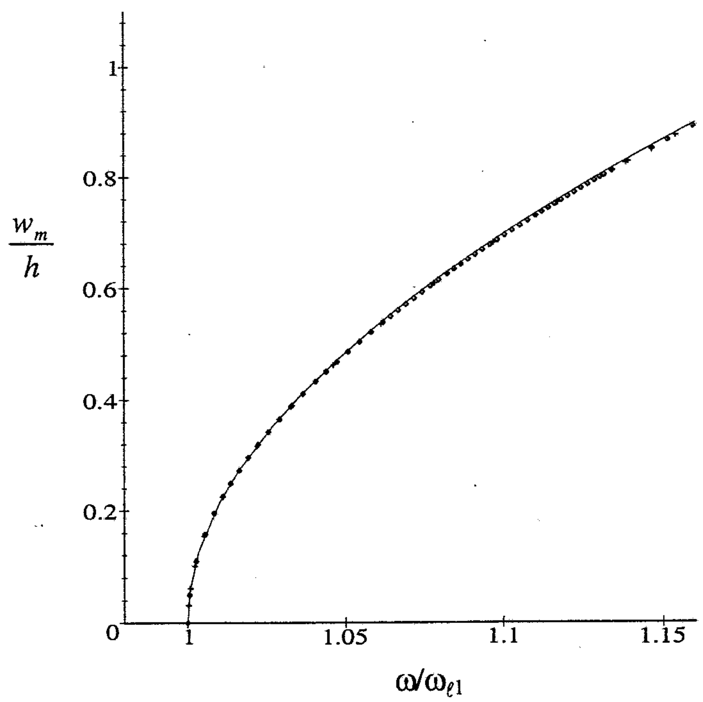

Figure 8.49 - Plate 7. Total displacement calculated at $(\xi,\eta)=(0.23,0.0)$ ($p_o=5$, $p_i=10$): - 1 harmonic, ◊ 2 harmonics, + three harmonics.

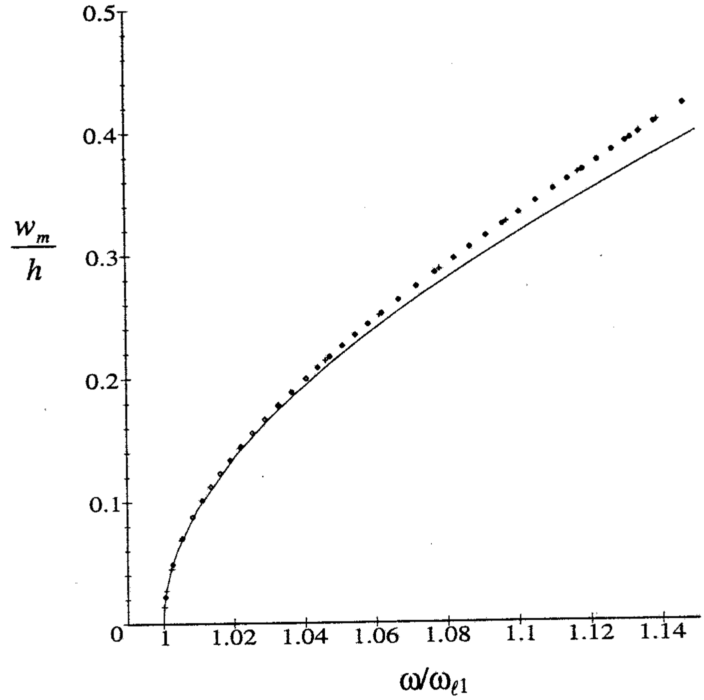

Figure 8.50 - Plate 7. Total displacement calculated at $(\xi,\eta)=(0.5,0.5)$ ($p_o=5$, $p_i=10$):
- 1 harmonic, ◊ 2 harmonics, + three harmonics.

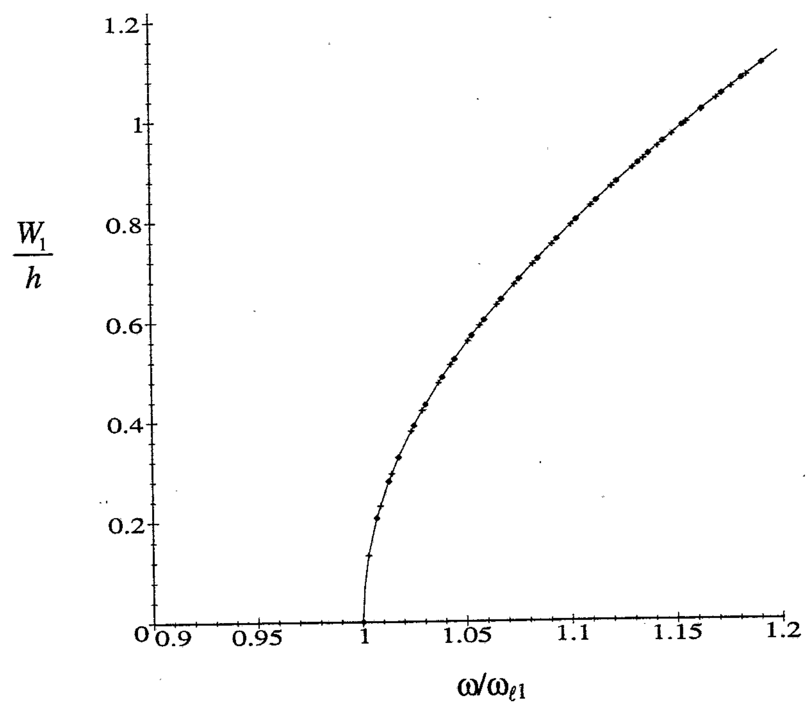

Figure 8.51 - Plate 6. First harmonic's amplitude calculated with $p_i=6$ and:
- $p_o=5$, ◊ $p_o = 6$, + $p_o=7$ $(\xi, \eta)=(0,0)$.

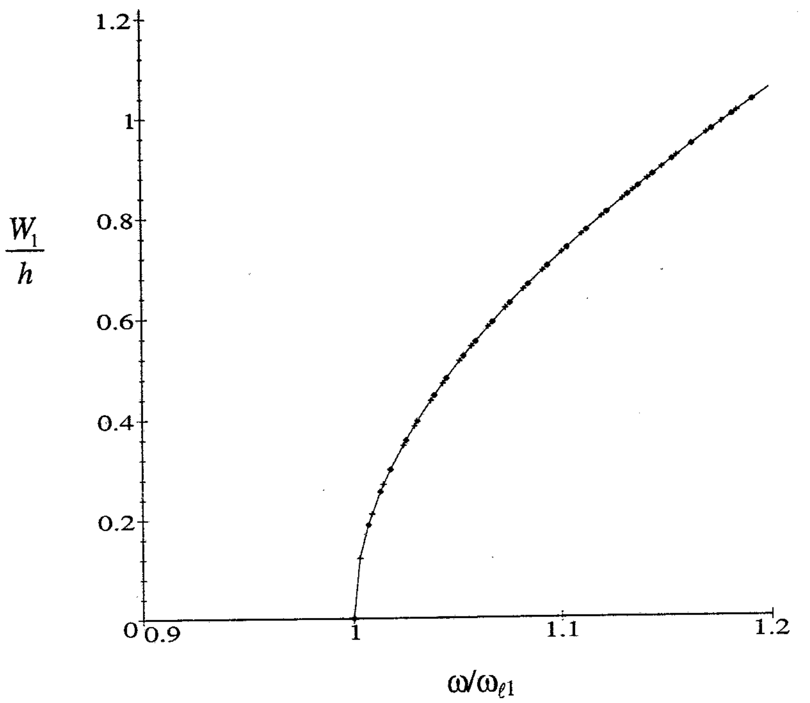

Figure 8.52 - Plate 6. First harmonic's amplitude calculated with p_i=6 and:
- p_o=5, ◊ p_o = 6, + p_o=7 (ξ, η)=(0.23,0).

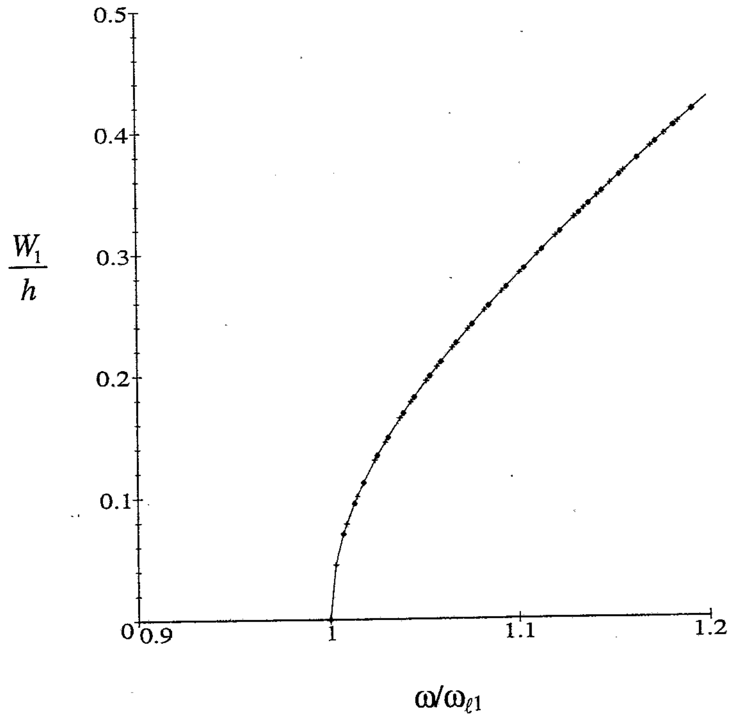

Figure 8.53 - Plate 6. First harmonic's amplitude calculated with p_i=6 and:
- p_o=5, ◊ p_o = 6, + p_o=7; (ξ, η) = (0.5, 0.5).

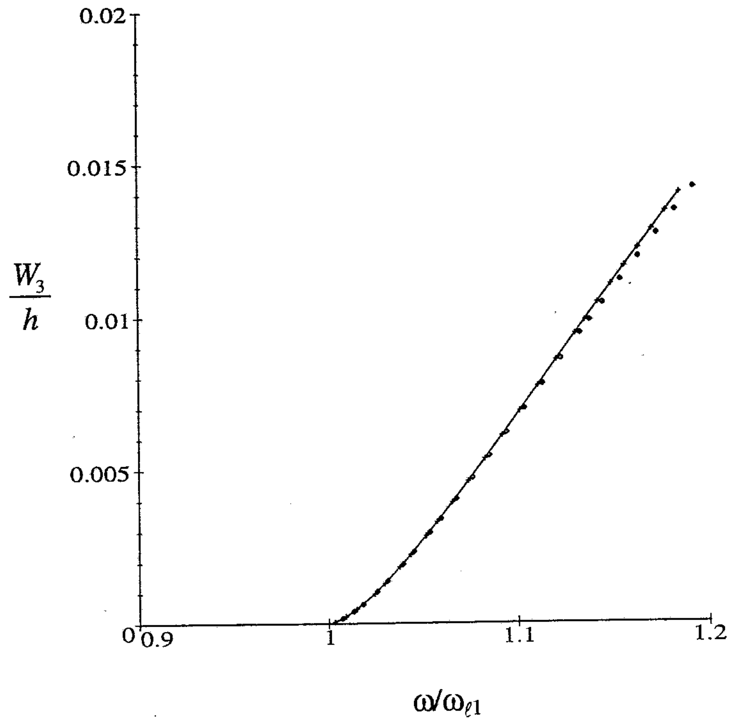

Figure 8.54 - Plate 6. Third harmonic's amplitude calculated with p_i=6 and:
◊ p_o=5, - p_o = 6, + p_o=7; (ξ,η) = (0, 0).

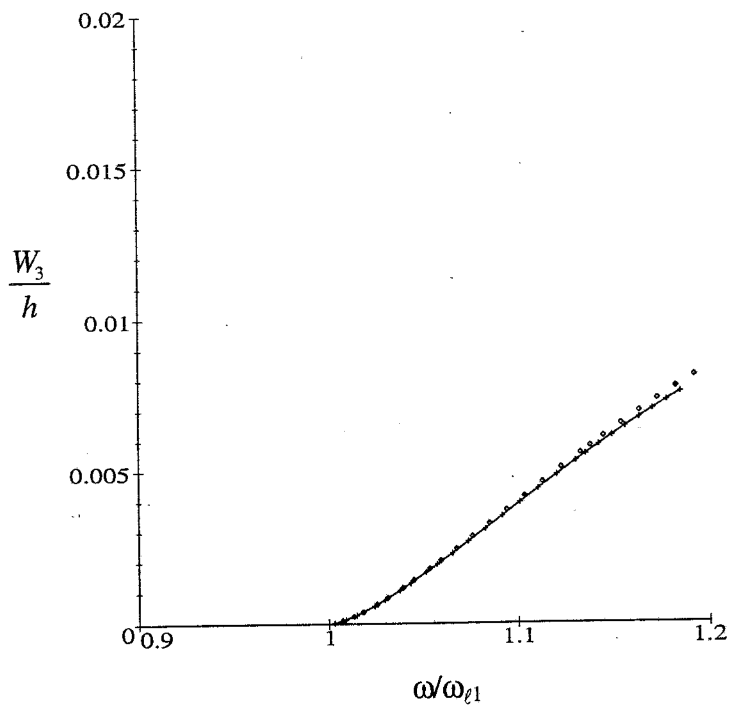

Figure 8.55 - Plate 6. Third harmonic's amplitude calculated with p_i=6 and:
◊ p_o=5, - p_o = 6, + p_o=7; (ξ, η) = (0.23, 0).

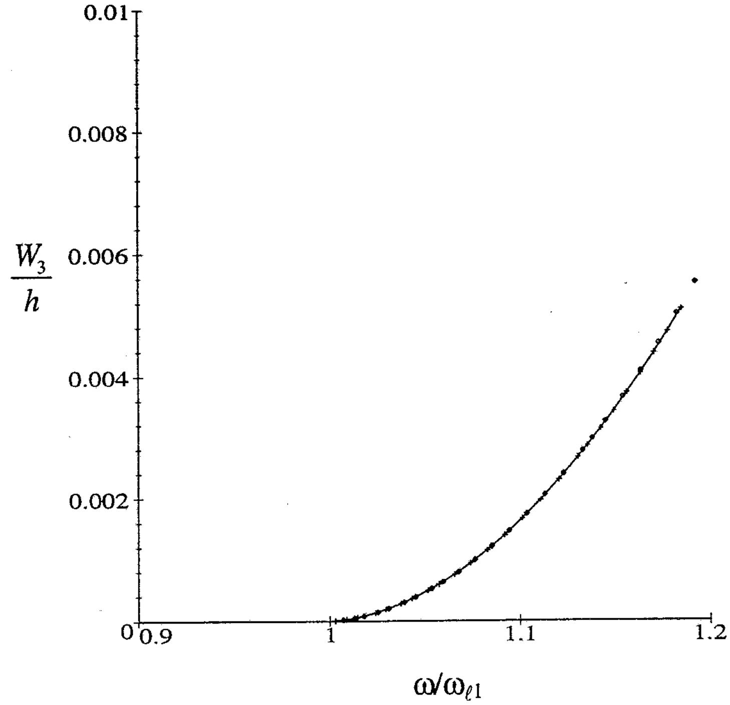

Figure 8.56 - Plate 6. Third harmonic's amplitude calculated with p_i=6 and:
◊ p_o=5, - p_o = 6, + p_o=7; (ξ, η) = (0.5, 0.5).

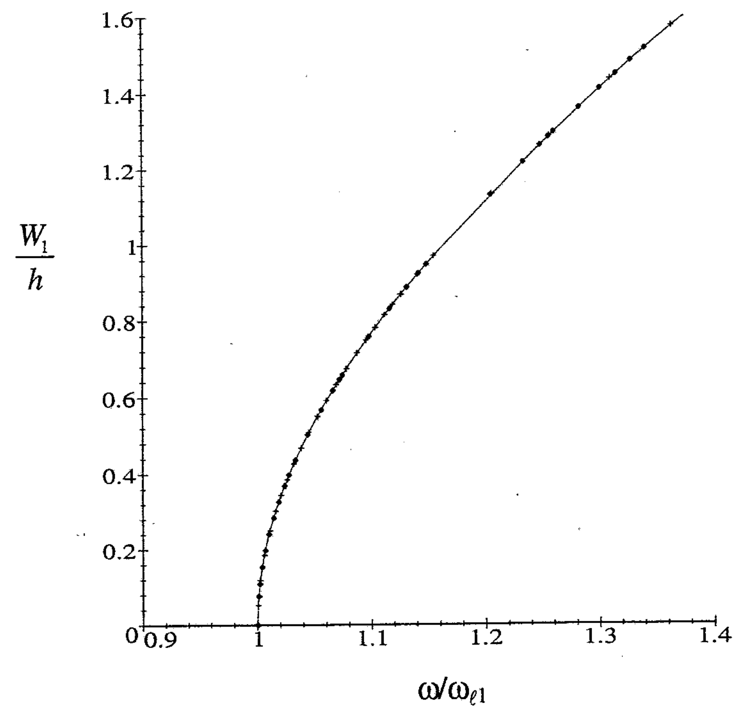

Figure 8.57 - Plate 7. First harmonic's amplitude calculated with p_i=10 and:
- p_o=5, ◊ p_o = 6, + p_o=7; (ξ, η) = (0.0, 0.0).

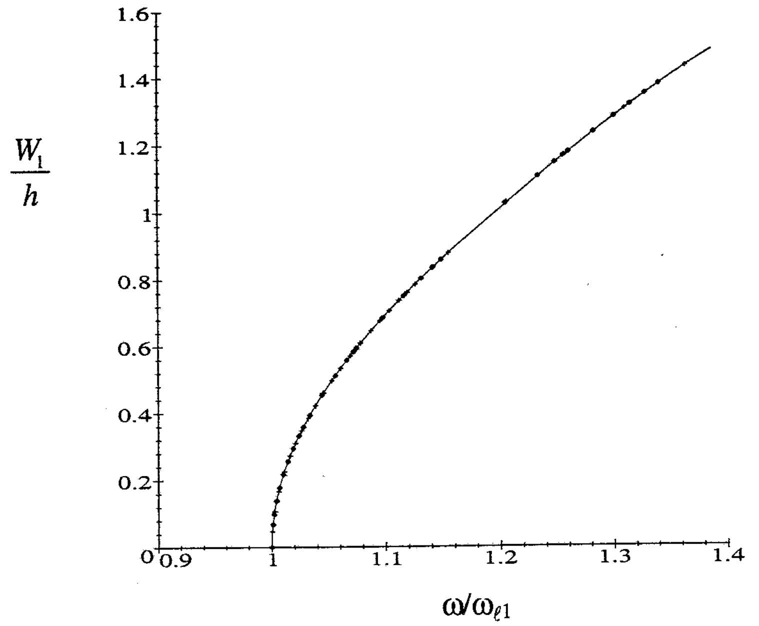

Figure 8.58 - Plate 7. First harmonic's amplitude calculated with p_i=10 and: - p_o=5, ◊ p_o = 6, + p_o=7; (ξ, η) = (0.23, 0.0).

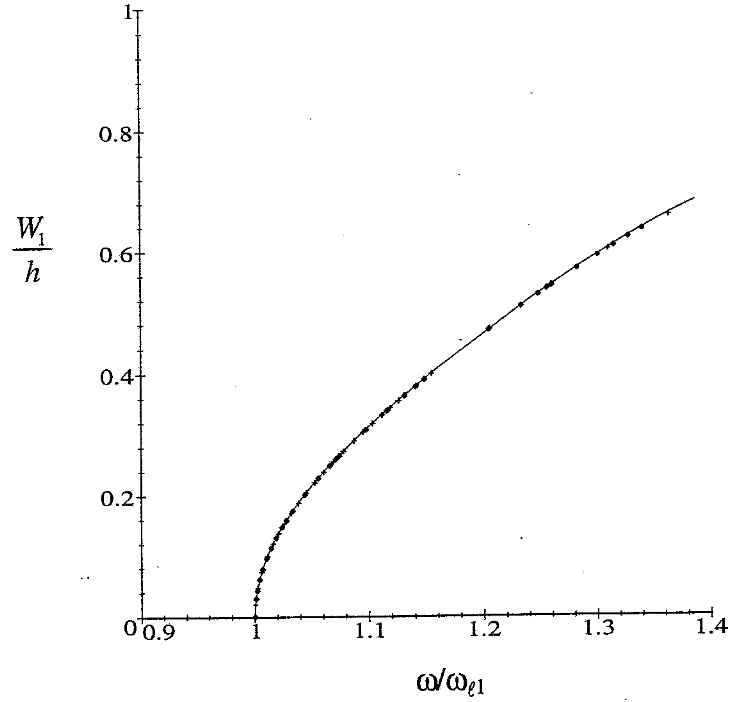

Figure 8.59 - Plate 7. First harmonic's amplitude calculated with p_i=10 and: - p_o=5, ◊ p_o = 6, + p_o=7; (ξ, η) = (0.5, 0.5).

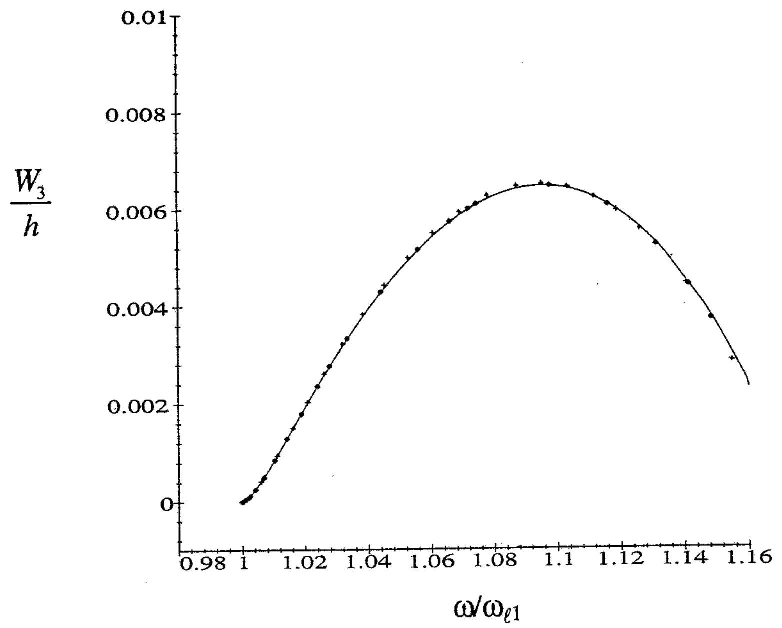

Figure 8.60 - Plate 7. Third harmonic's amplitude calculated with p_i=10 and:
◊ p_o=5, - p_o = 6, + p_o=7; (ξ, η) = (0, 0).

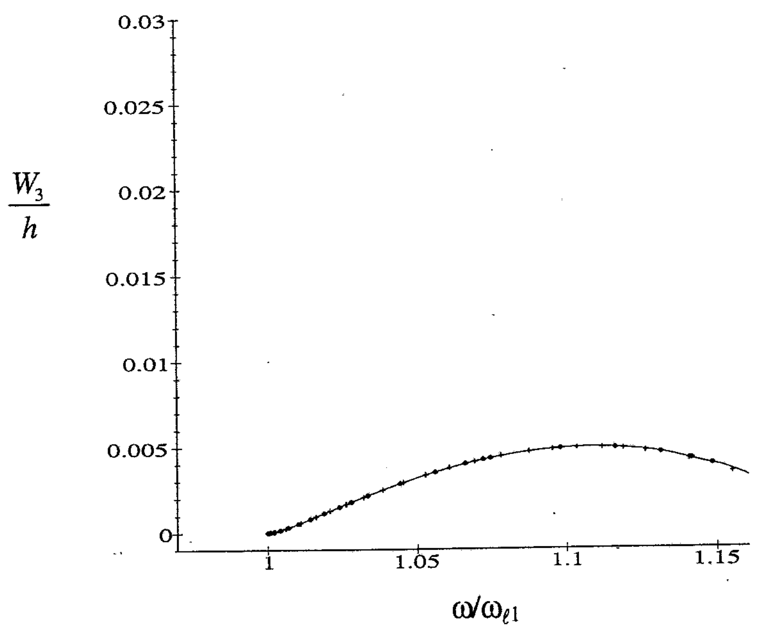

Figure 8.61 - Plate 7. Third harmonic's amplitude calculated with p_i=10 and:
◊ p_o=5, - p_o = 6, + p_o=7; (ξ, η) = (0.23, 0).

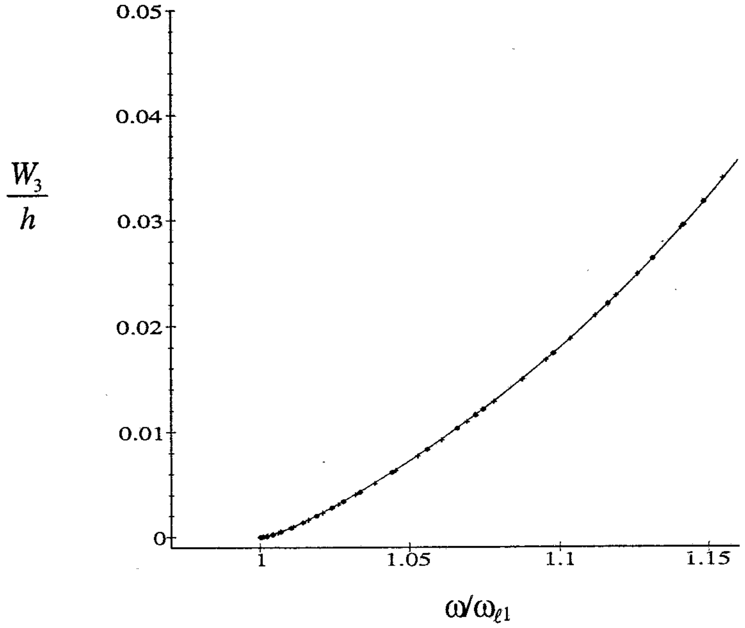

Figure 8.62 - Plate 7. Third harmonic's amplitude calculated with p_i=10 and:
◊ p_o=5, - p_o = 6, + p_o=7; (ξ, η) = (0.5, 0.5).

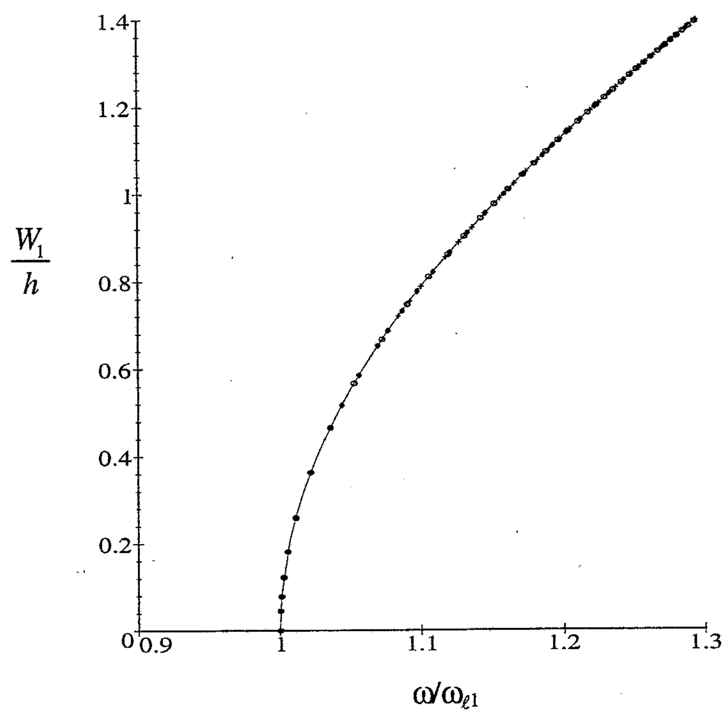

Figure 8.63 - Plate 6. First harmonic's amplitude calculated with p_o=6 and:
- p_i = 6, ◊ p_i=7, + p_i=8, o p_i=10; (ξ, η) = (0, 0).

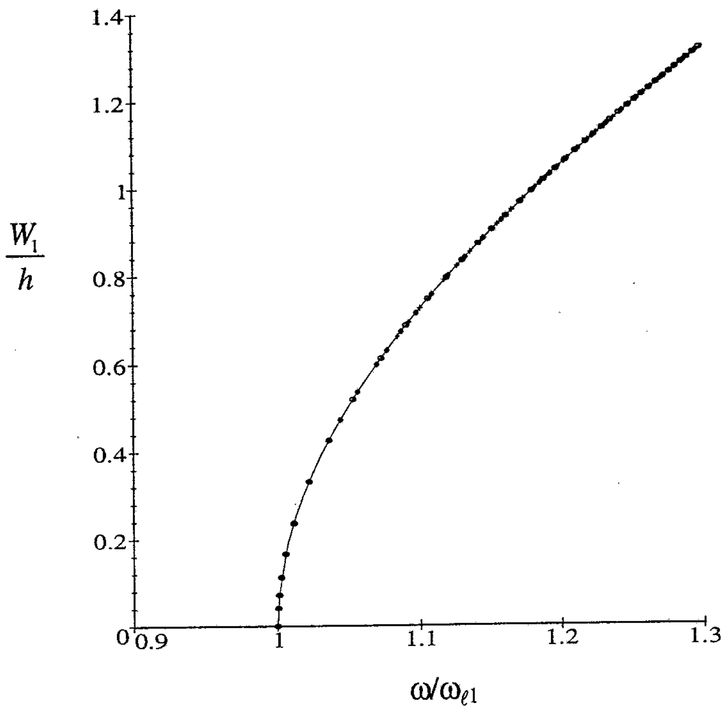

Figure 8.64 - Plate 6. First harmonic's amplitude calculated with p_o=6 and:
- p_i = 6, ◊ p_i=7, + p_i=8, o p_i=10; $(\xi, \eta) = (0.23, 0)$.

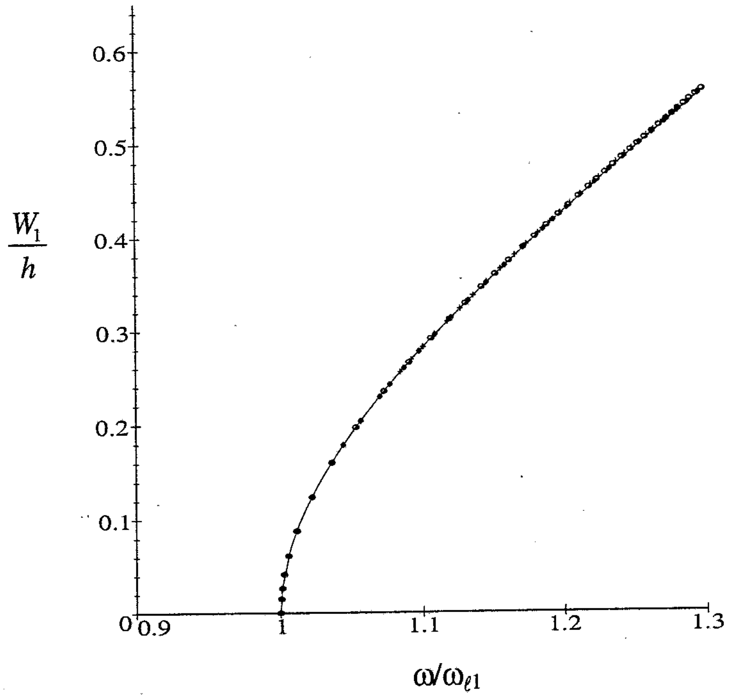

Figure 8.65 - Plate 6. First harmonic's amplitude calculated with p_o=6 and:
- p_i = 6, ◊ p_i=7, + p_i=8, o p_i=10; $(\xi, \eta) = (0.5, 0.5)$.

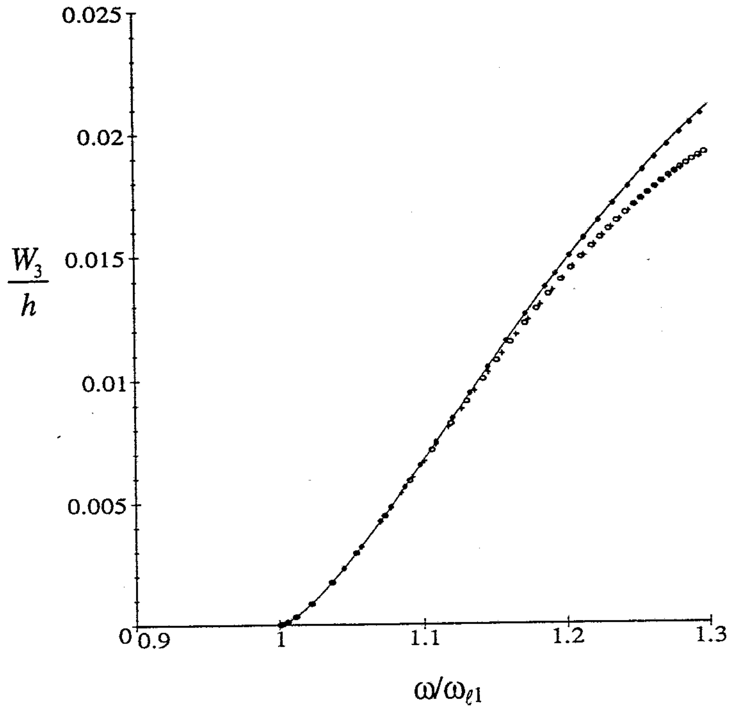

Figure 8.66 - Plate 6. Third harmonic's amplitude calculated with p_o=6 and:
- p_i=6, ◊ p_i=7, + p_i=8, o p_i=10; $(\xi, \eta) = (0, 0)$.

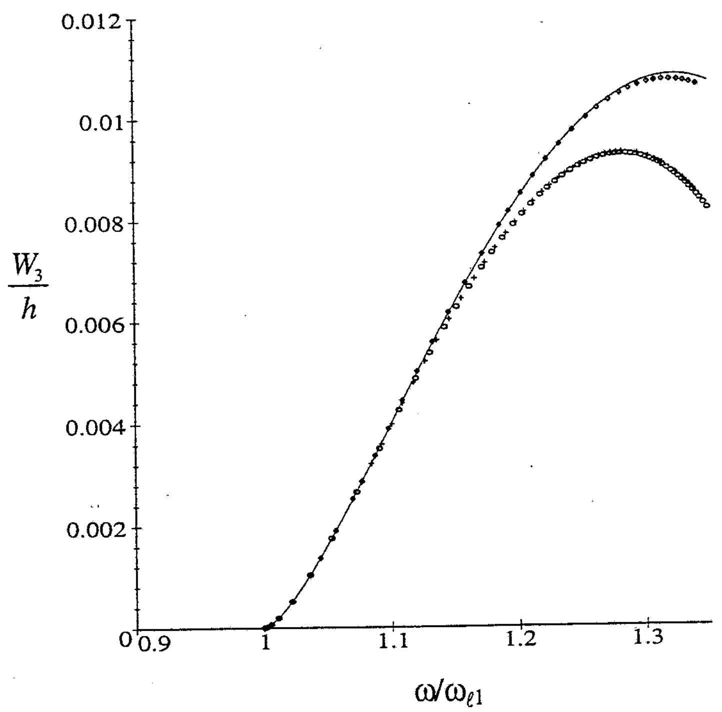

Figure 8.67 - Plate 6. Third harmonic's amplitude calculated with p_o=6 and:
- p_i=6, ◊ p_i=7, + p_i=8, o p_i=10; $(\xi, \eta) = (0.23, 0)$.

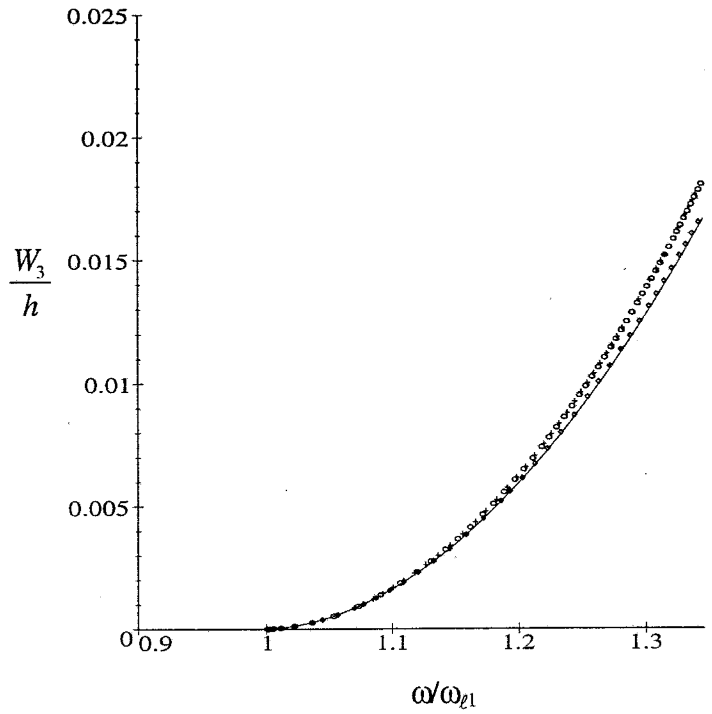

Figure 8.68 - Plate 6. Third harmonic's amplitude calculated with p_o=6 and:
- p_i=6, ◊ p_i=7, + p_i=8, o p_i=10; $(\xi, \eta) = (0.5, 0.5)$.

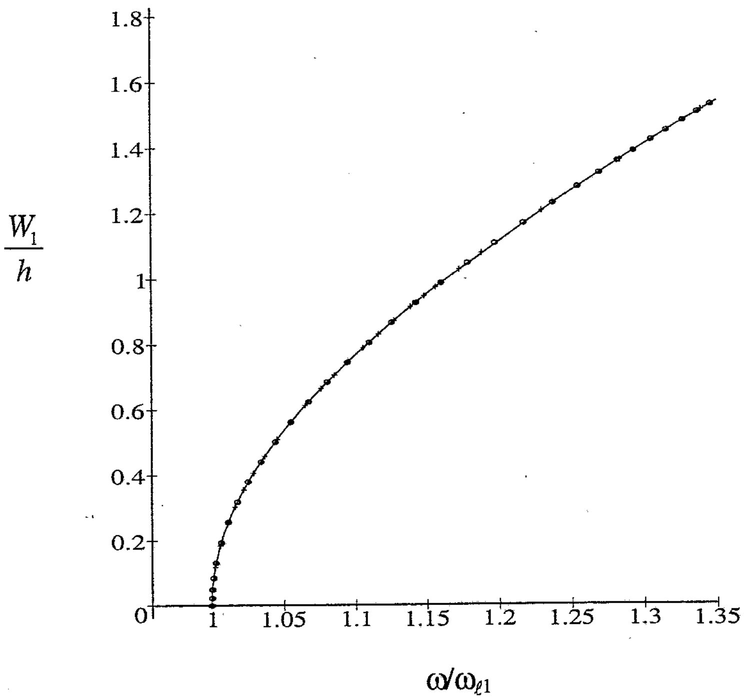

Figure 8.69 - Plate 7. First harmonic's amplitude calculated with p_o=5 and:
+ p_i=7, o p_i=8, - p_i=10; (ξ, η)=(0, 0).

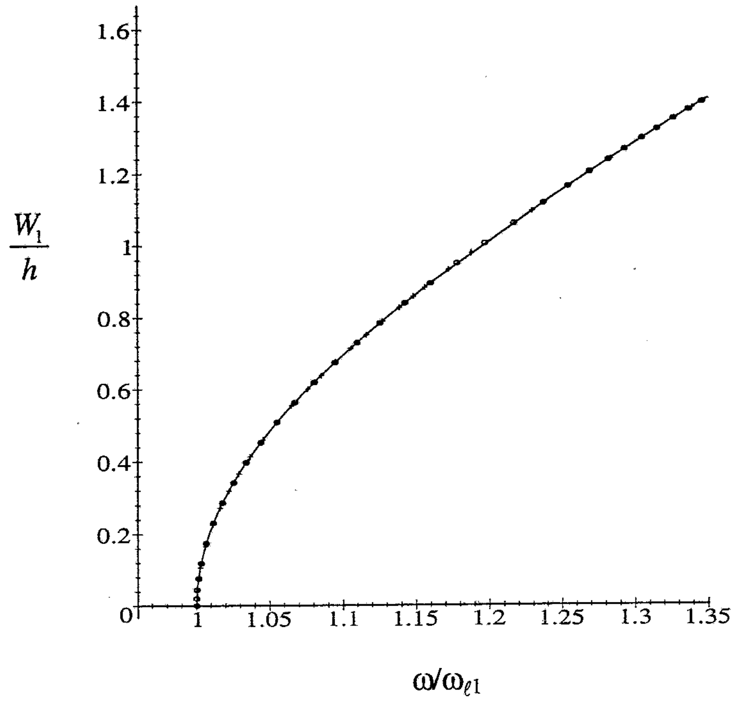

Figure 8.70 - Plate 7. First harmonic's amplitude calculated with p_o=5 and: + p_i=7, o p_i=8, - p_i=10; (ξ, η)=(0.23, 0).

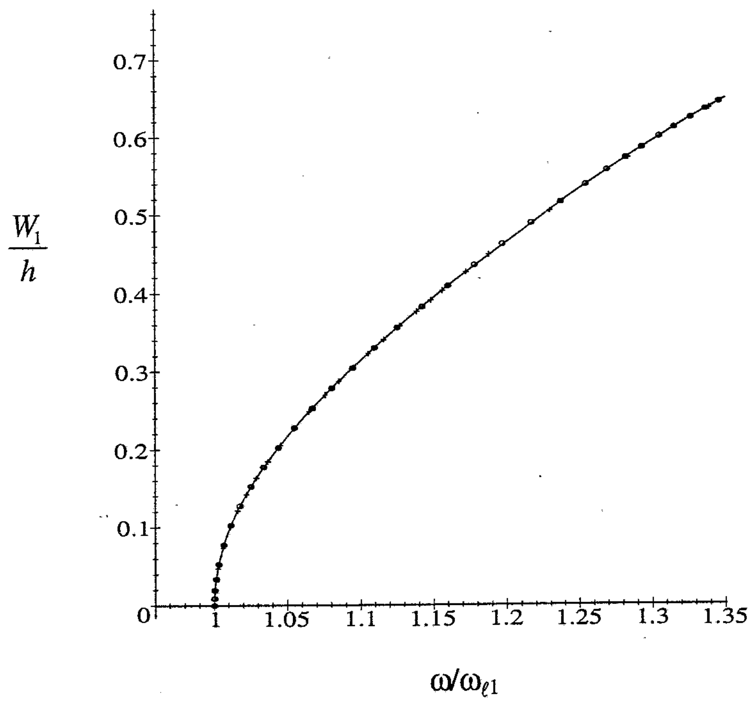

Figure 8.71 - Plate 7. First harmonic's amplitude calculated with p_o=5 and: + p_i=7, o p_i=8, - p_i=10; (ξ, η)=(0.5, 0.5).

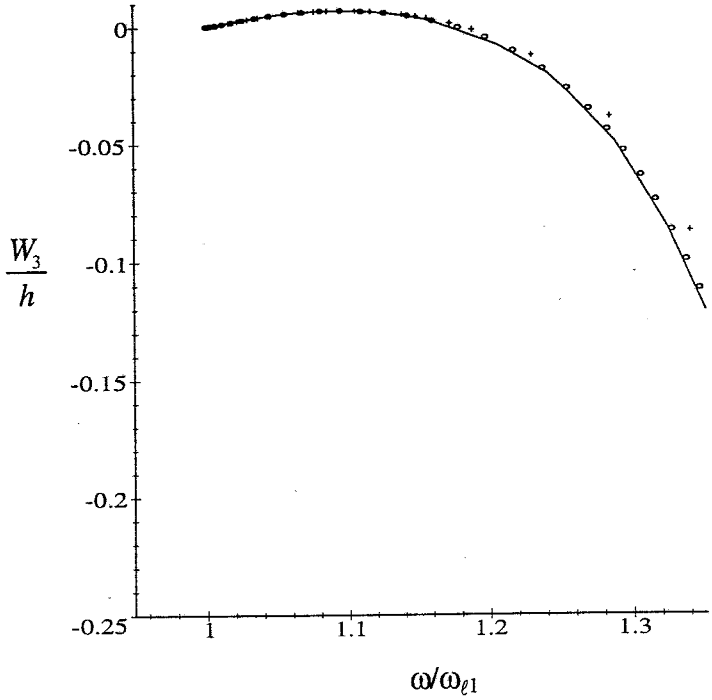

Figure 8.72 - Plate 7. Third harmonic's amplitude calculated with p_o=5 and: + p_i=7, o p_i=8, - p_i=10; (ξ,η)=(0, 0).

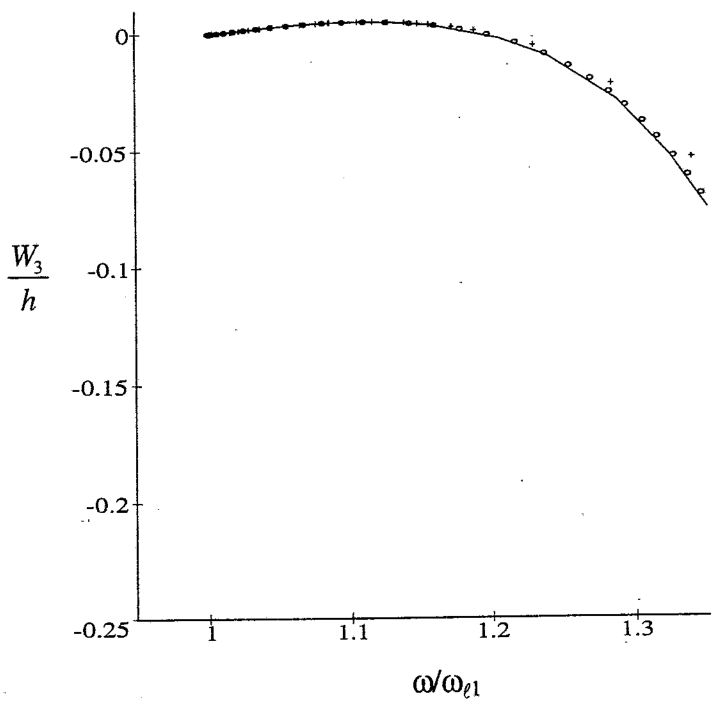

Figure 8.73 - Plate 7. Third harmonic's amplitude calculated with p_o=5 and: + p_i=7, o p_i=8, - p_i=10; (ξ,η)=(0.23, 0).

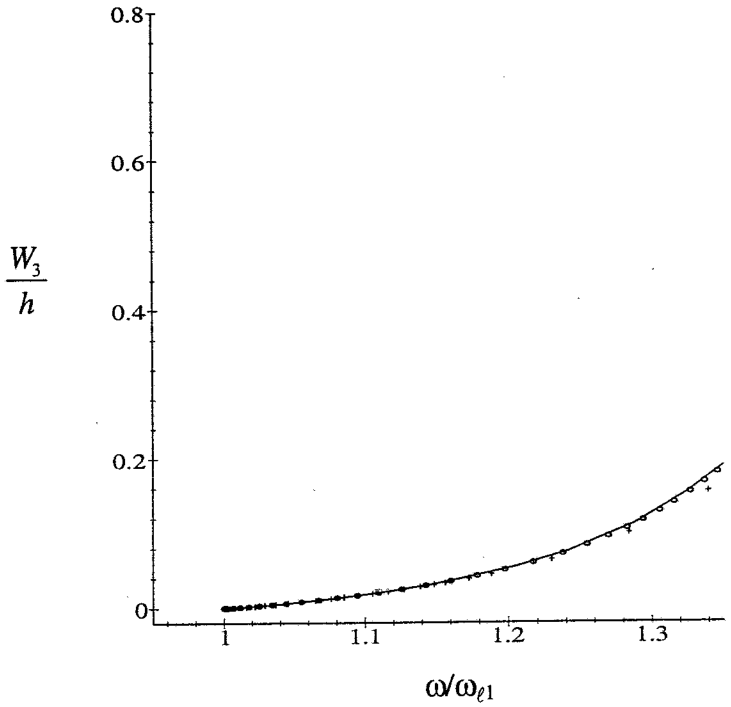

Figure 8.74 - Plate 7. Third harmonic's amplitude calculated with p_o=5 and: + p_i=7, o p_i=8, - p_i=10; (ξ,η)=(0.5, 0.5).

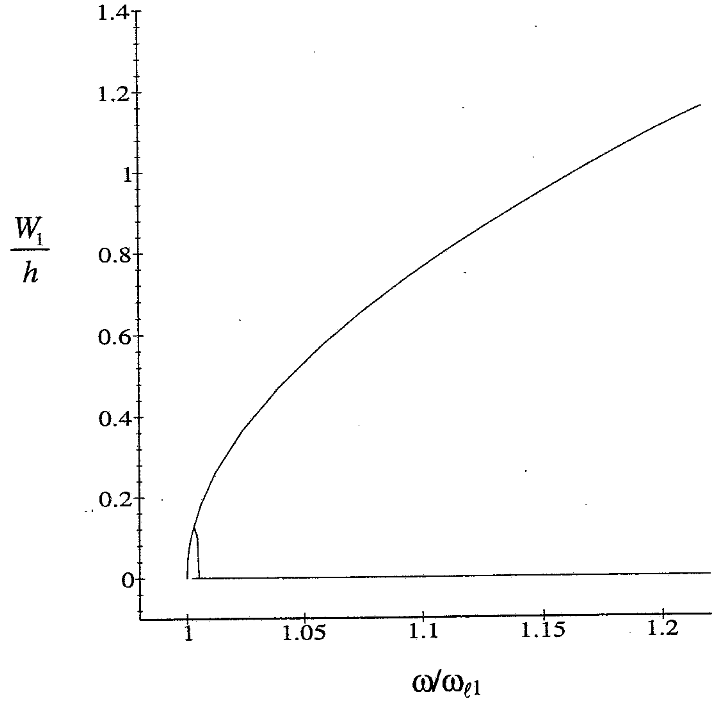

Figure 8.75 - Branch diagram of Plate 6. First harmonic's amplitude calculated at (ξ,η)=(0, 0) with p_o=6, p_i=10.

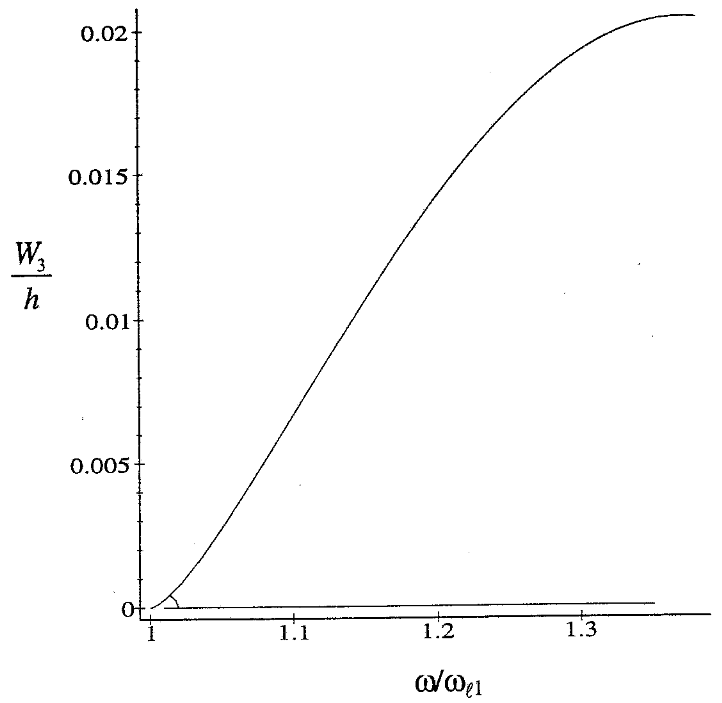

Figure 8.76 - Branch diagram of Plate 6. Third harmonic's amplitude calculated at (ξ,η)=(0, 0) with p_o=6, p_i=10.

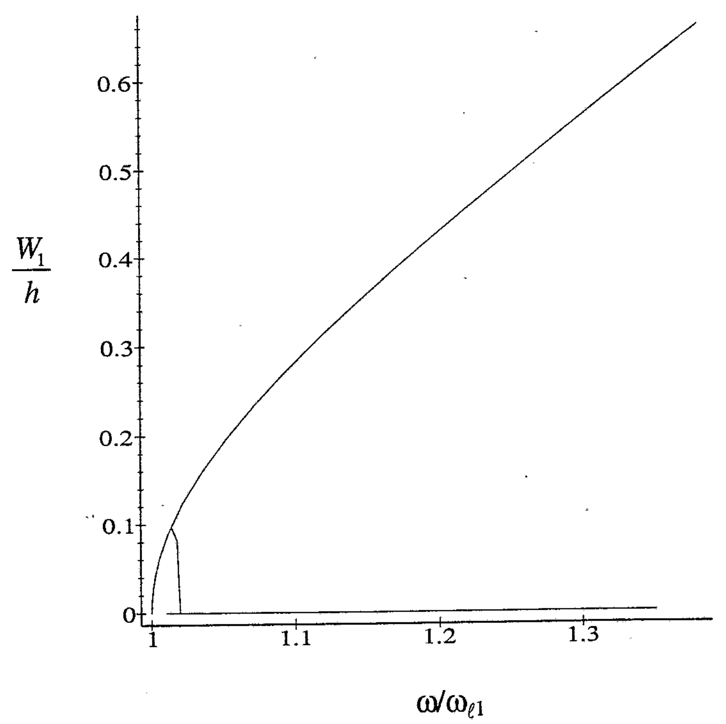

Figure 8.77 - Branch diagram of Plate 6. First harmonic's amplitude calculated at (ξ,η)=(0.5, 0.5) with p_o=6, p_i=10.

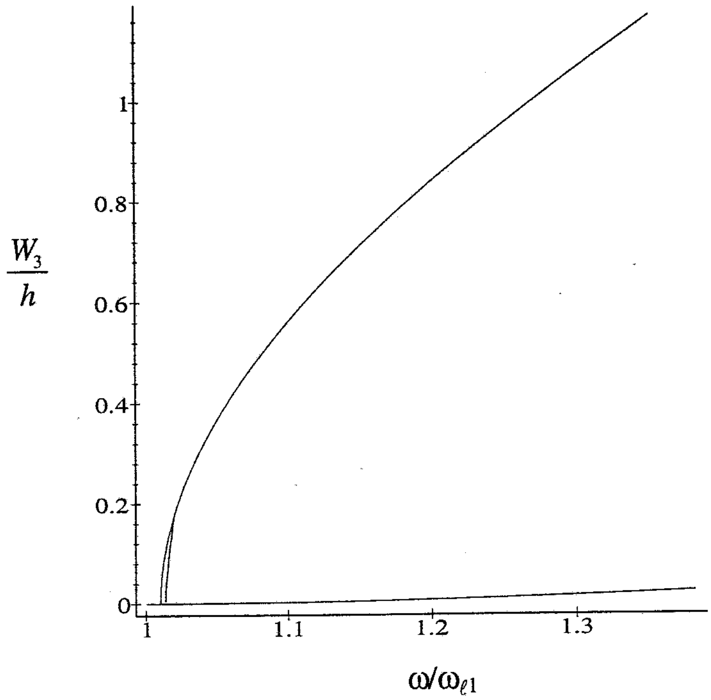

Figure 8.78 - Branch diagram of Plate 6. Third harmonic's amplitude calculated at $(\xi,\eta)=(0.5, 0.5)$ with $p_o=6$, $p_i=10$.

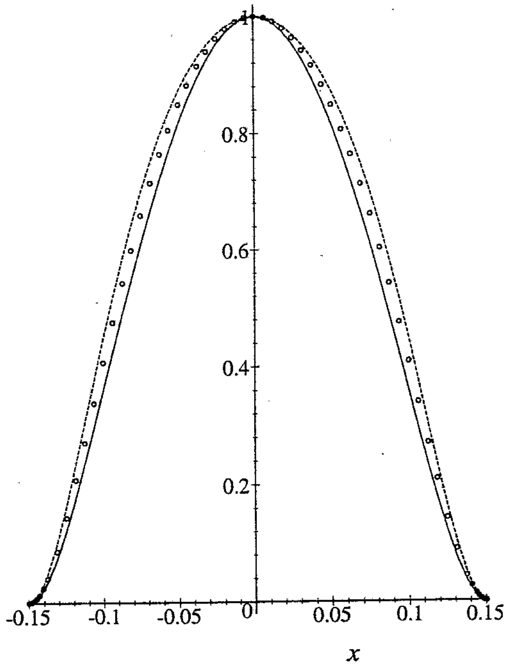

Figure 8.79 - Sections of modes of first harmonic of Plate 6, first main branch at points - $\omega/\omega_{\ell 1}=1.0004$, o $\omega/\omega_{\ell 1}=1.1883$, -- $\omega/\omega_{\ell 1}=1.3818$. $y=0$.

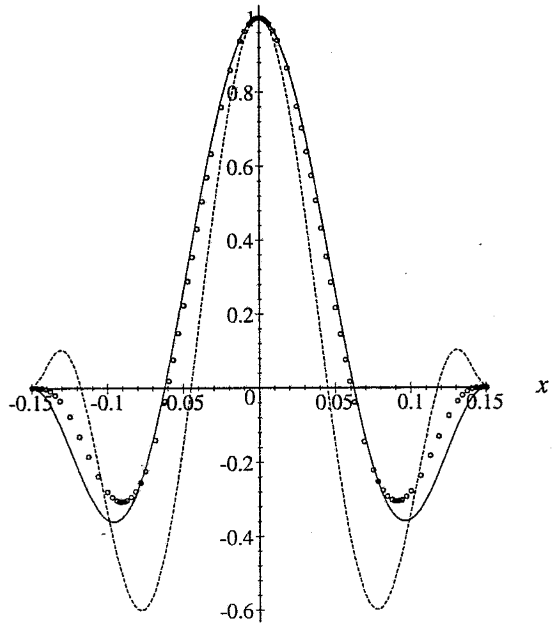

Figure 8.80 - Sections of modes of third harmonic of Plate 6, first main branch at points - $\omega/\omega_{\ell 1}$=1.0004, o $\omega/\omega_{\ell 1}$=1.1883, -- $\omega/\omega_{\ell 1}$=1.3818. y=0.

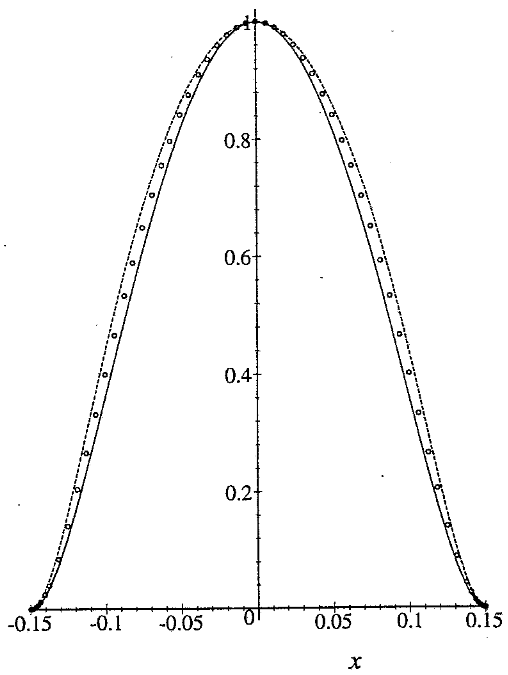

Figure 8.81 - Sections of shape of vibration (both harmonics) of Plate 6, first main branch, points $\omega/\omega_{\ell 1}$ = - 1.0004, - . $\omega/\omega_{\ell 1}$ = 1.1883, -- $\omega/\omega_{\ell 1}$ = 1.3818. y=0.

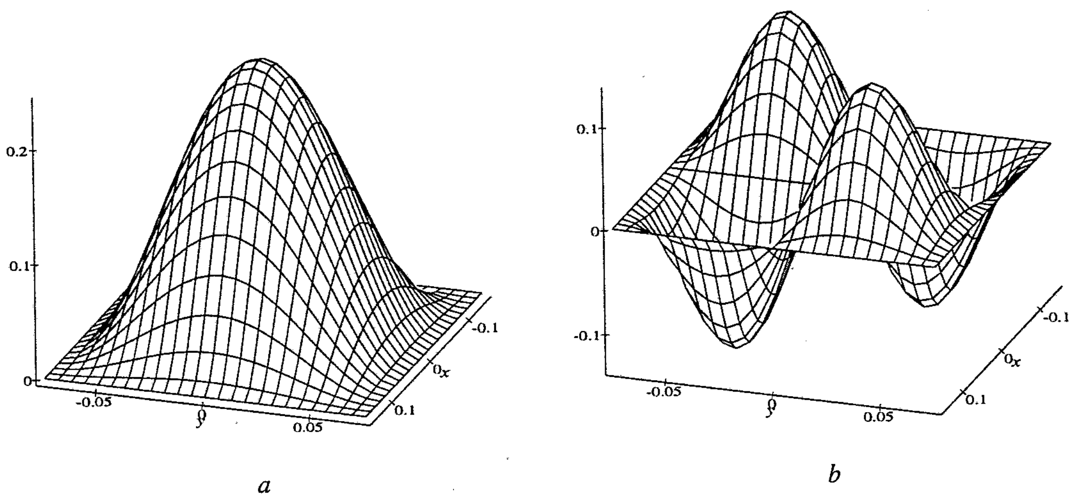

Figure 8.82 - Mode shapes associated with first and third harmonics, at point $\omega/\omega_{\ell 1}$ = 1.0179 of secondary branch. Plate 6.

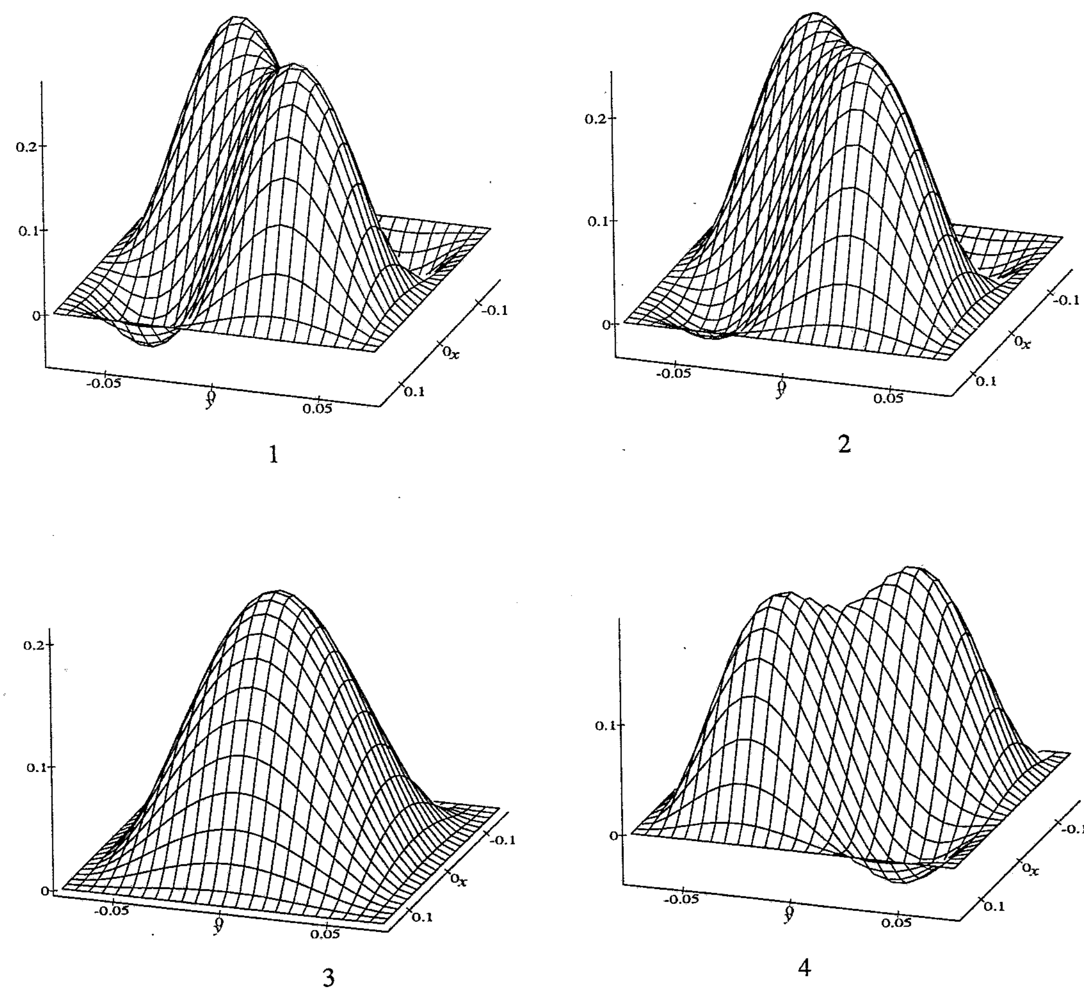

Figure 8.83*a* - Vibration of Plate 6 during half a cycle, at point $\omega/\omega_{\ell 1}$ = 1.0179 of secondary branch.

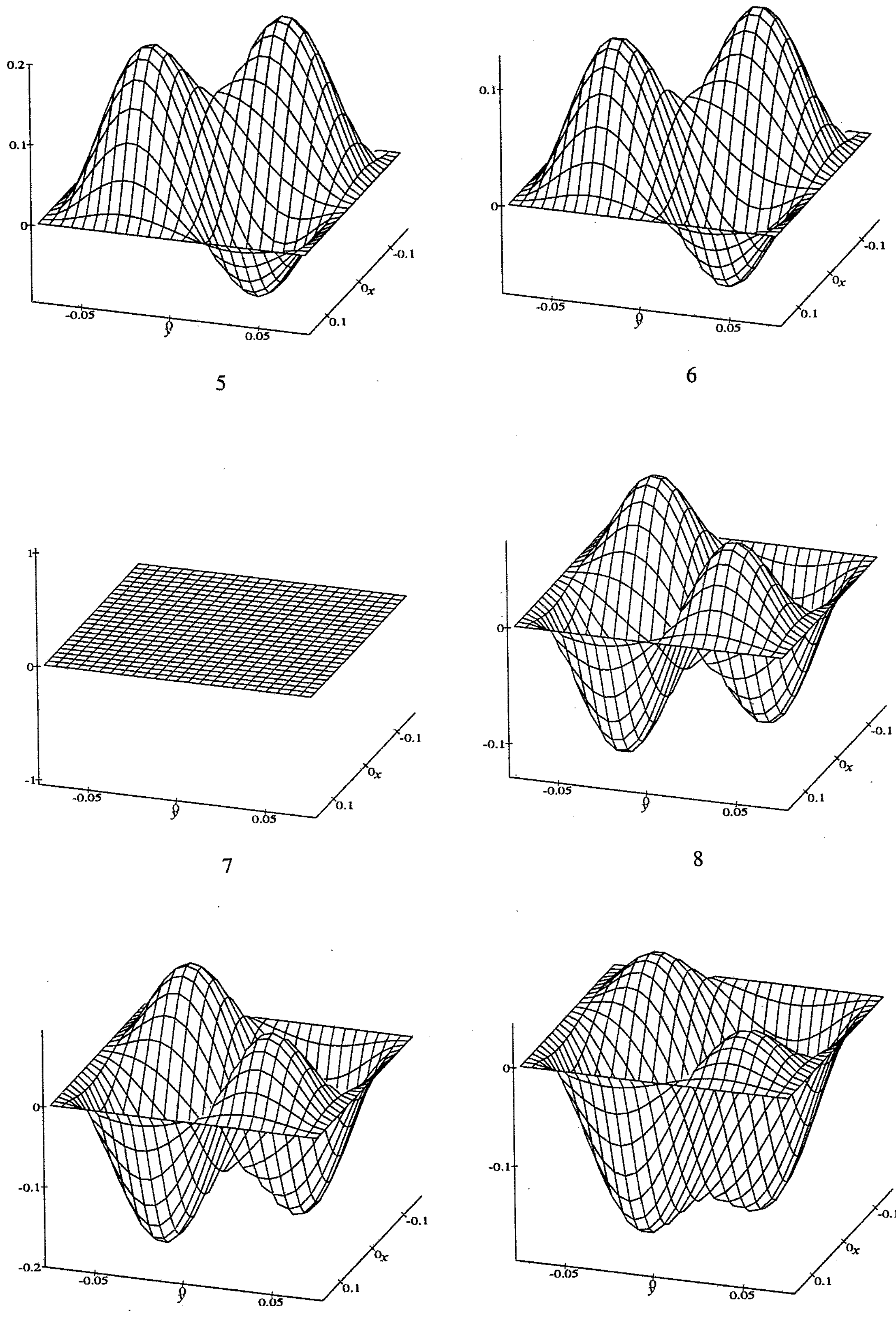

Figure 8.83*b* - Vibration of Plate 6 during half a cycle, at point $\omega/\omega_{\ell 1} = 1.0179$ of secondary branch.

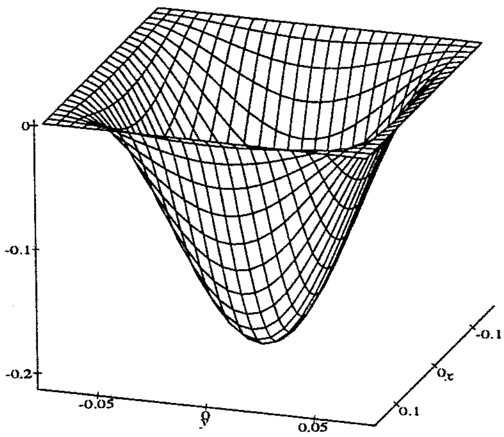

11

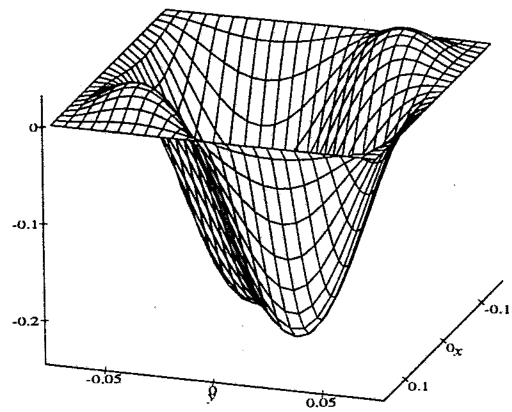

12

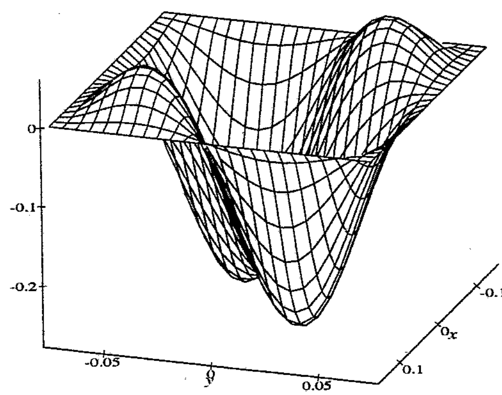

13

Figure 8.83*c* - Vibration of Plate 6 during half a cycle, at point $\omega/\omega_{\ell 1} = 1.0179$ of secondary branch.

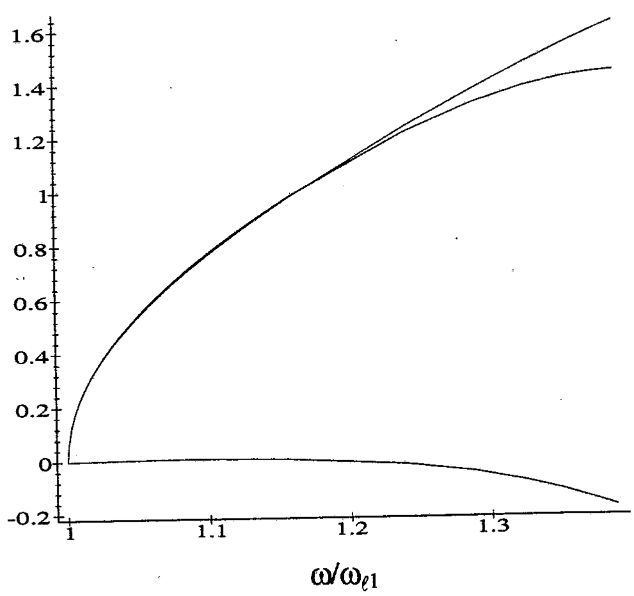

Figure 8.84 - Plate 7. p_o=5, p_i=10; (ξ,η)=(0,0). From the top: first harmonic, total and third harmonic nondimensional amplitudes.

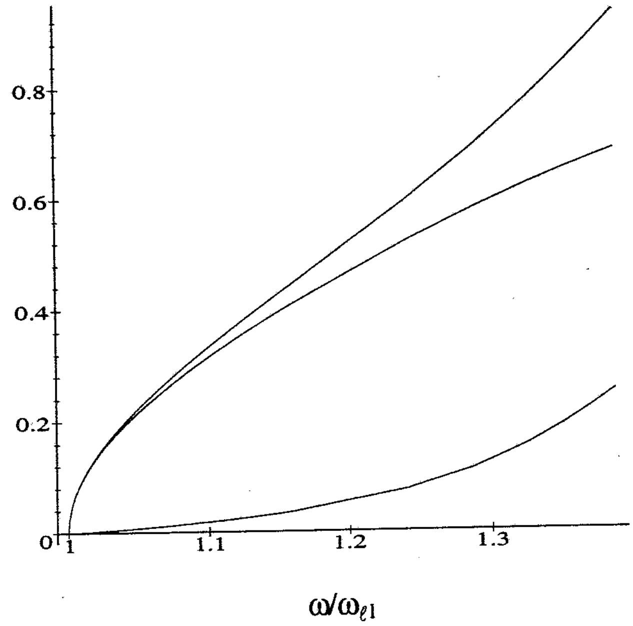

Figure 8.85 - Plate 7. p_o=5, p_i=10; (ξ,η)=(0.5,0.5). From the top: total, first harmonic's and third harmonic's nondimensional amplitudes.

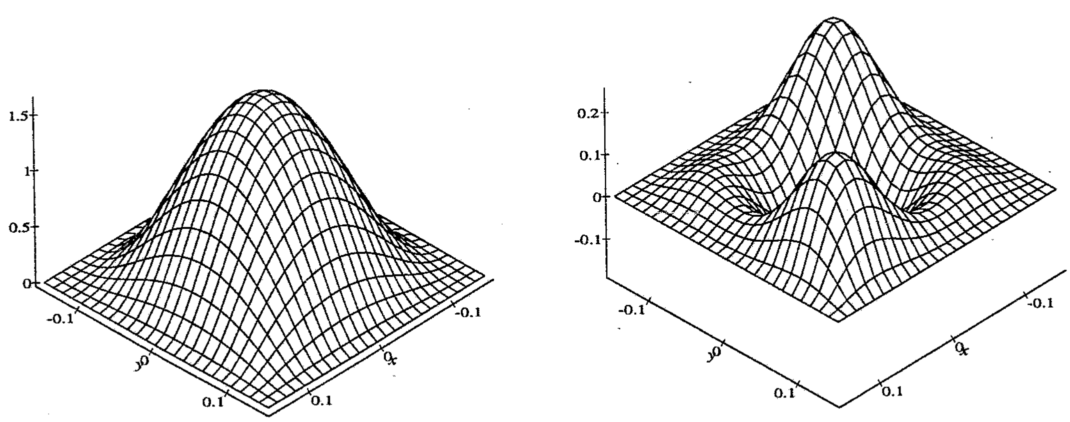

a *b*

Figure 8.86 - Mode shapes associated with first and third harmonics, at point $\omega/\omega_{\ell 1}$ = 1.3868 of secondary branch. Plate7.

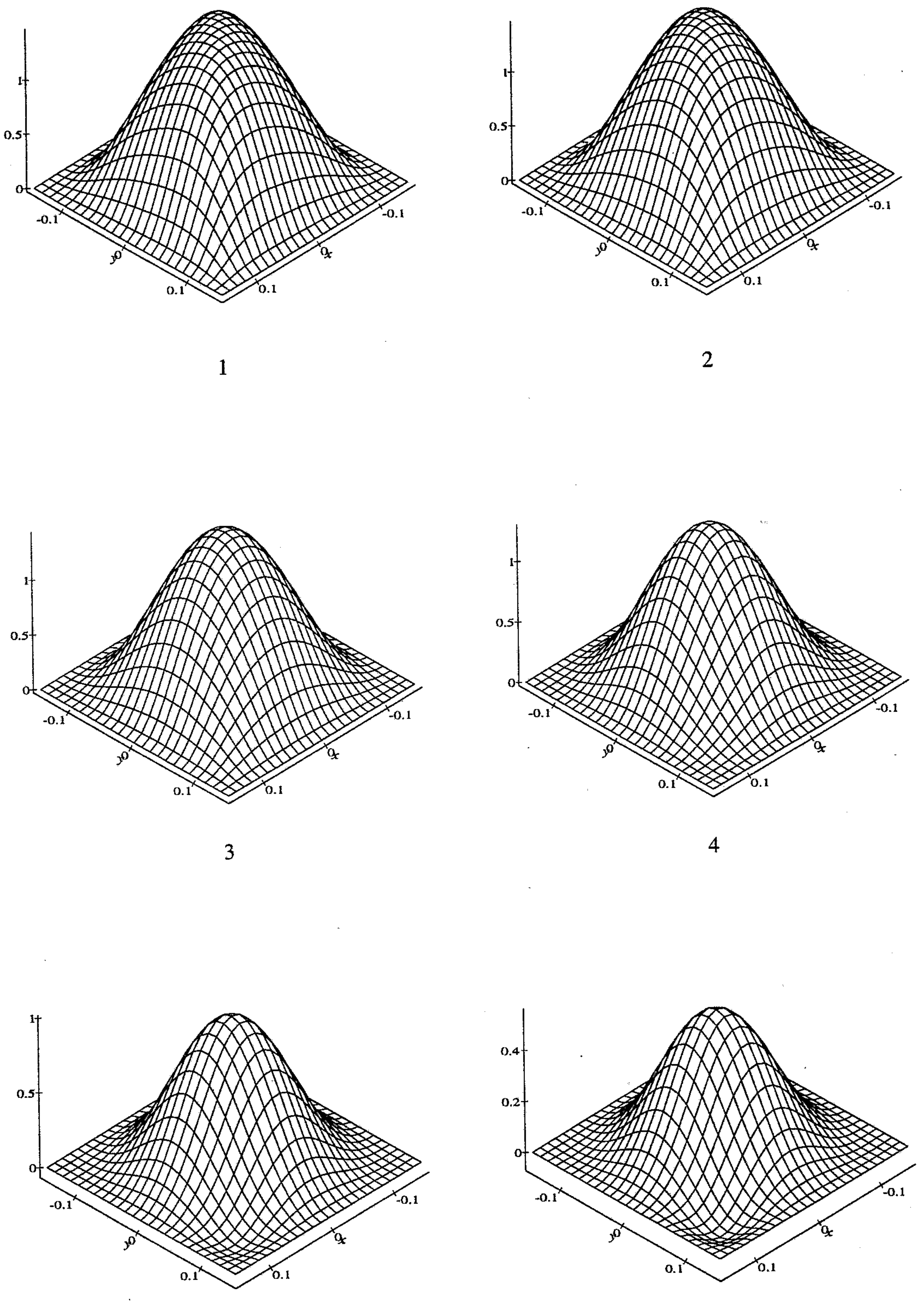

Figure 8.87a - Vibration of Plate 7 during half a cycle, at point $\omega/\omega_{\ell 1} = 1.3868$.

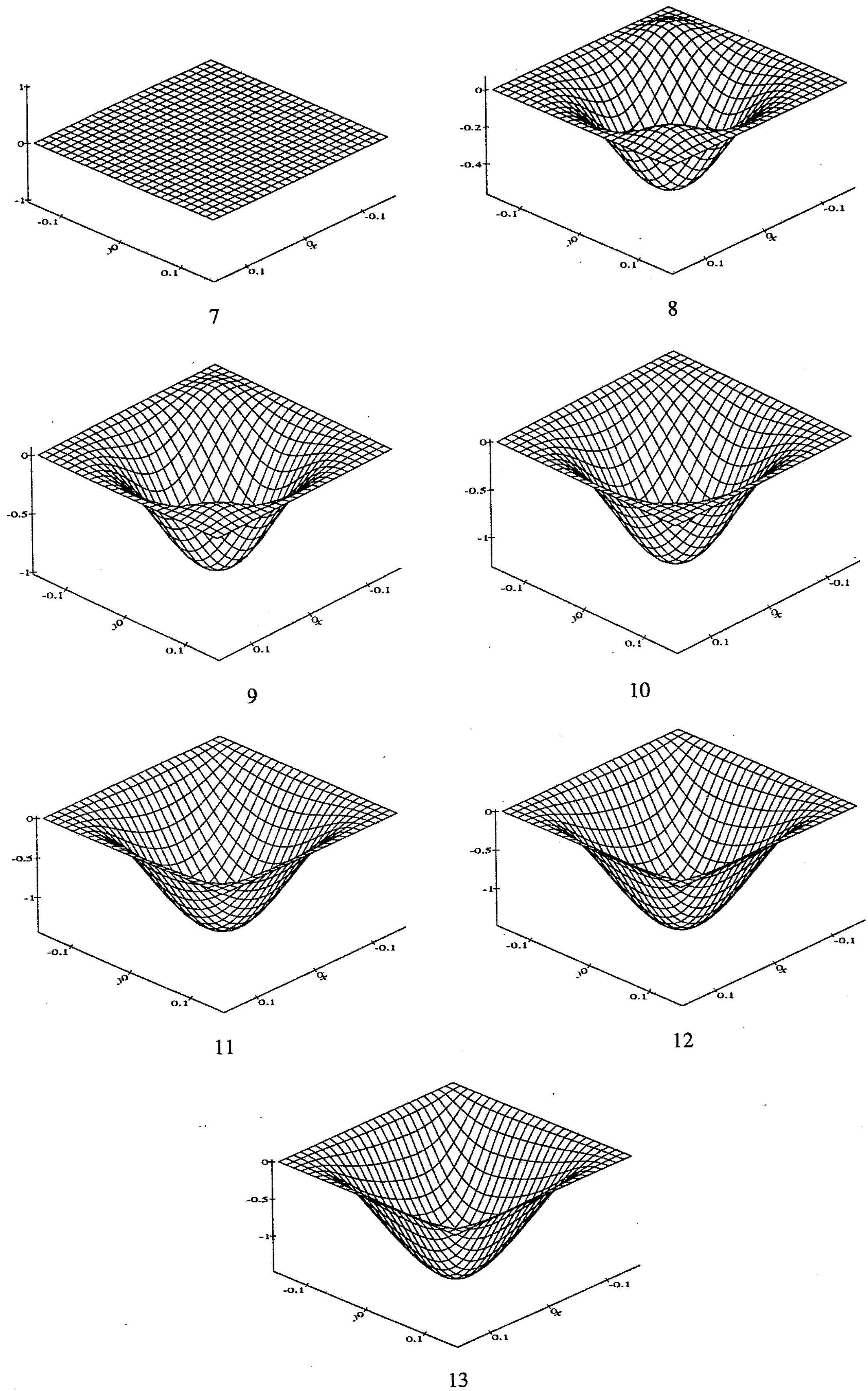

Figure 8.87*b* - Vibration of Plate 7 during half a cycle, at point $\omega/\omega_{\ell 1} = 1.3868$.

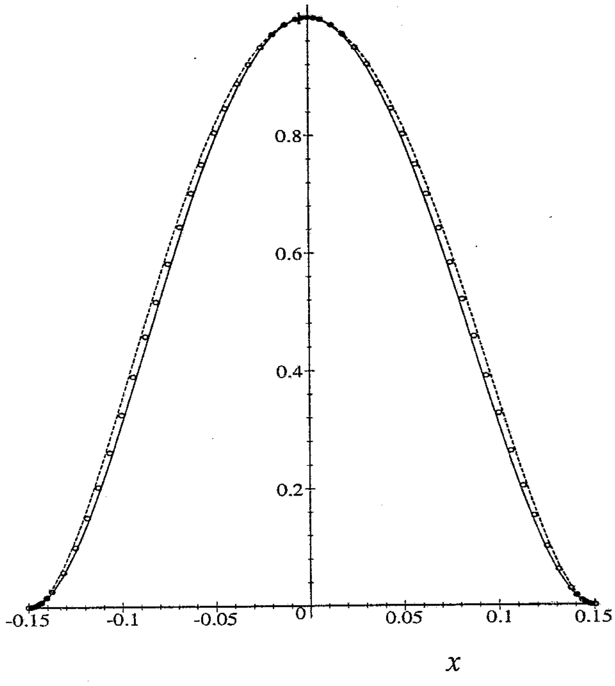

Figure 8.88 - Sections of modes of first harmonic of Plate 7 at points - $\omega/\omega_{\ell 1}$ = 1.0006, o $\omega/\omega_{\ell 1}$ =1.1306, -- $\omega/\omega_{\ell 1}$ = 1.3868. y=0.

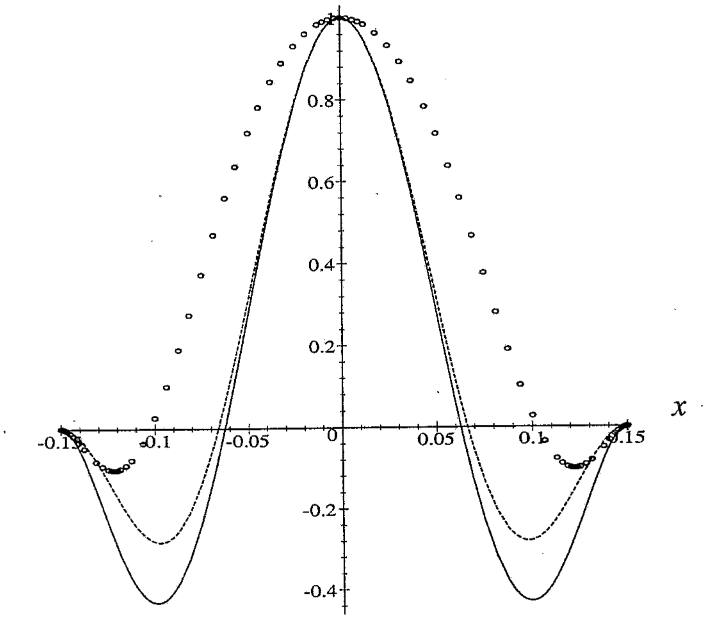

Figure 8.89 - Sections of modes of third harmonic of Plate 7 at points - $\omega/\omega_{\ell 1}$ = 1.0006, o $\omega/\omega_{\ell 1}$ =1.1306, -- $\omega/\omega_{\ell 1}$ = 1.3868. y=0.

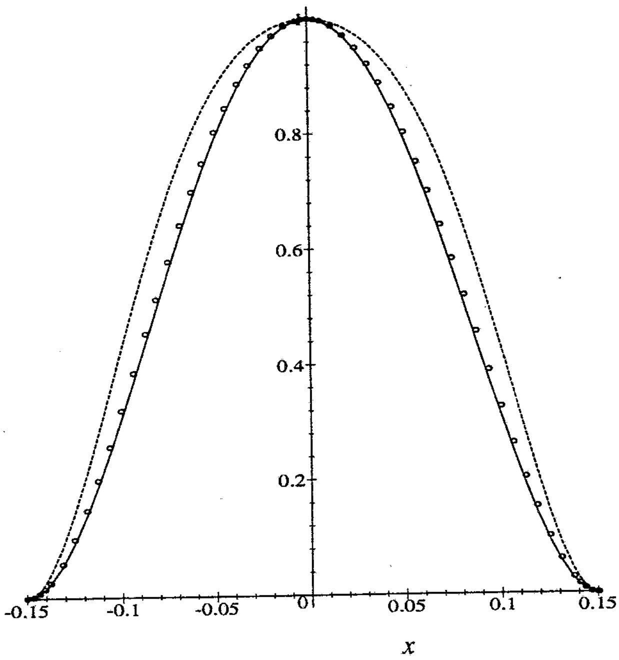

Figure 8.90 - Sections of shape of vibration (both harmonics) of Plate 7 at y=0, points - $\omega/\omega_{\ell 1}$ = 1.0006, o $\omega/\omega_{\ell 1}$ =1.1306, -- $\omega/\omega_{\ell 1}$ = 1.3868.

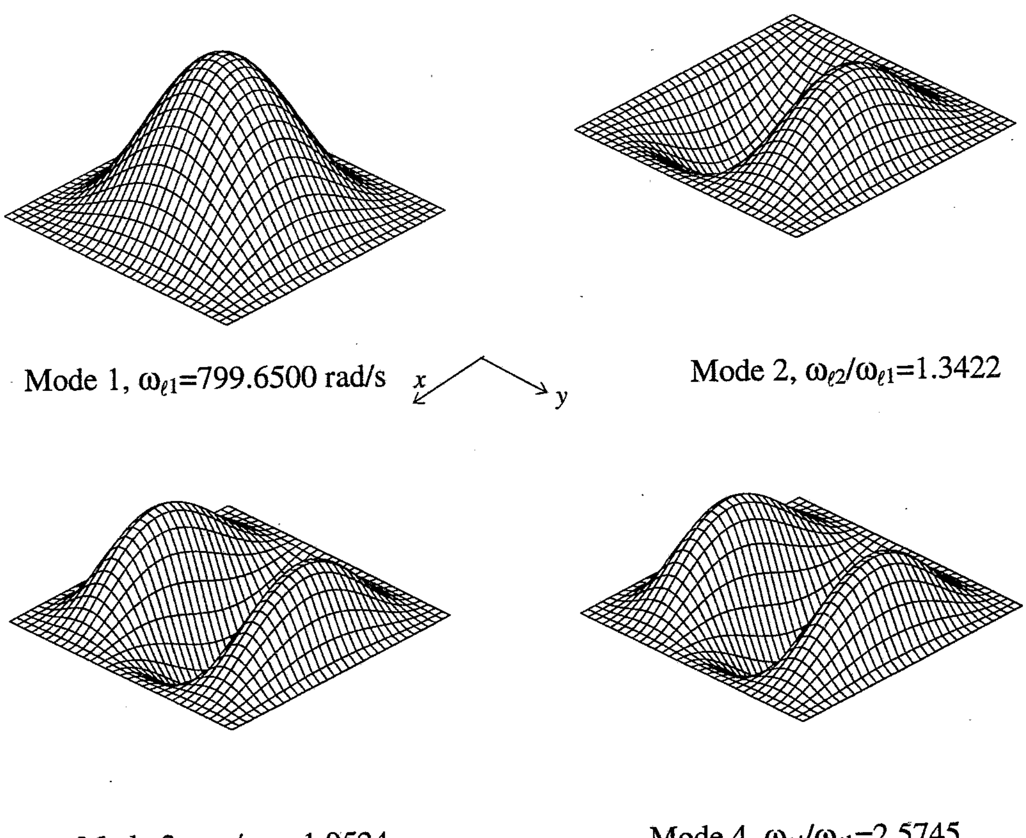

Figure 8.91a - Linear mode shapes and natural frequencies of Plate 7, θ=15°. p_o=8.

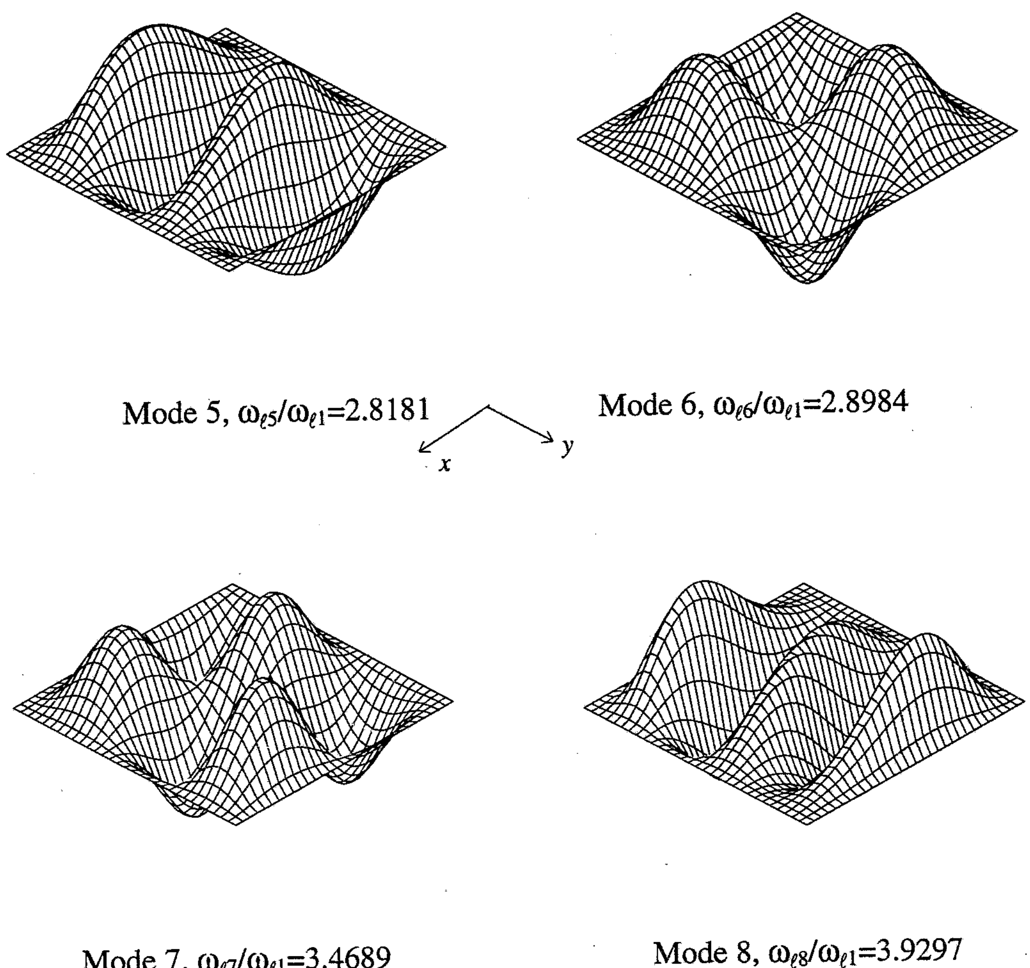

Figure 8.91*b* - Linear mode shapes and natural frequencies of Plate 7, θ=15°. p_o=8.

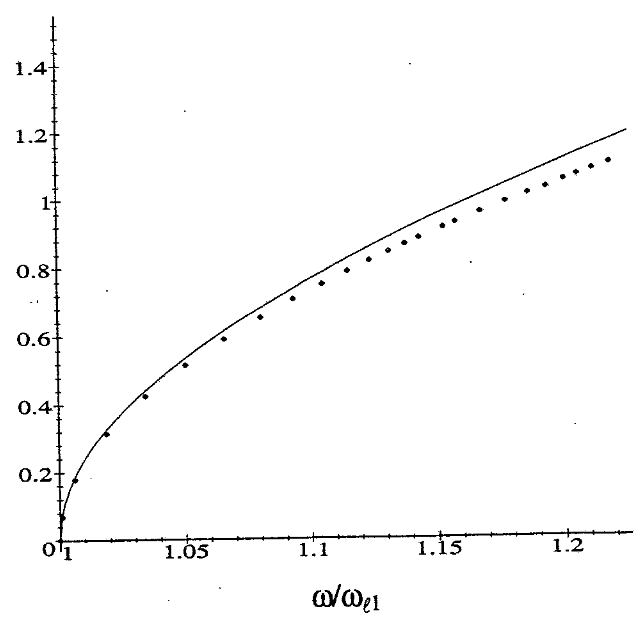

Figure 8.92 - Plate 7. First harmonic's amplitude: ◊ θ=15°, - θ=45°.
(ξ, η)=(0,0), p_o=6, p_i=10.

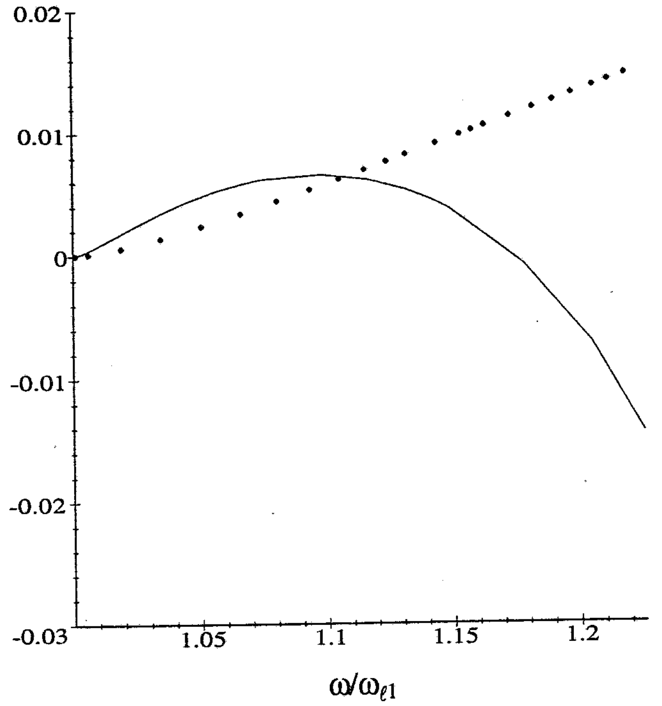

Figure 8.93 - Plate 7. Third harmonic's amplitude: ◊ θ=15°, - θ=45°.
(ξ, η)=(0,0), p_o=6, p_i=10.

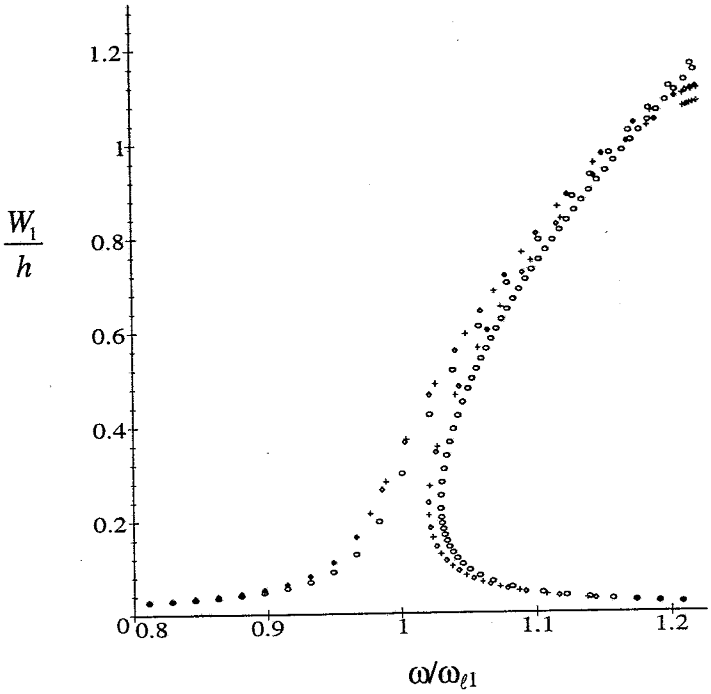

Figure 9.1 - Amplitude of first harmonic of Plate 3 calculated with: o 1 harmonic, ◊ 2 harmonics, + three harmonics, at (ξ,η) =(0,0). p_o=5, p_i=8.

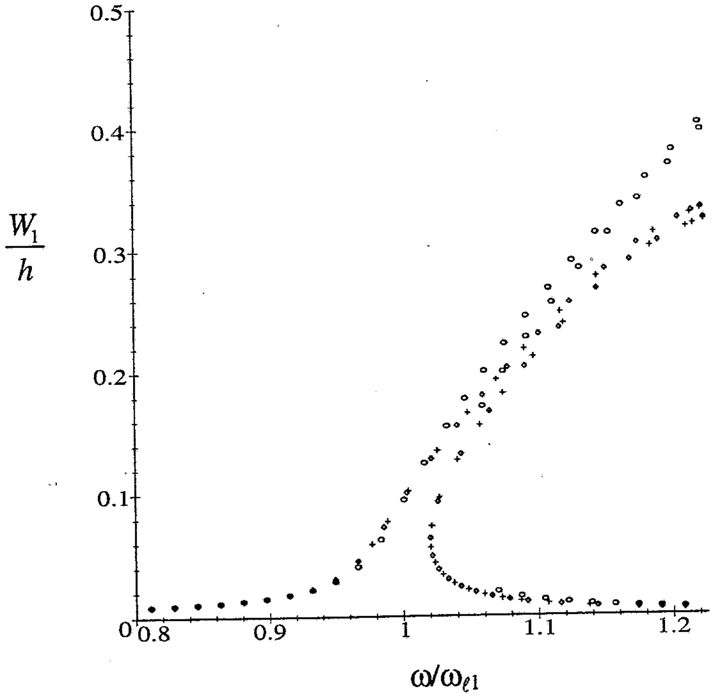

Figure 9.2 - Amplitude of first harmonic of Plate 3 calculated with: o 1 harmonic, ◊ 2 harmonics, + three harmonics, at (ξ,η) =(0.5, 0.5). p_o=5, p_i=8.

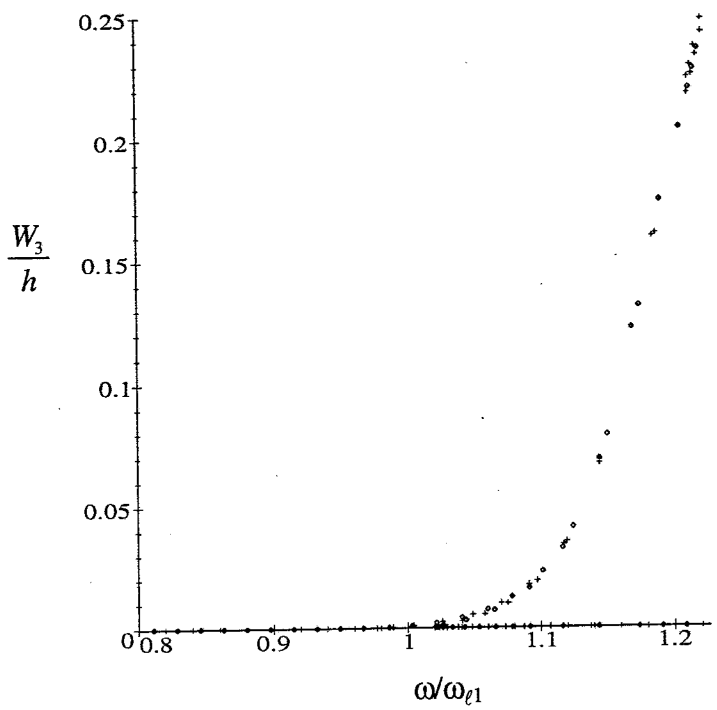

Figure 9.3 - Amplitude of third harmonic of Plate 3 calculated with: ◊ 2 harmonics, + three harmonics, at $(\xi, \eta) = (0, 0)$. p_o=5, p_i=8.

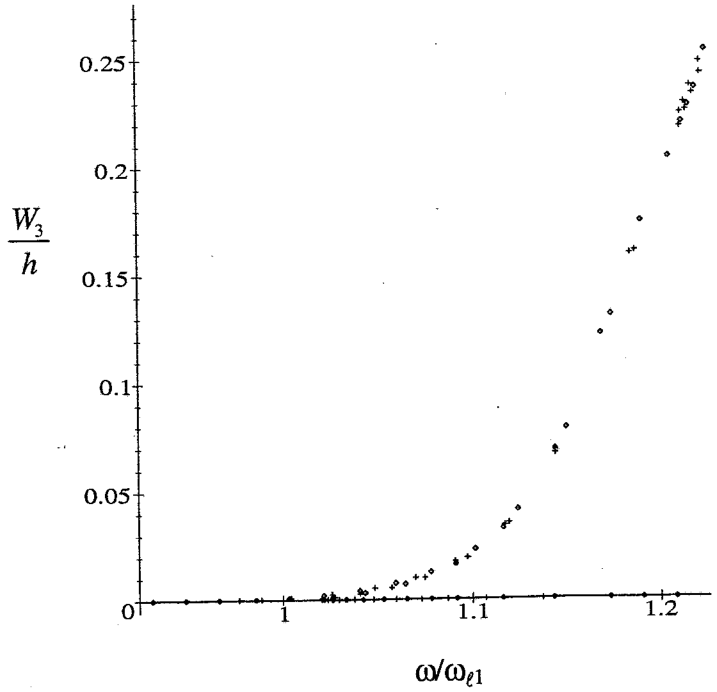

Figure 9.4 - Amplitude of third harmonic of Plate 3 calculated with: ◊ 2 harmonics, + three harmonics, at $(\xi, \eta) = (0.5, 0.5)$. p_o=5, p_i=8.

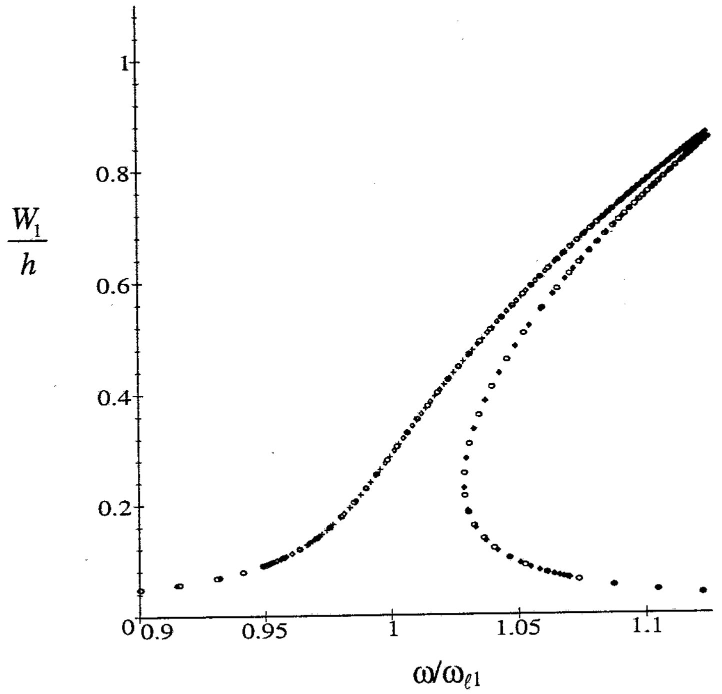

Figure 9.5 - Plate 3. First harmonic's amplitude calculated with p_i=10 and: o p_o=5, ◊ $p_o = 6$, + p_o=7 (ξ, η)=(0,0).

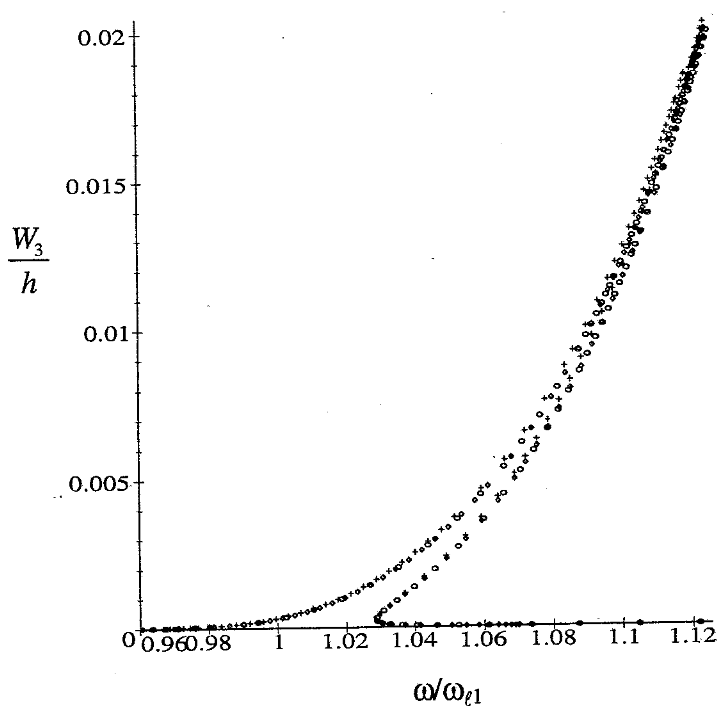

Figure 9.6 - Plate 3. Third harmonic's amplitude calculated with p_i=10 and: o p_o=5, ◊ $p_o = 6$, + p_o=7 (ξ, η)=(0,0).

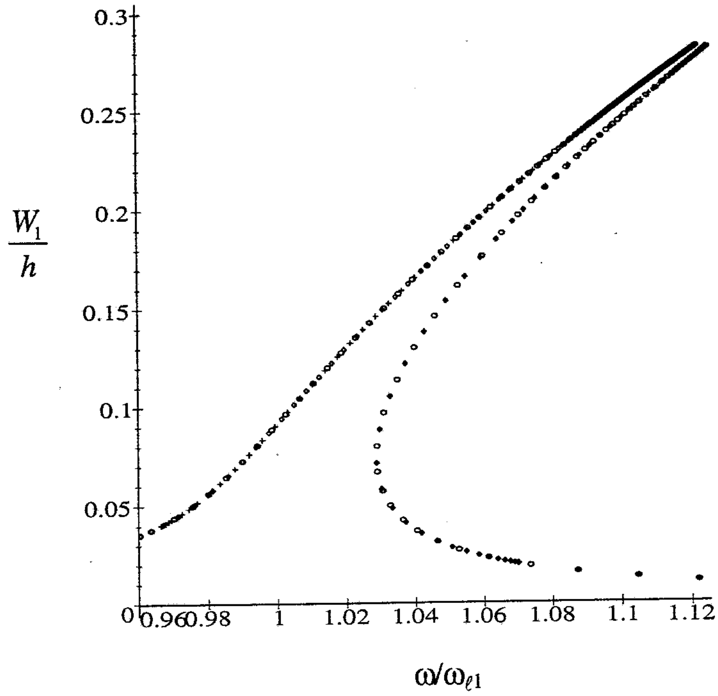

Figure 9.7 - Plate 3. First harmonic's amplitude calculated with p_i=10 and: o p_o=5, ◊ $p_o = 6$, + p_o=7 (ξ, η)=(0.5,0.5).

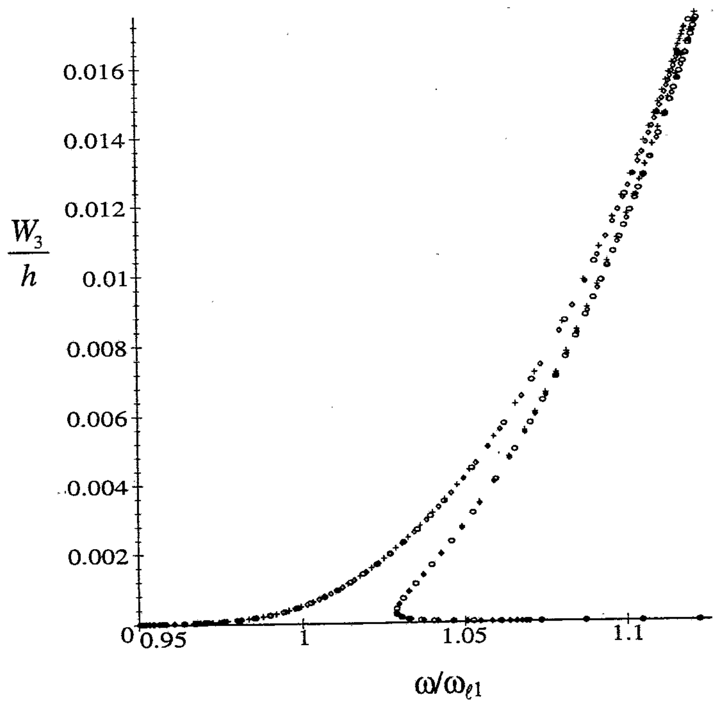

Figure 9.8 - Plate 3. Third harmonic's amplitude calculated with p_i=10 and: o p_o=5, ◊ $p_o = 6$, + p_o=7 (ξ, η)=(0.5,0.5).

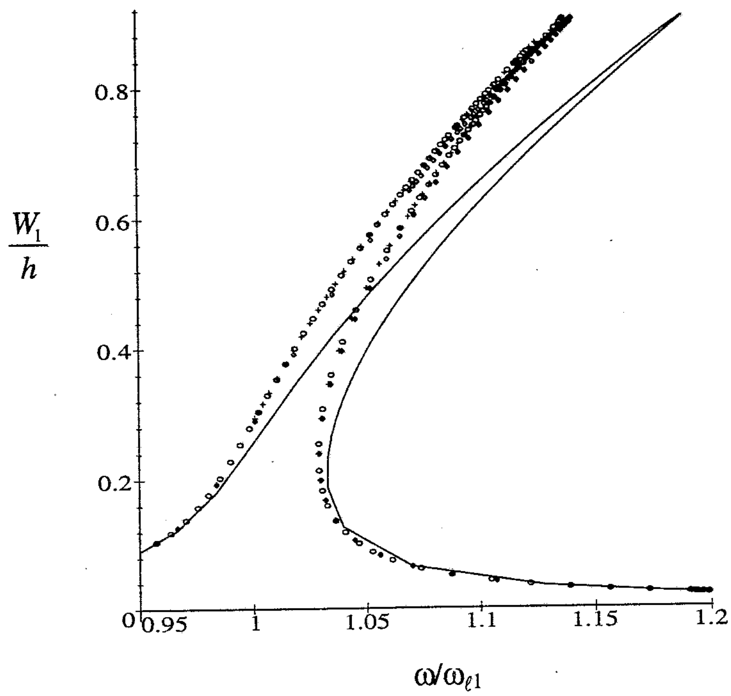

Figure 9.9 - First harmonic of Plate 3 calculated at $(\xi, \eta) = (0, 0)$ with p_o=5 and: - $p_i = 0$, ◊ p_i=5, + p_i=8, o p_i=10.

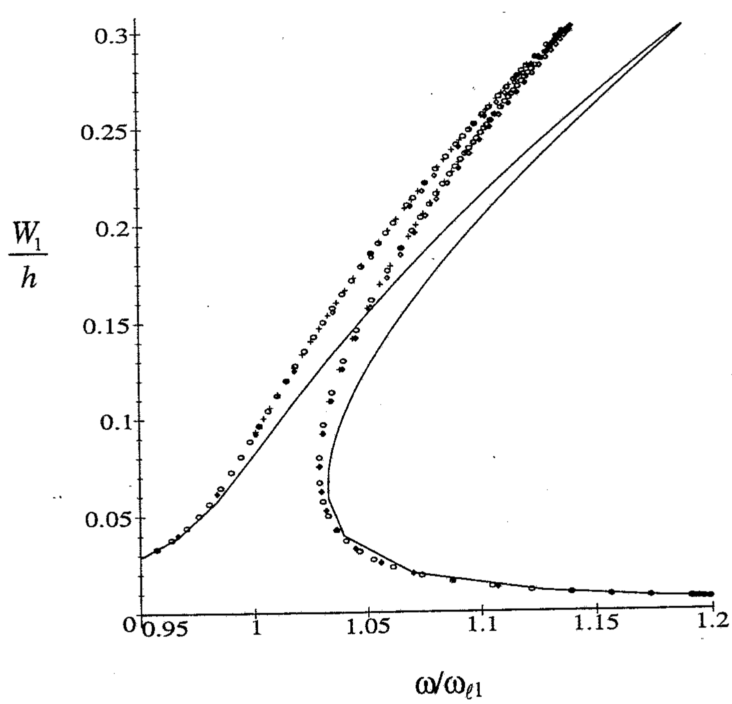

Figure 9.10 - First harmonic of Plate 3 calculated at $(\xi, \eta) = (0.5, 0.5)$ with p_o=5 and: - $p_i = 0$, ◊ p_i=5, + p_i=8, o p_i=10.

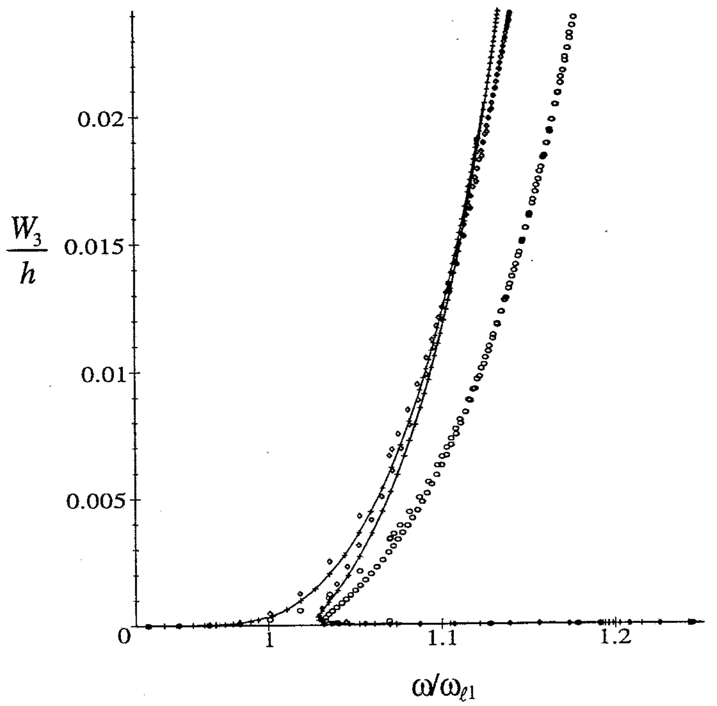

Figure 9.11 - Third harmonic of Plate 3 calculated at $(\xi, \eta) = (0, 0)$ with p_o=5 and:o $p_i = 0$, ◊ p_i=5, - p_i=8, + p_i=10.

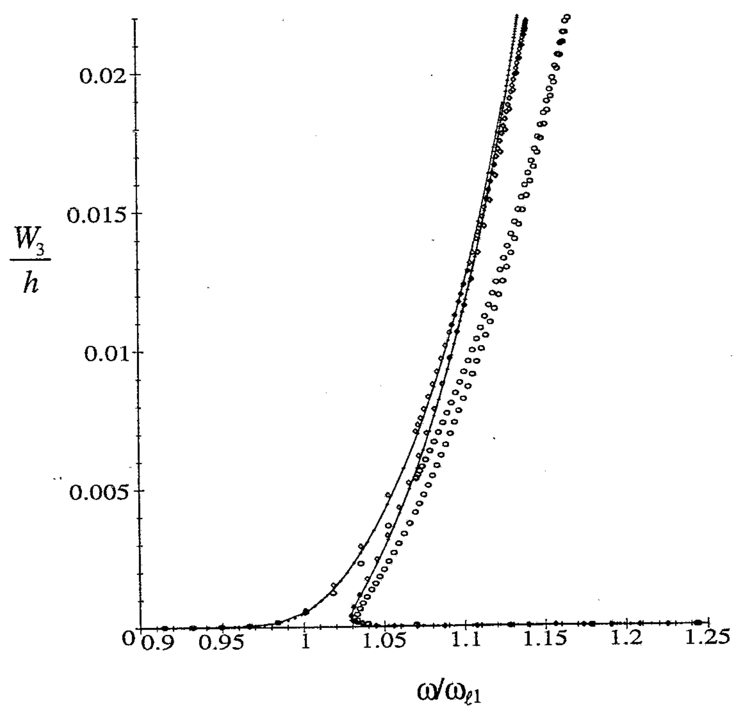

Figure 9.12 - Third harmonic of Plate 3 calculated at $(\xi, \eta) = (0.5, 0.5)$ with p_o=5 and: o $p_i = 0$, ◊ p_i=5, - p_i=8, + p_i=10.

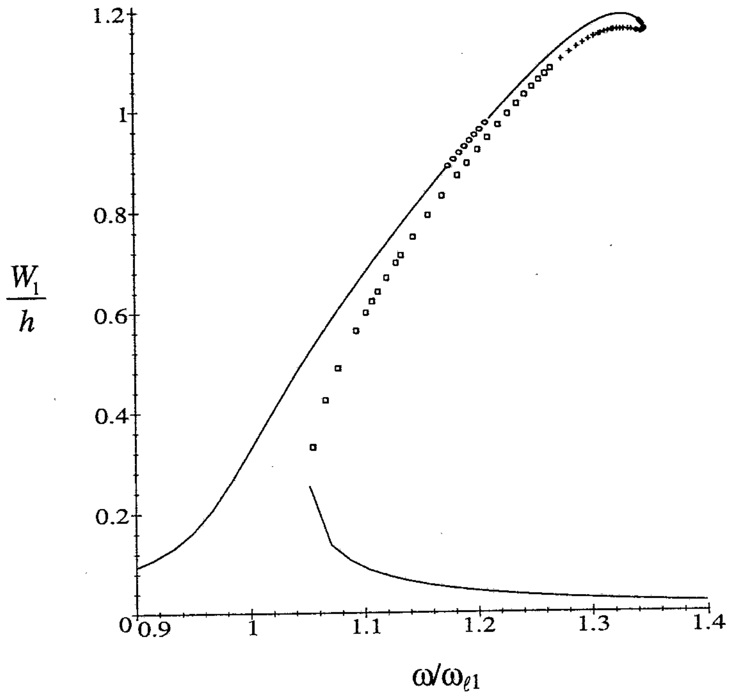

Figure 9.13 - Plate 3's first harmonic FRF at $(\xi, \eta) = (0, 0)$: - and + stable, o and ◊ third order instabilities, □ first order instability. (p_o=5, p_i = 0).

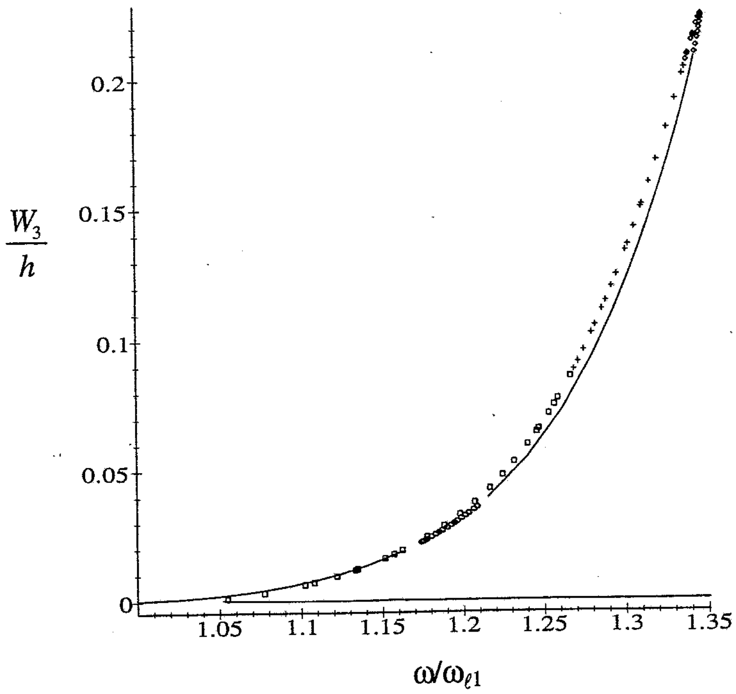

Figure 9.14 - Plate 3's third harmonic FRF at $(\xi, \eta) = (0, 0)$: - and + stable, o and ◊ third order instabilities, □ first order instability. (p_o=5, p_i =0)

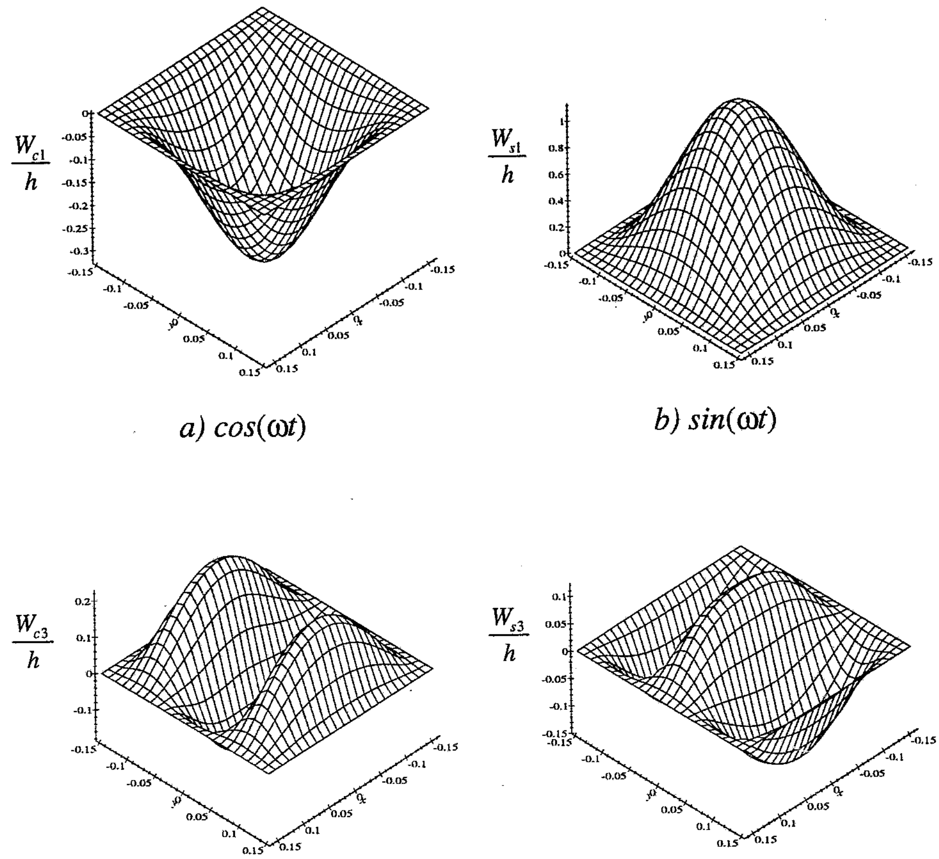

a) cos(ω*t*) *b) sin*(ω*t*)

c) cos(3ω*t*) *d) sin*(3ω*t*)

Figure 9.15 - Deformation of Plate 3 at point $\omega/\omega_{\ell 1}$=1.3416

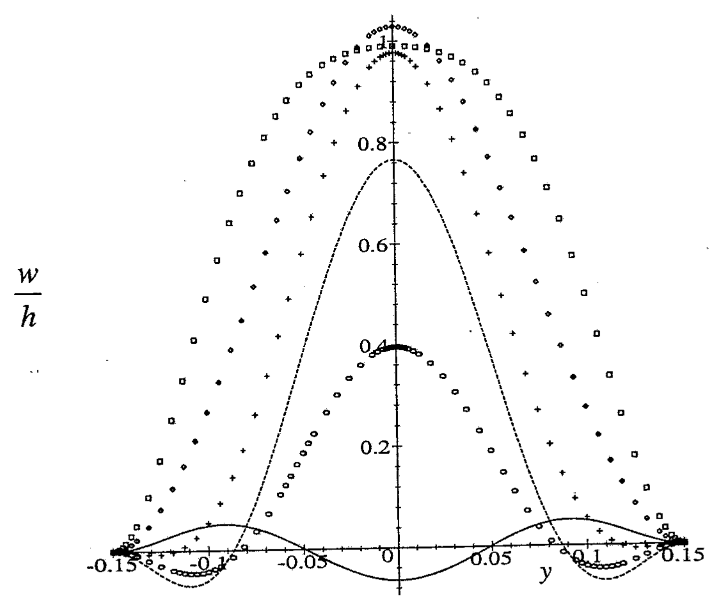

Figure 9.16 - Section of Plate 3 at x=0, frequency $\omega/\omega_{\ell 1}$=1.3416. - t = 0 s, o t=(1/24)T s, -- t=(2/24)T s, + t=(3/24)T s, ◊ t=(4/24)T s, □ t=(5/24)T s

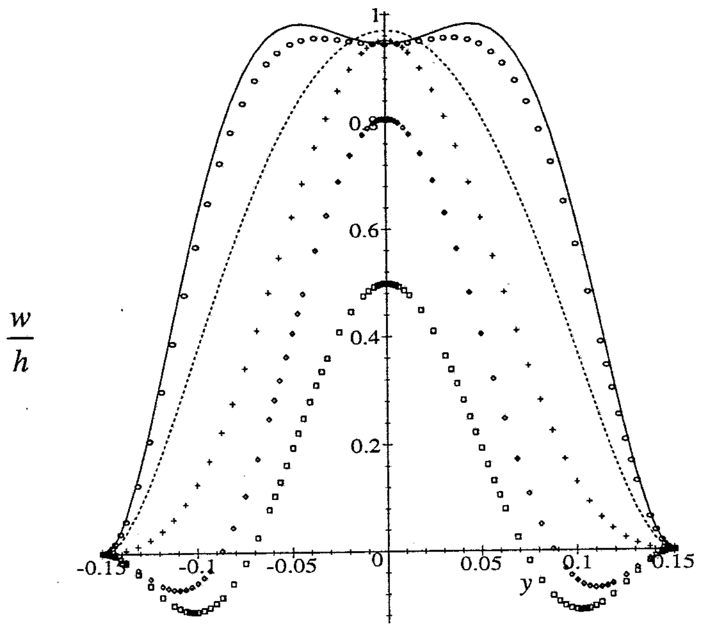

Figure 9.17 - Section of Plate 3 at x=0, frequency $\omega/\omega_{\ell 1}$=1.3416: - t=(6/24)T s, o t=(7/24)T s, -- t=(8/24)T s, + t=(9/24)T s, ◊ t=(10/24)T s, □ t=(11/24)T s

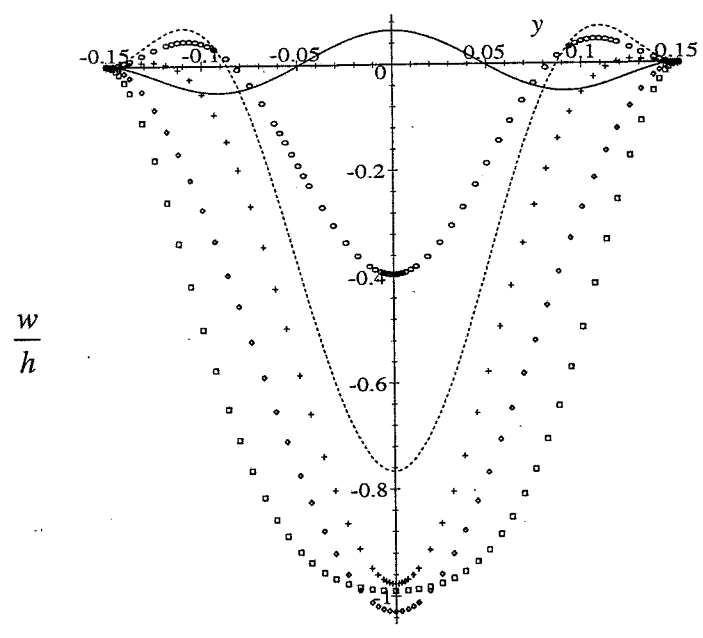

Figure 9.18 - Section of Plate 3 at x=0, frequency $\omega/\omega_{\ell 1}$=1.3416: - t=(12/24) s, o t=(13/24)T s, -- t=(14/12)T s, + t=(15/24)T s, ◊ t=(16/24)T s, □ t=(17/24)T s

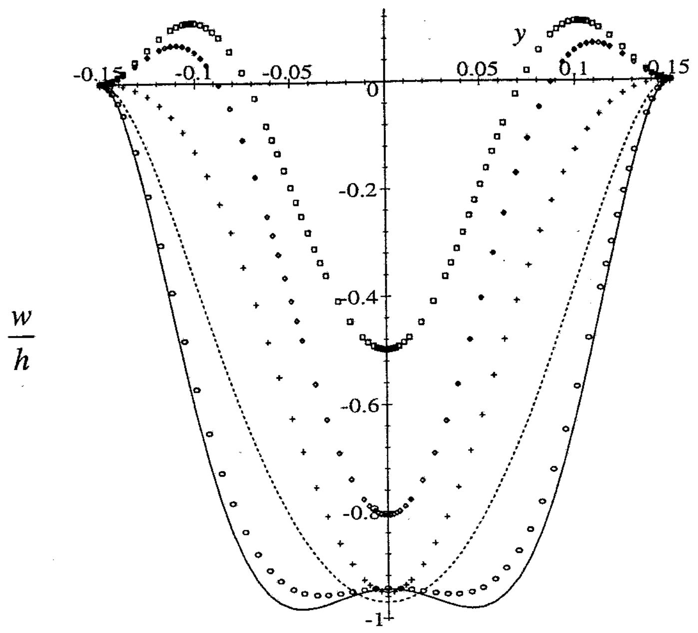

Figure 9.19 - Section of Plate 3 at x=0, frequency $\omega/\omega_{\ell 1}$=1.3416: t= - (18/24)T s, o t= (19/24)T s, -- t=(20/24)T s, + t=(21/24)T s, ◊ t=(22/24)T s, □t=(23/24)T s

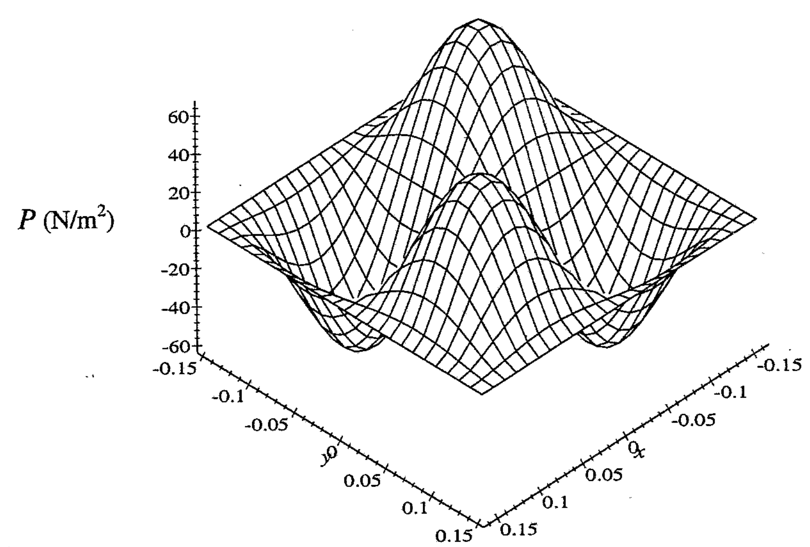

Figure 9.20 - Nonsymmetric excitation

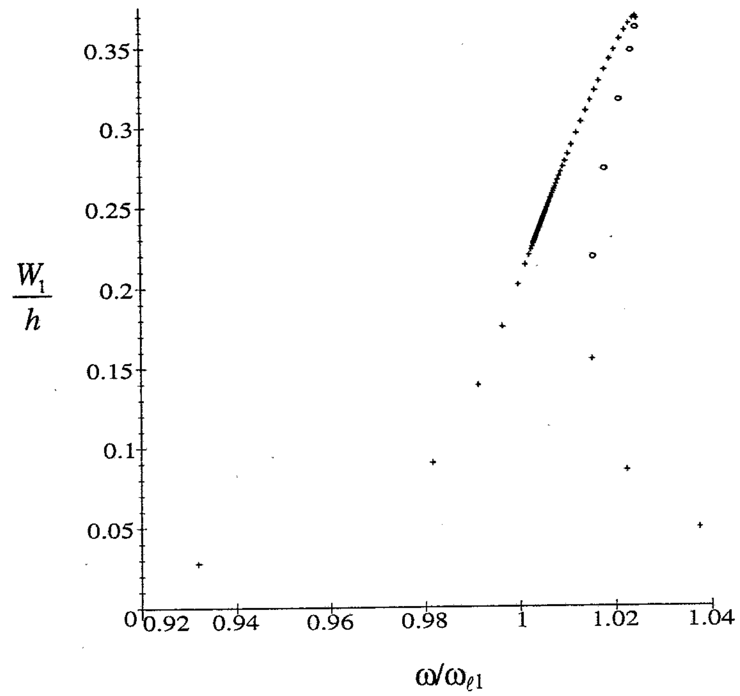

Figure 9.21 - FRF of first harmonic at $(\xi, \eta) = (0, 0)$ due to nonsymmetric excitation: + stable, o unstable. Plate 3 (p_o=5, p_i = 10).

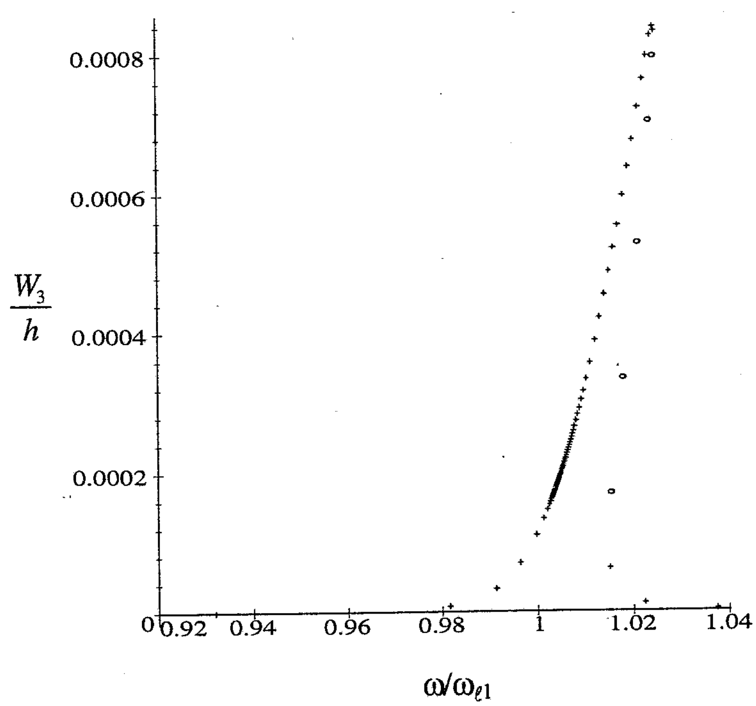

Figure 9.22 - FRF of third harmonic at $(\xi, \eta) = (0, 0)$ due to nonsymmetric excitation: + stable, o unstable. Plate 3 (p_o=5, p_i = 10).

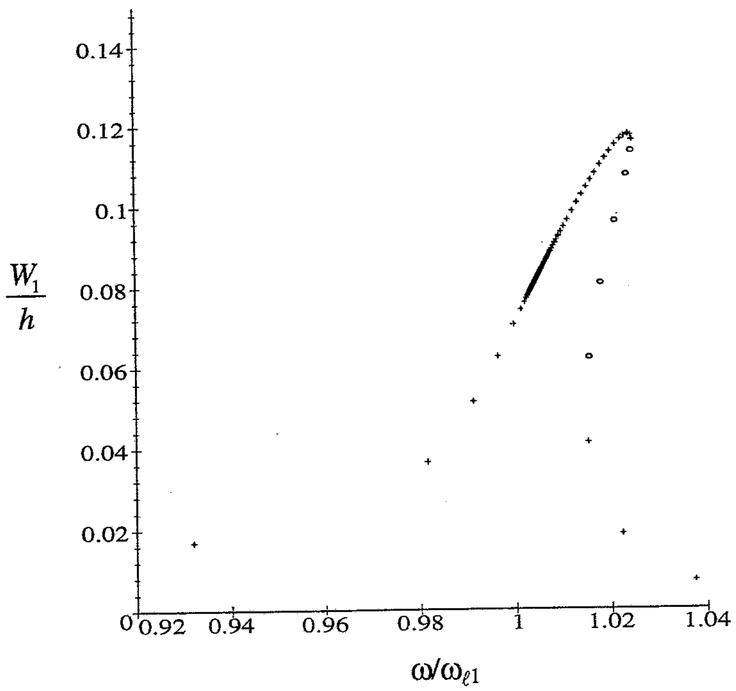

Figure 9.23 - FRF of first harmonic at $(\xi, \eta) = (0.5, 0.5)$ due to nonsymmetric excitation: + stable, o unstable. Plate 3 (p_o=5, p_i = 10).

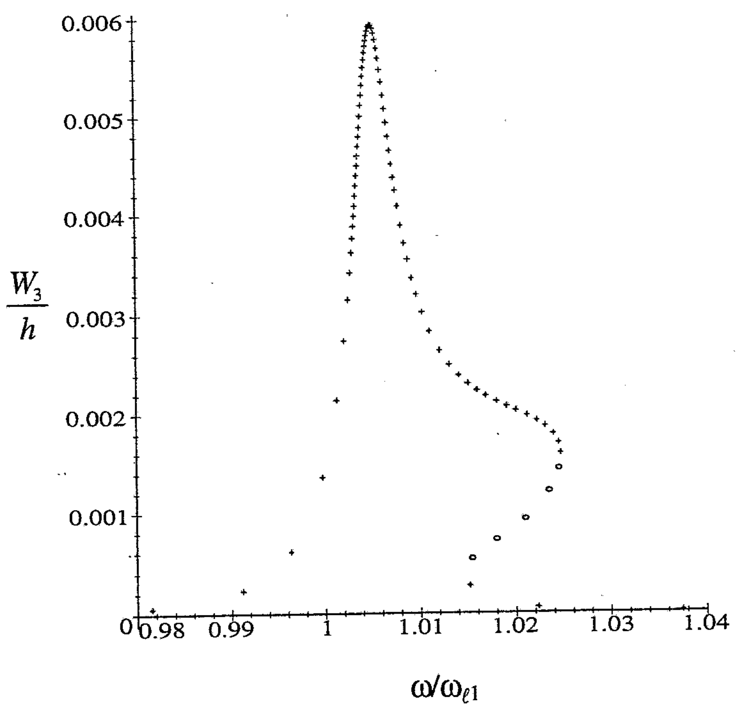

Figure 9.24 - FRF of third harmonic at $(\xi, \eta) = (0.5, 0.5)$ due to nonsymmetric excitation: + stable, o unstable. Plate 3 (p_o=5, p_i = 10).

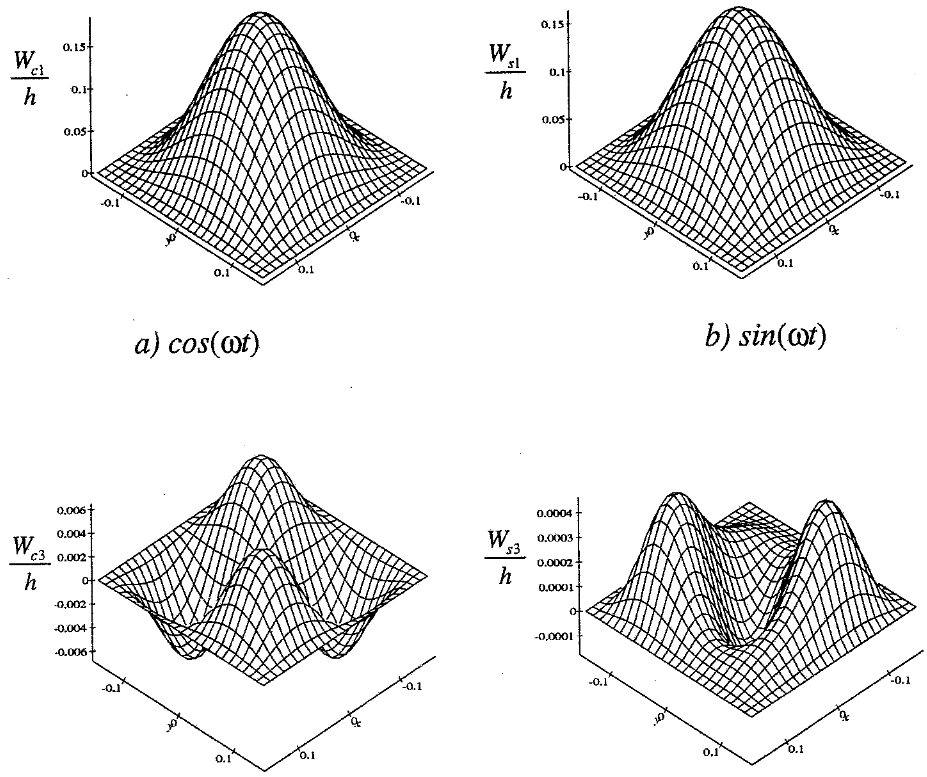

a) cos(ωt)

b) sin(ωt)

c) cos(3ωt)

d) sin(3ωt)

Figure 9.25 - Deformation of Plate 3 at point $\omega/\omega_{\ell 1}$=1.0050

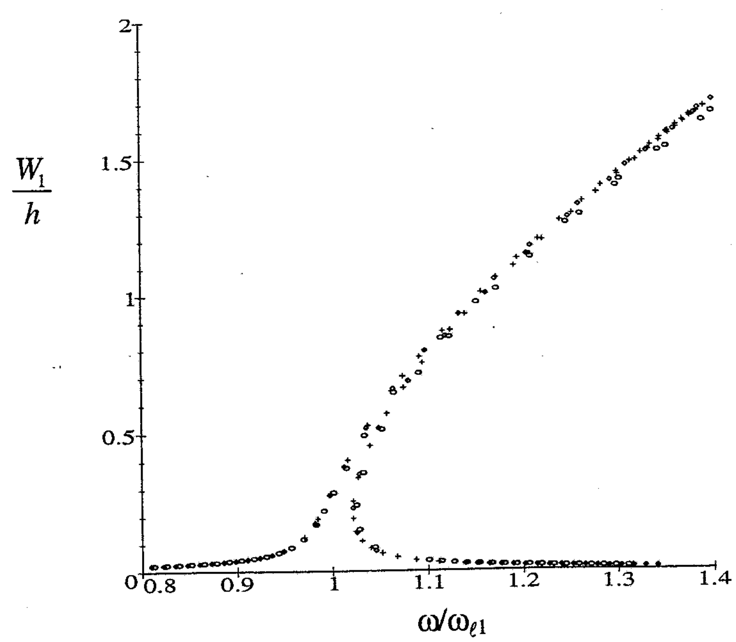

Figure 9.26 - First harmonic of Plate 7 calculated with: o 1 harmonic, ◊ 2 harmonics, + three harmonics, at (ξ,η) =(0,0). p_o=5, p_i=10.

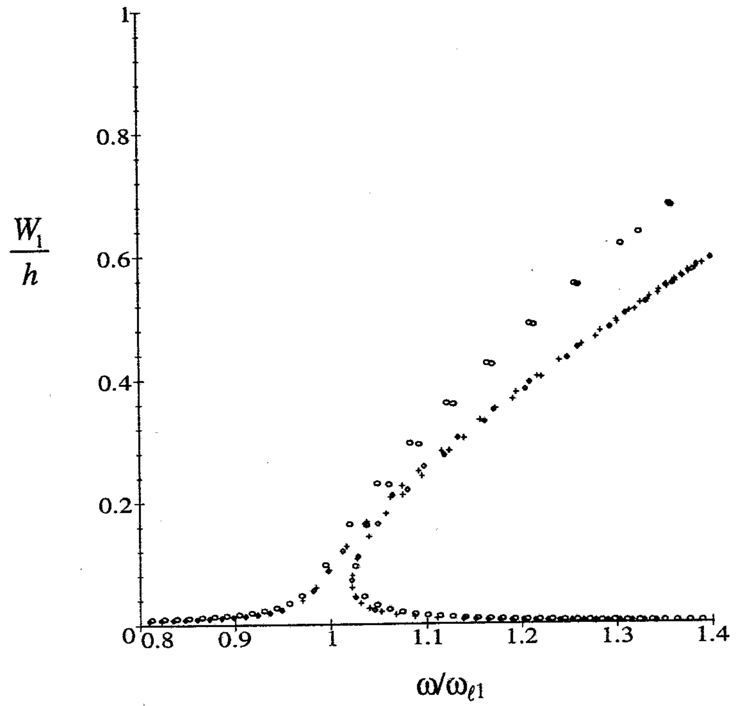

Figure 9.27 - First harmonic of Plate 7 calculated with: o 1 harmonic, ◊ 2 harmonics, + three harmonics, at $(\xi,\eta) = (0.5, 0.5)$. $p_o=5$, $p_i=10$.

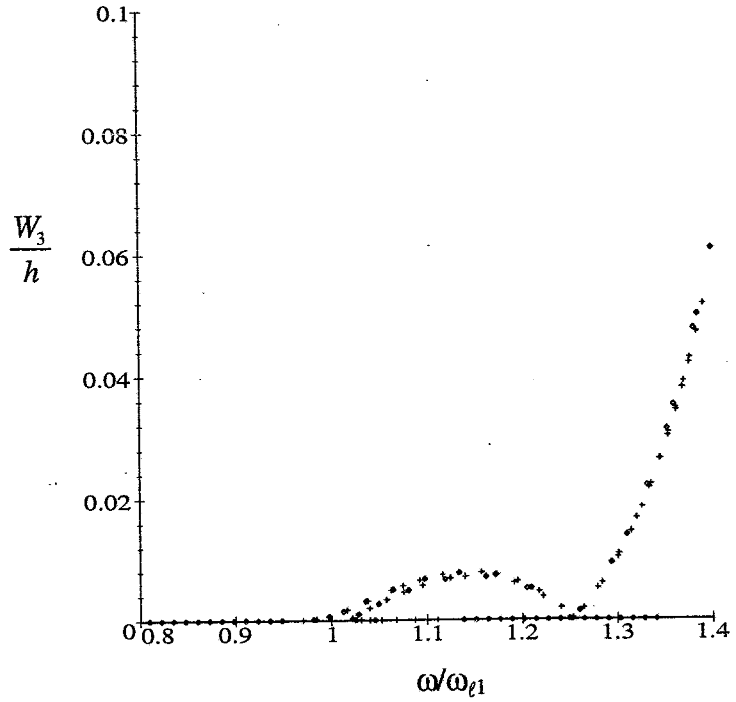

Figure 9.28 - Third harmonic of Plate 7 calculated with: ◊ 2 harmonics, + three harmonics, at $(\xi,\eta) = (0,0)$. $p_o=5$, $p_i=10$.

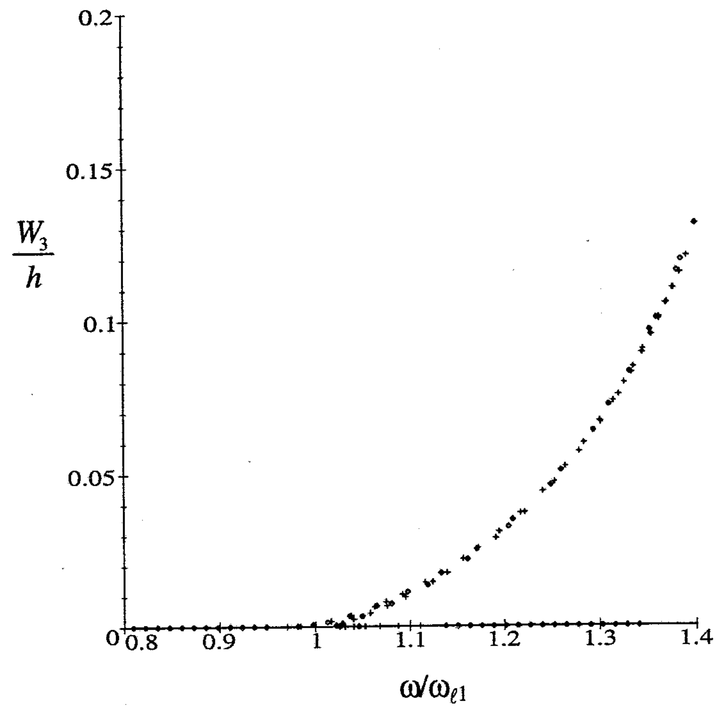

Figure 9.29 - Third harmonic of Plate 7 calculated with: ◊ 2 harmonics, + three harmonics, at $(\xi,\eta)=(0.5\ ,0.5)$. p_o=5, p_i=10.

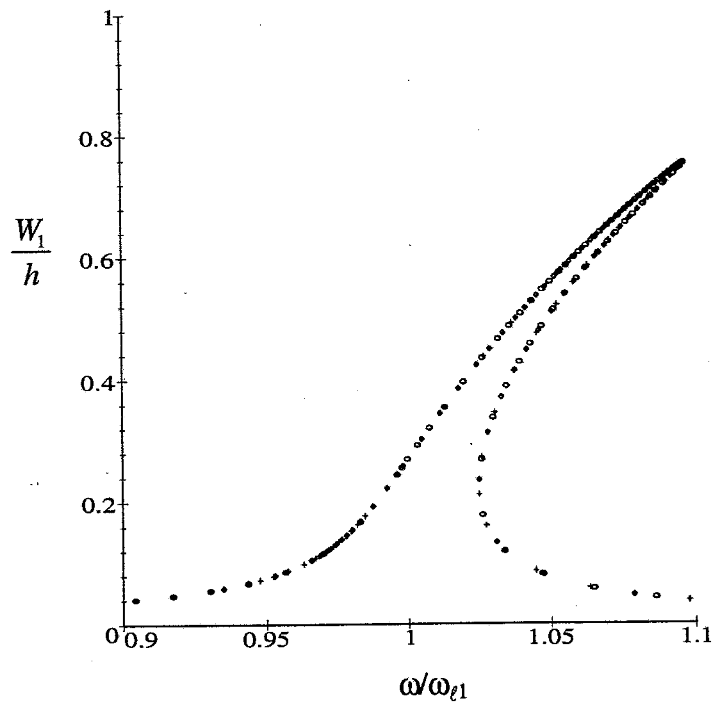

Figure 9.30 - Plate 7. First harmonic's amplitude calculated with p_i=10 and: o p_o=5, ◊ p_o = 6, + p_o=7 (ξ, η)=(0,0).

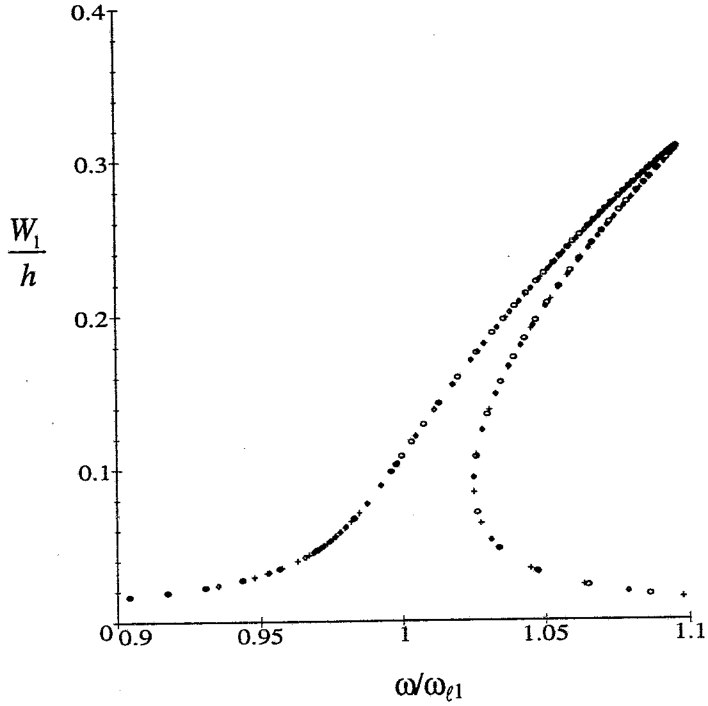

Figure 9.31 - Plate 7. First harmonic's amplitude calculated with p_i=10 and: o p_o=5, ◊ $p_o = 6$, + p_o=7 (ξ, η)=(0.5,0.5).

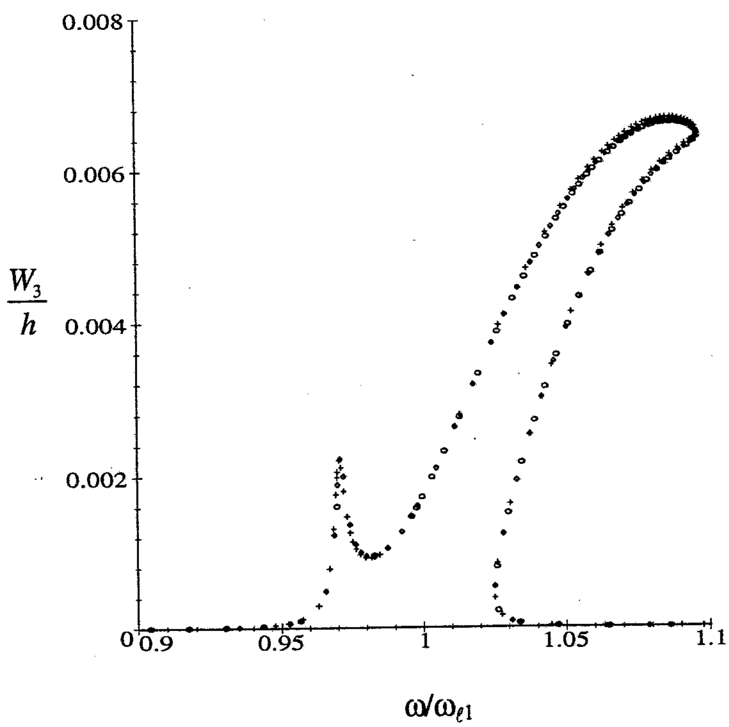

Figure 9.32 - Plate 7. Third harmonic's amplitude calculated with p_i=10 and: o p_o=5, ◊ $p_o = 6$, + p_o=7 (ξ, η)=(0,0).

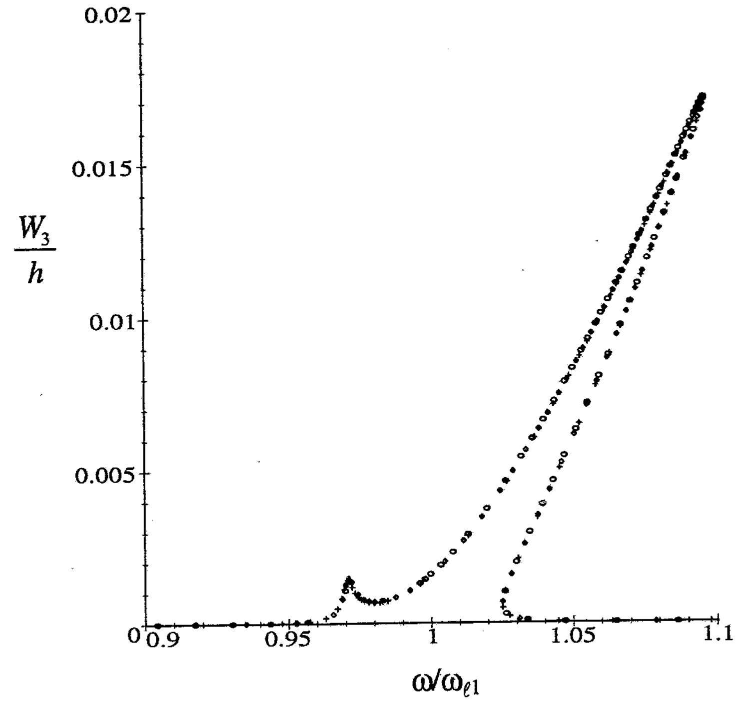

Figure 9.33 - Plate 7. Third harmonic's amplitude calculated with p_i=10 and: o p_o=5, ◊ p_o = 6, + p_o=7 (ξ, η)=(0.5,0.5).

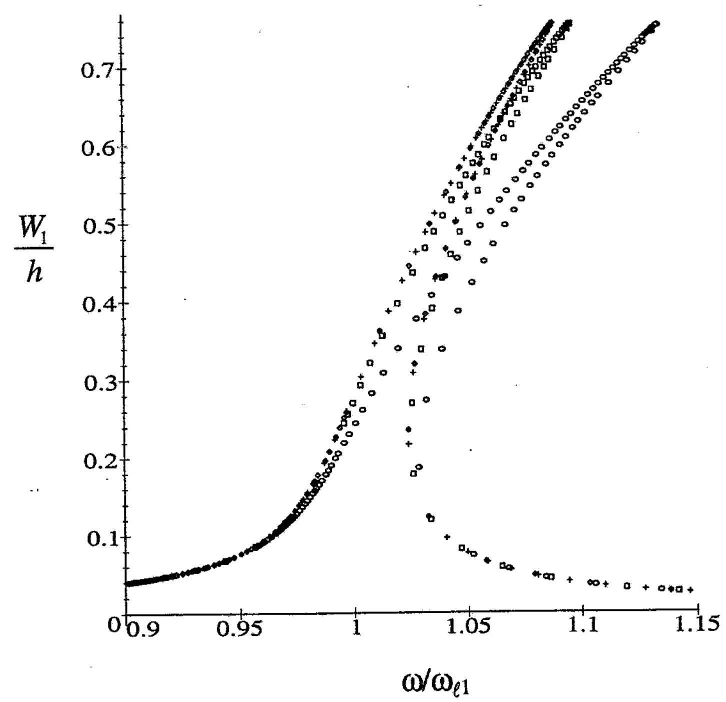

Figure 9.34 - Convergence with number of in-plane shape functions. Plate 7. (p_o=5). o p_i = 0,□ p_i=7, + p_i=8, ◊ p_i=10 ; (ξ, η) = (0, 0). First harmonic.

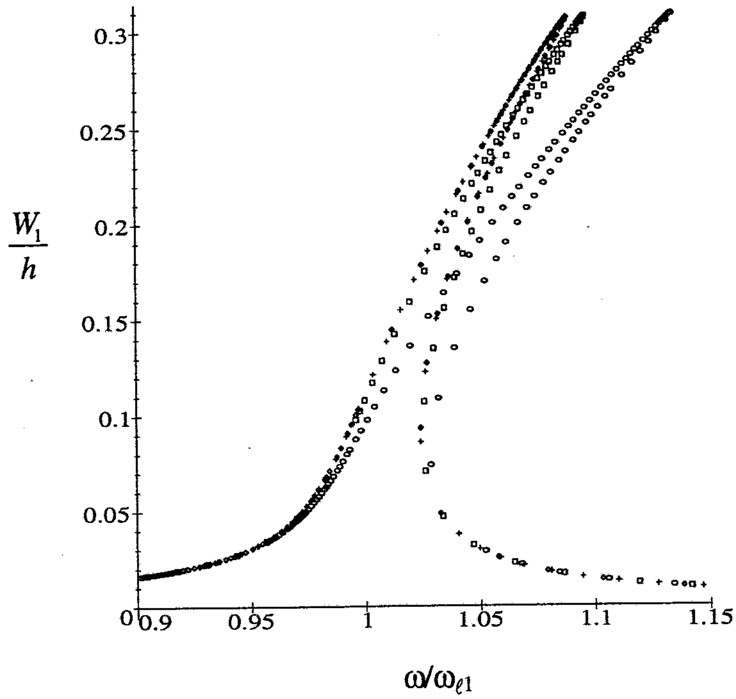

Figure 9.35 - Convergence with number of in-plane shape functions. Plate 7. (p_o=5). o $p_i = 0$, □ p_i=7, + p_i=8, ◊ p_i=10 ; (ξ, η) = (0.5, 0.5). First harmonic.

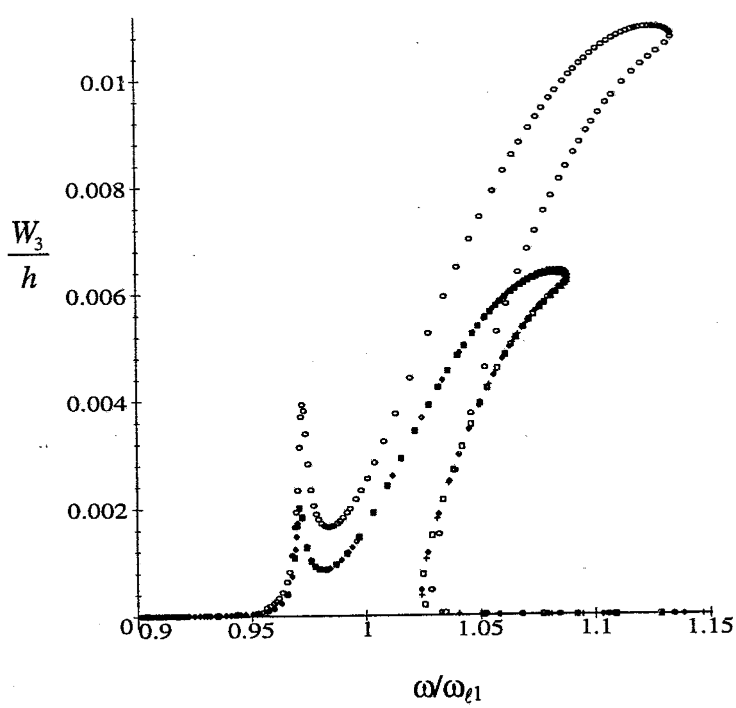

Figure 9.36 - Convergence with number of in-plane shape functions. Plate 7. (p_o=5). o $p_i = 0$,□ p_i=7, + p_i=8, ◊ p_i=10; (ξ, η) = (0, 0). Third harmonic.

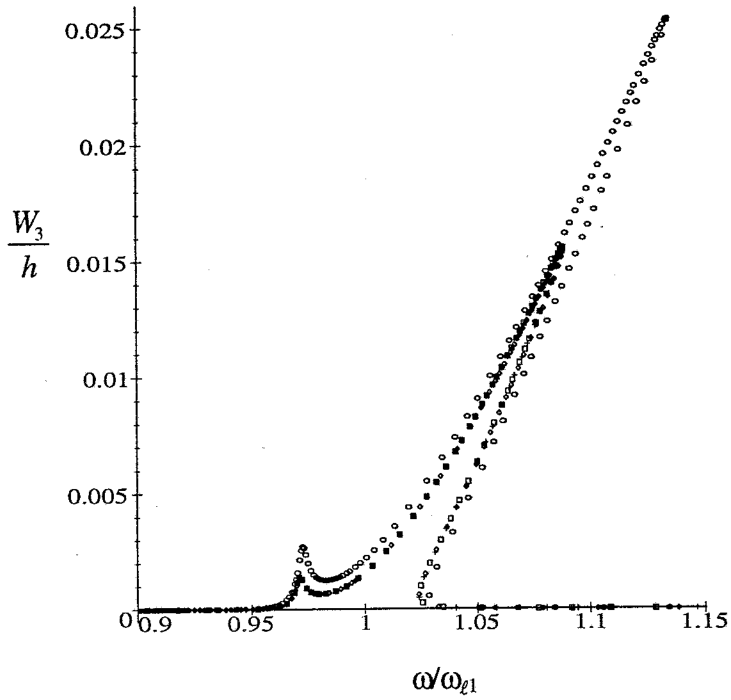

Figure 9.37 - Convergence with number of in-plane shape functions. Plate 7. (p_o=5). o $p_i = 0$,□ p_i=7, + p_i=8, ◊ p_i=10; (ξ, η) = (0.5, 0.5). Third harmonic.

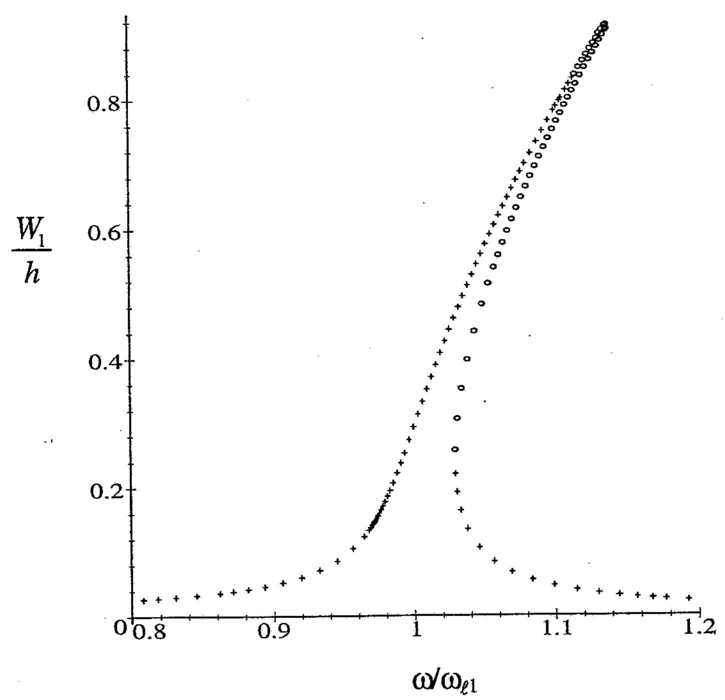

Figure 9.38 - FRF of first harmonic at (ξ, η) = (0, 0) due to symmetric excitation of large amplitude: + stable, o unstable. Plate 7 (p_o=5, p_i = 8).

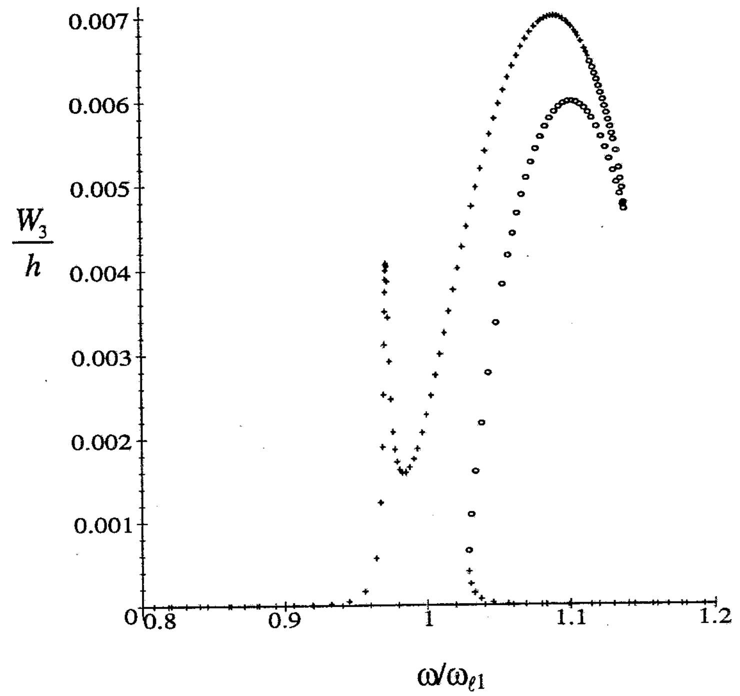

Figure 9.39 - FRF of third harmonic at $(\xi, \eta) = (0, 0)$ due to symmetric excitation of large amplitude: + stable, o unstable. Plate 7 (p_o=5, p_i = 8).

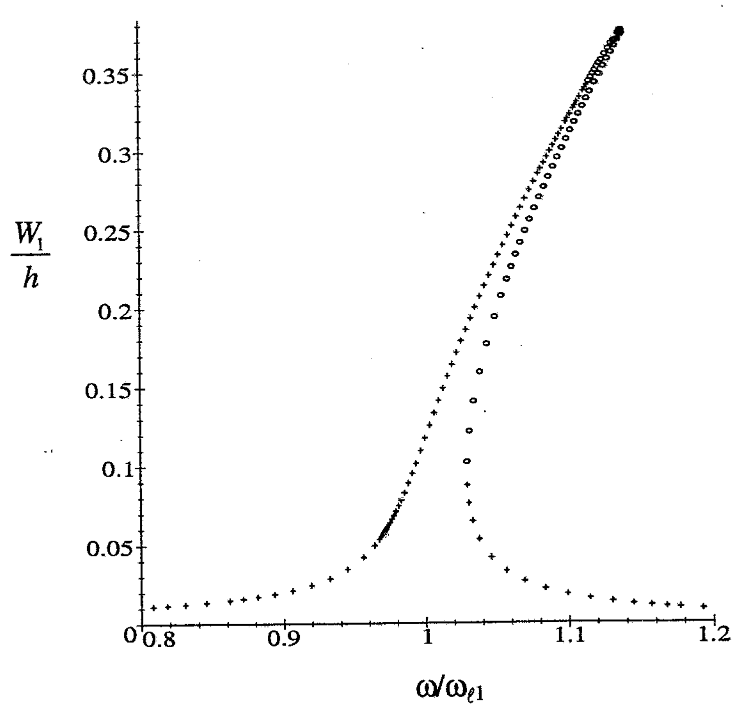

Figure 9.40 - FRF of first harmonic at $(\xi, \eta) = (0.5, 0.5)$ due to symmetric excitation of large amplitude: + stable, o unstable. Plate 7 (p_o=5, p_i = 8).

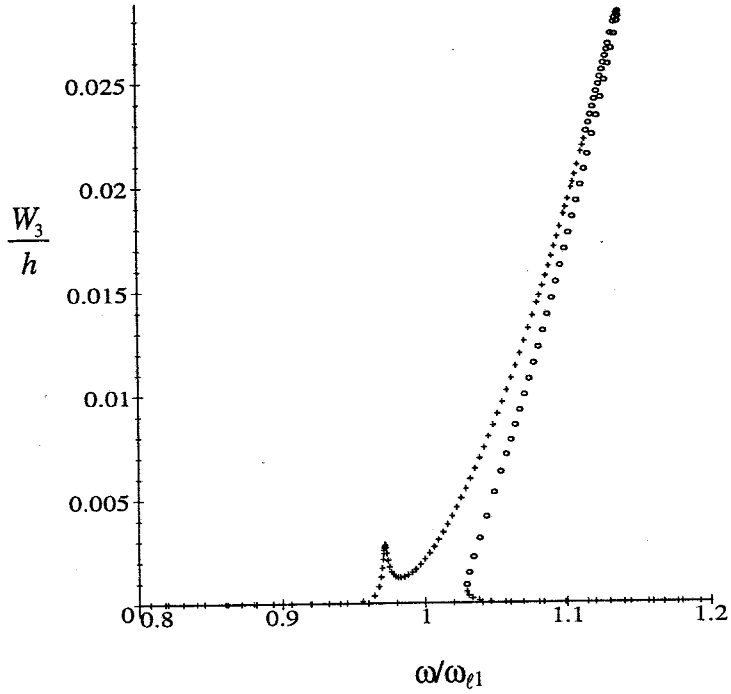

Figure 9.41 - FRF of third harmonic at $(\xi, \eta) = (0.5, 0.5)$ due to symmetric excitation of large amplitude: + stable, o unstable. Plate 7 (p_o=5, p_i = 8).

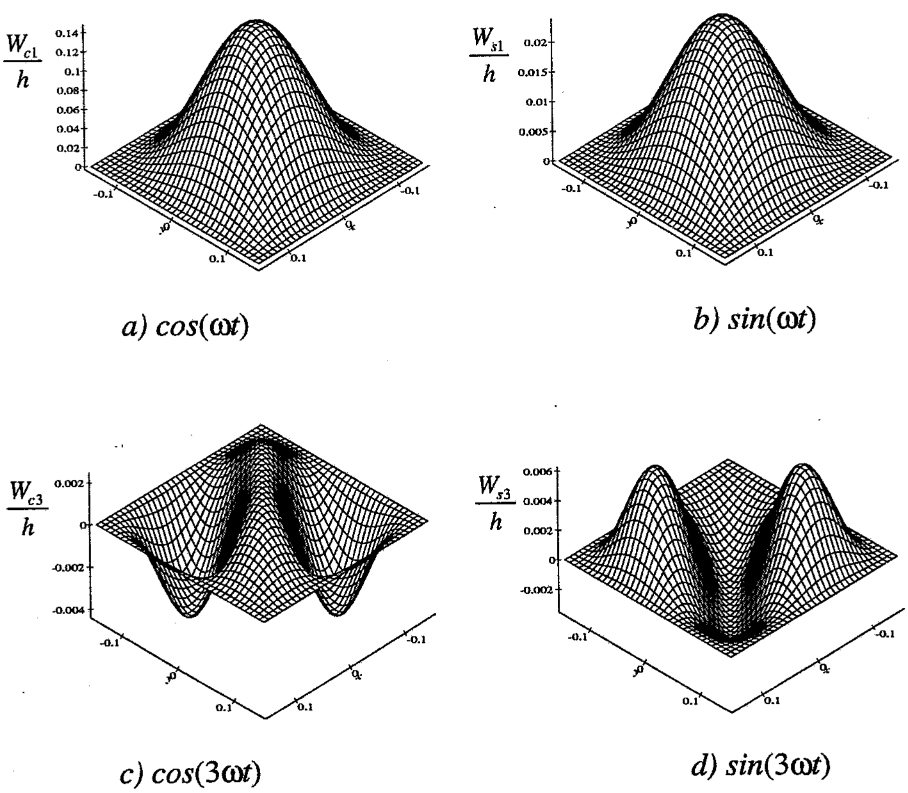

Figure 9.42 - Deformation of Plate 7 at point $\omega/\omega_{\ell 1}$=.97175.

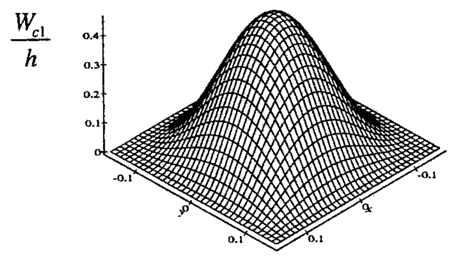

a) cos(ωt)

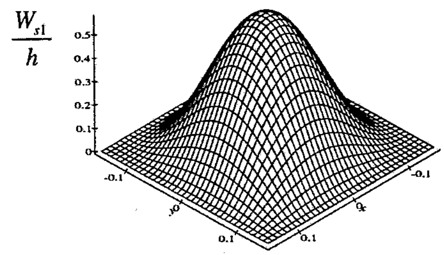

b) sin(ωt)

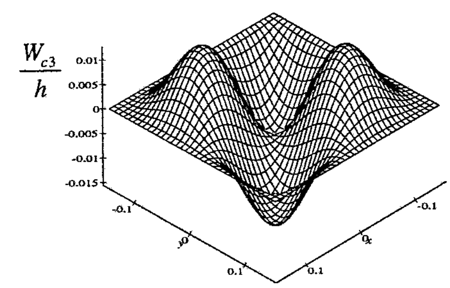

c) cos(3ωt)

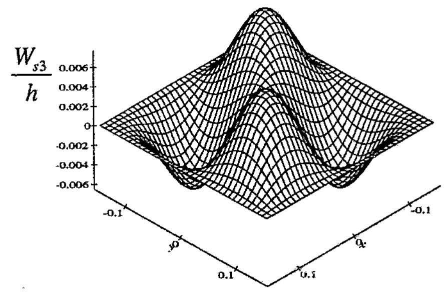

d) sin(3ωt)

Figure 9.43 - Deformation of Plate 7 at point $\omega/\omega_{\ell 1}$=1.08821.

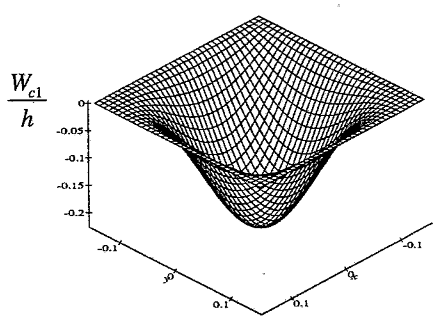

a) cos(ωt)

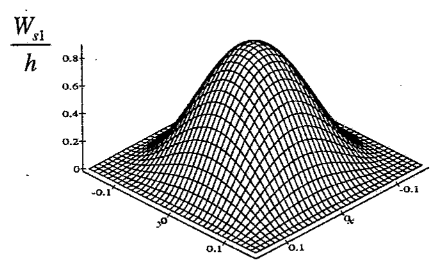

b) sin(ωt)

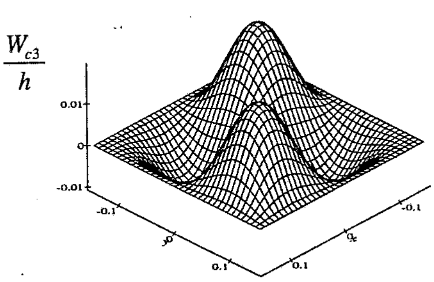

c) cos(3ωt)

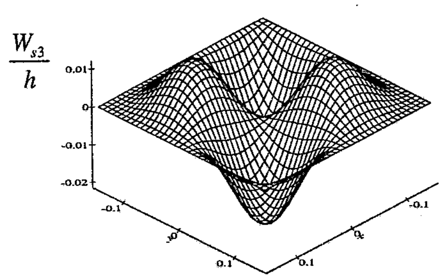

d) sin(3ωt)

Figure 9.44 - Deformation of Plate 7 at point $\omega/\omega_{\ell 1}$=1.13824.

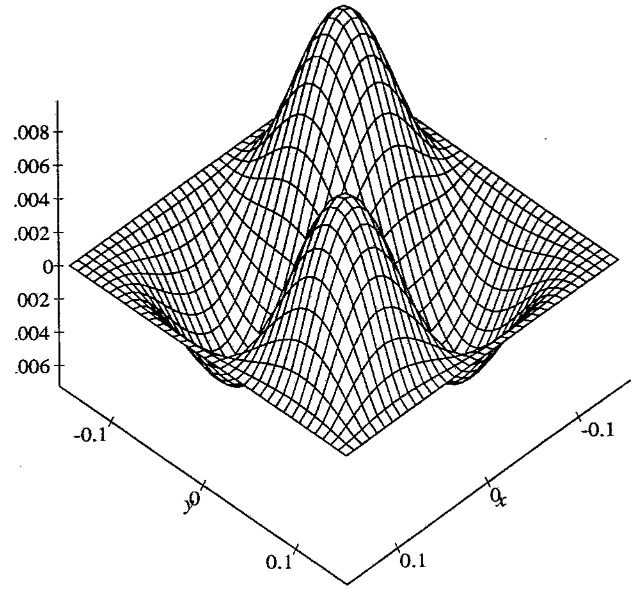

Figure 9.45 - Combination of modes 4 and 6 of Plate 7 (θ=45°).

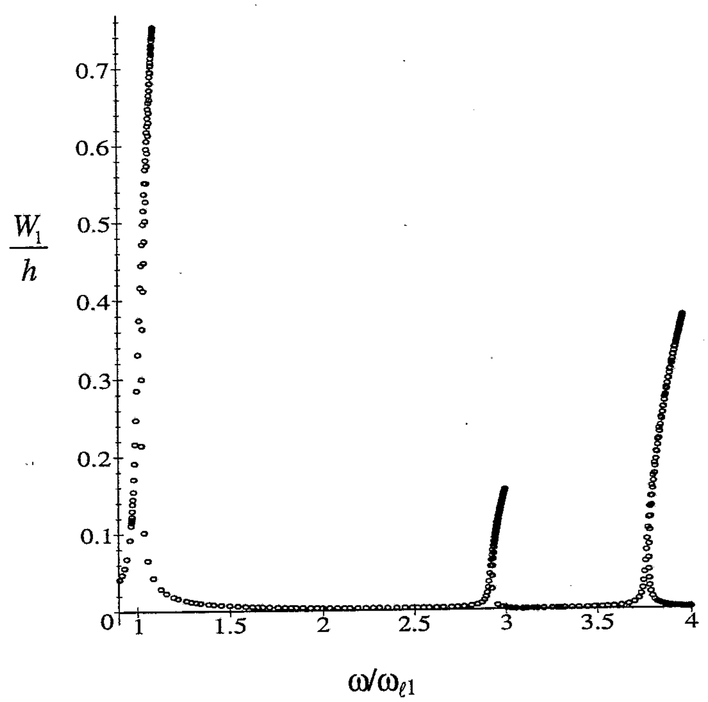

Figure 9.46 - Plate 7's first harmonic FRF at $(\xi, \eta) = (0, 0)$, p_o=6, $p_i = 10$.

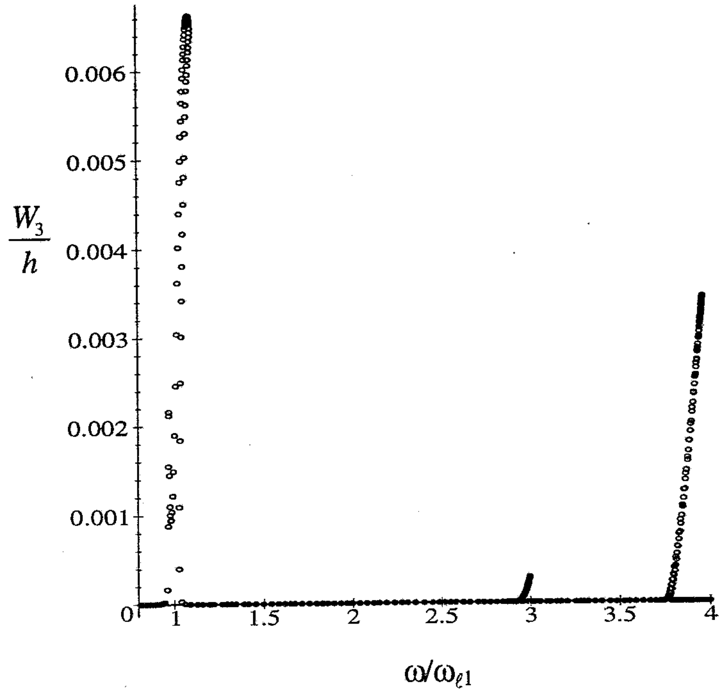

Figure 9.47 - Plate 7's third harmonic FRF at $(\xi, \eta) = (0, 0)$, p_o=6, p_i =10.

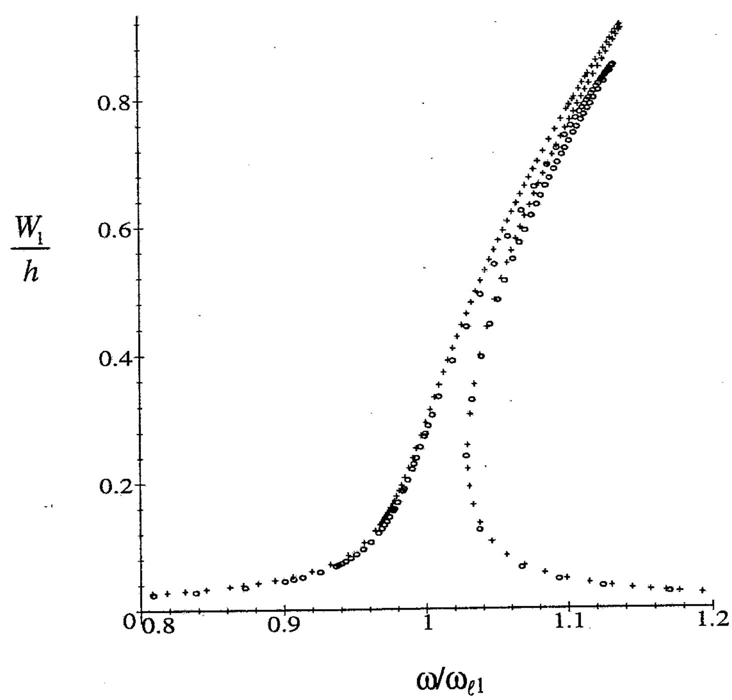

Figure 9.48 - Plate 7's first harmonic FRF at $(\xi, \eta) = (0, 0)$: o θ=15°, + θ=45°.

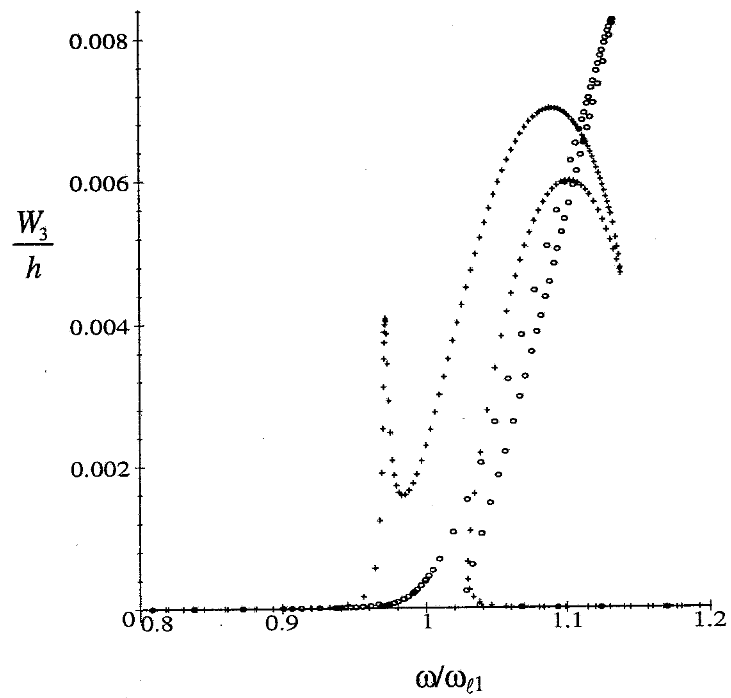

Figure 9.49 - Plate 7's third harmonic FRF at $(\xi, \eta) = (0, 0)$: o $\theta=15°$, + $\theta=45°$.

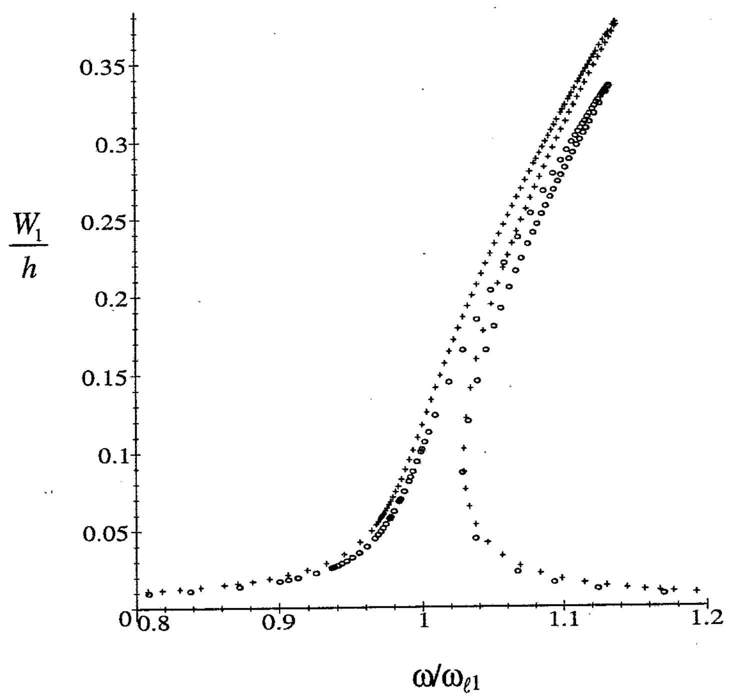

Figure 9.50 - Plate 7's first harmonic FRF at $(\xi, \eta) = (0.5, 0.5)$: o $\theta=15°$, + $\theta=45°$.

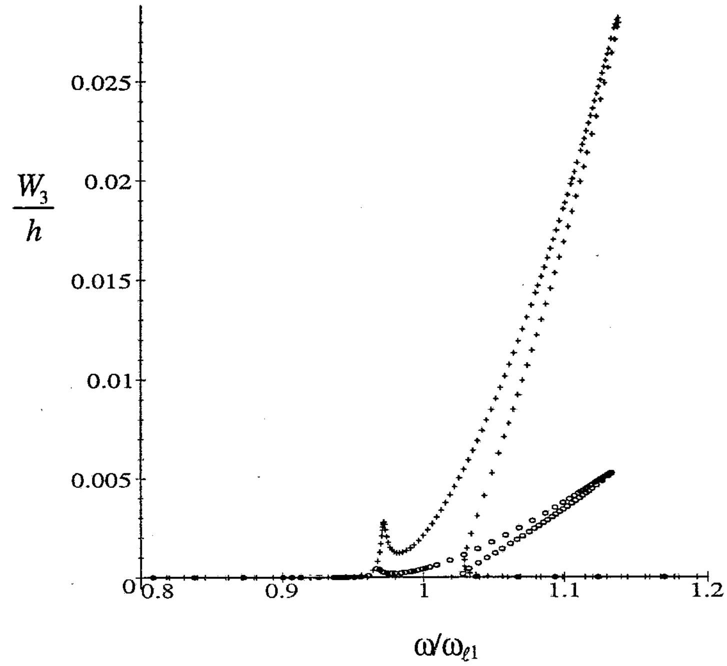

Figure 9.51 - Plate 7's third harmonic FRF at $(\xi, \eta) = (0.5, 0.5)$: o θ=15°, + θ=45°.

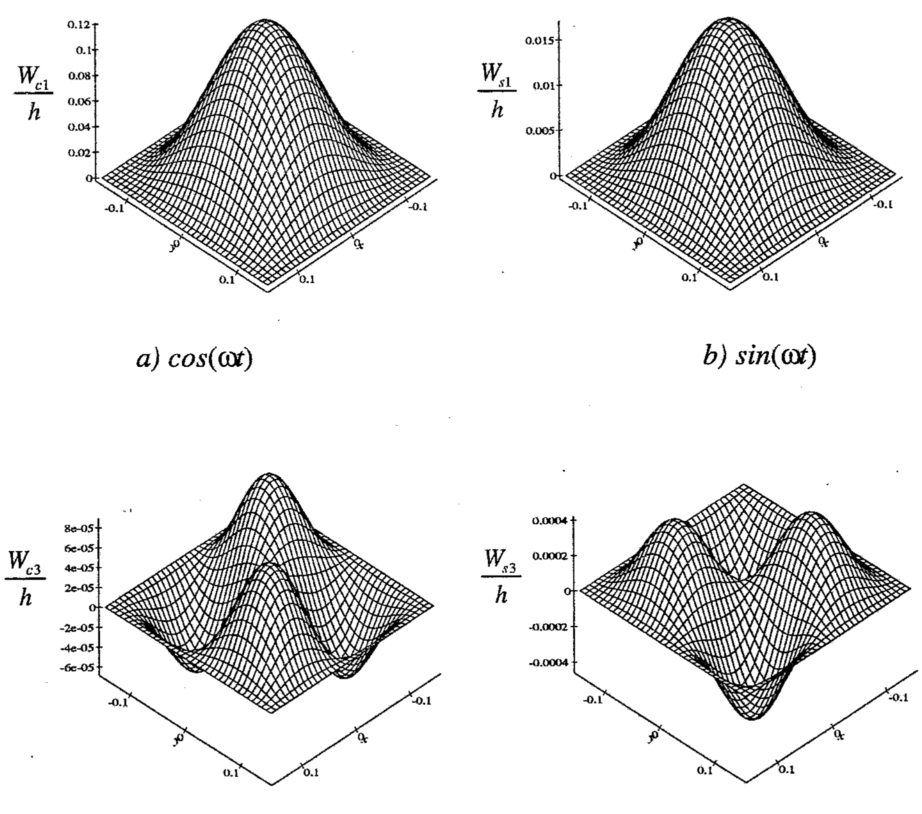

Figure 9.52 - Deformation of Plate 7.2 at point $\omega/\omega_{\ell 1}$= .96655.

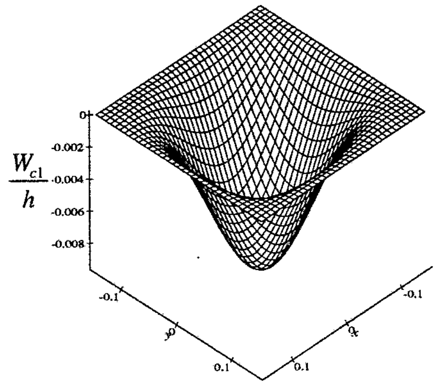

a) cos(ωt)

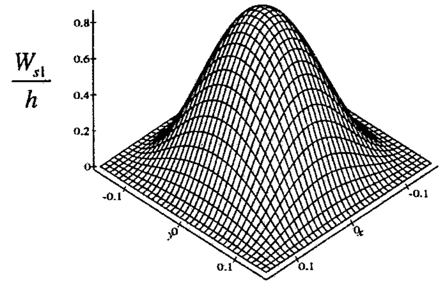

b) sin(ωt)

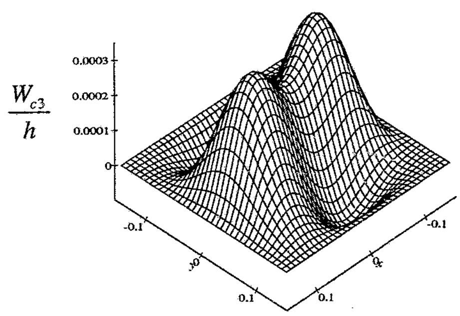

c) cos$(3\omega t)$

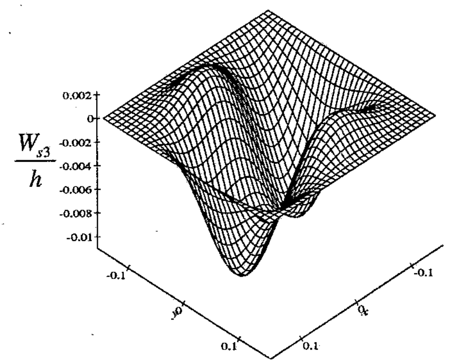

d) sin$(3\omega t)$

Figure 9.53 - Deformation of Plate 7.2 at point $\omega/\omega_{\ell 1}$= 1.13310.